

(NASA-SP-297) NUMERICAL MARCHING
TECHNIQUES FOR FLUID FLOWS WITH HEAT
TRANSFER (NASA) 349 p MP \$1.45; SOD HC
\$3.60

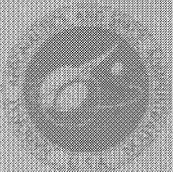
N74-12992

CSSL 20D

Unclas
24587

H1/12

Numerical Marching Techniques for Fluid Flows with Heat Transfer



Numerical Marching Techniques for Fluid Flows with Heat Transfer

Robert W. Hornbeck

*Lewis Research Center
Cleveland, Ohio*

and

*Carnegie-Mellon University
Pittsburgh, Pennsylvania*



Scientific and Technical Information Office 1973
NATIONAL AERONAUTICS AND SPACE ADMINISTRATION
Washington, D.C.

For Sale by the Superintendent of Documents,
U.S. Government Printing Office, Washington, D.C. 20402
Price \$3.60 Stock Number 3300-0430
Library of Congress Catalog Card Number 74-190300

PREFACE

In recent years there has been a large number of solutions presented in the fluid flow and heat transfer literature which have employed numerical marching techniques. However, most of these techniques seem to have been invented to solve the specific problem at hand, and they, therefore, seldom build on the work of previous investigators. To the author's knowledge, no unified presentation of these techniques, including the many aspects of their use, is available.

Any discussion of a field in science or technology must necessarily reflect the author's personal views about the evolution of that field. Since the author's interest in the numerical solution of fluid flow problems was begun and developed at the Carnegie Institute of Technology (now Carnegie-Mellon University), the natural evolution of the field appears to him to be that which has taken place at that institution, and in which he took part. Had the author, for example, come from the University of Michigan or the University of Wisconsin, where excellent numerical work of this type has also been done, it is likely that he would see the field from an entirely different perspective. This is particularly true in a field in which there is so much *art* rather than science in the evolution of the methods of solution. The author would therefore like to note at this point that much has been done in the field other than that referenced here and would like to apologize to those who may feel that their work has been slighted. It was felt, however, that much was to be gained by the unified approach used here rather than by presenting a motley literature survey of the vast number of techniques which have been employed in the past.

It is the purpose of this book to present the finite difference formulation and method of solution for a wide variety of fluid flow problems with associated heat transfer. Only a few direct results from these formulations will be given as examples, since the book is intended primarily to serve as a discussion of the techniques and as a starting point for further investigations; however, the formulations are sufficiently complete that a workable computer program may be written from them.

Some of the finite difference formulations given may be found complete with all results in the literature by the author and others; in these cases the references will be cited. For other problems apparently no finite difference formulation has

been previously employed, and in these cases the formulation is that of the author. For most of these cases the author or his associates have at least done experimental calculations which verify that the formulation and method of solution are workable. In a few cases such extensive work would be necessary to verify the formulation and method that a major research project would ensue, and in these cases the formulation must be considered as tentative, although no radical departures from the conventional techniques have been made. Such unproved formulations are clearly noted in the text.

It is hoped that the real utility of this book will be found not only in the actual formulations presented, which admittedly in a number of cases are for classical problems treated adequately by other means in the literature, but perhaps more importantly for situations in which the same or similar equations must be used for problems which are not readily amenable to other methods of analysis. Typical problems of this type are those which include any arbitrary distribution of suction or injection at a body surface, body forces such as MHD or EHD forces, any class of variable properties including those in which tabulated property variations must be used, and any type of velocity or temperature boundary condition. A number of such problems are presented and a solution formulated at the end of each chapter.

In the appendixes a number of topics are discussed which are of interest with respect to the finite difference equations presented in this book. These include a very rapid method for solving certain sets of linear algebraic equations, a discussion of numerical stability, the inherent error in flow rate for confined flow problems, and a method for obtaining high accuracy with a relatively small number of mesh points.

The author would also like to note that the use of the term *marching technique* is used here to apply to any numerical method of solving an initial value problem in the original sense of the term as used by L. F. Richardson in 1925. The term is thus applied equally to implicit and explicit techniques for the solution of parabolic and hyperbolic differential equations. There seems to be considerable current feeling that the term *marching* should apply only to explicit methods, but the author feels it is equally descriptive for implicit methods and it will be so used throughout this book.

CONTENTS

CHAPTER	PAGE
PREFACE.....	iii
1 INTRODUCTION.....	1
1.1 HISTORICAL BACKGROUND OF MARCHING PROCEDURES.....	1
1.2 RANGE OF APPLICABILITY OF MARCHING PROCEDURES.....	2
1.3 STABILITY, CONSISTENCY, AND CONVERGENCE...	3
1.4 EXPLICIT AND IMPLICIT DIFFERENCE REPRESENTATIONS.....	4
1.5 CHOICE OF MESH SIZE.....	7
REFERENCES.....	8
2 BOUNDARY LAYERS.....	11
2.1 TWO-DIMENSIONAL BOUNDARY LAYERS.....	11
2.1.1 Incompressible Constant Property Flow—Velocity Solution.....	11
2.1.2 Incompressible Constant Property Flow—Temperature Solution.....	16
2.1.3 Incompressible Constant Property Flow—Heat Transfer Solution.....	20
2.1.4 Compressible Flow—Velocity and Temperature Solutions.....	21
2.1.5 Compressible Flow—Nonlinear Finite Difference Representation.....	28
2.1.6 Compressible Flow—Heat Transfer Solution.....	29
2.2 AXISYMMETRIC BOUNDARY LAYERS.....	30
2.2.1 Incompressible Constant Property Flow—Velocity Solution.....	30
2.2.2 Incompressible Constant Property Flow—Temperature Solution.....	36

NUMERICAL MARCHING TECHNIQUES

CHAPTER	PAGE
2.2.3 Incompressible Constant Property Flow—Heat Transfer Solution	39
2.2.4 Compressible Flow—Velocity and Temperature Solutions.....	39
2.2.5 Compressible Flow—Heat Transfer Solution.....	48
2.3 OTHER PROBLEMS WITH A SIMILAR FORMULATION.....	48
2.3.1 Wake Behind a Flat Plate.....	48
2.3.2 Two-Dimensional or Axisymmetric Body With Suction or Injection at the Surface.....	50
2.3.3 Tangential Jet Adjacent to a Wall.....	50
2.3.4 Boundary Layer Flows With Body Forces (MHD, EHD, etc.).....	51
2.4 EXAMPLE PROBLEM—FLAT PLATE BOUNDARY LAYER.....	52
REFERENCES.....	55
3 JETS.....	57
3.1 PLANE JETS.....	57
3.1.1 Incompressible Constant Property Flow—Velocity Solution.....	57
3.1.1.1 <i>Highly implicit difference representation valid for small secondary velocities</i>	59
3.1.1.2 <i>Implicit formulation valid only for large secondary velocities</i>	63
3.1.2 Incompressible Constant Property Flow—Temperature Solution.....	65
3.1.3 Compressible Flow—Velocity and Temperature Solutions.....	67
3.1.3.1 <i>Highly implicit representation valid for small secondary velocities</i>	69
3.1.3.2 <i>Implicit representation valid only for large secondary velocities</i>	73
3.2 AXISYMMETRIC JETS.....	77
3.2.1 Incompressible Constant Property Flow—Velocity Solution.....	77
3.2.1.1 <i>Highly implicit difference representation valid for small secondary velocities</i>	78
3.2.1.2 <i>Implicit difference representation valid only for large secondary velocities</i>	82
3.2.2 Incompressible Constant Property Flow—Temperature Solution.....	84

CONTENTS

CHAPTER	PAGE
3.2.3 Compressible Flow—Velocity and Temperature Solutions	87
3.2.3.1 <i>Highly implicit difference representation valid for small secondary velocities</i>	89
3.2.3.2 <i>Implicit difference representation valid only for large secondary velocities</i>	94
3.3 OTHER PROBLEMS WITH A SIMILAR FORMULATION	99
3.3.1 Jets With Body Forces	99
3.3.2 Jet Mixing When Primary and Secondary Streams Are Different Compressible Fluids.....	99
3.4 EXAMPLE PROBLEM—TWO-DIMENSIONAL JET.....	111
REFERENCES	114
 4 FREE CONVECTION	 115
4.1 FLOW ON A VERTICAL HEATED PLATE.....	115
4.1.1 Velocity and Temperature Solutions.....	115
4.1.2 Heat Transfer Solution	121
4.2 OTHER PROBLEMS WITH SIMILAR FORMULATION.....	122
4.2.1 Combined Free and Forced Convection on a Vertical Heated Plate	122
4.2.2 Free Convection With Wall Temperature or Wall Heat Flux a Function of Position	123
4.2.3 Free Convection With MHD or EHD Body Forces	126
4.3 EXAMPLE PROBLEM—FREE CONVECTION FROM A HEATED VERTICAL PLATE	126
REFERENCES.....	128
 5 TIME DEPENDENT BOUNDARY LAYERS.....	 129
5.1 PLANE TRANSIENT BOUNDARY LAYER.....	129
5.1.1 Incompressible Flow—Velocity Solution	129
5.1.1.1 <i>Explicit representation</i>	131
5.1.1.2 <i>Implicit representation</i>	133
5.1.2 Incompressible Flow—Temperature Solution	135
5.1.2.1 <i>Explicit representation</i>	137
5.1.2.2 <i>Implicit representation</i>	138
5.1.3 Incompressible Flow—Heat Transfer Solution.....	140
5.1.4 Compressible Flow—Velocity and Temperature Solutions	140
5.1.5 Compressible Flow—Heat Transfer Solution.....	148
5.2 OTHER PROBLEMS WITH SIMILAR FORMULATIONS	148

5.3	EXAMPLE PROBLEM—OSCILLATING BOUNDARY LAYER ON A FLAT PLATE.....	149
	REFERENCES	151
6	PARALLEL PLATE CHANNEL.....	153
6.1	ENTRANCE FLOW AND HEAT TRANSFER IN A PARALLEL PLATE CHANNEL.....	153
6.1.1	Incompressible Constant Property Flow—Velocity Solution.....	153
6.1.2	Incompressible Constant Property Flow—Temperature Solution.....	160
6.1.3	Incompressible Constant Property Flow—Heat Transfer Solution.....	165
6.1.4	Compressible Flow—Velocity and Temperature Solutions.....	167
6.1.5	Compressible Flow—Heat Transfer Solution.....	178
6.2	OTHER PROBLEMS WITH A SIMILAR FORMULATION.....	181
6.2.1	Flow in Parallel Plate Channels With Porous Walls...	181
6.2.2	Developing Confined Free Convection Flow Between Parallel Plates.....	185
6.2.3	Flow in a Parallel Plate Channel With Body Forces.....	191
6.3	EXAMPLE PROBLEM — INCOMPRESSIBLE ENTRANCE FLOW IN A PARALLEL PLATE CHANNEL.....	191
	REFERENCES.....	194
7	CIRCULAR TUBE.....	195
7.1	ENTRANCE FLOW AND HEAT TRANSFER IN A CIRCULAR TUBE.....	195
7.1.1	Incompressible Constant Property Flow—Velocity Solution.....	196
7.1.2	Incompressible Constant Property Flow—Temperature Solution.....	202
7.1.3	Incompressible Constant Property Flow—Heat Transfer Solution	206
7.1.4	Compressible Flow—Velocity and Temperature Solutions.....	208
7.1.5	Compressible Flow—Heat Transfer Solution.....	219
7.2	OTHER PROBLEMS WITH A SIMILAR FORMULATION.....	221
7.2.1	Flow in Circular Tubes With Porous Walls.....	221
7.2.2	Developing Confined Free Convection Flow in a Circular Tube.....	225

CONTENTS

CHAPTER	PAGE
7.2.3 Flow in a Circular Tube With Body Forces.....	228
7.2.4 Entrance Flow and Heat Transfer in a Concentric Annulus.....	228
7.2.4.1 <i>Incompressible constant property flow—velocity solution</i>	228
7.2.4.2 <i>Incompressible constant property flow—temperature solution</i>	231
7.2.4.3 <i>Incompressible constant property flow—heat transfer</i>	233
7.3 EXAMPLE PROBLEM—INCOMPRESSIBLE FLOW IN THE ENTRANCE REGION OF A CIRCULAR TUBE...	235
REFERENCES.....	240
 8 RECTANGULAR CHANNEL.....	 241
8.1 ENTRANCE FLOW AND HEAT TRANSFER IN A RECTANGULAR CHANNEL.....	241
8.1.1 Incompressible Constant Property Flow—Velocity Solution—First Model.....	242
8.1.2 Incompressible Constant Property Flow—Velocity Solution—Second Model.....	252
8.1.3 Incompressible Constant Property Flow—Temperature and Heat Transfer Solutions.....	255
8.1.3.1 <i>Case 1—constant wall temperature</i>	257
8.1.3.2 <i>Case 2—constant heat input per unit length, uni- form peripheral temperature</i>	260
8.1.3.3 <i>Case 3—constant heat input per unit area of duct surface</i>	264
8.1.4 Compressible Flow in the Entrance of a Rectangular Channel—Proposed Velocity and Temperature Solutions.....	266
8.2 OTHER PROBLEMS WITH A SIMILAR FORMULA- TION.....	271
8.2.1 Flow in Rectangular Channels With Porous Walls.....	271
8.2.2 Entrance Flow in Channels With Cross Sections Com- posed of Rectangular Elements.....	273
8.2.3 Flow With Body Forces in Rectangular Channels.....	273
8.2.4 Confined Free Convection in a Vertical Rectangular Channel.....	274
8.3 EXAMPLE PROBLEM—LAMINAR INCOMPRESSIBLE ENTRANCE FLOW IN A SQUARE DUCT.....	276
REFERENCES.....	282

NUMERICAL MARCHING TECHNIQUES

CHAPTER		PAGE
9	OTHER NONCIRCULAR AND VARYING AREA CHANNELS .	283
	9.1 NONCIRCULAR CHANNELS OF CONSTANT AREA...	283
	9.1.1 Alternating Direction Implicit (ADI) Techniques.....	284
	9.1.2 Irregular Boundaries.....	287
	9.1.3 Normal Gradient Boundary Conditions.....	289
	9.1.4 General Remarks.....	290
	9.2 CHANNELS OF VARYING CROSS-SECTIONAL AREA.....	290
	9.3 EXAMPLE PROBLEM—COMPRESSIBLE FLOW IN VARYING AREA CHANNELS.....	293
	REFERENCES.....	299
APPENDIXES		
A	SOLUTION FOR A SET OF LINEAR ALGEBRAIC EQUATIONS HAVING A TRIDIAGONAL MATRIX OF COEFFICIENTS.....	301
B	FINITE DIFFERENCE REPRESENTATIONS, TRUNCATION ERROR ANALYSIS, AND STABILITY ANALYSIS.....	307
	B.1 FINITE DIFFERENCE REPRESENTATIONS.....	307
	B.2 TRUNCATION ERROR AND A SAMPLE TRUNCATION ERROR ANALYSIS.....	311
	B.3 GENERAL METHOD OF STABILITY ANALYSIS.....	312
	B.4 SAMPLE STABILITY ANALYSIS.....	316
C	ANALYSIS AND CORRECTION OF INHERENT ERROR IN FLOW RATE FOR CONFINED FLOW PROBLEMS IN CHANNELS OF CONSTANT AREA.....	323
D	VARIABLE MESH SIZE TECHNIQUE.....	329
E	GAUSS-JORDAN ELIMINATION ROUTINE.....	333
F	SPECIFICATION OF TRANSVERSE VELOCITIES AT LEADING EDGES AND CHANNEL ENTRANCES.....	337

CHAPTER 1

INTRODUCTION

1.1 HISTORICAL BACKGROUND OF MARCHING PROCEDURES

Marching procedures for the finite difference solution of parabolic partial difference equations (particularly the diffusion equation) have been known for many years (refs. 1 to 3). Only since the advent of the digital computer as an engineering tool, however, have these methods been widely used to obtain solutions to a variety of fluid flow and heat transfer problems. In many cases these numerical solutions represent the most accurate available solution to a given problem or at least the most accurate solution to the equations which are assumed to apply to the physical situation. In other cases the numerical solution represents the only one available. Any analytical solution of the momentum and energy equations is difficult because of the nonlinear convective terms. In most cases a solution can only be obtained by linearizations or approximations. On the other hand, the accuracy of a properly posed set of finite difference equations is limited only by the size of the grid spacing used in the solution.

Step-by-step integration processes (marching procedures) for boundary layer flows were employed by a number of investigators in the 1930's and 1940's (refs. 4 to 6). It was not, however, until the work of Friedrich and Forstall (ref. 7) in 1953 and Rouleau and Osterle (refs. 8 and 9) in 1954 and 1955 that these finite difference methods reached a sufficiently mature stage that they could be considered generally useful. Although in these investigations a desk calculator was employed, formulations were used which have been found of considerable value in electronic digital computer applications. Friedrich and Forstall (ref. 7) solved the problem of coaxial viscous jets using an explicit method with which some stability problems were encountered. Rouleau and Osterle (refs. 8 and 9) formulated an implicit finite difference scheme which was universally stable and then considered a variety of external flow problems. Bodoia and Osterle (ref. 10) extended this implicit formulation to confined flow situations. These four papers formed the basis for all of the steady flow solutions which were to follow. The

first extensive use of these methods for compressible flow problems was apparently that of Mitchel (ref. 11) for external flow problems, followed by Walker (ref. 12), Deissler and Presler (ref. 13), and Worsøe-Schmidt and Leppert (ref. 14), who solved internal flow problems.

The basic work on the numerical solution to transient flows of the boundary layer type was done at the University of Michigan. These investigations include those of Hellums (ref. 15), Farn (ref. 16), and Farn and Arpaci (ref. 17).

The pioneering work of Fromm and his associates at Los Alamos on the solution by numerical methods of the complete elliptic time-dependent Navier-Stokes equations will not be discussed here since this book will be restricted to equations of the parabolic and hyperbolic type. See reference 18 for a discussion of the work and further references.

1.2 RANGE OF APPLICABILITY OF MARCHING PROCEDURES

Numerical marching procedures are methods in which the solution is obtained in a step-by-step manner, always moving downstream in the flow field, forward in time, etc. Their use is restricted to certain classes of differential equations. The equations must be parabolic or hyperbolic (classical examples being the diffusion equation and the wave equation) and cannot be elliptic (e.g., Laplace's equation). The character of the basic equations of fluid flow and heat transfer, the Navier-Stokes equations and the energy equation, implies that there may be no derivatives higher than first order in the main flow direction. Thus, the second derivatives along the main flow direction in the viscous terms of the Navier-Stokes equations may not be present, nor can the axial conduction term in the energy equation. In many physical situations it is justifiable to neglect these terms, and if so, a marching procedure can be applied. As a general rule, the second axial derivatives may not be neglected if there is anything in the flow which will have an influence upstream (e.g., an object in the stream, a sharp constriction in the channel, or a heater grid in the stream). The second axial derivative may be neglected, and marching procedures may be applied, if the problem has an "open boundary" in the flow direction. Transient problems of the boundary-layer type have an "open boundary" in time as well as space, and marching techniques may be applied to these problems in the time (as well as the space) direction.

An additional restriction on fluid flow solutions using the marching technique is that large backflow is not permitted anywhere in the flow field. This condition is generally associated with separating flows, and, as a result, the solution cannot be carried far beyond the separation point. Of course, the physical validity of the parabolic equations may be questioned even slightly upstream of the separation point.

1.3 STABILITY, CONSISTENCY, AND CONVERGENCE

The terms stability, consistency, and convergence have acquired many meanings both in and out of numerical analysis, so it becomes necessary to define them as used in the context of this book.

The concept of stability of a numerical solution is somewhat difficult to precisely define, although, as anyone experienced in obtaining numerical solutions is well aware, instability usually manifests itself in a very obvious, usually catastrophic manner. This is actually a fortunate state of affairs in that, at least for all problems analyzed so far, there is a distinct dividing line between instability and stability. Instability is generally considered to be the result of either the cumulative growth of roundoff errors without bound as the solution is marched forward, or the growth of error due to the presence of an extraneous solution to the difference equations. Instability of either type will generally be seen as a strongly growing, oscillatory cumulative error which, in practice, rapidly causes a computer overflow. The usual distinction between stability and instability is that given by Forsythe and Wasow (ref. 19). This distinction is that a procedure is stable if the cumulative error as the solution is marched forward does not grow faster than some low power of the reciprocal of the mesh size in the marching direction; instability corresponds to the cumulative error being an exponential function of the reciprocal of the mesh size. There seems to be no intermediate condition.

The criteria for stability of many of the difference representations given in this book may be obtained in a relatively straightforward way. For some cases it is extremely difficult to obtain analytical expressions for the stability criteria; in these cases it is reasonable to simply proceed with the numerical solution. If instability develops, as was previously mentioned, it will do so rather quickly and violently, in which case adjustments in the mesh sizes and parameters may be tried until stability can hopefully be attained. Throughout the book, stability criteria are presented where available. Appendix B gives a stability analysis for a typical case and outlines the method in general.

A consistent finite difference representation has an exact solution (assuming no roundoff error) that approaches the solution of the differential equations which the difference equations replace as the mesh sizes used approach zero. Consistency of a difference representation is dependent on the difference forms used to replace the various terms in the differential equations and, to a certain extent, on the boundary conditions and difference representation of these boundary conditions. Where the term consistency is used in this book, many investigators use the term convergence, but since convergence is also widely used to describe a characteristic of an iterative process, the less widely used consistency seems a better choice.

All of the difference representations given in this book are consistent, except for certain formulations given for plane and axisymmetric jets which are consistent only for nonzero secondary velocities. Consistent representations which allow zero secondary velocities are also given for these cases.

If an iteratively obtained solution to a set of linear or nonlinear algebraic equations approaches the exact solution as the number of iterations becomes large, the method of solution is called convergent. As mentioned before, this term is also widely used to describe what in this book is called consistency.

1.4 EXPLICIT AND IMPLICIT DIFFERENCE REPRESENTATIONS

Explicit difference representations are those in which, as each step in the marching direction is taken, the unknown quantities in the equations may be solved for one at a time. Implicit representations require the solution of a set of simultaneous equations for the unknowns as each step is taken.

The choice of explicit or implicit finite difference representations will depend on many factors, including the problem itself and the size and speed of the available computer.

In order to examine the various representations, consider the flow field with a mesh imposed on it shown in figure 1-1. The main flow direction is x . No boundary conditions will be considered. Assuming the flow may be adequately described by the incompressible constant property Prandtl equations, the basic equations of motion are

$$u \frac{\partial u}{\partial x} + v \frac{\partial u}{\partial y} = \nu \frac{\partial^2 u}{\partial y^2} \quad (1-1)$$

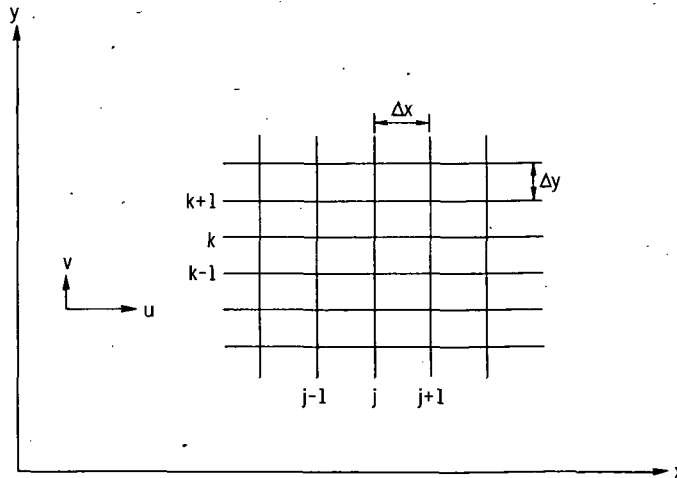


FIGURE 1-1.—Flow field and finite difference grid.

$$\frac{\partial u}{\partial x} + \frac{\partial v}{\partial y} = 0 \quad (1-2)$$

For any numerical work, the first step should be to put the basic equations in dimensionless form. However, since our interest here is in a discussion of explicit and implicit forms, this step is omitted. It is assumed that both u and v are known for all values of x and y in the region $0 \leq x \leq x_j$. It should now be possible by using a marching procedure to advance the solution to x_{j+1} , then to x_{j+2} , etc.

A number of difference forms are possible for the representation of equation (1-1). The following are examples:

Explicit:

$$\begin{aligned} u_{j,k} \left(\frac{u_{j+1,k} - u_{j,k}}{\Delta x} \right) + v_{j,k} \left(\frac{u_{j,k+1} - u_{j,k-1}}{2\Delta y} \right) \\ = v \left(\frac{u_{j,k+1} - 2u_{j,k} + u_{j,k-1}}{(\Delta y)^2} \right) \end{aligned} \quad (1-3)$$

Implicit:

$$\begin{aligned} u_{j,k} \left(\frac{u_{j+1,k} - u_{j,k}}{\Delta x} \right) + v_{j,k} \left(\frac{u_{j+1,k+1} - u_{j+1,k-1}}{2\Delta y} \right) \\ = v \frac{u_{j+1,k+1} - 2u_{j+1,k} + u_{j+1,k-1}}{(\Delta y)^2} \end{aligned} \quad (1-4)$$

Semi-implicit (Crank-Nicholson):

$$\begin{aligned} u_{j,k} \left(\frac{u_{j+1,k} - u_{j,k}}{\Delta x} \right) \\ + v_{j,k} \left(\frac{\frac{u_{j+1,k+1} - u_{j+1,k-1}}{2\Delta y} + \frac{u_{j,k+1} - u_{j,k-1}}{2\Delta y}}{2} \right) \\ = v \left(\frac{\frac{u_{j+1,k+1} - 2u_{j+1,k} + u_{j+1,k-1}}{(\Delta y)^2} + \frac{u_{j,k+1} - 2u_{j,k} + u_{j,k-1}}{(\Delta y)^2}}{2} \right) \end{aligned} \quad (1-5)$$

These representations are illustrated in figure 1-2. The explicit form (eq. (1-3)) has only one unknown, $u_{j+1,k}$, in each equation. Therefore this form can

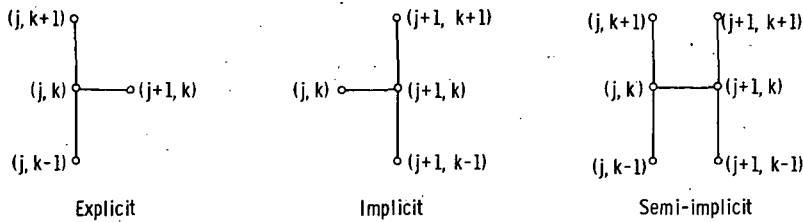


FIGURE 1-2.—Finite difference representations of momentum equation. (j , last x value at which velocities are known; $j+1$, x value at which velocities are to be found.)

be solved directly (explicitly) for the values of $u_{j+1, k}$ entirely in terms of known quantities. The explicit form has the advantages of high speed and simplicity of solution. The primary disadvantage of this form is that there are stability restrictions on its use. These restrictions are that $\nu \Delta x / [u_{j, k} (\Delta y)^2] \leq 1/2$ and $|v_{j, k} \Delta y / \nu| \leq 2$. These criteria are derived by Rouleau in reference 9. This restriction may not be too serious for such problems as free jets with moving secondaries, but for situations where u may become small or reach zero (as in cases where solid boundaries are present) this restriction can be so serious as to preclude the use of the explicit form.

The implicit form (eq. (1-4)) involves three unknowns: $u_{j+1, k-1}$, $u_{j+1, k}$, and $u_{j+1, k+1}$. When this difference equation is written for each value of k in the flow field, a set of simultaneous linear algebraic equations in the values of $u_{j+1, k}$ is formed. This set must be solved before another step can be taken in the x -direction. The implicit form has the advantage of universal stability for all mesh sizes so long as u does not become negative. The seeming disadvantage of the implicit representation is that the solution of a set of linear equations is, in general, time consuming. It should be noted, however, that for a set of linear algebraic equations of the type generated by equation (1-4) there exist methods which are very nearly as rapid as carrying out the explicit solution from equation (1-3). See appendix A for a description of one such method.

The semi-implicit representation (sometimes called a Crank-Nicholson representation), equation (1-5), is an effort to gain a more accurate representation of the differential equation by averaging the various terms wherever possible so that each of the terms will be evaluated at essentially the same point. The solution and stability criteria for the semi-implicit form are identical to those for the implicit form. In practice, the author has found the advantages of the semi-implicit form to be somewhat exaggerated, and that simply employing the implicit form with a slightly smaller mesh size results in virtually the same effect. Forsythe and Wasow (ref. 19) also note the lack of evidence for significant advantages of the semi-implicit approach. It should be noted that the representation in equation (1-5) has been chosen in such a way as to eliminate nonlinearities in the difference equations. It is questionable whether it is ever worthwhile to make the difference

equations nonlinear only to incorporate the advantages of the semi-implicit representation, since a considerable increase in computer time is required in order to solve the nonlinear equations.

The continuity equation has generally been written in a form which, for the present problem at least, is explicit. Only one of the many possible representations is

$$\frac{u_{j+1, k+1} - u_{j, k+1}}{\Delta x} + \frac{v_{j+1, k+1} - v_{j+1, k}}{\Delta y} = 0 \quad (1-6)$$

This equation may be solved in an explicit stepwise manner for $v_{j+1, k+1}$ assuming $v_{j+1, k}$ is known. The solution is started from a point where $v_{j+1, k}$ is known (a lower boundary, centerline, axis of symmetry, etc.) and marched upward. The values of $u_{j+1, k+1}$ and $u_{j+1, k}$ are known from the solution of the momentum equation. Various representations of the continuity equation are employed in this book for different flow situations. For external flows, the form of equation (1-6) will be almost universally used. For confined flows, the form employed will be dictated by the particular problem being considered and will be discussed in detail for each new situation.

1.5 CHOICE OF MESH SIZE

The choice of mesh sizes for the problems considered in this book is dictated primarily by the truncation error of the difference equations and, in some cases, by the stability criteria. The only way in which a final mesh size may be chosen with complete confidence is to run the problem with successively smaller mesh sizes until little or no change is observed in the results. Such a procedure may be impractical from the standpoint of computer time required, and in this case an alternative, although somewhat less desirable, solution is to run the problem for two mesh sizes and use one of the techniques for extrapolating to zero mesh size (refs. 19 and 20). This method will not produce satisfactory results if the mesh sizes chosen are not fairly close to the size required to give a reasonable solution.

No quantitative statements can be made about the choice of mesh sizes in various regions; however, smaller mesh sizes are required in regions of more rapidly changing velocity and temperature. This means that a fine mesh is required close to the wall in boundary layer problems, as well as close to the leading edge. It is worth noting that the leading edge (or the entrance in a channel flow problem) is a point of singularity in boundary layer theory, and that solutions obtained using the boundary layer equations in the region close to the entrance will be incorrect in this region. The effects of this point of singularity can be confined to the region very close to the singularity if very small mesh sizes in the downstream direction are used until the profiles smooth out somewhat. Typically, mesh sizes in the marching direction of the order of 1/100 of those employed further downstream

may be desirable in order to confine the leading edge effects to the region close to the singularity. A number of investigators have transformed the equations to boundary layer coordinates in an effort to minimize the effects of the singularity, but in view of the success of simply using a very small mesh size in this region, such a procedure becomes mainly useful in minimizing the effects of boundary layer thickness along the plate and its value must be weighed against its greater complexity. In chapter 2, section 2.4, a detailed discussion is presented of the effect of the leading edge singularity on the calculations for an actual problem.

In the region close to a wall, or in the mixing region of streams of different velocities, it is usually desirable to employ a finer mesh size than that needed far out in the free stream where velocity and temperature gradients are less steep. The technique for changing transverse mesh sizes in the flow field is discussed in appendix D.

To give a starting point for the choice of mesh sizes, it may be stated that transverse mesh sizes of the order of 10^{-1} to 10^{-2} will usually be sufficient, while mesh sizes in the downstream direction may vary from as small as 10^{-5} close to the leading edge to 10^{-3} farther downstream. These sizes are, of course, predicated on the use of the dimensionless variables used in succeeding chapters of this book. Any other choice of dimensionless variables may have a profound effect on the mesh sizes which are necessary.

REFERENCES

1. RICHARDSON, L. F.: The Approximate Arithmetical Solution by Finite Differences of Physical Problems Involving Differential Equations, with an Application to the Stresses in a Masonry Dam. Phil. Trans. Roy. Soc. London, Ser. A, vol. 210, 1910, pp. 307-357.
2. RICHARDSON, L. F.: How To Solve Differential Equations Approximately by Arithmetic. Math. Gazette, vol. 12, 1925, p. 415.
3. SCHMIDT, E.: Föppl's Festschrift. Joseph Springer, Berlin, 1924.
4. GOERTLER, H.: Weiterentwicklung eines Grenzschichtprofils bei gegebenem Druckverlauf. Zeit. f. Angew. Math. Mech., vol. 19, no. 3, June 1939, pp. 129-140.
5. GOERTLER, H.: Ein Differenzenverfahren zur Berechnung laminarer Grenzschichten. Ing.-Arch., vol. 16, 1948, pp. 173-187.
6. SCHROEDER, KURT: Ein einfaches numerisches Verfahren zur Berechnung der laminaren Grenzschicht. Math. Nachr., vol. 4, 1950-1951, pp. 439-467.
7. FRIEDRICH, CARL M.; AND FORSTALL, WALTON, JR.: A Numerical Method for Computing the Diffusion Rate of Coaxial Jets. Proceedings of the Third Midwestern Conference on Fluid Mechanics, Minneapolis, Minn., 1953, pp. 635-649.
8. ROULEAU, W. T.; AND OSTERLE, J. F.: The Application of Finite Difference Methods to Boundary-Layer Type Flows. J. Aeron. Sci., vol. 22, no. 4, Apr. 1955, pp. 249-254.
9. ROULEAU, WILFRED T.: Finite Difference Methods for the Solution of Fluid Flow Problems Described by the Prandtl Equations. Ph.D. Thesis, Carnegie Inst. Tech., 1954.
10. BODOIA, J. R.; AND OSTERLE, J. F.: Finite Difference Analysis of Plane Poiseuille and Couette Flow Developments. Appl. Sci. Res., Sec. A, vol. 10, no. 3-4, 1961, pp. 265-276.
11. MITCHEL, BARRY J.: Finite Difference Solution of the Development of Transpiration-Cooled Hypersonic Laminar Boundary Layers. Ph.D. Thesis, Carnegie Inst. Tech., 1961.

12. WALKER, M. L., JR.: Laminar Compressible Flow in the Entrance Region of a Tube. Ph.D. Thesis, Carnegie Inst. Tech., 1965.
13. DEISSLER, ROBERT G.; AND PRESLER, ALDEN F.: Analysis of Developing Laminar Flow and Heat Transfer in a Tube for a Gas with Variable Properties. Proceedings of the Third International Heat Transfer Conference. Vol. 1, AIChE, 1966, pp. 250-256.
14. WORSØE-SCHMIDT, P. M.; AND LEPPERT, G.: Heat Transfer and Friction for Laminar Flow of Gas in a Circular Tube at High Heating Rate. Int. J. Heat Mass Transfer, vol. 8, no. 10, Oct. 1965, pp. 1281-1301.
15. HELSUMS, JESSE D.: Finite Difference Computation of Natural Convection Heat Transfer. Ph. D. Thesis, Univ. Michigan, 1960.
16. FARN, CHARLES L. S.: A Finite Difference Method for Computing Unsteady, Incompressible, Laminar Boundary-Layer Flows. Ph. D. Thesis, Univ. Michigan, 1965.
17. FARN, CHARLES L. S.; AND ARPACI, VEDAT S.: On the Numerical Solution of Unsteady, Laminar Boundary Layers. AIAA J., vol. 4, no. 4, Apr. 1966, pp. 730-732.
18. FROMM, J.: The Time Dependent Flow of an Incompressible Viscous Fluid. Methods in Computational Physics. Vol. 3. Academic Press, 1964, pp. 346-382.
19. FORSYTHE, GEORGE E.; AND WASOW, WOLFGANG R.: Finite-Difference Methods for Partial Differential Equations. John Wiley & Sons, Inc., 1960.
20. CRANDALL, STEPHEN H.: Engineering Analysis, A Survey of Numerical Procedures. McGraw-Hill Book Co., Inc., 1956.

CHAPTER 2

BOUNDARY LAYERS

This detailed discussion of numerical techniques is begun by considering the external laminar boundary layer which forms on the surface of a body when the body is placed in a free stream of a viscous fluid.

2.1 TWO-DIMENSIONAL BOUNDARY LAYERS

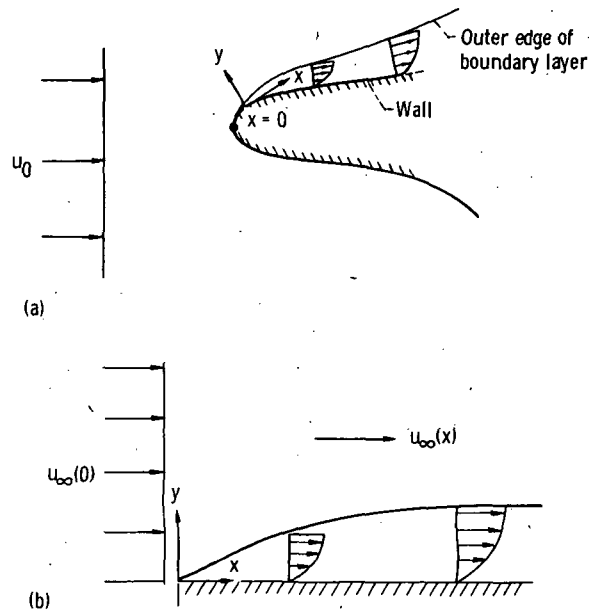
For our purposes it is convenient to reformulate the general two-dimensional boundary layer problem (of which an example is shown in fig. 2-1(a)) into a flat plate boundary layer problem (as shown in fig. 2-1(b)). The pressure gradient and velocity far above the plate may be functions of x . Their values are determined from the solution for potential flow around a body having the shape of the actual body. This potential flow solution, evaluated at the surface of the body, yields the desired values of $u_\infty(x)$ and $dp(x)/dx$. The flow at the "leading edge" of the flat plate is a uniform velocity with a value equal to that obtained from the potential flow solution evaluated at the surface of the body and $x=0$ (e.g., if $x=0$ is a stagnation point on the original body, then this velocity will be zero).

The temperatures in the stream far above the plate and at the "leading edge" are assumed constant for the incompressible case, but they must be computed from the energy equation for the compressible case since the velocity and pressure fields of the potential flow solution affect the temperature.

2.1.1 Incompressible Constant Property Flow - Velocity Solution

For the incompressible flow case, the equations of momentum and energy are uncoupled so that they may be solved separately. The basic equations of motion, making the usual boundary layer assumptions, are

$$\rho \left(u \frac{\partial u}{\partial x} + v \frac{\partial u}{\partial y} \right) = -\frac{dp}{dx} + \mu \left(\frac{\partial^2 u}{\partial y^2} \right) \quad (2-1)$$



(a) Typical two-dimensional boundary layer configuration.
 (b) Two-dimensional boundary layer problem reformulated as flat plate boundary layer.

FIGURE 2-1.—Modeling of a two-dimensional boundary layer as a flat plate boundary layer.

$$\frac{\partial u}{\partial x} + \frac{\partial v}{\partial y} = 0 \quad (2-2)$$

The boundary conditions are

$$\left. \begin{aligned} u(x, 0) &= 0 \\ v(x, 0) &= 0 \\ u(x, \infty) &= u_\infty(x) \\ u(0, y) &= u_\infty(0) \quad (\text{see appendix F}) \end{aligned} \right\} \quad (2-3)$$

Before undertaking a numerical solution, the first step should invariably be to place the equations to be solved in a dimensionless form having as few parameters as possible. This may be accomplished for equations (2-1) and (2-2) by employing the following dimensionless variables:

$$\left. \begin{aligned} U &= u/u_0 \\ V &= \frac{\rho v L}{\mu} \\ P &= \frac{p - p_0}{\rho u_0^2} \end{aligned} \right\} \begin{aligned} X &= \frac{x\mu}{L^2 \rho u_0} \\ Y &= y/L \end{aligned} \quad (2-4)$$

where the characteristic velocity u_0 will usually be chosen as the velocity far upstream from the body, and a typical length L is measured along the surface in the x -direction. For the flat plate case $u_\infty(0) = u_0$.

The differential equations in dimensionless form become

$$U \frac{\partial U}{\partial X} + V \frac{\partial U}{\partial Y} = -\frac{dP}{dX} + \frac{\partial^2 U}{\partial Y^2} \quad (2-5)$$

$$\frac{\partial U}{\partial X} + \frac{\partial V}{\partial Y} = 0 \quad (2-6)$$

with boundary conditions

$$\left. \begin{aligned} U(X, 0) &= 0 \\ V(X, 0) &= 0 \\ U(X, \infty) &= u_\infty/u_0 = U_\infty(X) \\ U(0, Y) &= U_\infty(0) \end{aligned} \right\} \quad (2-7)$$

From the potential flow solution, U_∞ and $dP(X)/dX$ are known.

Equations (2-5) and (2-6) may now be written in difference form. A difference grid is imposed on the flow field as shown in figure 2-2. The most useful representation for equation (2-5) is the following implicit form:

$$\begin{aligned} U_{j,k} \frac{U_{j+1,k} - U_{j,k}}{\Delta X} + V_{j,k} \frac{U_{j+1,k+1} - U_{j+1,k-1}}{2\Delta Y} \\ = -\frac{P_{j+1} - P_j}{\Delta X} + \frac{U_{j+1,k+1} - 2U_{j+1,k} + U_{j+1,k-1}}{(\Delta Y)^2} \end{aligned} \quad (2-8)$$

A simple explicit form is used for equation (2-6):

$$\frac{U_{j+1,k+1} - U_{j,k+1}}{\Delta X} + \frac{V_{j+1,k+1} - V_{j+1,k}}{\Delta Y} = 0 \quad (2-9)$$

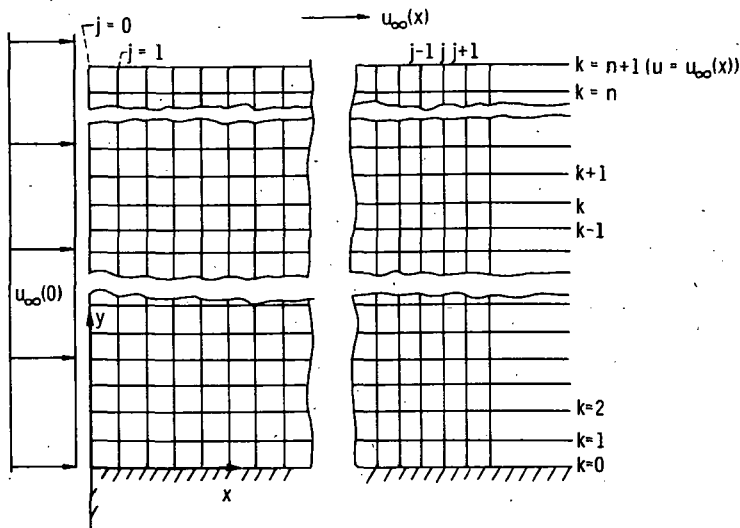


FIGURE 2-2.—Finite difference grid.

Equation (2-8) may now be rewritten in a more useful form as

$$\left[-\frac{V_{j,k}}{2\Delta Y} - \frac{1}{(\Delta Y)^2} \right] U_{j+1,k-1} + \left[\frac{U_{j,k}}{\Delta X} + \frac{2}{(\Delta Y)^2} \right] U_{j+1,k}$$

$$\left[\frac{V_{j,k}}{2\Delta Y} - \frac{1}{(\Delta Y)^2} \right] U_{j+1,k+1} = \frac{P_j - P_{j+1} + U_{j,k}^2}{\Delta X} \quad (2-10)$$

Equation (2-10) is now written for all values of k from $k=1$ to a sufficiently large value of Y to ensure that the free stream has been reached; this value of Y will correspond to $k=n$. The free stream boundary condition will then be $U=U_\infty$ at $k=n+1$. As a general rule, the value of n should be chosen to ensure that there are several points (3 or 4) for $k < n+1$ such that $U \cong U_\infty$. If the solution is actually started from the leading edge, it will be relatively simple to find an adequate value of n as the solution is carried downstream. The value of n must be increased as the boundary layer grows in thickness if a fixed ΔY is used. When n reaches a sufficiently large value that computations become awkward (perhaps 50 or 60) it will be found worthwhile to double ΔY and halve n before continuing.

The set of linear algebraic equations corresponding to equation (2-10) for $k=1(1)n$ (k varying from 1 to n in steps of 1) may be written in matrix form as

$$\left. \begin{aligned} \frac{\Delta X}{|U|(\Delta Y^2)} &\geq \frac{1}{2} \\ V &\geq \sqrt{\frac{2|U|}{\Delta X}} \end{aligned} \right\} \quad (2-13)$$

These conditions will be satisfied only if the negative value of U is very small; hence, the solution may be carried only up to and perhaps very slightly past the separation point. A complete solution to the problem posed in this section is presented in section 2.4 as a representative example of the use of the techniques of this chapter. The solution is carried out for the case of $dP(X)/dX=0$.

2.1.2 Incompressible Constant Property Flow—Temperature Solution

For constant properties, the energy equation is uncoupled from the flow equations. Neglecting viscous dissipation (which may readily be included if desired), the energy equation may be written as

$$\rho c_p \left(u \frac{\partial t}{\partial x} + v \frac{\partial t}{\partial y} \right) = k \frac{\partial^2 t}{\partial y^2} \quad (2-14)$$

A number of temperature boundary conditions at the wall are possible. Two commonly employed conditions will be considered here—constant wall temperature or constant wall heat flux. The complete boundary conditions for the problem are

$$t(x, 0) = t_w \quad (\text{constant wall temperature})$$

or

$$-k \left. \frac{\partial t}{\partial y} \right|_{y=0} = q \quad (\text{constant wall heat flux})$$

and

$$t(0, y) = t_\infty$$

$$t(x, \infty) = t_\infty$$

(2-15)

The choice of dimensionless variables is

$$\begin{aligned}
 U &= u/u_0 & X &= \frac{x\mu}{L^2\rho u_0} \\
 V &= \frac{\rho v L}{\mu} & Y &= \frac{y}{L} \\
 T &= \frac{t-t_w}{t_\infty-t_w} \quad (\text{constant wall temperature}) \\
 \text{or} \\
 T &= \frac{k}{qL} (t-t_\infty) \quad (\text{constant heat flux})
 \end{aligned}
 \tag{2-16}$$

Inserting these dimensionless variables into equation (2-14) yields

$$U \frac{\partial T}{\partial X} + V \frac{\partial T}{\partial Y} = \frac{1}{Pr} \frac{\partial^2 T}{\partial Y^2} \tag{2-17a}$$

where

$$Pr = \frac{\mu c_p}{k} \tag{2-17b}$$

In dimensionless form, the boundary conditions (2-15) become

$$\begin{aligned}
 T(X, 0) &= 0 \\
 T(0, Y) &= 1 \\
 T(X, \infty) &= 1
 \end{aligned}
 \left. \vphantom{\begin{aligned} T(X, 0) \\ T(0, Y) \\ T(X, \infty) \end{aligned}} \right\} (\text{constant wall temperature})$$

or

$$\begin{aligned}
 \frac{\partial T}{\partial Y}(X, 0) &= -1 \\
 T(0, Y) &= 0 \\
 T(X, \infty) &= 0
 \end{aligned}
 \left. \vphantom{\begin{aligned} \frac{\partial T}{\partial Y}(X, 0) \\ T(0, Y) \\ T(X, \infty) \end{aligned}} \right\} (\text{constant heat flux})$$

$$\tag{2-18}$$

Since an implicit difference scheme has been used to solve the momentum equation and since it is most desirable to use the same mesh sizes for the temperature solution and not to be limited by stability criteria, an implicit difference scheme is also employed for the energy equation. Equation (2-17a) may be written in difference form as

$$\begin{aligned}
 U_{j,k} \frac{T_{j+1,k} - T_{j,k}}{\Delta X} + V_{j,k} \frac{T_{j+1,k+1} - T_{j+1,k-1}}{2\Delta Y} \\
 = \frac{1}{Pr} \frac{T_{j+1,k+1} - 2T_{j+1,k} + T_{j+1,k-1}}{(\Delta Y)^2}
 \end{aligned} \quad (2-19)$$

This may be rewritten in a more convenient form as

$$\begin{aligned}
 \left[-\frac{V_{j,k}}{2\Delta Y} - \frac{1}{Pr(\Delta Y)^2} \right] T_{j+1,k-1} + \left[\frac{U_{j,k}}{\Delta X} + \frac{2}{Pr(\Delta Y)^2} \right] T_{j+1,k} \\
 + \left[\frac{V_{j,k}}{2\Delta Y} - \frac{1}{Pr(\Delta Y)^2} \right] T_{j+1,k+1} = \frac{U_{j,k} T_{j,k}}{\Delta X}
 \end{aligned} \quad (2-20)$$

The marked similarity of equation (2-20) to the momentum equation difference representation (2-10) can be useful in the writing of a computer program.

The finite difference forms of the boundary conditions (2-18) are obvious except for the gradient condition on the constant heat flux case. A difference form for the gradient which is consistent in truncation error with the energy equation (see appendix B, section B.1) is

$$\left. \frac{\partial T}{\partial Y} \right|_{Y=0} = \frac{-3T_{j+1,0} + 4T_{j+1,1} - T_{j+1,2}}{2(\Delta Y)} = -1 \quad (2-21)$$

where $T_{j+1,0} = T_w$ which for the constant wall heat flux case is unknown. The difference representations of both the basic equation and the boundary conditions must have truncation error of the same order so that accuracy is not lost. Combining representations of one error order for the basic equation and a different error order for the boundary conditions may give results which are less accurate than either representation alone.

The matrix formulation of equation (2-20) written for $k=1(1)n$ with constant wall temperature is

$$\begin{array}{|ccc|} \hline \beta'_1 & \Omega'_1 & \\ \alpha'_2 & \beta'_2 & \Omega'_2 \\ & \text{---} & \text{---} \\ & \text{---} & \text{---} \\ & & \alpha'_{n-1} & \beta'_{n-1} & \Omega'_{n-1} \\ & & \alpha'_n & \beta'_n & \\ \hline \end{array} \times \begin{array}{|c|} \hline T_{j+1,1} \\ T_{j+1,2} \\ T_{j+1,3} \\ \text{---} \\ \text{---} \\ T_{j+1,n-1} \\ T_{j+1,n} \\ \hline \end{array} = \begin{array}{|c|} \hline \phi'_1 - \alpha'_1 \\ \phi'_2 \\ \phi'_3 \\ \text{---} \\ \text{---} \\ \phi'_{n-1} \\ \phi'_n \\ \hline \end{array} \quad (2-22)$$

the next step should be computed next, then the temperature at that step, etc. In this way only one column of velocities and temperatures need be saved at any one time. Of course, the same mesh sizes should be used for the velocity and temperature solutions.

In solving for both the velocity and temperature, it may be found advantageous to employ a fine mesh size near the wall and a coarser one near the free stream. The details of this technique are discussed in appendix D. Usually the velocity solution requires finer mesh sizes near the wall than does the temperature solution so that the velocity solution is the determining factor in the choice of mesh size. An exception is for high Prandtl number fluids, for which the thermal boundary layer becomes very thin. In this case, the temperature solution becomes the determining factor in the choice of mesh size, and even finer mesh sizes are needed than those required for an accurate velocity solution.

2.1.3 Incompressible Constant Property Flow – Heat Transfer Solution

The local Nusselt number is given by

$$Nu_x = \frac{qx}{k(t_w - t_\infty)} \quad (2-25)$$

where q is the local heat flux. In dimensionless form; the local Nusselt number is, for constant wall temperature,

$$Nu_x = \frac{\partial T}{\partial Y} X Re \quad (2-26)$$

where

$$Re = \frac{\rho u_0 L}{\mu}$$

and for constant wall heat flux

$$Nu_x = \frac{1}{T_w} X Re \quad (2-27)$$

The mean Nusselt number is given by

$$Nu_m = \frac{1}{X} \int_0^X Nu_x dX \quad (2-28)$$

Equations (2-26) to (2-28) may now be expressed in finite difference form. For constant wall temperature,

$$Nu_x = \left[\frac{-3T_{j+1,0} + 4T_{j+1,1} - T_{j+1,2}}{2(\Delta Y)} \right] X_{j+1} Re \quad (2-29)$$

and for constant wall heat flux,

$$Nu_x = \frac{X_{j+1}}{T_{j+1,0}} Re \quad (2-30)$$

To find the mean Nusselt number, Simpson's rule (ref. 2) may be used. Since, however, an even number of intervals are required for integration by Simpson's rule, the value of Nu_m can only be obtained at every other step. The mean Nusselt number is given by

$$Nu_m \Big|_{j+1} = \left[\left(Nu_x \Big|_{j-1} + 4Nu_x \Big|_j + Nu_x \Big|_{j+1} \right) \left(\frac{\Delta X}{3} \right) + Nu_m \Big|_{j-1} (X_{j-1}) \right] \left(\frac{1}{X_{j+1}} \right) \quad (2-31)$$

2.1.4 Compressible Flow – Velocity and Temperature Solutions

For the compressible flow case, the equations of momentum and energy are coupled and must be solved simultaneously. The compressible flat plate boundary layer problem has been solved numerically by Mitchel (ref. 3). The formulation given here draws on the work of Mitchel, as well as that of Walker (ref. 4).

The basic equations for the compressible boundary layer are

$$\rho \left(u \frac{\partial u}{\partial x} + v \frac{\partial u}{\partial y} \right) = -\frac{dp}{dx} + \frac{\partial}{\partial y} \left(\mu \frac{\partial u}{\partial y} \right) \quad (2-32)$$

$$\frac{\partial(\rho u)}{\partial x} + \frac{\partial(\rho v)}{\partial y} = 0 \quad (2-33)$$

$$\rho c_p \left(u \frac{\partial t}{\partial x} + v \frac{\partial t}{\partial y} \right) = u \frac{dp}{dx} + \frac{\partial}{\partial y} \left(k \frac{\partial t}{\partial y} \right) + \mu \left(\frac{\partial u}{\partial y} \right)^2 \quad (2-34)$$

$$p = \rho \mathcal{R} t \quad (2-35)$$

The viscosity and thermal conductivity are generally assumed as functions of temperature only. As an example of such functions, the commonly employed power-law relationships will be used here, although of course any desired relationship could be readily substituted. The assumed expressions for viscosity and thermal conductivity are

$$\mu = \mu(t) = \mu_0(t/t_0)^f \quad (2-36)$$

$$k = k(t) = k_0(t/t_0)^g \quad (2-37)$$

where μ_0 and k_0 are the viscosity and thermal conductivity at a reference temperature t_0 .

Equations (2-32) to (2-37) constitute six equations in the six unknowns $u, v, t, \rho, \mu,$ and k .

The boundary conditions on velocity for this problem are

$$\left. \begin{aligned} u(x, 0) &= 0 \\ v(x, 0) &= 0 \\ u(x, \infty) &= u_\infty(x) \\ u(0, y) &= u_\infty(0) \text{ (see appendix F)} \end{aligned} \right\} \quad (2-38)$$

As in the incompressible case, only the commonly considered thermal conditions of constant wall temperature and constant wall heat flux will be used here, although any other temperature boundary conditions can easily be accommodated. For constant wall temperature the boundary conditions are

$$\left. \begin{aligned} t(x, 0) &= t_w \\ t(x, \infty) &= t_\infty(x) \\ t(0, y) &= t_0 = t_\infty(0) \end{aligned} \right\} \quad (2-39)$$

For constant wall heat flux, the temperature boundary conditions are

$$\left. \begin{aligned} -k \frac{\partial t}{\partial y} \Big|_{y=0} &= q \\ t(x, \infty) &= t_\infty(x) \\ t(0, y) &= t_0 = t_\infty(0) \end{aligned} \right\} \quad (2-40)$$

In equations (2-38), (2-39) and (2-40), the values of u_∞ and t_∞ , both of which are functions of x , are presumed known from the inviscid flow solution in the free stream.

The next step in obtaining a numerical solution should be to put the basic equations and boundary conditions in dimensionless form. The dimensionless variables are chosen as

$$\left. \begin{aligned}
 U &= \frac{u}{u_0} & T &= \frac{t}{t_0} \\
 V &= \frac{\rho_0 v L}{\mu_0} & P &= \frac{p}{p_0} \\
 X &= \frac{x \mu_0}{\rho_0 u_0 L^2} & \rho^* &= \frac{\rho}{\rho_0} \\
 Y &= \frac{y}{L} & k^* &= \frac{k}{k_0} \\
 & & \mu^* &= \frac{\mu}{\mu_0}
 \end{aligned} \right\} \quad (2-41)$$

All quantities with subscript 0 are evaluated in the free stream at the leading edge.

When these variables are inserted into equations (2-32) to (2-37), the dimensionless forms of these equations may be written as

$$\rho^* \left(U \frac{\partial U}{\partial X} + V \frac{\partial U}{\partial Y} \right) = -\frac{1}{\gamma M_0^2} \frac{dP}{dX} + \frac{\partial}{\partial Y} \left(\mu^* \frac{\partial U}{\partial Y} \right) \quad (2-42)$$

$$\frac{\partial(\rho^* U)}{\partial X} + \frac{\partial(\rho^* V)}{\partial Y} = 0 \quad (2-43)$$

$$\rho^* \left(U \frac{\partial T}{\partial X} + V \frac{\partial T}{\partial Y} \right) = \frac{\gamma-1}{\gamma} U \frac{dP}{dX} + \frac{1}{Pr} \frac{\partial}{\partial Y} \left(k^* \frac{\partial T}{\partial Y} \right) + (\gamma-1) M_0^2 \mu^* \left(\frac{\partial U}{\partial Y} \right)^2 \quad (2-44)$$

$$P = \rho^* T \quad (2-45)$$

$$\mu^* = T^f \quad (2-46)$$

$$k^* = T^g \quad (2-47)$$

where the free-stream Mach number at the leading edge is $M_0 = u_0 / \sqrt{\gamma \mathcal{R} t_0}$ and the Prandtl number evaluated at the same location is $Pr = \mu_0 c_p / k_0$. Equations (2-42) to (2-47) now constitute a complete set of dimensionless equations.

The boundary conditions may now be written in dimensionless form. The velocity conditions are

$$\left. \begin{aligned} U(X, 0) &= 0 \\ V(X, 0) &= 0 \\ U(X, \infty) &= \frac{u_\infty(X)}{u_0} = U_\infty(X) \\ U(0, Y) &= 1 \end{aligned} \right\} \quad (2-48)$$

For constant wall temperature, the temperature boundary conditions are

$$\left. \begin{aligned} T(X, 0) &= T_w \\ T(X, \infty) &= \frac{t_\infty(X)}{t_0} = T_\infty(X) \\ T(0, Y) &= 1 \end{aligned} \right\} \quad (2-49)$$

For constant heat flux, the temperature conditions become

$$\left. \begin{aligned} -k^* \frac{\partial T}{\partial Y} \Big|_{Y=0} &= \frac{qL}{k_0 t_0} \\ T(X, \infty) &= T_\infty(X) \\ T(0, Y) &= 1 \end{aligned} \right\} \quad (2-50)$$

The basic equations may now be written in finite difference form. An implicit form is chosen. The difference equations are

$$\begin{aligned} \rho_{j,k}^* \left[U_{j,k} \frac{U_{j+1,k} - U_{j,k}}{\Delta X} + V_{j,k} \frac{U_{j+1,k+1} - U_{j+1,k-1}}{2(\Delta Y)} \right] \\ = -\frac{1}{\gamma M_0^2} \frac{P_{j+1} - P_j}{\Delta X} + \mu_{j,k}^* \left[\frac{U_{j+1,k+1} - 2U_{j+1,k} + U_{j+1,k-1}}{(\Delta Y)^2} \right] \\ + \left[\frac{\mu_{j,k+1}^* - \mu_{j,k-1}^*}{2(\Delta Y)} \right] \left[\frac{U_{j+1,k+1} - U_{j+1,k-1}}{2(\Delta Y)} \right] \end{aligned} \quad (2-51)$$

$$\frac{\rho_{j+1,k+1}^* U_{j+1,k+1} - \rho_{j,k+1}^* U_{j,k+1}}{\Delta X} + \frac{\rho_{j+1,k+1}^* V_{j+1,k+1} - \rho_{j+1,k}^* V_{j+1,k}}{\Delta Y} = 0 \quad (2-52)$$

$$\begin{aligned} \rho_{j,k}^* \left[U_{j,k} \frac{T_{j+1,k} - T_{j,k}}{\Delta X} + V_{j,k} \frac{T_{j+1,k+1} - T_{j+1,k-1}}{2(\Delta Y)} \right] \\ = \frac{\gamma - 1}{\gamma} U_{j,k} \frac{P_{j+1} - P_j}{\Delta X} + \frac{1}{Pr} k_{j,k}^* \left[\frac{T_{j+1,k+1} - 2T_{j+1,k} + T_{j+1,k-1}}{(\Delta Y)^2} \right] \end{aligned}$$

$$\begin{aligned}
& + \frac{1}{Pr} \left[\frac{k_{j,k+1}^* - k_{j,k-1}^*}{2(\Delta Y)} \right] \left[\frac{T_{j+1,k+1} - T_{j+1,k-1}}{2(\Delta Y)} \right] \\
& + M_0^2 (\gamma - 1) \mu_{j,k}^* \left[\frac{U_{j+1,k+1} - U_{j+1,k-1}}{2(\Delta Y)} \right]^2 \quad (2-53)
\end{aligned}$$

$$\rho_{j+1,k}^* = \frac{P_{j+1}}{T_{j+1,k}} \quad (2-54)$$

$$\mu_{j+1,k}^* = (T_{j+1,k})^f \quad (2-55)$$

$$k_{j+1,k}^* = (T_{j+1,k})^g \quad (2-56)$$

This finite difference representation presents distinct advantages in that all equations are linear in the various unknowns. Thus at each step the equations represented by equation (2-51) may be solved for the values of $U_{j+1,k}$, then equation (2-53) for the values of $T_{j+1,k}$, equation (2-54) for $\rho_{j+1,k}^*$, equation (2-52) for $V_{j+1,k}$, and finally equations (2-55) and (2-56) for $\mu_{j+1,k}^*$, and $k_{j+1,k}^*$.

Before this solution can be carried out, it is necessary to express the boundary conditions in finite difference form. The only condition which it is necessary to discuss here is the heat flux condition in (2-50), which may be represented as

$$k_{j,0}^* \left[\frac{-3T_{j+1,0} + 4T_{j+1,1} - T_{j+1,2}}{2(\Delta Y)} \right] = \frac{-q_0 L}{k_{ot0}} \quad (2-57)$$

The method of solution for the basic equations may now be presented.

The momentum equation (eq. (2-51)) may be rewritten in a more convenient form as

$$\begin{aligned}
& \left[\frac{-\rho_{j,k}^* V_{j,k}}{2(\Delta Y)} - \frac{\mu_{j,k}^*}{(\Delta Y)^2} + \frac{\mu_{j,k+1}^* - \mu_{j,k-1}^*}{4(\Delta Y)^2} \right] U_{j+1,k-1} \\
& + \left[\frac{\rho_{j,k}^* U_{j,k}}{\Delta X} + \frac{2\mu_{j,k}^*}{(\Delta Y)^2} \right] U_{j+1,k} \\
& + \left[\frac{\rho_{j,k}^* V_{j,k}}{2(\Delta Y)} - \frac{\mu_{j,k}^*}{(\Delta Y)^2} - \frac{\mu_{j,k+1}^* - \mu_{j,k-1}^*}{4(\Delta Y)^2} \right] U_{j+1,k+1} \\
& = \frac{\rho_{j,k}^* U_{j,k}^2}{\Delta X} - \frac{1}{\gamma M_0^2} \frac{P_{j+1} - P_j}{\Delta X} \quad (2-58)
\end{aligned}$$

$$\rho_{j+1,k}^* = \frac{P_{j+1}}{T_{j+1,k}} \quad (2-62)$$

Next the continuity equation (eq. (2-52)) may be solved for the transverse velocities yielding

$$V_{j+1,k+1} = \left(\frac{\rho_{j+1,k}^*}{\rho_{j+1,k+1}^*} \right) V_{j+1,k} + \frac{\Delta Y}{\Delta X} \left[\left(\frac{\rho_{j,k+1}^*}{\rho_{j+1,k+1}^*} \right) U_{j,k+1} - U_{j+1,k+1} \right] \quad (2-63)$$

This solution is started at the plate ($Y=0$) where $V_{j+1,0}=0$ and marched out to the free stream.

Finally, the dimensionless viscosity and thermal conductivity are found from equations (2-55) and (2-56):

$$\mu_{j+1,k}^* = (T_{j+1,k})^f \quad (2-64)$$

$$k_{j+1,k}^* = (T_{j+1,k})^g \quad (2-65)$$

This solution at $j+1$ is now complete and the solution may be advanced another step downstream. The process may be continued as far as desired.

The truncation error for both the momentum and energy equations is of $\mathcal{O}(\Delta Y^2)$ and $\mathcal{O}(\Delta X)$. For continuity the truncation error is of $\mathcal{O}(\Delta X)$ and $\mathcal{O}(\Delta Y)$.

The difference representation given here is stable for all mesh sizes so long as $U \geq 0$.

2.1.5 Compressible Flow—Nonlinear Finite Difference Representation

Many finite difference representations of the momentum and energy equations are possible, including a number which are not linear in the unknowns. These nonlinear representations, such as those used by Walker (ref. 4), must be solved iteratively, but their advantage is a possibly more accurate influence of the variable properties on the solution (i.e., a possible use of larger mesh sizes). Except for the use of the iterative method, the solution for these representations is quite similar to that used for the linear difference equations. As an example, consider the following possible representations of the momentum equation (2-42) and the energy equation (2-44). The momentum equation may be written as

$$\rho_{j,k}^* \left[U_{j,k} \frac{U_{j+1,k} - U_{j,k}}{\Delta X} + V_{j,k} \frac{U_{j+1,k+1} - U_{j+1,k-1}}{2(\Delta Y)} \right] =$$

$$\begin{aligned}
&= -\frac{1}{\gamma M_0^2} \frac{P_{j+1} - P_j}{\Delta X} + \mu_{j+1,k}^* \left[\frac{U_{j+1,k+1} - 2U_{j+1,k} + U_{j+1,k-1}}{(\Delta Y)^2} \right] \\
&\quad + \left[\frac{\mu_{j+1,k+1}^* - \mu_{j+1,k-1}^*}{2(\Delta Y)} \right] \left[\frac{U_{j+1,k+1} - U_{j+1,k-1}}{2(\Delta Y)} \right] \quad (2-66)
\end{aligned}$$

And the energy equation becomes

$$\begin{aligned}
&\rho_{j,k}^* \left[U_{j,k} \frac{T_{j+1,k} - T_{j,k}}{\Delta X} + V_{j,k} \frac{T_{j+1,k+1} - T_{j+1,k-1}}{2(\Delta Y)} \right] \\
&= \frac{\gamma - 1}{\gamma} U_{j,k} \frac{P_{j+1} - P_j}{\Delta X} + \frac{1}{Pr} k_{j+1,k}^* \left[\frac{T_{j+1,k+1} - 2T_{j+1,k} + T_{j+1,k-1}}{(\Delta Y)^2} \right] \\
&\quad + \frac{1}{Pr} \left[\frac{k_{j+1,k+1}^* - k_{j+1,k-1}^*}{2(\Delta Y)} \right] \left[\frac{T_{j+1,k+1} - T_{j+1,k-1}}{2(\Delta Y)} \right] \\
&\quad + M_0^2 (\gamma - 1) \mu_{j+1,k}^* \left[\frac{U_{j+1,k+1} - U_{j+1,k-1}}{2(\Delta Y)} \right]^2 \quad (2-67)
\end{aligned}$$

The viscous term in equation (2-66) and the conduction term in equation (2-67) have been represented by using the dimensionless viscosity and thermal conductivity at the unknown $(j+1)$ position. Since $\mu_{j+1,k}^*$ is a function of temperature, equation (2-66) cannot be solved directly for the $U_{j+1,k}$ values, and since $k_{j+1,k}^*$ is also a function of temperature and appears in equation (2-67), this equation is no longer linear in $T_{j+1,k}$. However, a straightforward procedure is simply to guess values for $\mu_{j+1,k}^*$ and $k_{j+1,k}^*$ (probably the values from the last column). The properties are then considered as known and equations (2-66) and (2-67) may be solved in exactly the same manner as in the previous section for $U_{j+1,k}$ and $T_{j+1,k}$. The property relations are then re-evaluated using the new values of $T_{j+1,k}$ and the process repeated until the values of $U_{j+1,k}$ and $T_{j+1,k}$ agree with those obtained on the previous iteration to any desired degree of accuracy. In general, only a few iterations (less than 10) will be required to give good accuracy. The values of $V_{j+1,k}$ can now be determined from continuity, equation (2-63), and another step taken downstream. The procedure may be continued as far downstream as desired.

2.1.6 Compressible Flow—Heat Transfer Solution

The heat transfer solution is identical to that for the incompressible case (section 2.1.3) except that $k_{j,0}^*$ will appear in the heat flux expression.

2.2 AXISYMMETRIC BOUNDARY LAYERS

For axial flow and heat transfer along a body of revolution, approximations to the basic equations of momentum, continuity, and energy result in two different sets of equations of the boundary layer type. These two sets of equations correspond to two different physical situations. In one case the body has a radius of the order of the boundary layer thickness (i.e., a slender body) and in the other case the radius of the body is large compared to the boundary layer thickness. In both cases it is assumed that there are no steep variations of radius with axial distance.

For the large radius case, transverse curvature may be neglected in the momentum and energy equations and the equations are quite similar to those for two-dimensional flow. This led Mangler (ref. 5) to develop a transformation which maps the axisymmetric problem into an equivalent two-dimensional problem. Since we have already discussed two-dimensional boundary layer solutions, the large radius solution will be considered as formulated and we shall not discuss it further. It should be noted that for compressible flow the Mangler transformation is only valid for perfect gases and constant specific heats.

The formulation for the slender body will be of value for several reasons. The formulation is valid not only for slender bodies but also for axial flow along a circular cylinder of constant radius of any size and includes the transverse curvature effects which are of considerable interest (refs. 6 to 8). In addition, the difference equations derived here will also be valid for the axisymmetric jet with moving secondary which will be discussed in chapter 3.

The problem configuration and coordinate system are shown in figure 2-3. The inviscid flow solution around the body is assumed known, giving u_∞ , t_∞ , and dp/dz . The free stream velocity far upstream from the body is u_0 . Within the limitations of the assumptions (slender body, only small variations in radius) it is adequate to consider the coordinate system as the r, z -system rather than going to a curvilinear coordinate system in which the coordinates are normal and tangential to the surface of the body. Depending on the nose shape, the formulation given here may not be valid close to the nose of the body.

2.2.1 Incompressible Constant Property Flow—Velocity Solution

The equations of motion for the constant property incompressible flow problem are

$$\rho \left(u \frac{\partial u}{\partial z} + v \frac{\partial u}{\partial r} \right) = - \frac{dp}{dz} + \mu \left(\frac{1}{r} \frac{\partial u}{\partial r} + \frac{\partial^2 u}{\partial r^2} \right) \quad (2-68)$$

$$\frac{\partial u}{\partial z} + \frac{1}{r} \frac{\partial (vr)}{\partial r} = 0 \quad (2-69)$$

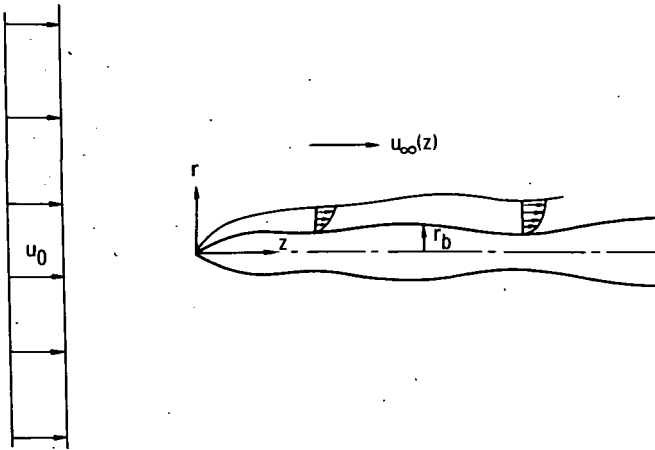


FIGURE 2-3.— Configuration for boundary layer flow on slender axisymmetric body.

The boundary conditions for the problem are

$$\left. \begin{aligned}
 u(r_b, z) &= 0 \\
 u(\infty, z) &= u_\infty(z) \\
 v(r_b, z) &= 0 \\
 u(r, 0) &= u_\infty(0) \text{ (see appendix F)}
 \end{aligned} \right\} \quad (2-70)$$

The problem must now be restated in dimensionless form. This can be accomplished by the following choice of dimensionless variables:

$$\left. \begin{aligned}
 U &= \frac{u}{u_0} & Z &= \frac{z\mu}{\rho u_0 a^2} \\
 V &= \frac{\rho v a}{\mu} & R &= \frac{r}{a} \\
 P &= \frac{p - p_0}{\rho u_0^2} & R_b &= \frac{r_b}{a}
 \end{aligned} \right\} \quad (2-71)$$

In equations (2-71), a is a characteristic value of the radius.

When these dimensionless variables are used, equations (2-68) and (2-69) become

$$U \frac{\partial U}{\partial Z} + V \frac{\partial U}{\partial R} = -\frac{dP}{dZ} + \frac{1}{R} \frac{\partial U}{\partial R} + \frac{\partial^2 U}{\partial R^2} \quad (2-72)$$

$$\frac{\partial U}{\partial Z} + \frac{1}{R} \frac{\partial (VR)}{\partial R} = 0 \quad (2-73)$$

The boundary conditions in dimensionless form are

$$\left. \begin{aligned} U(R_b, Z) &= 0 \\ U(\infty, Z) &= \frac{u_\infty(Z)}{u_0} = U_\infty(Z) \\ V(R_b, Z) &= 0 \\ U(R, 0) &= \frac{u_\infty(0)}{u_0} = U_\infty(0) \end{aligned} \right\} \quad (2-74)$$

A finite difference grid is now imposed on the flow field. This grid is shown in figure 2-4 for the case of a cylindrical body ($R_b = \text{a constant}$) with $k=0$ at the surface of the body. Variations in R_b introduce certain computational difficulties which will be dealt with later. Equations (2-72) and (2-73) may now be expressed in finite difference form as

$$\begin{aligned} U_{j,k} \frac{U_{j+1,k} - U_{j,k}}{\Delta Z} + V_{j,k} \frac{U_{j+1,k+1} - U_{j+1,k-1}}{2(\Delta R)} \\ = -\frac{P_{j+1} - P_j}{\Delta Z} + \frac{1}{R_k} \frac{U_{j+1,k+1} - U_{j+1,k-1}}{2(\Delta R)} \\ + \frac{U_{j+1,k+1} - 2U_{j+1,k} + U_{j+1,k-1}}{(\Delta R)^2} \end{aligned} \quad (2-75)$$

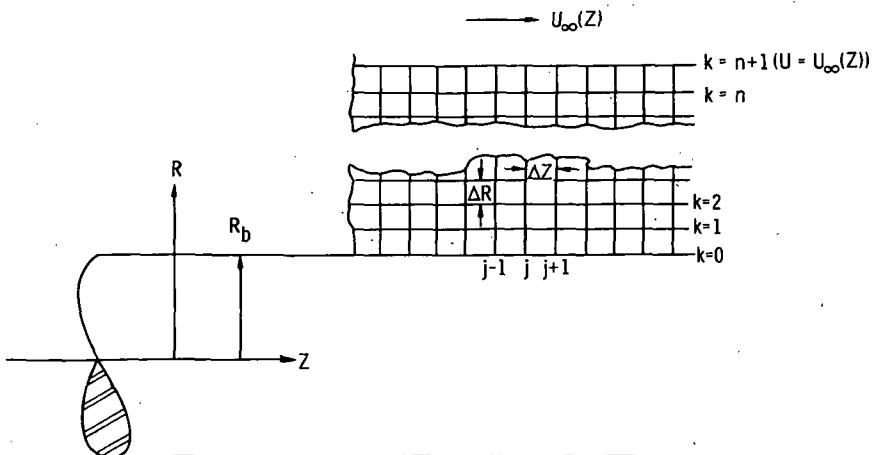


FIGURE 2-4. — Finite difference grid for constant radius cylinder.

The matrix of coefficients in equation (2-78) is tridiagonal and the method of appendix A may be applied to solve for the values $U_{j+1,k}$.

The continuity equation (eq. (2-76)) may now be solved for $V_{j+1,k+1}$ to yield:

$$V_{j+1,k+1} = V_{j+1,k} \left(\frac{R_k}{R_{k+1}} \right) - \frac{\Delta R}{\Delta Z} \frac{R_k}{R_{k+1}} (U_{j+1,k+1} - U_{j,k+1}) \quad (2-79)$$

Since $V_{j+1,0} = 0$, this equation may be solved in a stepwise manner from $k=0$ (the surface of the body) and marched out into the free stream, obtaining a value of $V_{j+1,k+1}$ for each k .

The solution may now be advanced downstream one ΔZ and the previous process repeated. In this manner the solution may be carried as far downstream as desired.

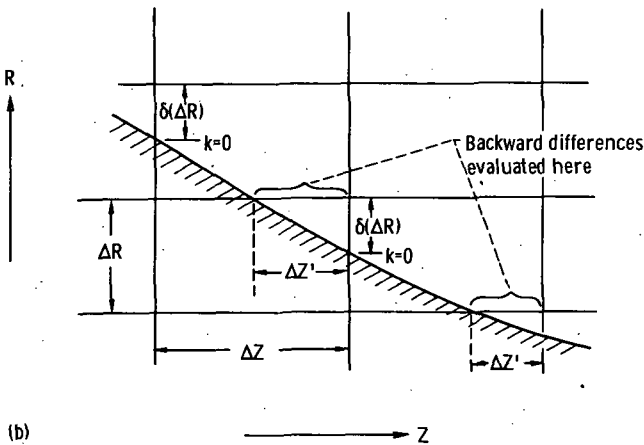
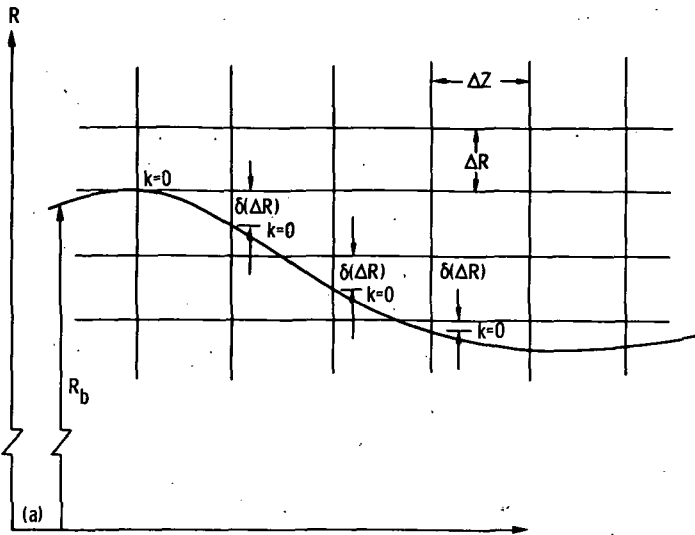
The variation of the radius of the body with Z may slightly complicate the orderly advancement of the solution downstream. If R_b varies with Z , and at the axial station j the surface of the body is set on a mesh point, then at station $j+1$ the surface will not fall on a mesh point for arbitrary ΔZ . One possible solution is to transform to a coordinate system in which R_b does not appear to vary, but this is difficult to generalize, and the viewpoint taken in this report is to solve the basic equations directly without recourse to transformations.

The method for accommodating R_b variations with Z which seems to best combine accuracy and simplicity is to let the surface of the body fall on the mesh where it may and call this point $k=0$. Then at $k=1$, the first mesh point above the surface, the difference equations must be slightly modified to account for the fact that the space between this point and the surface is only a fraction of a full ΔR (see fig. 2-5). The method for doing this is identical to that for changing to a different mesh size in a field and is discussed in detail in appendix D. The only modifications to the matrix equation (2-78) are in β_1 and Ω_1 , and these become

$$\beta_1 = \frac{U_{j,1}}{\Delta Z} + \left[V_{j,1} - \frac{1}{\delta(\Delta R)} \right] \left[\frac{1-\delta}{\delta(\Delta R)} \right] + \frac{2}{\delta(\Delta R)^2} \quad (2-80)$$

$$\Omega_1 = \left[\frac{V_{j,1}}{\Delta R} - \frac{1}{\delta(\Delta R)^2} \right] \left(\frac{\delta}{1+\delta} \right) - \frac{2}{(\Delta R)^2} \left(\frac{1}{1+\delta} \right) \quad (2-81)$$

where δ is the fraction of a full ΔR mesh space from the surface to the first mesh point above it. The only modification necessary to continuity (eq. (2-79)) is to use $\delta(\Delta R)$ in place of ΔR for $k=0$. Note that the $k=0$ point may shift as the radius changes. Care must be taken to incorporate this shift in k in the values in the j th column—for example, what was $V_{j,k}$ before may be $V_{j,k+1}$ now in reference to the new origin for $k=0$.



(a) Overall view of mesh configurations.

(b) Enlarged view of body surface crossing horizontal grid lines.

FIGURE 2-5. — Mesh configurations for slender body of varying radius.

Another problem becomes evident if the body is decreasing in size with increasing Z and the body surface crosses a horizontal grid line as occurs at two points in figure 2-5(a). In this case, the backward differences may be evaluated by employing $\Delta Z'$ instead of ΔZ as shown in the enlarged view in figure 2-5(b), and by using the values of the variables at the surface of the body for $U_{j,1}$ and $V_{j,1}$ (both are of course zero).

As in all external flows, the thickness of the boundary layer will determine where the edge of the numerical field should be and how many points are required. This was discussed in detail in the flat plate boundary layer formulation (section 2.1.1).

The solution will be stable for all $U \geq 0$. For $U < 0$, it is necessary that

$$\frac{\Delta Z}{|U|(\Delta R)^2} \geq \frac{1}{2} \quad (2-82)$$

and

$$\left| V - \frac{1}{R_k} \right| \geq \sqrt{\frac{2|U|}{\Delta Z}} \quad (2-83)$$

These stability criteria were obtained by Hornbeck (ref. 9).

The truncation error of the momentum equation is of $\mathcal{O}(\Delta Z)$ and $\mathcal{O}(\Delta R^2)$. For continuity the truncation error is of $\mathcal{O}(\Delta Z)$ and $\mathcal{O}(\Delta R)$.

2.2.2 Incompressible Constant Property Flow—Temperature Solution

The energy equation corresponding to the slender body assumption is

$$\rho c_p \left(u \frac{\partial t}{\partial z} + v \frac{\partial t}{\partial r} \right) = k \left(\frac{\partial^2 t}{\partial r^2} + \frac{1}{r} \frac{\partial t}{\partial r} \right) \quad (2-84)$$

As in the flat plate case, only the common temperature boundary conditions of constant surface temperature or constant surface heat flux will be considered here. However, any other conditions may be readily substituted. The boundary conditions are

$$\left. \begin{aligned} & t(r_b, z) = t_w \quad (\text{constant surface temperature}) \\ \text{or} & \\ & -k \frac{\partial t}{\partial r} \Big|_{r=r_b} = q \quad (\text{constant surface heat flux}) \\ \text{and} & \\ & t(\infty, z) = t_\infty(z) \\ & t(r, 0) = t_\infty(0) \end{aligned} \right\} \quad (2-85)$$

The following dimensionless variables may now be defined:

$$\begin{aligned}
 U &= u/u_0 & Z &= \frac{z\mu}{a^2\rho u_0} \\
 V &= \frac{\rho va}{\mu} & R &= r/a \\
 T &= \frac{t-t_w}{t_x-t_w} \quad (\text{constant surface temperature}) \\
 \text{or} \\
 T &= \frac{k}{qa} (t-t_x) \quad (\text{constant heat flux})
 \end{aligned} \tag{2-86}$$

Equation (2-84) in dimensionless form becomes

$$U \frac{\partial T}{\partial Z} + V \frac{\partial T}{\partial R} = \frac{1}{Pr} \left(\frac{\partial^2 T}{\partial R^2} + \frac{1}{R} \frac{\partial T}{\partial R} \right) \tag{2-87}$$

and the boundary conditions written in dimensionless form are

$$\begin{aligned}
 & \left. \begin{aligned}
 T(R_b, Z) &= 0 \\
 T(R, 0) &= 1 \\
 T(\infty, Z) &= 1
 \end{aligned} \right\} (\text{constant surface temperature}) \\
 \text{or} \\
 & \left. \begin{aligned}
 \frac{\partial T}{\partial R}(R_b, Z) &= -1 \\
 T(R, 0) &= 0 \\
 T(\infty, Z) &= 0
 \end{aligned} \right\} (\text{constant wall heat flux})
 \end{aligned} \tag{2-88}$$

Equation (2-87) may be written in finite difference form as

$$\begin{aligned}
 U_{j,k} \frac{T_{j+1,k} - T_{j,k}}{\Delta Z} + V_{j,k} \frac{T_{j+1,k+1} - T_{j+1,k-1}}{2(\Delta R)} \\
 = \frac{1}{Pr} \left\{ \frac{T_{j+1,k+1} - 2T_{j+1,k} + T_{j+1,k-1}}{(\Delta R)^2} + \frac{1}{R_k} \left[\frac{T_{j+1,k+1} - T_{j+1,k-1}}{2(\Delta R)} \right] \right\} \tag{2-89}
 \end{aligned}$$

This may be rewritten in a more useful form as

If the method discussed in the velocity solution section to allow for R_b variations with Z is used, then β'_1 and Ω'_1 must be modified to become

$$\beta'_1 = \frac{U_{j,1}}{\Delta Z} + \left[V_{j,1} - \frac{1}{Pr(\delta)(\Delta R)} \right] \left[\frac{1-\delta}{\delta(\Delta R)} \right] + \frac{2}{\delta(Pr)(\Delta R)^2} \quad (2-93)$$

$$\Omega'_1 = \left[\frac{V_{j,1}}{\Delta R} - \frac{1}{Pr(\delta)(\Delta R)^2} \right] \left(\frac{\delta}{1+\delta} \right) - \frac{2}{Pr(\Delta R)^2} \left(\frac{1}{1+\delta} \right) \quad (2-94)$$

The matrix of coefficients in equation (2-92) is tridiagonal, and the method of appendix A may be applied to solve for $T_{j+1,k}$ at each step downstream.

For the constant heat flux case, α'_1 also appears and is given by

$$\alpha'_1 = \frac{-2}{\delta(Pr)(1+\delta)(\Delta R)^2} - \left(V_{j,1} - \frac{1}{Pr(\delta)(\Delta R)} \right) \left(\frac{1}{\delta(1+\delta)(\Delta R)} \right) \quad (2-95)$$

The heat flux expression (2-91) becomes

$$\left. \frac{\partial T}{\partial R} \right|_{R=R_b} = \frac{-(1+2\delta)T_{j+1,0} + (1+\delta)^2 T_{j+1,1} - (\delta)^2 T_{j+1,2}}{\delta(1+\delta)\Delta R} = -1 \quad (2-96)$$

As in the velocity solution, if the body surface crosses horizontal grid lines as shown in figure 2-5(b), then $\Delta Z'$ may be employed in evaluating the backward differences and $U_{j,1}$, $V_{j,1}$, and $T_{j,1}$ are evaluated at the surface of the body. The quantities $U_{j,1}$ and $V_{j,1}$ are zero, and $T_{j,1}$ will be known for the constant wall temperature case and may be found by linear extrapolation of the surface temperatures at the two preceding axial steps for the constant wall heat flux case.

The temperature formulation for the axisymmetric boundary layer problem is universally stable. The truncation error of the finite difference representation is of $\mathcal{O}(\Delta Z)$ and $\mathcal{O}(\Delta R)^2$.

2.2.3 Incompressible Constant Property Flow—Heat Transfer Solution

The heat transfer solution for the slender body of revolution is identical to that for the flat plate (section 2.1.3) except that the characteristic length L is replaced by the characteristic radius a .

2.2.4 Compressible Flow—Velocity and Temperature Solutions

As in the two-dimensional case, a perfect gas has been assumed and the viscosity and thermal conductivity relations have been assumed as a simple power law. These relations between properties are for illustrative purposes only and any

other relationships may be substituted. The coupled fundamental equations for the compressible flow—slender body case are

$$\rho \left(u \frac{\partial u}{\partial z} + v \frac{\partial u}{\partial r} \right) = - \frac{dp}{dz} + \frac{1}{r} \frac{\partial}{\partial r} \left(\mu r \frac{\partial u}{\partial r} \right) \quad (2-97)$$

$$\frac{\partial(\rho u)}{\partial z} + \frac{1}{r} \frac{\partial(\rho r v)}{\partial r} = 0 \quad (2-98)$$

$$\rho c_p \left(u \frac{\partial t}{\partial z} + v \frac{\partial t}{\partial r} \right) = u \frac{dp}{dz} + \frac{1}{r} \frac{\partial}{\partial r} \left(kr \frac{\partial t}{\partial r} \right) + \mu \left(\frac{\partial u}{\partial r} \right)^2 \quad (2-99)$$

$$p = \rho \mathcal{R} t \quad (2-100)$$

$$\mu = \mu(t) = \mu_0 (t/t_0)^f \quad (2-101)$$

$$k = k(t) = k_0 (t/t_0)^g \quad (2-102)$$

The velocity boundary conditions are assumed to be

$$\left. \begin{aligned} u(r_b, z) &= 0 \\ v(r_b, z) &= 0 \\ u(r, 0) &= u_\infty(0) \quad (\text{see appendix F}) \\ u(\infty, z) &= u_\infty(z) \end{aligned} \right\} \quad (2-103)$$

As examples of typical temperature boundary conditions, constant surface temperature and constant surface heat flux will be considered here. For constant surface temperature the boundary conditions are

$$\left. \begin{aligned} t(r_b, z) &= t_w \\ t(r, 0) &= t_\infty(0) \\ t(\infty, z) &= t_\infty(z) \end{aligned} \right\} \quad (2-104)$$

and for constant heat flux,

$$\left. \begin{aligned} -k \frac{\partial t}{\partial r} \Big|_{r=r_b} &= q \\ t(r, 0) &= t_\infty(0) \\ t(\infty, z) &= t_\infty(z) \end{aligned} \right\} \quad (2-105)$$

The dimensionless variables which seem to offer the most advantages are

$$\left. \begin{aligned} U &= \frac{u}{u_0} & Z &= \frac{z\mu_0}{\rho_0 u_0 a^2} \\ V &= \frac{\rho_0 v a}{\mu_0} & R &= \frac{r}{a} \quad \left(R_b = \frac{r_b}{a} \right) \\ T &= \frac{t}{t_0} & k^* &= \frac{k}{k_0} \\ P &= \frac{p}{p_0} & \mu^* &= \frac{\mu}{\mu_0} \\ & & \rho^* &= \frac{\rho}{\rho_0} \end{aligned} \right\} \quad (2-106)$$

If these variables are used, equations (2-97) to (2-102) may be written as

$$\rho^* \left(U \frac{\partial U}{\partial Z} + V \frac{\partial U}{\partial R} \right) = -\frac{1}{\gamma M_0^2} \frac{dP}{dZ} + \frac{1}{R} \frac{\partial}{\partial R} \left(\mu^* R \frac{\partial U}{\partial R} \right) \quad (2-107)$$

$$\frac{\partial(\rho^* U)}{\partial Z} + \frac{1}{R} \frac{\partial(\rho^* R V)}{\partial R} = 0 \quad (2-108)$$

$$\begin{aligned} \rho^* \left(U \frac{\partial T}{\partial Z} + V \frac{\partial T}{\partial R} \right) &= \frac{\gamma-1}{\gamma} U \frac{dP}{dZ} + \frac{1}{(Pr)R} \frac{\partial}{\partial R} \left(k^* R \frac{\partial T}{\partial R} \right) \\ &+ (\gamma-1) M_0^2 \mu^* \left(\frac{\partial U}{\partial R} \right)^2 \end{aligned} \quad (2-109)$$

$$P = \rho^* T \quad (2-110)$$

$$\mu^* = (T)^f \quad (2-111)$$

$$k^* = (T)^g \quad (2-112)$$

where the Mach number evaluated at t_0 is $M_0 = u_0 / \sqrt{\gamma \mathcal{R} t_0}$, and the Prandtl number evaluated at t_0 is $Pr = \mu_0 c_p / k_0$.

The boundary conditions on velocity in dimensionless form are

$$\left. \begin{aligned} U(R_b, Z) &= 0 \\ V(R_b, Z) &= 0 \\ U(\infty, Z) &= u_\infty(Z) / u_0 = U_\infty(Z) \\ U(R, 0) &= U_\infty(0) / u_0 = U_\infty(0) \end{aligned} \right\} \quad (2-113)$$

and those on temperature for constant surface temperature are

$$\left. \begin{aligned} T(R, 0) &= 1 \\ T(\infty, Z) &= t_\infty(Z)/t_0 = T_\infty(Z) \\ T(R_b, Z) &= t_w/t_0 = T_w \end{aligned} \right\} \quad (2-114)$$

or for constant heat flux

$$\left. \begin{aligned} T(R, 0) &= 1 \\ T(\infty, Z) &= t_\infty(Z)/t_0 = T_\infty(Z) \\ -k^* \frac{\partial T}{\partial R} \Big|_{R=R_b} &= \frac{qa}{k_0 t_0} \end{aligned} \right\} \quad (2-115)$$

Equations (2-107) to (2-112) may now be written in difference form. An implicit representation is used for momentum and energy and all representations are chosen in such a way as to make all difference equations linear in the various unknowns. The difference representations of equations (2-107) to (2-112) are

$$\begin{aligned} &\rho_{j,k}^* \left(U_{j,k} \frac{U_{j+1,k} - U_{j,k}}{\Delta Z} + V_{j,k} \frac{U_{j+1,k+1} - U_{j+1,k-1}}{2\Delta R} \right) \\ &= -\frac{1}{\gamma M_0^2} \frac{P_{j+1} - P_j}{\Delta Z} + \mu_{j,k}^* \left[\frac{U_{j+1,k+1} - 2U_{j+1,k} + U_{j+1,k-1}}{(\Delta R)^2} \right. \\ &\quad \left. + \frac{1}{R_k} \frac{U_{j+1,k+1} - U_{j+1,k-1}}{2\Delta R} \right] \\ &\quad + \left[\frac{\mu_{j,k+1}^* - \mu_{j,k-1}^*}{2(\Delta R)} \right] \left[\frac{U_{j+1,k+1} - U_{j+1,k-1}}{2(\Delta R)} \right] \end{aligned} \quad (2-116)$$

$$\frac{\rho_{j+1,k}^* U_{j+1,k} - \rho_{j,k}^* U_{j,k}}{\Delta Z} + \frac{\rho_{j+1,k+1}^* R_{k+1} V_{j+1,k+1} - \rho_{j+1,k}^* R_k V_{j+1,k}}{R_k (\Delta R)} = 0 \quad (2-117)$$

$$\begin{aligned} &\rho_{j,k}^* \left[U_{j,k} \frac{T_{j+1,k} - T_{j,k}}{\Delta Z} + V_{j,k} \frac{T_{j+1,k+1} - T_{j+1,k-1}}{2(\Delta R)} \right] = \frac{\gamma - 1}{\gamma} U_{j,k} \frac{P_{j+1} - P_j}{\Delta Z} \\ &\quad + \frac{1}{Pr} \left\{ k_{j,k}^* \left[\frac{T_{j+1,k+1} - 2T_{j+1,k} + T_{j+1,k-1}}{(\Delta R)^2} + \frac{1}{R_k} \frac{T_{j+1,k+1} - T_{j+1,k-1}}{2(\Delta R)} \right] + \right. \end{aligned}$$

$$\begin{aligned}
& + \left[\frac{k_{j,k+1}^* - k_{j,k-1}^*}{2(\Delta R)} \right] \left[\frac{T_{j+1,k+1} - T_{j+1,k-1}}{2(\Delta R)} \right] \\
& + (\gamma - 1) M_0^2 \mu_{j,k}^* \left[\frac{U_{j+1,k+1} - U_{j+1,k-1}}{2(\Delta R)} \right]^2 \quad (2-118)
\end{aligned}$$

$$\rho_{j+1,k}^* = \frac{P_{j+1}}{T_{j+1,k}} \quad (2-119)$$

$$\mu_{j+1,k}^* = (T_{j+1,k})^f \quad (2-120)$$

$$k_{j+1,k}^* = (T_{j+1,k})^g \quad (2-121)$$

As in the two-dimensional case discussed in section 2.1.4, these equations may be solved successively in the following order which essentially decouples them: equation (2-116) for the $U_{j+1,k}$'s, equation (2-118) for the $T_{j+1,k}$'s, equation (2-119) for the $\rho_{j+1,k}$'s, equation (2-117) for the $V_{j+1,k}$'s and finally equations (2-120) and (2-121) for $\mu_{j+1,k}^*$ and $k_{j+1,k}^*$.

The only boundary condition for which the finite difference form need be discussed is the heat flux condition in equation (2-115). This may be represented by

$$k_{j,0}^* \left[\frac{-3T_{j+1,0} + 4T_{j+1,1} - T_{j+1,2}}{2(\Delta R)} \right] = \frac{-qa}{k_0 t_0} \quad (2-122)$$

The relation (2-122) must be solved simultaneously with the energy equation (2-118).

Equation (2-116) may be rewritten in a more useful form as

$$\begin{aligned}
& \left[\frac{-\rho_{j,k}^* V_{j,k}}{2(\Delta R)} - \frac{\mu_{j,k}^*}{(\Delta R)^2} + \frac{\mu_{j,k}^*}{2(R_k)\Delta R} + \frac{\mu_{j,k+1}^* - \mu_{j,k-1}^*}{4(\Delta R)^2} \right] U_{j+1,k-1} \\
& + \left[\frac{\rho_{j,k}^* U_{j,k}}{\Delta Z} + \frac{2\mu_{j,k}^*}{(\Delta R)^2} \right] U_{j+1,k} + \left[\frac{\rho_{j,k}^* V_{j,k}}{2(\Delta R)} - \frac{\mu_{j,k}^*}{(\Delta R)^2} - \frac{\mu_{j,k}^*}{2(R_k)\Delta R} \right. \\
& \left. - \frac{\mu_{j,k+1}^* - \mu_{j,k-1}^*}{4(\Delta R)^2} \right] U_{j+1,k+1} = -\frac{1}{\gamma M_0^2} \frac{P_{j+1} - P_j}{\Delta Z} + \frac{\rho_{j,k}^* U_{j,k}^2}{\Delta Z} \quad (2-123)
\end{aligned}$$

Equation (2-123), written for $k=1(1)n$, now constitutes a complete set of equations for the values of $U_{j+1,k}$. This set may be written in matrix form as

$$V_{j+1,k+1} = \frac{\rho_{j+1,k}^* R_k}{\rho_{j+1,k+1}^* R_{k+1}} V_{j+1,k} + \left(\frac{\Delta R}{\Delta Z} \right) \frac{R_k}{\rho_{j+1,k+1}^* R_{k+1}} (\rho_{j,k}^* U_{j,k} - \rho_{j+1,k}^* U_{j+1,k}) \quad (2-127)$$

Equation (2-127) may be marched outward from the surface ($k = 0$) to give all values of $V_{j+1,k+1}$.

Finally, equations (2-120) and (2-121) can be solved for $\mu_{j+1,k}^*$ and $k_{j+1,k}^*$.

If R_b is a function of Z , then the difficulty of the surface not falling exactly on a mesh point will be encountered. The method of attack applied here is the same as that described in section 2.2.1 for the incompressible case. The matrix equations (2-124) and (2-126) must be modified to account for the partial grid space at the surface. As before, δ is the fraction of the grid space adjacent to the surface. The modifications are, for equation (2-124),

$$\beta_1 = \frac{\rho_{j,1}^* U_{j,1}}{\Delta Z} + \frac{\rho_{j,1}^* V_{j,1}(1-\delta)}{\delta(\Delta R)} + \frac{2\mu_{j,1}^*}{\delta(\Delta R)^2} - \frac{(1-\delta)\mu_{j,1}^*}{\delta^2(\Delta R)^2} - \frac{(\mu_{j,q}^* - \mu_{j,0}^*)(1-\delta)}{2\delta^2(\Delta R)^2} \quad (2-128)$$

$$\Omega_1 = \frac{\rho_{j,1}^* V_{j,1}\delta}{(1+\delta)(\Delta R)} - \frac{3\mu_{j,1}^*}{(1+\delta)(\Delta R)^2} - \frac{(\mu_{j,q}^* - \mu_{j,0}^*)}{2(1+\delta)(\Delta R)^2} \quad (2-129)$$

where

$$\mu_{j,q}^* = \mu_{j,0}^* \left(\frac{\delta-1}{\delta+1} \right) + 2\mu_{j,1}^* (1-\delta) + 2\mu_{j,2}^* \left(\frac{\delta^2}{1+\delta} \right)$$

and the modifications to equation (2-126) are, for constant surface temperature,

$$\beta_1' = \frac{\rho_{j,1}^* U_{j,1}}{\Delta Z} + \frac{\rho_{j,1}^* V_{j,1}(1-\delta)}{\delta(\Delta R)} + \frac{2k_{j,1}^*}{(Pr)\delta(\Delta R)^2} - \frac{(1-\delta)k_{j,1}^*}{(Pr)\delta^2(\Delta R)^2} - \frac{(k_{j,q}^* - k_{j,0}^*)(1-\delta)}{2(Pr)\delta^2(\Delta R)^2} \quad (2-130)$$

$$\Omega_1' = \frac{\rho_{j,1}^* V_{j,1}\delta}{(1+\delta)(\Delta R)} - \frac{3k_{j,1}^*}{(1+\delta)(Pr)(\Delta R)^2} - \frac{(k_{j,q}^* - k_{j,0}^*)}{2(Pr)(1+\delta)(\Delta R)^2} \quad (2-131)$$

and

$$\begin{aligned}
\phi'_1 - \alpha'_1 T_w &= \frac{\gamma-1}{\gamma} U_{j,1} \frac{P_{j+1} - P_j}{\Delta Z} + \frac{\rho_{j,1}^* U_{j,1} T_{j,1}}{\Delta Z} \\
&+ (\gamma-1) M_\delta^2 \mu_{j,1}^* \left[\frac{U_{j+1,1}(1-\delta) + U_{j+1,2} \left(\frac{\delta^2}{1+\delta} \right)}{\delta(\Delta R)} \right]^2 \\
&- \left[\frac{-\rho_{j,1}^* V_{j,1}}{\delta(\delta+1)\Delta R} - \frac{2k_{j,1}^*}{\delta(1+\delta)(Pr)(\Delta R)^2} + \frac{k_{j,1}^*}{\delta^2(1+\delta)(Pr)(\Delta R)^2} \right. \\
&\quad \left. + \frac{k_{j,q}^* - k_{j,0}^*}{2(Pr)(\delta+1)\delta^2(\Delta R)^2} \right] T_w \quad (2-132)
\end{aligned}$$

where

$$k_{j,q}^* = k_{j,0}^* \left(\frac{\delta-1}{\delta+1} \right) + 2k_{j,1}^*(1-\delta) + 2k_{j,2}^* \left(\frac{\delta^2}{1+\delta} \right)$$

For constant wall heat flux, an expression for α'_1 is also needed along with modifications of ϕ'_1 and the heat flux expression. The necessary quantities are

$$\begin{aligned}
\alpha'_1 &= \frac{-\rho_{j,1}^* V_{j,1}}{\delta(\delta+1)\Delta R} - \frac{2k_{j,1}^*}{\delta(1+\delta)(Pr)(\Delta R)^2} + \frac{k_{j,1}^*}{\delta^2(1+\delta)(Pr)(\Delta R)^2} \\
&\quad + \frac{k_{j,q}^* - k_{j,0}^*}{2(Pr)(\delta+1)\delta^2(\Delta R)^2} \quad (2-133)
\end{aligned}$$

$$\begin{aligned}
\phi'_1 &= \frac{\gamma-1}{\gamma} U_{j,1} \frac{P_{j+1} - P_j}{\Delta Z} + \frac{\rho_{j,1}^* U_{j,1} T_{j,1}}{\Delta Z} \\
&+ (\gamma-1) M_\delta^2 \mu_{j,1}^* \left[\frac{U_{j+1,1}(1-\delta) + U_{j+1,2} \left(\frac{\delta^2}{1+\delta} \right)}{\delta(\Delta R)} \right]^2 \quad (2-134)
\end{aligned}$$

and the heat flux condition

$$\begin{aligned}
-k^* \frac{\partial T}{\partial R} \Big|_{R=R_b} &= -k_{j,0}^* \left[\frac{T_{j+1,1}(1+\delta)^2 - T_{j+1,2}(\delta^2) - T_{j+1,0}(1+2\delta)}{\delta(1+\delta)(\Delta R)} \right] \\
&= \frac{qa}{k_0 t_0} \quad (2-135)
\end{aligned}$$

For details of handling the constant heat flux case see section 2.1.2.

When all quantities have been obtained at the station $(j+1)$, the solution may be advanced downstream one ΔZ and the process repeated. The representation is universally stable for all $U \geq 0$. The truncation error is of $\mathcal{O}(\Delta R^2)$ and $\mathcal{O}(\Delta Z)$ for momentum and energy and of $\mathcal{O}(\Delta R)$ and $\mathcal{O}(\Delta Z)$ for continuity.

2.2.5 Compressible Flow—Heat Transfer Solution

The heat transfer solution is identical to that for the incompressible case (section 2.2.3) except that $k_{j,0}^*$ will appear in the heat flux expression (see eq. (2-135)).

2.3 OTHER PROBLEMS WITH A SIMILAR FORMULATION

2.3.1 Wake Behind a Flat Plate

The problem is illustrated in figure 2-6. Rouleau (ref. 10) solved the incompressible wake problem using a finite difference formulation similar to that to be presented here in order that he might evaluate the finite difference results in comparison with the classical solution of Goldstein (ref. 11). The formulation is virtually identical to that for the flat plate boundary layer with $dp/dx=0$ except that the boundary condition

$$U(X, 0) = 0$$

for the boundary layer problem is replaced by

$$\frac{\partial U}{\partial Y}(X, 0) = 0 \quad (2-136)$$

Because the additional unknown $U_{j+1,0}$ has been introduced, it will be necessary to write the momentum equation at $Y=0$. Consider, for example, the incompressible case. The momentum equation in difference form at $Y=0$ may be written as

$$U_{j,0} \frac{U_{j+1,0} - U_{j,0}}{\Delta X} + V_{j,0} \frac{U_{j+1,1} - U_{j+1,-1}}{2(\Delta Y)} = \frac{U_{j+1,1} - 2U_{j+1,0} + U_{j+1,-1}}{(\Delta Y)^2} \quad (2-137)$$

The boundary condition (2-136) in difference form is

$$\frac{U_{j+1,1} - U_{j+1,-1}}{2(\Delta Y)} = 0 \quad (2-138)$$

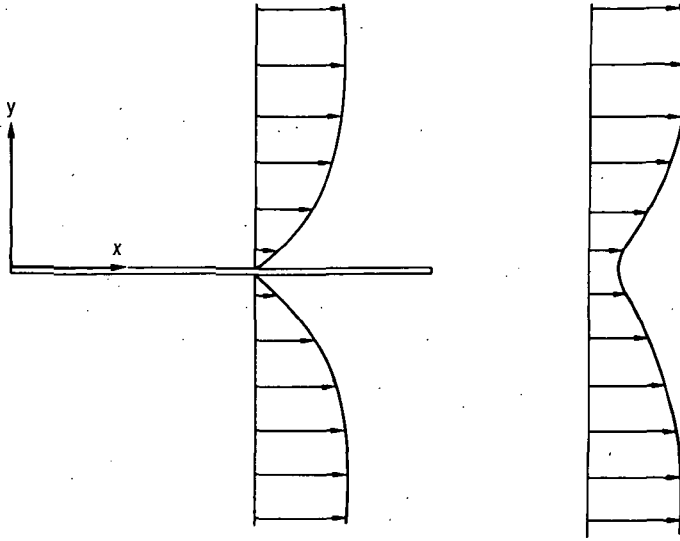


FIGURE 2-6. - Wake behind flat plate.

and hence

$$U_{j+1,1} = U_{j+1,-1} \quad (2-139)$$

When equation (2-139) is used, equation (2-137) may be rewritten as

$$U_{j,0} \frac{U_{j+1,0} - U_{j,0}}{\Delta X} = 2 \left[\frac{U_{j+1,1} - U_{j+1,0}}{(\Delta Y)^2} \right] \quad (2-140)$$

or

$$\left[\frac{U_{j,0}}{\Delta X} + \frac{2}{(\Delta Y)^2} \right] U_{j+1,0} + \left[\frac{-2}{(\Delta Y)^2} \right] U_{j+1,1} = \frac{U_{j,0}^2}{\Delta X} \quad (2-141)$$

This equation, along with the momentum equation (2-10), written for $k=1(1)n$ now forms a complete set of algebraic equations for the values of $U_{j+1,k}$. The resulting matrix equation, in which equation (2-141) now forms the top row, retains the desirable tridiagonal form of the coefficient matrix. A similar change must be made for the energy equation, with a symmetry condition $\partial T / \partial Y = 0$ applying at $Y=0$. The extension to the compressible case is straightforward. In all cases the velocity profile used for starting the solution at the end of the plate will be a boundary layer profile, obtained either by the numerical methods of this chapter or by classical analytical techniques.

2.3.2 Two-Dimensional or Axisymmetric Body With Suction or Injection at the Surface

The only change to the formulations given in this chapter to accommodate suction or injection at the surface is that instead of the transverse velocity being zero at the surface of the body a transverse velocity is specified. For the two-dimensional case

$$V(X, 0) = V_w(X) \quad (2-142)$$

and for the axisymmetric case

$$V(R_b, Z) = V_w(Z) \quad (2-143)$$

where V_w can be any desired function of the axial coordinate. No changes in the difference equations are necessary.

2.3.3 Tangential Jet Adjacent to a Wall

The problem configuration is shown in figure 2-7. Tangential jet injection has recently received considerable attention as a means of providing boundary layer and heat transfer control (refs. 12 and 13).

Several minor modifications to the two-dimensional formulation are necessary in order to consider this case. The dimensionless variables should be redefined so that the characteristic length L is replaced by the jet height d , and the proper velocity and temperature profiles must be used at the "leading edge" (actually any-

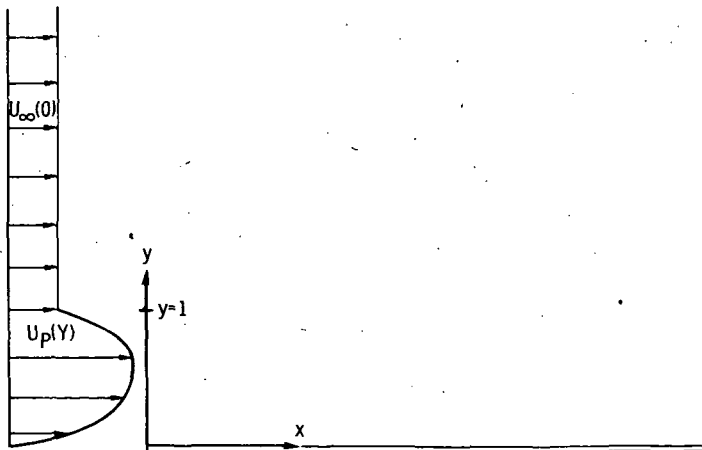


FIGURE 2-7. — Tangential jet adjacent to wall.

where on the surface that the jet is injected). This initial profile may be expressed as

$$U(0, Y) = u_p(Y)/u_0 = U_p(Y) \quad \text{for } Y \leq 1 \quad (2-144)$$

and

$$U(0, Y) = u_\infty(0)/u_0 = U_\infty(0) \quad \text{for } Y > 1 \quad (2-145)$$

Possibilities for $U_p(Y)$ include a uniform profile of any desired magnitude or a parabolic profile. It is also possible to modify equation (2-145) to represent a Blasius type profile corresponding to the situation of a jet injected somewhere downstream of the leading edge of the plate where a boundary layer has already begun to develop before the jet is reached. A very wide variety of boundary conditions on temperature are possible so none will be discussed in detail here, but their application to the finite difference problem is straightforward.

It should be noted that difficulties have been encountered by the author and others when jet velocities become very large compared to the secondary velocity. This difficulty generally is manifested as an oscillatory character of the profile in the mixing region of the jet and secondary. This phenomenon has not yet been satisfactorily explained.

2.3.4 Boundary Layer Flows With Body Forces (MHD, EHD, etc.)

A large class of problems in which there is a body force on the fluid may be approximated by using an equation of motion for two-dimensional flows of the form

$$\rho \left(u \frac{\partial u}{\partial x} + v \frac{\partial u}{\partial y} \right) = -\frac{dp}{dx} + \frac{\partial}{\partial y} \left(\mu \frac{\partial u}{\partial y} \right) + F(x, y, u, v) \quad (2-146)$$

where F is the body force on the fluid. An equivalent equation for axisymmetric flows is

$$\rho \left(u \frac{\partial u}{\partial z} + v \frac{\partial u}{\partial r} \right) = -\frac{dp}{dz} + \frac{1}{r} \frac{\partial}{\partial r} \left(r\mu \frac{\partial u}{\partial r} \right) + F(r, z, u, v) \quad (2-147)$$

A complete discussion of magnetohydrodynamics and electrohydrodynamics cannot, of course, be undertaken here; the reader is referred to any of the standard references such as Pai (ref. 14) or Hughes and Young (ref. 15). However, the problems encountered may be placed in two broad categories; those in which the form of the body force as a function of the velocity may be determined without simultaneously solving for the velocity distribution (that is, where the induced

fields are small compared to the applied fields), and those in which the solution for the velocity distribution and the body force distribution must be obtained simultaneously.

If the induced fields are neglected, then the body force distribution as a function of velocity may be inserted in equation (2-146) or (2-147) and, with some variations to allow for the form of the body force, the fluid flow and heat transfer problems may be solved essentially as before. The continuity equation will be unchanged, and the proper form of the energy equation (refs. 14 and 15) must be used. A number of different forms of the body force distribution may be encountered. If the body force is a function of position only, it adds only to the right side of the difference representation of the momentum equation and does not affect the method of solution at all. If, as is often the case, the body force is a linear function of u , then the only change in the difference equation is an addition to the coefficient of $U_{j+1,k}$ in the difference equation. If the body force were a nonlinear function of u or v then it would be necessary to employ an iterative method to obtain a solution to the resulting set of difference equations. The methods discussed in the next chapter for jet flows with zero secondary velocity may be useful in this context.

If, for incompressible flow, the induced field effects must be included and it becomes necessary to simultaneously solve for the velocity and body force distributions, then the difference forms of both the equation of motion and the necessary field equation (e.g., one of Maxwell's equations) must be solved simultaneously. The resulting difference equations, at least for MHD, will be linear. The matrix of coefficients will not be tridiagonal, however, so the solution will necessarily be somewhat time consuming. An iterative method in which all off-tridiagonal terms are evaluated at the last iteration may be found useful.

If the flow is compressible, the energy and continuity equations will have to be solved simultaneously with the equation of motion and field equations, and an iterative scheme becomes almost mandatory.

2.4 EXAMPLE PROBLEM—FLAT PLATE BOUNDARY LAYER

As an example of the use of the numerical technique and of the problems which may be encountered near a leading edge, we shall now consider the classical problem of the incompressible boundary layer on a flat plate.

Since for the flat plate case $dp/dx = 0$, the dimensionless form of the differential equations of motion and the associated boundary conditions (eqs. (2-5) to (2-7)) become

$$U \frac{\partial U}{\partial X} + V \frac{\partial U}{\partial Y} = \frac{\partial^2 U}{\partial Y^2} \quad (2-148)$$

$$\frac{\partial U}{\partial X} + \frac{\partial V}{\partial Y} = 0 \quad (2-149)$$

$$\left. \begin{aligned} U(X, 0) &= 0 \\ V(X, 0) &= 0 \\ U(X, \infty) &= 1 \\ U(0, Y) &= 1 \end{aligned} \right\} \quad (2-150)$$

With the similarity transformation

$$\eta = \frac{Y}{X^{1/2}} \quad (2-151)$$

equation (2-148) may be transformed into a total differential equation, the solution of which is the Blasius series (see Schlichting, ref. 16). This solution is shown as the dotted line in figure 2-8.

Numerical solutions to the set (eqs. (2-148) to (2-150)) were obtained using the difference representations (2-8) and (2-9). The U velocity profiles are shown as solid lines in figure 2-8. The mesh sizes used were $\Delta X = 0.001$ and $\Delta Y = 0.025$ with $n = 80$ (i.e., with 80 increments from the plate to the free stream).

If the numerical solutions were exact (no truncation or roundoff error), then when plotted as a function of η all values $U(\eta)$ should fall on the same curve, and that curve would be the one obtained from the Blasius series. In actuality, since

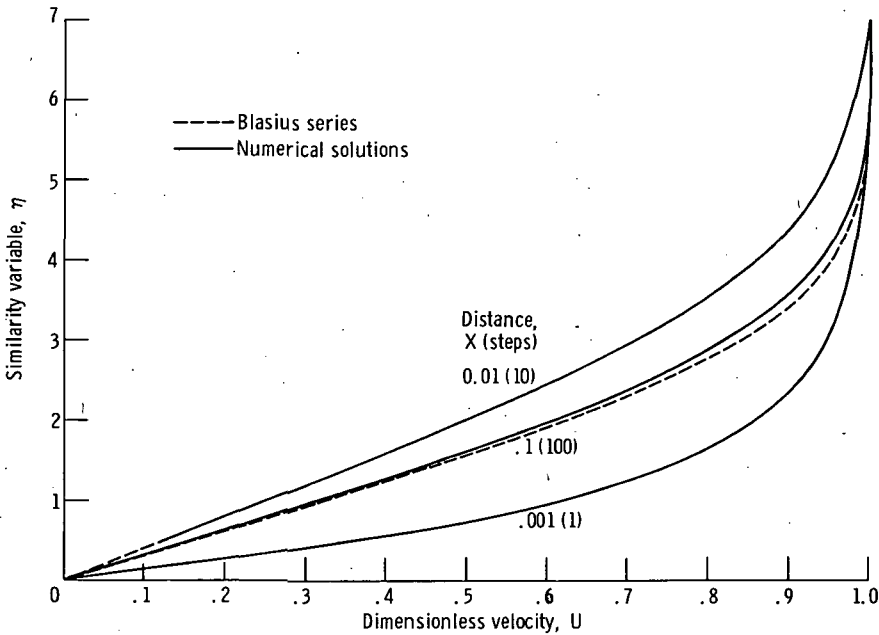


FIGURE 2-8.—Comparison of numerical solution with Blasius series solution for flat plate boundary layer.

the boundary condition at the leading edge is such that the velocity at the plate drops abruptly to zero, two sources of error are introduced. The first of these is truncation error, since only a few mesh points in the transverse direction will be affected due to the thinness of the boundary layer at the first step downstream of the leading edge. The second, and far more serious, error is introduced by the fact that the leading edge is a singular point, and hence the solution in the neighborhood of that point cannot be adequately represented by a Taylor series expansion. Since a finite difference representation is simply the first few terms of a Taylor series expansion, it cannot be expected that a finite difference solution will be accurate in the neighborhood of the leading edge. The solution should improve in accuracy as more downstream steps are taken and the singularity left behind.

The curves shown in figure 2-8 demonstrate the expected behavior. The influence of the singularity is very strongly felt at 1 step and 10 steps (although the boundary layer thickness is surprisingly good). After 100 steps (at $X=0.10$), the numerical solution deviates from the Blasius solution by at most about 6 percent.

The question now arises as to how the effect of the singularity may be confined to the region close to the leading edge. To help to answer this question, a numerical solution was then obtained using $\Delta X = 0.00025$, one-fourth of the value of ΔX used in the previous solution, with ΔY and n remaining the same. Curves virtually identical to those shown in figure 2-8 were obtained when the same number of ΔX steps were used. This was true despite the fact that these curves were obtained at an X value only one-fourth of that at which the previous profiles were obtained. This result indicates that the downstream effect of the singularity is a function primarily of *how many* ΔX steps are taken from the leading edge and *not* the value of X . The effect of the singularity may thus be confined to the region very close to the leading edge by simply taking a large number of steps with a small ΔX in that region.

A common criticism of the approach employed here, in which the partial differential equations are solved directly, is that it is not an effective way to obtain very accurate answers, due to the leading edge singularity and the effects of large variations in boundary layer thickness along the plate. As mentioned in chapter 1, a change to boundary layer coordinates is helpful in overcoming this problem, and many numerical schemes of varying complexity have been evolved which are based on this transformation. However, since the approach taken in this book is to solve the partial differential equations directly without transformations, it was felt worthwhile to determine the mesh sizes and computer time required in order to obtain an accurate solution by this direct approach. After some experimentation, results were obtained for the U velocity distribution which varied from the exact solution by no more than two digits in the third decimal place (less than 0.5 percent error). This solution required mesh sizes as follows: $\Delta X = 1.5 \times 10^{-5}$, $\Delta Y = 0.003425$ up to $k=180$, and $\Delta Y = 0.01370$ from $k=180$ to $k=n=320$ (a total of 320 transverse mesh points; see appendix D for details of employing two different transverse mesh sizes). Five thousand steps were taken in the downstream (X) direction from the

leading edge to reach $X = 0.075$ where the comparison with the exact solutions was made. This procedure took slightly over $2\frac{1}{2}$ minutes of high speed digital computer time. This time could have been shortened considerably if a variable number of transverse mesh points were used, depending on the local boundary layer thickness, but in the interests of simplicity a constant number of transverse mesh points was employed.

REFERENCES

1. BODOIA, JOHN R.: The Finite Difference Analysis of Confined Viscous Flows. Ph.D. Thesis, Carnegie Inst. Tech., 1959.
2. RALSTON, ANTHONY: A First Course in Numerical Analysis. McGraw-Hill Book Co., Inc., 1965.
3. MITCHEL, BARRY J.: Finite Difference Solution of the Development of Transpiration-Cooled Hypersonic Laminar Boundary Layers, Ph.D. Thesis, Carnegie Inst. Tech., 1961.
4. WALKER, M. L., JR.: Laminar Compressible Flow in the Entrance Region of a Tube. Ph.D. Thesis, Carnegie Inst. Tech., 1965.
5. MANGLER, W.: Zusammenhang zwischen ebenen und rotationssymmetrischen Grenzsichten in kompressiblen Flüssigkeiten. Zeit. f. Angew. Math. Mech., vol. 28, Apr. 1948, pp. 97-103.
6. GLAUERT, M. B.; and LICHTHILL, M. J.: The Axisymmetric Boundary Layer on a Long Thin Cylinder. Proc. Roy. Soc. (London), Ser. A, vol. 230, No. 1181, June 21, 1955, pp. 188-203.
7. SEBAN, R. A.; AND BOND, R.: Skin-Friction and Heat-Transfer Characteristics of a Laminar Boundary Layer on a Cylinder in Axial Incompressible Flow. J. Aeron. Sci., vol. 18, No. 10, Oct. 1951, pp. 671-675.
8. ESHGHI, SIAVASH; AND HORNBECK, ROBERT W.: Flow and Heat Transfer in the Axisymmetric Boundary Layer Over a Circular Cylinder. Int. Heat Mass Transfer, vol. 10, No. 12, Dec. 1967, pp. 1757-1766.
9. HORNBECK, ROBERT W.: The Entry Problem in Pipes with Porous Walls. Ph.D. Thesis, Carnegie Inst. Tech., 1961.
10. ROULEAU, WILFRED T.: Finite Difference Methods for the Solution of Fluid Flow Problems Described by the Prandtl Equations. Ph.D. Thesis, Carnegie Inst. Tech., 1954.
11. GOLDSTEIN, S.: Concerning Some Solutions of the Boundary-Layer Equations in Hydrodynamics. Proc. Cambridge Phil. Soc., vol. 26, Jan. 1930, pp. 1-30.
12. SCHETZ, J. A.; AND JANNONE, J.: Initial Boundary Layer Effects on Laminar Flows with Wall Slot Injection. J. Heat Transfer, vol. 87, No. 1, Feb. 1965, pp. 157-160.
13. LIBBY, PAUL A.; AND SCHETZ, JOSEPH A.: Approximate Analysis of the Slot Injection of a Gas in Laminar Flow. AIAA J., vol. 1, No. 5, May 1963, pp. 1056-1061.
14. PAI, SHIH-I.: Magnetogasdynamics and Plasma Dynamics. Prentice-Hall, Inc., 1962.
15. HUGHES, WILLIAM F.; AND YOUNG, F. J.: The Electromagnetodynamics of Fluids. John Wiley & Sons, Inc., 1966.
16. SCHLICHTING, HERMANN (J. Kestin, Trans.): Boundary Layer Theory. Fourth ed., McGraw-Hill Book Co., Inc., 1960.

CHAPTER 3

JETS

In this chapter solutions are formulated for the problem of a laminar plane or axisymmetric jet issuing into an infinite medium, either stationary or moving. For a first approach the surrounding medium is assumed to be of the same fluid as the jet. More complex situations will be considered in later sections of this chapter. A uniform external pressure field in the surrounding medium is assumed.

The equations employed in this chapter are valid only if the pressure in the interior of the jet may be considered equal to that of the surrounding medium. This requires that the surface tension of the jet be negligible and that the jet be fully expanded. A fully expanded jet is one in which the pressure at the jet mouth is equal to the pressure in the surrounding fluid (e.g., a jet emerging from a tube); an underexpanded jet is one in which the pressure is higher at the jet mouth than that of the surrounding fluid (e.g., a jet emerging from a reservoir). In the latter case the pressure in the jet interior does not reach the pressure in the surrounding fluid until after the *vena contracta* is reached. This situation is not considered here.

3.1 PLANE JETS

The plane jet is illustrated in figure 3-1 along with the coordinate system used in this chapter.

3.1.1 Incompressible Constant Property Flow—Velocity Solution

The incompressible constant property equations of motion for a plane jet in a uniform pressure field are

$$\rho \left(u \frac{\partial u}{\partial x} + v \frac{\partial u}{\partial y} \right) = \mu \frac{\partial^2 u}{\partial y^2} \quad (3-1)$$

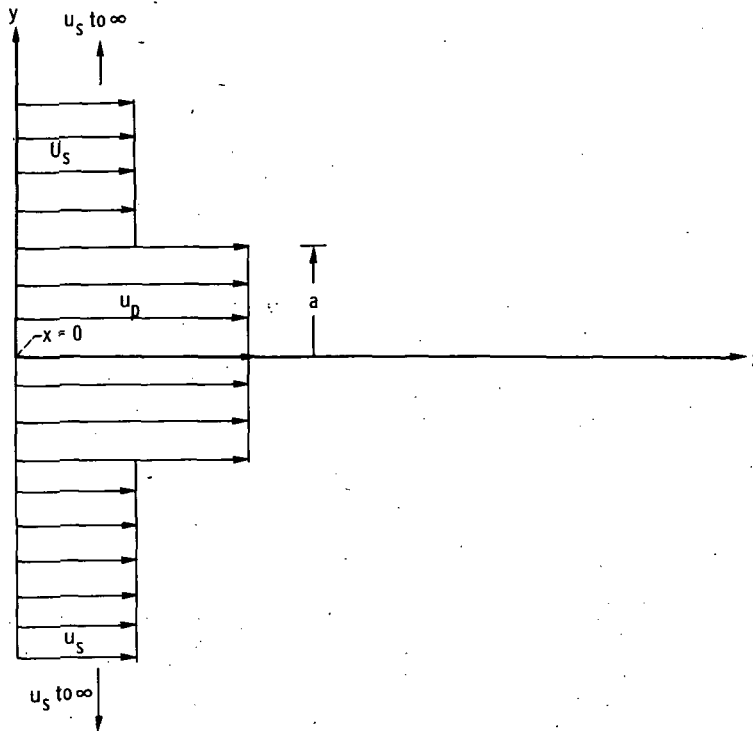


FIGURE 3-1.—Plane jet configuration showing velocity profile at $x=0$.

$$\frac{\partial u}{\partial x} + \frac{\partial v}{\partial y} = 0 \quad (3-2)$$

The boundary conditions to be considered are

$$\left. \begin{aligned} u(0, y) &= u_p(y) & y \leq a \text{ (see appendix F)} \\ u(0, y) &= u_s(y) & y > a \\ u(x, \infty) &= u_s \\ \frac{\partial u}{\partial y}(x, 0) &= 0 \\ v(x, 0) &= 0 \end{aligned} \right\} \quad (3-3)$$

The basic equations are made dimensionless by the following choices of dimensionless variables:

$$\begin{aligned}
 U &= \frac{u}{u_c} & X &= \frac{x\mu}{\rho u_c a^2} \\
 V &= \frac{\rho v a}{\mu} & Y &= \frac{y}{a}
 \end{aligned}
 \quad \left. \vphantom{\begin{aligned} U \\ V \end{aligned}} \right\} \quad (3-4)$$

Equations (3-1) and (3-2) may be rewritten in dimensionless form using the variables (3-4) as

$$U \frac{\partial U}{\partial X} + V \frac{\partial U}{\partial Y} = \frac{\partial^2 U}{\partial Y^2} \quad (3-5)$$

$$\frac{\partial U}{\partial X} + \frac{\partial V}{\partial Y} = 0 \quad (3-6)$$

The boundary conditions (3-3) in dimensionless form are

$$\begin{aligned}
 U(0, Y) &= U_p(Y) & Y &\leq 1 \\
 U(0, Y) &= U_s(Y) & Y &> 1 \\
 U(X, \infty) &= U_s(\infty) \\
 \frac{\partial U}{\partial Y}(X, 0) &= 0 \\
 V(X, 0) &= 0
 \end{aligned}
 \quad \left. \vphantom{\begin{aligned} U(0, Y) \\ U(X, \infty) \\ \frac{\partial U}{\partial Y}(X, 0) \\ V(X, 0) \end{aligned}} \right\} \quad (3-7)$$

3.1.1.1 Highly implicit difference representation valid for small secondary velocities. — A finite difference representation must now be chosen for equations (3-5) and (3-6). The finite difference grid is shown in figure 3-2. The difference form selected for equation (3-5) is highly implicit in that not only are all Y -derivatives evaluated at $j+1$ but, in addition, the coefficients of the nonlinear convective terms are also evaluated at $j+1$. This representation, which results in nonlinear algebraic equations for the unknowns $U_{j+1, k}$ and $V_{j+1, k}$, is necessary if zero and small secondary velocities are to be considered, since the usual implicit scheme with the coefficients evaluated at j is inconsistent for these conditions. This inconsistency is not discussed in detail, but for zero secondary velocity the usual implicit form results in the U velocity profile decreasing linearly from the edge of the jet to whatever value of Y is chosen as infinity. This result is obviously incorrect. The usual implicit scheme, which is also discussed in this chapter, does give correct results if the secondary velocity is of the order of the primary velocity or larger.

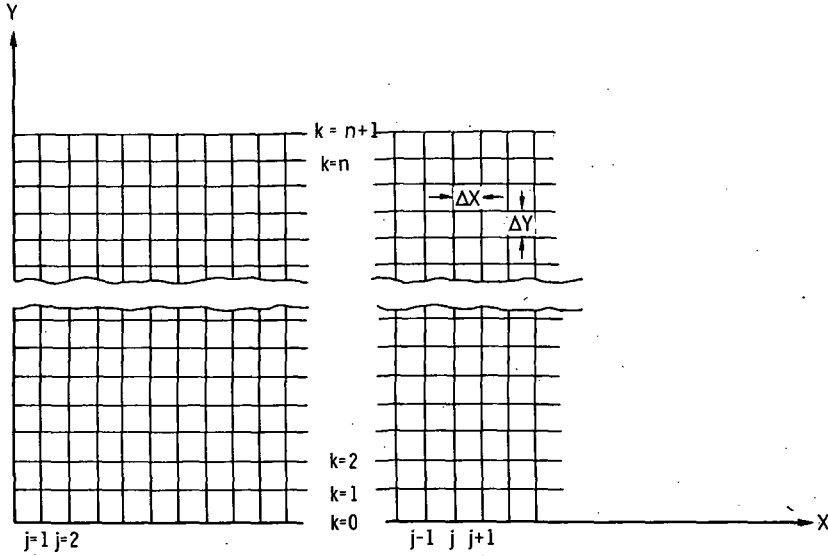


FIGURE 3-2. — Finite difference grid for plane jet.

The nonlinear difference representation chosen here is valid for all values of u_s/u_p :

$$U_{j+1,k} \left(\frac{U_{j+1,k} - U_{j,k}}{\Delta X} \right) + V_{j+1,k} \left[\frac{U_{j+1,k+1} - U_{j+1,k-1}}{2(\Delta Y)} \right] = \frac{U_{j+1,k+1} - 2U_{j+1,k} + U_{j+1,k-1}}{(\Delta Y)^2} \quad (3-8)$$

The representation of the continuity equation (3-6) is conventional:

$$\frac{U_{j+1,k+1} - U_{j,k+1}}{\Delta X} + \frac{V_{j+1,k+1} - V_{j+1,k}}{\Delta Y} = 0 \quad (3-9)$$

Equation (3-8) is nonlinear so that none of the usual techniques for linear algebraic equations may be employed. However, one very simple and effective iterative technique is now described. First, equation (3-8) is rewritten, using superscripts to indicate on which iteration that value was obtained; for example, $U_{j+1,k}^{(l)}$ is obtained on the (l)th iteration while $U_{j+1,k}^{(l+1)}$ is obtained on the ($l+1$)th iteration. Equation (3-8) becomes

$$U_{j+1,k}^{(l)} \left(\frac{U_{j+1,k}^{(l+1)} - U_{j,k}^{(l)}}{\Delta X} \right) + V_{j+1,k}^{(l)} \left[\frac{U_{j+1,k+1}^{(l+1)} - U_{j+1,k-1}^{(l+1)}}{2(\Delta Y)} \right] = \frac{U_{j+1,k+1}^{(l+1)} - 2U_{j+1,k}^{(l+1)} + U_{j+1,k-1}^{(l+1)}}{(\Delta Y)^2} \quad (3-10)$$

where

$$\alpha_k^{(l)} = -\frac{V_{j+1,k}^{(l)}}{2(\Delta Y)} - \frac{1}{(\Delta Y)^2}$$

$$\beta_k^{(l)} = \frac{U_{j+1,k}^{(l)}}{\Delta X} + \frac{2}{(\Delta Y)^2}$$

$$\Omega_k^{(l)} = \frac{V_{j+1,k}^{(l)}}{2(\Delta Y)} - \frac{1}{(\Delta Y)^2}$$

$$\phi_k^{(l)} = \frac{U_{j+1,k}^{(l)} U_{j,k}}{\Delta X}$$

Equation (3-13) incorporates the symmetry condition at $k=0$ which in finite difference form is

$$U_{j+1,1} = U_{j+1,-1}$$

The coefficient matrix of equation (3-13) is tridiagonal and the method of appendix A may be used at each iteration to solve for the values of $U_{j+1,k}^{(l+1)}$. After the iteration process has converged, another step downstream may be taken and the process repeated.

It might be noted that this iterative procedure is a composite of Jacobi and Gauss-Siedel iterative techniques as extended to nonlinear equations. Crandall (ref. 1) discusses these methods for linear equations.

In some cases it may be desirable or necessary to either overrelax or underrelax the iterative procedure. If difficulty in obtaining convergence of the iterative process is encountered, then underrelaxation is indicated; overrelaxation is usually employed to accelerate an already convergent iterative process. The author's experience with jet flows having uniform velocity profiles at the point where mixing of the two streams begins is that underrelaxation is not necessary to obtain convergence. However, for the example discussed in section 3-4, where the velocity profile in the primary was parabolic and the secondary was at rest, underrelaxation was necessary.

Before discussing the relaxation procedure, we shall briefly mention the notation to be used. In the straight iterative procedure, the quantities $U_{j+1,k}^{(l)}$ appearing in the equation of motion take on the values of $U_{j+1,k}^{(l+1)}$ after each iteration, and then a new set of $U_{j+1,k}^{(l+1)}$'s is solved for on the next iteration. Symbolically this may be written as

$$U_{j+1,k}^{(l)} \leftarrow U_{j+1,k}^{(l+1)}$$

In the relaxation procedure, the values of $U_{j+1,k}^{(l)}$ are modified somewhat from the previous ones. This modification may be expressed as

$$U_{j+1,k}^{(l)} \leftarrow U_{j+1,k}^{(l)} + \lambda (U_{j+1,k}^{(l+1)} - U_{j+1,k}^{(l)})$$

where λ is called a relaxation factor. Values of λ in the range $0 \leq \lambda < 1$ correspond to underrelaxation while $1 < \lambda \leq 2$ correspond to overrelaxation. For $\lambda = 1$ the procedure again becomes straight iteration which simply corresponds to replacing the old value with the newly computed value.

An iterative method such as this will necessarily be more time consuming than the usual implicit scheme in which only one set of simultaneous linear equations of the type (3-13) need be solved at each step; however, this representation is necessary to ensure a consistent solution for zero or small secondary velocities.

One interesting consequence of employing the highly implicit technique is that since $V_{j,k}$ does not appear in the equations, $V(0, Y)$ need not be specified at the mouth of the jet to start the marching procedure. Since $V(0, Y)$ is not truly a boundary condition (see appendix F), this is at least esthetically pleasing.

3.1.1.2 Implicit formulation valid only for large secondary velocities. — We now present an alternative formulation to the jet problem which is valid only if the secondary velocity is at least of the order of the primary velocity. This implicit scheme is very similar to the implicit scheme used for boundary layer problems in chapter 2 and in those cases where it can be used has a considerable time-saving advantage over the iterative method just discussed.

The difference representation of equation (3-5) for this alternative formulation is

$$U_{j,k} \frac{U_{j+1,k} - U_{j,k}}{\Delta X} + V_{j,k} \frac{U_{j+1,k+1} - U_{j+1,k-1}}{2(\Delta Y)} = \frac{U_{j+1,k+1} - 2U_{j+1,k} + U_{j+1,k-1}}{(\Delta Y)^2} \quad (3-14)$$

In order to facilitate a matrix representation, equation (3-14) may now be rearranged as

$$\left[-\frac{V_{j,k}}{2(\Delta Y)} - \frac{1}{(\Delta Y)^2} \right] U_{j+1,k-1} + \left[\frac{U_{j,k}}{\Delta X} + \frac{2}{(\Delta Y)^2} \right] U_{j+1,k} + \left[\frac{V_{j,k}}{2(\Delta Y)} - \frac{1}{(\Delta Y)^2} \right] U_{j+1,k+1} = \frac{(U_{j,k})^2}{\Delta X} \quad (3-15)$$

Equation (3-15) written for $k=0(1)n$ constitutes a set of $(n+1)$ linear equations in $(n+1)$ unknowns which may be rewritten in matrix form as

secondary velocities. The explicit formulation would have no advantages over the implicit formulation (3-14), since the times required for solution are comparable and there are stability restrictions on the mesh sizes which can be used with an explicit form. The explicit form, therefore, is not considered here.

The truncation error of the finite difference representation at each step is of $\mathcal{O}(\Delta Y)^2$ and $\mathcal{O}(\Delta X)$ for the momentum equation (both forms) and of $\mathcal{O}(\Delta Y)$ and $\mathcal{O}(\Delta X)$ for continuity.

The implicit solutions are stable for all $U \geq 0$. This has been demonstrated by Rouleau (ref. 2) for the form (3-14) and has been found to be true for form (3-8) by experience, although a stability analysis cannot be readily carried out because of the nonlinearity of the difference equation. Since only positive values of U should be encountered in the jet problem, the solution can be considered universally stable. It should be noted, however, that difficulties similar to those discussed in section 2.3.3 may occur if the disparity in velocity between the primary and secondary streams is too great. This can result in small oscillations in the axial velocity in the mixing region. The reason for this behavior is not understood.

3.1.2 Incompressible Constant Property Flow – Temperature Solution

Assuming constant properties and neglecting viscous dissipation, the energy equation for this problem may be written as

$$\rho c_p \left(u \frac{\partial t}{\partial x} + v \frac{\partial t}{\partial y} \right) = k \frac{\partial^2 t}{\partial y^2} \tag{3-18}$$

The boundary conditions are

$$\left. \begin{aligned} t(0, y) &= t_p & y &\leq a \\ t(0, y) &= t_s & y &> a \\ t(x, \infty) &= t_s \\ \frac{\partial t}{\partial y}(x, 0) &= 0 \end{aligned} \right\} \tag{3-19}$$

Equation (3-18) may be made dimensionless by the following choice of dimensionless variables:

$$\left. \begin{aligned} T &= \frac{t - t_s}{t_p - t_s} & X &= \frac{x\mu}{\rho u_p a^2} \\ U &= u/u_p & Y &= y/a \\ V &= \rho v a / \mu \end{aligned} \right\} \tag{3-20}$$

When these variables are inserted in equations (3-18) and (3-19), the problem may be restated in dimensionless form as

$$U \frac{\partial T}{\partial X} + V \frac{\partial T}{\partial Y} = \frac{1}{Pr} \frac{\partial^2 T}{\partial Y^2} \quad (3-21)$$

$$\left. \begin{aligned} T(0, Y) &= 1 & Y \leq 1 \\ T(0, Y) &= 0 & Y > 1 \\ T(X, \infty) &= 0 \\ \frac{\partial T}{\partial Y}(X, 0) &= 0 \end{aligned} \right\} \quad (3-22)$$

A finite difference representation may now be chosen. The finite difference form given here will correspond to the finite difference form of the momentum equation (3-8) and should be used when that form is used. If the secondary velocity is sufficiently high to allow the use of the form (3-14) for the momentum equation, then the coefficients of the convective terms in the following equation should be made $U_{j,k}$ and $V_{j,k}$. The difference form of equation (3-21) is

$$\begin{aligned} U_{j+1,k} \frac{T_{j+1,k} - T_{j,k}}{\Delta X} + V_{j+1,k} \frac{T_{j+1,k+1} - T_{j+1,k-1}}{2(\Delta Y)} \\ = \frac{1}{Pr} \frac{T_{j+1,k+1} - 2T_{j+1,k} + T_{j+1,k-1}}{(\Delta Y)^2} \end{aligned} \quad (3-23)$$

Equation (3-23) is similar to equation (3-8) in that the coefficients are evaluated at $j+1$. However, in the incompressible case being considered, the flow equations are solved first and the coefficients are hence known and the difference equation remains linear in T .

Equation (3-23) may be rearranged in a more useful form as

$$\begin{aligned} \left[-\frac{V_{j+1,k}}{2(\Delta Y)} - \frac{1}{Pr(\Delta Y)^2} \right] T_{j+1,k-1} + \left[\frac{U_{j+1,k}}{\Delta X} + \frac{2}{Pr(\Delta Y)^2} \right] T_{j+1,k} \\ + \left[\frac{V_{j+1,k}}{2(\Delta Y)} - \frac{1}{Pr(\Delta Y)^2} \right] T_{j+1,k+1} = \frac{U_{j+1,k} T_{j,k}}{\Delta X} \end{aligned} \quad (3-24)$$

Equation (3-24) written for $k=0(1)n$ and expressed in matrix form is

$$\rho c_p \left(u \frac{\partial t}{\partial x} + v \frac{\partial t}{\partial y} \right) = \frac{\partial}{\partial y} \left(k \frac{\partial t}{\partial y} \right) + \mu \left(\frac{\partial u}{\partial y} \right)^2 \quad (3-28)$$

$$\rho t = \text{constant} \quad (3-29)$$

$$\mu = \mu(t) \quad (3-30)$$

$$k = k(t) \quad (3-31)$$

Equation (3-29) assumes a perfect gas at constant pressure. Any other equation of state may be used if desired.

The boundary conditions are

$$\left. \begin{aligned} u(0, y) &= u_p & y \leq a \text{ (see appendix F)} \\ u(0, y) &= u_s & y > a \\ u(x, \infty) &= u_s \\ \frac{\partial u}{\partial y}(x, 0) &= 0 \\ v(x, 0) &= 0 \\ t(0, y) &= t_p & y \leq a \\ t(0, y) &= t_s & y > a \\ t(x, \infty) &= t_s \\ \frac{\partial t}{\partial y}(x, 0) &= 0 \end{aligned} \right\} \quad (3-32)$$

These equations may be put in dimensionless form by the following choice of dimensionless variables:

$$\left. \begin{aligned} U &= \frac{u}{u_p} & X &= \frac{x\mu_p}{\rho_p u_p a^2} \\ V &= \frac{\rho_p v a}{\mu_p} & Y &= \frac{y}{a} \\ T &= \frac{t}{t_p} & k^* &= \frac{k}{k_p} \\ & & \mu^* &= \frac{\mu}{\mu_p} \\ & & \rho^* &= \frac{\rho}{\rho_p} \end{aligned} \right\} \quad (3-33)$$

For these dimensionless representations the conditions in the primary stream at the jet mouth have been chosen as reference values. Inserting these variables into equations (3-26) to (3-31) gives

$$\rho^* \left(U \frac{\partial U}{\partial X} + V \frac{\partial U}{\partial Y} \right) = \frac{\partial}{\partial Y} \left(\mu^* \frac{\partial U}{\partial Y} \right) \quad (3-34)$$

$$\frac{\partial(\rho^*U)}{\partial X} + \frac{\partial(\rho^*V)}{\partial Y} = 0 \quad (3-35)$$

$$\rho^* \left(U \frac{\partial T}{\partial X} + V \frac{\partial T}{\partial Y} \right) = \frac{1}{Pr} \frac{\partial}{\partial Y} \left(k^* \frac{\partial T}{\partial Y} \right) + (\gamma - 1) M_p^2 \mu^* \left(\frac{\partial U}{\partial Y} \right)^2 \quad (3-36)$$

(where the Mach number in the primary stream at $X=0$ is $M_p = u_p / \sqrt{\gamma \mathcal{R} t_p}$, and the Prandtl number at the same location is $Pr = (\mu c_p / k)_p$)

$$\rho^* = \frac{1}{T} \quad (3-37)$$

$$\mu^* = (T)^f \quad (3-38)$$

$$k^* = (T)^g \quad (3-39)$$

The usual power law relations for μ and k have been assumed as in the preceding chapter. Any other relationship may be readily considered.

The boundary conditions (3-23) in dimensionless form become

$$\left. \begin{aligned} U(0, Y) &= 1 & Y \leq 1 \\ U(0, Y) &= u_s / u_p & Y > 1 \\ U(X, \infty) &= u_s / u_p \\ \frac{\partial U}{\partial Y}(X, 0) &= 0 \\ V(X, 0) &= 0 \\ T(0, Y) &= 1 & Y \leq 1 \\ T(0, Y) &= t_s / t_p & Y > 1 \\ T(X, \infty) &= t_s / t_p \\ \frac{\partial T}{\partial Y}(X, 0) &= 0 \end{aligned} \right\} \quad (3-40)$$

3.1.3.1 Highly implicit representation valid for small secondary velocities.— Equations (3-34) to (3-39) may now be expressed in finite difference form. An implicit representation similar to that used for equation (3-8) in section 3.1.1

is used here for both momentum and energy in order that the formulation may be valid for zero and small secondary velocities. The representation which must be used results in nonlinear difference equations. Since this is the case, the equations must be solved using an iterative method; therefore, it is not necessary to always evaluate the properties in such a way that they are known when a given equation is considered. Evaluating the properties in this way was useful in sections 2.1.4 and 2.2.4 since the linearity of the difference equations was preserved. Somewhat better accuracy can presumably be obtained, however, by evaluating the properties simultaneously with the velocities and temperatures in each equation. The solution in this case can be accomplished by using an iterative method, and since an iterative method is already necessary, no complications are added to the solution.

The difference representations of equations (3-34) to (3-39) are

$$\begin{aligned} \rho_{j+1,k}^* & \left[U_{j+1,k} \frac{U_{j+1,k} - U_{j,k}}{\Delta X} + V_{j+1,k} \frac{U_{j+1,k+1} - U_{j+1,k-1}}{2(\Delta Y)} \right] \\ & = \mu_{j+1,k}^* \left[\frac{U_{j+1,k+1} - 2U_{j+1,k} + U_{j+1,k-1}}{(\Delta Y)^2} \right] \\ & + \left[\frac{\mu_{j+1,k+1}^* - \mu_{j+1,k-1}^*}{2(\Delta Y)} \right] \left[\frac{U_{j+1,k+1} - U_{j+1,k-1}}{2(\Delta Y)} \right] \end{aligned} \quad (3-41)$$

$$\frac{\rho_{j+1,k}^* U_{j+1,k} - \rho_{j,k}^* U_{j,k}}{\Delta X} + \frac{\rho_{j+1,k+1}^* V_{j+1,k+1} - \rho_{j+1,k}^* V_{j+1,k}}{\Delta Y} = 0 \quad (3-42)$$

$$\begin{aligned} \rho_{j+1,k}^* & \left[U_{j+1,k} \frac{T_{j+1,k} - T_{j,k}}{\Delta X} + V_{j+1,k} \frac{T_{j+1,k+1} - T_{j+1,k-1}}{2(\Delta Y)} \right] \\ & = \frac{1}{Pr} \left\{ k_{j+1,k}^* \left[\frac{T_{j+1,k+1} - 2T_{j+1,k} + T_{j+1,k-1}}{(\Delta Y)^2} \right] \right. \\ & + \left. \left[\frac{k_{j+1,k+1}^* - k_{j+1,k-1}^*}{2(\Delta Y)} \right] \left[\frac{T_{j+1,k+1} - T_{j+1,k-1}}{2(\Delta Y)} \right] \right\} \\ & + (\gamma - 1) M_p^2 \mu_{j+1,k}^* \left[\frac{U_{j+1,k+1} - U_{j+1,k-1}}{2(\Delta Y)} \right]^2 \end{aligned} \quad (3-43)$$

$$\rho_{j+1,k}^* = \frac{1}{T_{j+1,k}} \quad (3-44)$$

$$\mu_{j+1,k}^* = (T_{j+1,k})^f \quad (3-45)$$

$$k_{j+1,k}^* = (T_{j+1,k})^g \quad (3-46)$$

The iterative method of solution for equations (3-41) to (3-46) discussed here is quite similar to that employed in section 3.1.1 for the incompressible mo-

mentum equation. It is not necessarily the fastest way to solve the set of difference equations but it is reasonably fast and is very straightforward. As in section 3.1.1, the superscript l on a quantity indicates that quantity was obtained on the (l) th iteration, while the superscript $(l+1)$ indicates the $(l+1)$ th iteration. Equations (3-41) and (3-43) are rewritten as

$$\begin{aligned} & \left[\frac{-\rho_{j+1,k}^{*(l)} V_{j+1,k}^{(l)}}{2(\Delta Y)} - \frac{\mu_{j+1,k}^{*(l)}}{(\Delta Y)^2} + \frac{\mu_{j+1,k+1}^{*(l)} - \mu_{j+1,k-1}^{*(l)}}{4(\Delta Y)^2} \right] U_{j+1,k-1}^{(l+1)} + \left[\frac{\rho_{j+1,k}^{*(l)} U_{j+1,k}^{(l)}}{\Delta X} \right. \\ & \left. + \frac{2\mu_{j+1,k}^{*(l)}}{(\Delta Y)^2} \right] U_{j+1,k}^{(l+1)} + \left[\frac{\rho_{j+1,k}^{*(l)} V_{j+1,k}^{(l)}}{2(\Delta Y)} - \frac{\mu_{j+1,k}^{*(l)}}{(\Delta Y)^2} - \frac{\mu_{j+1,k+1}^{*(l)} - \mu_{j+1,k-1}^{*(l)}}{4(\Delta Y)^2} \right] U_{j+1,k+1}^{(l+1)} \\ & = \frac{\rho_{j+1,k}^{*(l)} U_{j+1,k}^{(l)} U_{j,k}}{\Delta X} \end{aligned} \quad (3-47)$$

and

$$\begin{aligned} & \left[\frac{-\rho_{j+1,k}^{*(l)} V_{j+1,k}^{(l)}}{2(\Delta Y)} - \frac{k_{j+1,k}^{*(l)}}{Pr(\Delta Y)^2} + \frac{(k_{j+1,k+1}^{*(l)} - k_{j+1,k-1}^{*(l)})}{4Pr(\Delta Y)^2} \right] T_{j+1,k-1}^{(l+1)} \\ & + \left[\frac{\rho_{j+1,k}^{*(l)} U_{j+1,k}^{(l+1)}}{\Delta X} + \frac{2k_{j+1,k}^{*(l)}}{Pr(\Delta Y)^2} \right] T_{j+1,k}^{(l+1)} + \left[\frac{\rho_{j+1,k}^{*(l)} V_{j+1,k}^{(l)}}{2(\Delta Y)} - \frac{k_{j+1,k}^{*(l)}}{Pr(\Delta Y)^2} \right. \\ & \quad \left. - \frac{(k_{j+1,k+1}^{*(l)} - k_{j+1,k-1}^{*(l)})}{4Pr(\Delta Y)^2} \right] T_{j+1,k+1}^{(l+1)} \\ & = (\gamma - 1) M_p^2 \mu_{j+1,k}^{*(l)} \left(\frac{U_{j+1,k+1}^{(l+1)} - U_{j+1,k-1}^{(l+1)}}{2(\Delta Y)} \right)^2 + \frac{\rho_{j+1,k}^{*(l)} U_{j+1,k}^{(l+1)} T_{j,k}}{\Delta X} \end{aligned} \quad (3-48)$$

Equation (3-47) written for $k=0(1)n$ now constitutes $(n+1)$ linear equations in the $(n+1)$ unknowns $U_{j+1,k}^{(l+1)}$, since those quantities with superscript (l) are considered known from the previous iteration. Equation (3-48) represents a similar set of equations in $T_{j+1,k}^{(l+1)}$. For each iteration the procedure is to solve the set of equations represented by equation (3-47) for $U_{j+1,k}^{(l+1)}$, then the set represented by equation (3-48) for $T_{j+1,k}^{(l+1)}$, and finally the equation of state (3-44) for $\rho_{j+1,k}^{*(l+1)}$ to yield

$$\rho_{j+1,k}^{*(l+1)} = \frac{1}{T_{j+1,k}^{(l+1)}} \quad (3-49)$$

The continuity equation (3-42) may now be solved for $V_{j+1,k}^{(l+1)}$ giving

$$V_{j+1,k+1}^{(l+1)} = \frac{\rho_{j+1,k}^{*(l+1)}}{\rho_{j+1,k+1}^{*(l+1)}} V_{j+1,k}^{(l+1)} - \frac{\Delta Y}{\Delta X} \left(\frac{\rho_{j+1,k}^{*(l+1)}}{\rho_{j+1,k+1}^{*(l+1)}} U_{j+1,k}^{(l+1)} - \frac{\rho_{j,k}^*}{\rho_{j+1,k+1}^{*(l+1)}} U_{j,k} \right) \quad (3-50)$$

The linear difference representations of equations (3-34) to (3-39), valid only for high secondary velocities, are

$$\begin{aligned} \rho_{j,k}^* \left[U_{j,k} \frac{U_{j+1,k} - U_{j,k}}{\Delta X} + V_{j,k} \frac{U_{j+1,k+1} - U_{j+1,k-1}}{2(\Delta Y)} \right] \\ = \mu_{j,k}^* \left[\frac{U_{j+1,k+1} - 2U_{j+1,k} + U_{j+1,k-1}}{(\Delta Y)^2} \right] \\ + \left[\frac{\mu_{j,k+1}^* - \mu_{j,k-1}^*}{2(\Delta Y)} \right] \left[\frac{U_{j+1,k+1} - U_{j+1,k-1}}{2(\Delta Y)} \right] \end{aligned} \quad (3-53)$$

$$\frac{\rho_{j+1,k}^* U_{j+1,k} - \rho_{j,k}^* U_{j,k}}{\Delta X} + \frac{\rho_{j+1,k+1}^* V_{j+1,k+1} - \rho_{j+1,k}^* V_{j+1,k}}{\Delta Y} = 0 \quad (3-54)$$

$$\begin{aligned} \rho_{j,k}^* \left[U_{j,k} \frac{T_{j+1,k} - T_{j,k}}{\Delta X} + V_{j,k} \frac{T_{j+1,k+1} - T_{j+1,k-1}}{2(\Delta Y)} \right] \\ = \frac{1}{Pr} \left\{ k_{j,k}^* \left[\frac{T_{j+1,k+1} - 2T_{j+1,k} + T_{j+1,k-1}}{(\Delta Y)^2} \right] \right. \\ \left. + \left[\frac{k_{j,k+1}^* - k_{j,k-1}^*}{2(\Delta Y)} \right] \left[\frac{T_{j+1,k+1} - T_{j+1,k-1}}{2(\Delta Y)} \right] \right\} \\ + (\gamma - 1) M_b^2 \mu_{j,k}^* \left[\frac{U_{j+1,k+1} - U_{j+1,k-1}}{2(\Delta Y)} \right]^2 \end{aligned} \quad (3-55)$$

$$\rho_{j+1,k}^* = \frac{1}{T_{j+1,k}} \quad (3-56)$$

$$\mu_{j+1,k}^* = (T_{j+1,k})^f \quad (3-57)$$

$$k_{j+1,k}^* = (T_{j+1,k})^g \quad (3-58)$$

Equations (3-53) and (3-55) may be rewritten in more useful forms. Equation (3-53) becomes

$$\begin{aligned} \left[\frac{-\rho_{j,k}^* V_{j,k}}{2(\Delta Y)} - \frac{\mu_{j,k}^*}{(\Delta Y)^2} + \frac{\mu_{j,k+1}^* - \mu_{j,k-1}^*}{4(\Delta Y)^2} \right] U_{j+1,k-1} \\ + \left[\frac{\rho_{j,k}^* U_{j,k}}{\Delta X} + \frac{2\mu_{j,k}^*}{(\Delta Y)^2} \right] U_{j+1,k} \\ + \left[\frac{\rho_{j,k}^* V_{j,k}}{2(\Delta Y)} - \frac{\mu_{j,k}^*}{(\Delta Y)^2} - \frac{\mu_{j,k+1}^* - \mu_{j,k-1}^*}{4(\Delta Y)^2} \right] U_{j+1,k+1} = \frac{\rho_{j,k}^* U_{j,k}^2}{\Delta X} \end{aligned} \quad (3-59)$$

and equation (3-55) becomes

3.2 AXISYMMETRIC JETS

The problem configuration and coordinate system for the axisymmetric jet flows to be considered are shown in figure 3-3. While there is considerable similarity between the formulations for the plane and axisymmetric cases, variations in difference representations and techniques due to the different form of the basic equations in the two cases would appear to make a complete presentation of the axisymmetric formulation worthwhile.

3.2.1 Incompressible Constant Property Flow—Velocity Solution

The incompressible equations of motion for the axisymmetric jet are

$$\rho \left(u \frac{\partial u}{\partial z} + v \frac{\partial u}{\partial r} \right) = \frac{\mu}{r} \frac{\partial}{\partial r} \left(r \frac{\partial u}{\partial r} \right) \quad (3-64)$$

$$\frac{\partial u}{\partial z} + \frac{1}{r} \frac{\partial (rv)}{\partial r} = 0 \quad (3-65)$$

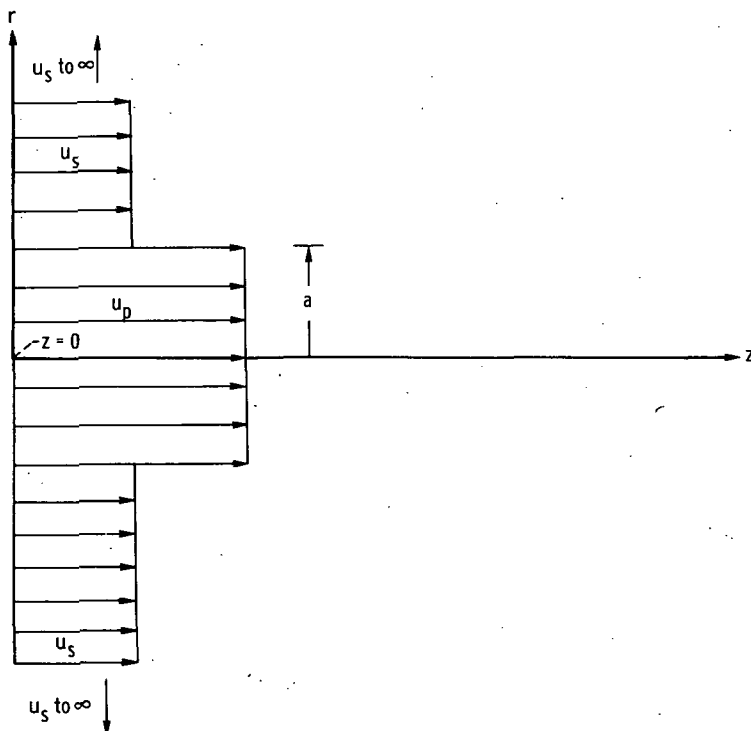


FIGURE 3-3.— Axisymmetric jet configuration showing velocity profile at $z=0$.

The boundary conditions to be considered here are

$$\left. \begin{aligned} u(r, 0) &= u_p & r \leq a & \quad (\text{see appendix F}) \\ u(r, 0) &= u_s & r > a \\ u(\infty, z) &= u_s \\ \frac{\partial u}{\partial r}(0, z) &= 0 \\ v(0, z) &= 0 \end{aligned} \right\} \quad (3-66)$$

The basic equations may be made dimensionless by the following choice of dimensionless variables:

$$\left. \begin{aligned} U &= \frac{u}{u_p} & Z &= \frac{z\mu}{\rho u_p a^2} \\ V &= \frac{\rho v a}{\mu} & R &= \frac{r}{a} \end{aligned} \right\} \quad (3-67)$$

Equations (3-64) and (3-65) in dimensionless form are

$$U \frac{\partial U}{\partial Z} + V \frac{\partial U}{\partial R} = \frac{1}{R} \frac{\partial U}{\partial R} + \frac{\partial^2 U}{\partial R^2} \quad (3-68)$$

$$\frac{\partial U}{\partial Z} + \frac{1}{R} \frac{\partial (VR)}{\partial R} = 0 \quad (3-69)$$

The boundary conditions in dimensionless form are

$$\left. \begin{aligned} U(R, 0) &= 1 & R \leq 1 \\ U(R, 0) &= \frac{U_s}{U_p} & R > 1 \\ U(\infty, Z) &= \frac{U_s}{U_p} \\ \frac{\partial U}{\partial R}(0, Z) &= 0 \\ V(0, Z) &= 0 \end{aligned} \right\} \quad (3-70)$$

3.2.1.1 Highly implicit difference representation valid for small secondary velocities.—Equation (3-68) must now be placed in finite difference form. The

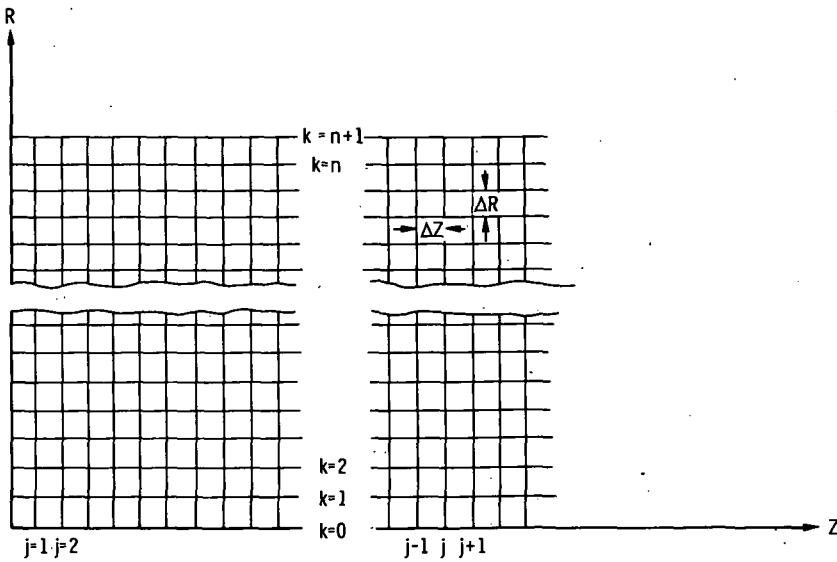


FIGURE 3-4. — Finite difference grid for axisymmetric jet.

finite difference grid is shown in figure 3-4. As in the two-dimensional case, a nonlinear finite difference form of the momentum equation is necessary in order that the representation be consistent for zero or small secondary velocities. The finite difference form chosen for equation (3-68) is

$$\begin{aligned}
 U_{j+1,k} \frac{U_{j+1,k} - U_{j,k}}{\Delta Z} + V_{j+1,k} \frac{U_{j+1,k+1} - U_{j+1,k-1}}{2(\Delta R)} \\
 = \frac{1}{R_k} \frac{U_{j+1,k+1} - U_{j+1,k-1}}{2(\Delta R)} + \frac{U_{j+1,k+1} - 2U_{j+1,k} + U_{j+1,k-1}}{(\Delta R)^2} \quad (3-71)
 \end{aligned}$$

Equation (3-71) applies for all $k > 0$. For $k = 0$, a special form of the equation must be obtained by letting $R \rightarrow 0$ in equation (3-68). Equation (3-68) then becomes

$$U \frac{\partial U}{\partial Z} \Big|_{R=0} = \lim_{R \rightarrow 0} \left(\frac{1}{R} \frac{\partial U}{\partial R} \right) + \frac{\partial^2 U}{\partial R^2} \Big|_{R=0} \quad (3-72)$$

When L'Hospital's rule is applied to the first term on the right side, equation (3-72) becomes

$$U \frac{\partial U}{\partial Z} \Big|_{R=0} = 2 \frac{\partial^2 U}{\partial R^2} \Big|_{R=0} \quad (3-73)$$

Equation (3-73) may be written in difference form as

$$U_{j+1,0} \frac{U_{j+1,0} - U_{j,0}}{\Delta Z} = 4 \left[\frac{U_{j+1,1} - U_{j+1,0}}{(\Delta R)^2} \right] \quad (3-74)$$

Incorporated in equation (3-74) is the symmetry condition

$$U_{j+1,1} = U_{j+1,-1}$$

Continuity (eq. (3-69)) may be written in finite difference form as

$$\frac{U_{j+1,k} - U_{j,k}}{\Delta Z} + \frac{1}{R_k} \left(\frac{V_{j+1,k+1} R_{k+1} - V_{j+1,k} R_k}{\Delta R} \right) = 0 \quad (3-75)$$

A special form of continuity is also necessary for $k=0$. This may be found by letting $R \rightarrow 0$ in equation (3-69). This gives

$$\left. \frac{\partial U}{\partial Z} \right|_{R=0} + 2 \left. \frac{\partial V}{\partial R} \right|_{R=0} = 0 \quad (3-76)$$

The finite difference form used for (3-76) is

$$\frac{U_{j+1,0} - U_{j,0}}{\Delta Z} + 2 \left(\frac{V_{j+1,1}}{\Delta R} \right) = 0 \quad (3-77)$$

Equation (3-75) then applies for $k > 0$ and equation (3-77) for $k=0$.

The method of solution for equations (3-71) and (3-74) is very similar to that used for the plane jet in section 3.1.1. The superscript (l) indicates values obtained on the (l)th iteration while those with superscript ($l+1$) are the ones obtained on the ($l+1$)th iteration. Equation (3-71), valid for $k > 0$, may be written in the form

$$\left[-\frac{V_{j+1,k}^{(l)}}{2(\Delta R)} + \frac{1}{2R_k(\Delta R)} - \frac{1}{(\Delta R)^2} \right] U_{j+1,k-1}^{(l+1)} + \left[\frac{U_{j+1,k}^{(l)}}{\Delta Z} + \frac{2}{(\Delta R)^2} \right] U_{j+1,k}^{(l+1)} \\ + \left[\frac{V_{j+1,k}^{(l)}}{2(\Delta R)} - \frac{1}{2R_k(\Delta R)} - \frac{1}{(\Delta R)^2} \right] U_{j+1,k+1}^{(l+1)} = \frac{U_{j+1,k}^{(l)} U_{j,k}}{\Delta Z} \quad (3-78)$$

Equation (3-74), valid for $k=0$, may be written as

$$\left[\frac{U_{j+1,0}^{(l)}}{\Delta Z} + \frac{4}{(\Delta R)^2} \right] U_{j+1,0}^{(l+1)} + \left[\frac{-4}{(\Delta R)^2} \right] U_{j+1,1}^{(l+1)} = \frac{U_{j+1,0}^{(l)} U_{j,0}}{\Delta Z} \quad (3-79)$$

Equation (3-78) written for $k=1(1)n$ along with equation (3-79) for $k=0$ now constitute $(n+1)$ equations in the $(n+1)$ unknowns $U_{j+1,k}^{(l+1)}$. At each iteration, these may be considered as linear since all values with superscript (l) are known

and from equation (3-75) for $k > 0$

$$V_{j+1,k+1}^{(l+1)} = V_{j+1,k}^{(l+1)} \left(\frac{R_k}{R_{k+1}} \right) - \frac{(\Delta R)R_k}{(\Delta Z)R_{k+1}} (U_{j+1,k}^{(l+1)} - U_{j,k}) \quad (3-82)$$

The values of $V_{j+1,k}^{(l+1)}$ can be found in a stepwise manner working outward from $k=0$.

The iteration is now complete and the values just determined now assume a superscript (l) and the process is repeated. This is continued until the values of $U_{j+1,k}^{(l+1)}$ and $U_{j+1,k}^{(l)}$ as well as $V_{j+1,k}^{(l+1)}$ and $V_{j+1,k}^{(l)}$ agree to within some predetermined accuracy. Then another step ΔZ downstream may be taken and the iterative procedure again employed.

3.2.1.2 Implicit difference representation valid only for large secondary velocities.—As in the plane case, if the secondary velocity is sufficiently high, a linear representation of the difference equation for momentum may be used. This representation of equation (3-68) is, for $k > 0$,

$$U_{j,k} \frac{U_{j+1,k} - U_{j,k}}{\Delta Z} + V_{j,k} \frac{U_{j+1,k+1} - U_{j+1,k-1}}{2(\Delta R)} \\ = \frac{1}{R_k} \frac{U_{j+1,k+1} - U_{j+1,k-1}}{2(\Delta R)} + \frac{U_{j+1,k+1} - 2U_{j+1,k} + U_{j+1,k-1}}{(\Delta R)^2} \quad (3-83)$$

and the finite difference form of equation (3-73) is, for $k = 0$,

$$U_{j,0} \frac{U_{j+1,0} - U_{j,0}}{\Delta Z} = 4 \frac{U_{j+1,1} - U_{j+1,0}}{(\Delta R)^2} \quad (3-84)$$

Equations (3-83) and (3-84) may be written in more useful forms as

$$\left[-\frac{V_{j,k}}{2(\Delta R)} + \frac{1}{2R_k(\Delta R)} - \frac{1}{(\Delta R)^2} \right] U_{j+1,k-1} + \left[\frac{U_{j,k}}{\Delta Z} + \frac{2}{(\Delta R)^2} \right] U_{j+1,k} \\ + \left[\frac{V_{j,k}}{2(\Delta R)} - \frac{1}{2R_k(\Delta R)} - \frac{1}{(\Delta R)^2} \right] U_{j+1,k+1} = \frac{U_{j,k}^2}{\Delta Z} \quad (3-85)$$

and

$$\left[\frac{U_{j,0}}{\Delta Z} + \frac{4}{(\Delta R)^2} \right] U_{j+1,0} + \left[-\frac{4}{(\Delta R)^2} \right] U_{j+1,1} = \frac{U_{j,0}^2}{\Delta Z} \quad (3-86)$$

Equation (3-85) written for $k=1(1)n$ along with equation (3-86) for $k=0$ constitutes a complete set of linear equations in the values of $U_{j+1,k}$ and may be

$$V_{j+1, k+1} = V_{j+1, k} \left(\frac{R_k}{R_{k+1}} \right) - \frac{(\Delta R)R_k}{(\Delta Z)R_{k+1}} (U_{j+1, k} - U_{j, k}) \quad (3-89)$$

Another step ΔZ downstream may now be taken and the procedure repeated.

3.2.2 Incompressible Constant Property Flow – Temperature Solution

Under the assumption of constant properties and neglecting viscous dissipation, the energy equation for the axisymmetric jet is given by

$$\rho c_p \left(u \frac{\partial t}{\partial z} + v \frac{\partial t}{\partial r} \right) = k \left(\frac{\partial^2 t}{\partial r^2} + \frac{1}{r} \frac{\partial t}{\partial r} \right) \quad (3-90)$$

The boundary conditions are

$$\left. \begin{aligned} t(r, 0) &= t_p & (r \leq a) \\ t(r, 0) &= t_s & (r > a) \\ t(\infty, z) &= t_s \\ \frac{\partial t}{\partial r}(0, z) &= 0 \end{aligned} \right\} \quad (3-91)$$

Equation (3-90) may be made dimensionless by the following choice of dimensionless variables:

$$\left. \begin{aligned} T &= \frac{t - t_s}{t_p - t_s} & U &= \frac{u}{u_p} \\ Z &= \frac{z\mu}{\rho u_p a^2} & V &= \frac{\rho v a}{\mu} \\ R &= \frac{r}{a} \end{aligned} \right\} \quad (3-92)$$

If these variables are inserted into equations (3-90) and (3-91) the problem may be restated in dimensionless terms as

$$U \frac{\partial T}{\partial Z} + V \frac{\partial T}{\partial R} = \frac{1}{Pr} \left(\frac{\partial^2 T}{\partial R^2} + \frac{1}{R} \frac{\partial T}{\partial R} \right) \quad (3-93)$$

subject to

$$\left. \begin{aligned} T(R, 0) &= 1 & (R \leq 1) \\ T(R, 0) &= 0 & (R > 1) \\ T(\infty, Z) &= 0 \\ \frac{\partial T}{\partial R}(0, Z) &= 0 \end{aligned} \right\} \quad (3-94)$$

As in the plane case, the difference representation for the energy equation will correspond to the nonlinear representation of the momentum equation, which in this case is equation (3-71). If the form (3-83) can be used for the momentum equation, the coefficients of the convective terms in the next equation should be replaced by $U_{j,k}$ and $V_{j,k}$.

The finite difference form of (3-93) chosen is

$$\begin{aligned} U_{j+1,k} \frac{T_{j+1,k} - T_{j,k}}{\Delta Z} + V_{j+1,k} \frac{T_{j+1,k+1} - T_{j+1,k-1}}{2(\Delta R)} \\ = \frac{1}{Pr} \left[\frac{T_{j+1,k+1} - 2T_{j+1,k} + T_{j+1,k-1}}{(\Delta R)^2} + \frac{1}{R_k} \frac{T_{j+1,k+1} - T_{j+1,k-1}}{2(\Delta R)} \right] \end{aligned} \quad (3-95)$$

This equation is valid for $k > 0$ and may more conveniently be written as

$$\begin{aligned} \left[\frac{-V_{j+1,k}}{2(\Delta R)} - \frac{1}{Pr(\Delta R)^2} + \frac{1}{2(Pr)R_k(\Delta R)} \right] T_{j+1,k-1} + \left[\frac{U_{j+1,k}}{\Delta Z} + \frac{2}{Pr(\Delta R)^2} \right] T_{j+1,k} \\ + \left[\frac{V_{j+1,k}}{2(\Delta R)} - \frac{1}{Pr(\Delta R)^2} - \frac{1}{2(Pr)R_k(\Delta R)} \right] T_{j+1,k+1} = \frac{U_{j+1,k}T_{j,k}}{\Delta Z} \end{aligned} \quad (3-96)$$

For $k=0$ a special form is necessary. Taking the limit of equation (3-93) as $R \rightarrow 0$ gives

$$U \frac{\partial T}{\partial Z} \Big|_{R=0} = \frac{2}{Pr} \frac{\partial^2 T}{\partial R^2} \Big|_{R=0} \quad (3-97)$$

This may be written in finite difference form as

$$U_{j+1,0} \frac{T_{j+1,0} - T_{j,0}}{\Delta Z} = \frac{4}{Pr} \frac{T_{j+1,1} - T_{j+1,0}}{(\Delta R)^2} \quad (3-98)$$

Equation (3-98) incorporates the symmetry condition $T_{j+1,1} = T_{j+1,-1}$. This may be rearranged in a more useful form as

while keeping the total number of points reasonably small should be employed. Details are given in section 2.1.1. It is, of course, most desirable to employ the same grid for the velocity and temperature solutions.

The finite difference representation is universally stable for all mesh sizes. The truncation error of the energy equation is of $\mathcal{O}(\Delta R^2)$ and $\mathcal{O}(\Delta Z)$.

3.2.3 Compressible Flow—Velocity and Temperature Solutions

In the compressible flow situation the basic equations are coupled. For this case they are

$$\rho \left(u \frac{\partial u}{\partial z} + v \frac{\partial u}{\partial r} \right) = \frac{1}{r} \frac{\partial}{\partial r} \left(\mu r \frac{\partial u}{\partial r} \right) \quad (3-101)$$

$$\frac{\partial(\rho u)}{\partial z} + \frac{1}{r} \frac{\partial(\rho r v)}{\partial r} = 0 \quad (3-102)$$

$$\rho c_p \left(u \frac{\partial t}{\partial z} + v \frac{\partial t}{\partial r} \right) = \frac{1}{r} \frac{\partial}{\partial r} \left(k r \frac{\partial t}{\partial r} \right) + \mu \left(\frac{\partial u}{\partial r} \right)^2 \quad (3-103)$$

$$\rho t = \text{constant} \quad (3-104)$$

$$\mu = \mu(t) \quad (3-105)$$

$$k = k(t) \quad (3-106)$$

subject to the boundary conditions

$$\left. \begin{aligned} u(r, 0) &= u_p && (r \leq a) \text{ (see appendix F)} \\ u(r, 0) &= u_s && (r > a) \\ u(\infty, z) &= u_s \\ \frac{\partial u}{\partial r}(0, z) &= 0 \\ v(0, z) &= 0 \\ t(r, 0) &= t_p && (r \leq a) \\ t(r, 0) &= t_s && (r > a) \\ t(\infty, z) &= t_s \\ \frac{\partial t}{\partial r}(0, z) &= 0 \end{aligned} \right\} \quad (3-107)$$

The basic equations may be put in dimensionless form by the following choice of dimensionless variables:

$$\left. \begin{aligned} U &= u/u_p \\ V &= \frac{\rho_p v a}{\mu_p} \\ T &= t/t_p \\ Z &= \frac{z \mu_p}{\rho_p u_p a^2} \\ R &= r/a \\ k^* &= k/k_p \\ \mu^* &= \mu/\mu_p \\ \rho^* &= \rho/\rho_p \end{aligned} \right\} \quad (3-108)$$

As in the plane case, the primary conditions at the jet mouth have been chosen as reference values. Inserting the dimensionless variables (3-108) into equations (3-101) to (3-106) gives

$$\rho^* \left(U \frac{\partial U}{\partial Z} + V \frac{\partial U}{\partial R} \right) = \frac{1}{R} \frac{\partial}{\partial R} \left(\mu^* R \frac{\partial U}{\partial R} \right) \quad (3-109)$$

$$\frac{\partial(\rho^* U)}{\partial Z} + \frac{1}{R} \frac{\partial(\rho^* R V)}{\partial R} = 0 \quad (3-110)$$

$$\rho^* \left(U \frac{\partial T}{\partial Z} + V \frac{\partial T}{\partial R} \right) = \frac{1}{Pr(R)} \frac{\partial}{\partial R} \left(k^* R \frac{\partial T}{\partial R} \right) + (\gamma - 1) M_p^2 \mu^* \left(\frac{\partial U}{\partial R} \right)^2 \quad (3-111)$$

$$\rho^* T = 1 \quad (3-112)$$

$$\mu^* = (T)^f \quad (3-113)$$

$$k^* = (T)^g \quad (3-114)$$

where

$$M_p = \frac{u_p}{\sqrt{\gamma R t_p}}$$

and

$$Pr = \left(\frac{\mu c_p}{k} \right)_p$$

The usual power law relationships have been assumed for equations (3-113) and (3-114).

The transformed boundary conditions in dimensionless form are

$$\left. \begin{aligned}
 U(R, 0) &= 1 & (R \leq 1) \\
 U(R, 0) &= \frac{u_s}{u_p} & (R > 1) \\
 U(\infty, Z) &= \frac{u_s}{u_p} \\
 \frac{\partial U}{\partial R}(0, Z) &= 0 \\
 V(0, Z) &= 0 \\
 T(R, 0) &= 1 & (R \leq 1) \\
 T(R, 0) &= \frac{t_s}{t_p} & (R > 1) \\
 T(\infty, Z) &= \frac{t_s}{t_p} \\
 \frac{\partial T}{\partial R}(0, Z) &= 0
 \end{aligned} \right\} \quad (3-115)$$

3.2.3.1 *Highly implicit difference representation valid for small secondary velocities.*—Equations (3-109) to (3-114) may now be expressed in finite difference form. The form chosen is quite similar to that used for the plane case in section 3.1.3 and the discussions given there also apply to this case. The form is consistent for all secondary velocities including zero. Equations (3-109) to (3-114) are represented as

$$\begin{aligned}
 \rho_{j+1,k}^* & \left[U_{j+1,k} \frac{U_{j+1,k} - U_{j,k}}{\Delta Z} + V_{j+1,k} \frac{U_{j+1,k+1} - U_{j+1,k-1}}{2(\Delta R)} \right] \\
 &= \mu_{j+1,k}^* \left[\frac{U_{j+1,k+1} - 2U_{j+1,k} + U_{j+1,k-1}}{(\Delta R)^2} \right. \\
 & \quad \left. + \frac{1}{R_k} \frac{U_{j+1,k+1} - U_{j+1,k-1}}{2(\Delta R)} \right] \\
 & \quad + \left[\frac{\mu_{j+1,k+1}^* - \mu_{j+1,k-1}^*}{2(\Delta R)} \right] \left[\frac{U_{j+1,k+1} - U_{j+1,k-1}}{2(\Delta R)} \right] \quad (3-116)
 \end{aligned}$$

$$\frac{\rho_{j+1,k}^* U_{j+1,k} - \rho_{j,k}^* U_{j,k}}{\Delta Z} + \frac{\rho_{j+1,k+1}^* R_{k+1} V_{j+1,k+1} - \rho_{j+1,k}^* R_k V_{j+1,k}}{R_k \Delta R} = 0 \quad (3-117)$$

CG

$$\begin{aligned}
 & \rho_{j+1,k}^* \left[U_{j+1,k} \frac{T_{j+1,k} - T_{j,k}}{\Delta Z} + V_{j+1,k} \frac{T_{j+1,k+1} - T_{j+1,k-1}}{2(\Delta R)} \right] \\
 &= \frac{1}{Pr} \left\{ k_{j+1,k}^* \left[\frac{T_{j+1,k+1} - 2T_{j+1,k} + T_{j+1,k-1}}{(\Delta R)^2} + \frac{1}{R_k} \frac{T_{j+1,k+1} - T_{j+1,k-1}}{2(\Delta R)} \right] \right. \\
 & \quad \left. + \left[\frac{k_{j+1,k+1}^* - k_{j+1,k-1}^*}{2(\Delta R)} \right] \left[\frac{T_{j+1,k+1} - T_{j+1,k-1}}{2(\Delta R)} \right] \right\} \\
 & \quad + (\gamma - 1) M_p^2 \mu_{j+1,k}^* \left[\frac{U_{j+1,k+1} - U_{j+1,k-1}}{2(\Delta R)} \right]^2 \quad (3-118)
 \end{aligned}$$

$$\rho_{j+1,k}^* = \frac{1}{T_{j+1,k}} \quad (3-119)$$

$$\mu_{j+1,k}^* = (T_{j+1,k})^f \quad (3-120)$$

$$k_{j+1,k}^* = (T_{j+1,k})^g \quad (3-121)$$

Equations (3-116), (3-117), and (3-118) are valid for $k > 0$ only. For $k = 0$, special forms are required. These are found by first taking the limits of equations (3-109), (3-110), and (3-111) as $R \rightarrow 0$. Equation (3-109) becomes

$$\rho^* U \frac{\partial U}{\partial Z} \Big|_{R=0} = 2\mu^* \left(\frac{\partial^2 U}{\partial R^2} \right) \Big|_{R=0} \quad (3-122)$$

equation (3-110) becomes

$$\frac{\partial(\rho^* U)}{\partial Z} \Big|_{R=0} + 2\rho^* \left(\frac{\partial V}{\partial R} \right) \Big|_{R=0} = 0 \quad (3-123)$$

and equation (3-111) becomes

$$\rho^* U \frac{\partial T}{\partial Z} \Big|_{R=0} = \frac{2k^*}{Pr} \left(\frac{\partial^2 T}{\partial R^2} \right) \Big|_{R=0} \quad (3-124)$$

Equations (3-122), (3-123), and (3-124) may be rewritten in finite difference form as

$$\rho_{j+1,0}^* U_{j+1,0} \left(\frac{U_{j+1,0} - U_{j,0}}{\Delta Z} \right) = 4\mu_{j+1,0}^* \left[\frac{U_{j+1,1} - U_{j+1,0}}{(\Delta R)^2} \right] \quad (3-125)$$

$$\frac{\rho_{j+1,0}^* U_{j+1,0} - \rho_{j,0}^* U_{j,0}}{\Delta Z} + 2\rho_{j+1,0}^* \left(\frac{V_{j+1,1}}{\Delta R} \right) = 0 \quad (3-126)$$

$$\rho_{j+1,0}^* U_{j+1,0} \left(\frac{T_{j+1,0} - T_{j,0}}{\Delta Z} \right) = \frac{4k_{j+1,0}^*}{Pr} \left[\frac{T_{j+1,1} - T_{j+1,0}}{(\Delta R)^2} \right] \quad (3-127)$$

These equations are valid for $k=0$.

The iterative method of solution to equations (3-116) to (3-121) and (3-125) to (3-127) is identical to that used in section 3.1.3 for the plane compressible jet and described in detail in that section; therefore much of the description is omitted in the following presentation. As before, the superscript (l) indicates values obtained on the (l) th iteration while the superscript $(l+1)$ indicates values obtained in the $(l+1)$ th iteration. Equations (3-116), (3-118), (3-125), and (3-127) are now rewritten as

$$\begin{aligned} & \left[-\frac{\rho_{j+1,k}^{*(l)} V_{j+1,k}^{(l)}}{2(\Delta R)} - \frac{\mu_{j+1,k}^{*(l)}}{(\Delta R)^2} + \frac{\mu_{j+1,k}^{*(l)}}{2(R_k) \Delta R} + \frac{\mu_{j+1,k+1}^{*(l)} - \mu_{j+1,k-1}^{*(l)}}{4(\Delta R)^2} \right] U_{j+1,k-1}^{(l+1)} \\ & + \left[\frac{\rho_{j+1,k}^{*(l)} U_{j+1,k}^{(l)}}{\Delta Z} + \frac{2\mu_{j+1,k}^{*(l)}}{(\Delta R)^2} \right] U_{j+1,k}^{(l+1)} \\ & + \left[\frac{\rho_{j+1,k}^{*(l)} V_{j+1,k}^{(l)}}{2(\Delta R)} - \frac{\mu_{j+1,k}^{*(l)}}{(\Delta R)^2} - \frac{\mu_{j+1,k}^{*(l)}}{2(R_k) \Delta R} - \frac{\mu_{j+1,k+1}^{*(l)} - \mu_{j+1,k-1}^{*(l)}}{4(\Delta R)^2} \right] U_{j+1,k+1}^{(l+1)} \\ & = \frac{\rho_{j+1,k}^{*(l)} U_{j+1,k}^{(l)} U_{j,k}}{\Delta Z} \end{aligned} \quad (3-128)$$

$$\begin{aligned} & \left[-\frac{\rho_{j+1,k}^{*(l)} V_{j+1,k}^{(l)}}{2(\Delta R)} - \frac{k_{j+1,k}^{*(l)}}{Pr(\Delta R)^2} + \frac{k_{j+1,k}^{*(l)}}{2R_k(\Delta R)Pr} + \frac{k_{j+1,k+1}^{*(l)} - k_{j+1,k-1}^{*(l)}}{4(Pr)(\Delta R)^2} \right] T_{j+1,k-1}^{(l+1)} \\ & + \left[\frac{\rho_{j+1,k}^{*(l)} U_{j+1,k}^{(l+1)}}{\Delta Z} + \frac{2k_{j+1,k}^{*(l)}}{Pr(\Delta R)^2} \right] T_{j+1,k}^{(l+1)} \\ & + \left[\frac{\rho_{j+1,k}^{*(l)} V_{j+1,k}^{(l)}}{2(\Delta R)} - \frac{k_{j+1,k}^{*(l)}}{Pr(\Delta R)^2} - \frac{k_{j+1,k}^{*(l)}}{2R_k(\Delta R)Pr} - \frac{k_{j+1,k+1}^{*(l)} - k_{j+1,k-1}^{*(l)}}{4(Pr)(\Delta R)^2} \right] T_{j+1,k+1}^{(l+1)} \\ & = \frac{\rho_{j+1,k}^{*(l)} U_{j+1,k}^{(l+1)} T_{j,k}}{\Delta Z} + (\gamma - 1) M_p^2 \mu_{j+1,k}^{*(l)} \left(\frac{U_{j+1,k+1}^{(l+1)} - U_{j+1,k-1}^{(l+1)}}{2(\Delta R)} \right)^2 \end{aligned} \quad (3-129)$$

$$\begin{aligned} & \left[\frac{\rho_{j+1,0}^{*(l)} U_{j+1,0}^{(l)}}{\Delta Z} + \frac{4\mu_{j+1,0}^{*(l)}}{(\Delta R)^2} \right] U_{j+1,0}^{(l+1)} + \left[-\frac{4}{(\Delta R)^2} \mu_{j+1,0}^{*(l)} \right] U_{j+1,1}^{(l+1)} \\ & = \frac{\rho_{j+1,0}^{*(l)} U_{j+1,0}^{(l)} U_{j,0}}{\Delta Z} \end{aligned} \quad (3-130)$$

$$\beta_0^{(l)} = \frac{\rho_{j+1,0}^{*(l)} U_{j+1,0}^{(l)}}{\Delta Z} + \frac{4\mu_{j+1,0}^{*(l)}}{(\Delta R)^2} \quad (k=0)$$

The set of linear equations resulting when (3-129) is written for $k=1(l)n$ plus (3-131) for $k=0$ may be combined in matrix form as

$$\begin{pmatrix} \beta_0^{(l)} & -4k_{j+1,0}^{*(l)} \\ \alpha_1^{(l)} & \beta_1^{(l)} & \Omega_1^{(l)} \\ & \alpha_2^{(l)} & \beta_2^{(l)} & \Omega_2^{(l)} \\ & & \dots & \dots \\ & & & \alpha_{n-1}^{(l)} & \beta_{n-1}^{(l)} & \Omega_{n-1}^{(l)} \\ & & & & \alpha_n^{(l)} & \beta_n^{(l)} \end{pmatrix} \times \begin{pmatrix} T_{j+1,0}^{(l+1)} \\ T_{j+1,1}^{(l+1)} \\ T_{j+1,2}^{(l+1)} \\ \dots \\ T_{j+1,n-1}^{(l+1)} \\ T_{j+1,n}^{(l+1)} \end{pmatrix} = \begin{pmatrix} \phi_0^{(l)} \\ \phi_1^{(l)} \\ \phi_2^{(l)} \\ \dots \\ \phi_{n-1}^{(l)} \\ \phi_n^{(l)} - \Omega_n^{(l)}(t_s/t_n) \end{pmatrix} \quad (3-133)$$

where

$$\alpha_k^{(l)} = \frac{-\rho_{j+1,k}^{*(l)} V_{j+1,k}^{(l)}}{2(\Delta R)} - \frac{k_{j+1,k}^{*(l)}}{Pr(\Delta R)^2} + \frac{k_{j+1,k}^{*(l)}}{2(R_k)(\Delta R)Pr} + \frac{k_{j+1,k+1}^{*(l)} - k_{j+1,k-1}^{*(l)}}{4(Pr)(\Delta R)^2}$$

$$\beta_k^{(l)} = \frac{\rho_{j+1,k}^{*(l)} U_{j+1,k}^{(l+1)}}{\Delta Z} + \frac{2k_{j+1,k}^{*(l)}}{Pr(\Delta R)^2} \quad (k > 0)$$

$$\Omega_k^{(l)} = \frac{\rho_{j+1,k}^{*(l)} V_{j+1,k}^{(l)}}{2(\Delta R)} - \frac{k_{j+1,k}^{*(l)}}{Pr(\Delta R)^2} - \frac{k_{j+1,k}^{*(l)}}{2(R_k)(\Delta R)Pr} - \frac{k_{j+1,k+1}^{*(l)} - k_{j+1,k-1}^{*(l)}}{4(Pr)(\Delta R)^2}$$

$$\phi_k^{(l)} = \frac{\rho_{j+1,k}^{*(l)} U_{j+1,k}^{(l+1)} T_{j,k}}{\Delta Z} + (\gamma - 1) M_d^2 \mu_{j+1,k}^{*(l)} \left[\frac{U_{j+1,k+1}^{(l+1)} - U_{j+1,k-1}^{(l+1)}}{2(\Delta R)} \right]^2$$

and

$$\beta_0^{(l)} = \frac{\rho_{j+1,0}^{*(l)} U_{j+1,0}^{(l+1)}}{\Delta Z} + \frac{4k_{j+1,0}^{*(l)}}{(\Delta R)^2} \quad (k=0)$$

For each iteration the set of equations represented by (3-132) is first solved for $U_{j+1,k}^{(l+1)}$, then the set represented by (3-133) is solved for $T_{j+1,k}^{(l+1)}$, and finally the

equation of state (3-119) is solved for $\rho_{j+1,k}^{*(l+1)}$ to yield

$$\rho_{j+1,k}^{*(l+1)} = \frac{1}{T_{j+1,k}^{(l+1)}} \quad (3-134)$$

The continuity equation for $k=0$ (eq. (3-126)) may now be solved for $V_{j+1,1}^{(l+1)}$:

$$V_{j+1,1}^{(l+1)} = \frac{\Delta R}{2(\Delta Z)} \left[\frac{\rho_{j,0}^*}{\rho_{j+1,0}^{*(l+1)}} U_{j,0} - U_{j+1,0}^{(l+1)} \right] \quad (3-135)$$

The remaining values of $V_{j+1,k}^{(l+1)}$ are found from equation (3-117):

$$V_{j+1,k+1}^{(l+1)} = \frac{\rho_{j+1,k}^{*(l+1)} R_k}{\rho_{j+1,k+1}^{*(l+1)} R_{k+1}} V_{j+1,k}^{(l+1)} + \frac{R_k \Delta R}{R_{k+1} \Delta Z} \frac{(\rho_{j,k}^* U_{j,k} - \rho_{j+1,k}^{*(l+1)} U_{j+1,k}^{(l+1)})}{\rho_{j+1,k+1}^{*(l+1)}} \quad (3-136)$$

Equation (3-136) may be solved in a stepwise manner working outward from $k=1$. Finally, equations (3-120) and (3-121) are solved to find $\mu_{j+1,k}^{*(l+1)}$ and $k_{j+1,k}^{*(l+1)}$. The iterative process is repeated until the solution has converged to the desired accuracy and then another step downstream may be taken.

3.2.3.2 Implicit difference representation valid only for large secondary velocities.—As in the plane case in section 3.1.3, if the secondary velocity is large, the difference equations may be written in a linear form. The forms chosen for equations (3-109) to (3-114) are

$$\begin{aligned} \rho_{j,k}^* \left[U_{j,k} \frac{U_{j+1,k} - U_{j,k}}{\Delta Z} + V_{j,k} \frac{U_{j+1,k+1} - U_{j+1,k-1}}{2(\Delta R)} \right] \\ = \mu_{j,k}^* \left[\frac{U_{j+1,k+1} - 2U_{j+1,k} + U_{j+1,k-1}}{(\Delta R)^2} + \frac{1}{R_k} \frac{U_{j+1,k+1} - U_{j+1,k-1}}{2(\Delta R)} \right] \\ + \left[\frac{\mu_{j,k+1}^* - \mu_{j,k}^*}{2(\Delta R)} \right] \left[\frac{U_{j+1,k+1} - U_{j+1,k-1}}{2(\Delta R)} \right] \quad (3-137) \end{aligned}$$

$$\frac{\rho_{j+1,k}^* U_{j+1,k} - \rho_{j,k}^* U_{j,k}}{\Delta Z} + \frac{\rho_{j+1,k+1}^* R_{k+1} V_{j+1,k+1} - \rho_{j+1,k}^* R_k V_{j+1,k}}{\Delta R} = 0 \quad (3-138)$$

$$\begin{aligned} \rho_{j,k}^* \left[U_{j,k} \frac{T_{j+1,k} - T_{j,k}}{\Delta Z} + V_{j,k} \frac{T_{j+1,k+1} - T_{j+1,k-1}}{2(\Delta R)} \right] \\ = \frac{1}{Pr} \left\{ k_{j,k}^* \left[\frac{T_{j+1,k+1} - 2T_{j+1,k} + T_{j+1,k-1}}{(\Delta R)^2} + \frac{1}{R_k} \frac{T_{j+1,k+1} - T_{j+1,k-1}}{2(\Delta R)} \right] + \right. \end{aligned}$$

$$\begin{aligned}
 & + \left[\frac{k_{j,k+1}^* - k_{j,k-1}^*}{2(\Delta R)} \right] \left[\frac{T_{j+1,k+1} - T_{j+1,k-1}}{2(\Delta R)} \right] \\
 & + (\gamma - 1) M_p^2 \mu_{j,k}^* \left[\frac{U_{j+1,k+1} - U_{j+1,k-1}}{2(\Delta R)} \right]^2 \tag{3-139}
 \end{aligned}$$

$$\rho_{j+1,k}^* T_{j+1,k} = 1 \tag{3-140}$$

$$\mu_{j+1,k}^* = (T_{j+1,k})^f \tag{3-141}$$

$$k_{j+1,k}^* = (T_{j+1,k})^g \tag{3-142}$$

For $k=0$, the following forms are needed for equations (3-122) to (3-124):

$$\rho_{j,0}^* U_{j,0} \left(\frac{U_{j+1,0} - U_{j,0}}{\Delta Z} \right) = 4\mu_{j,0}^* \left[\frac{U_{j+1,1} - U_{j+1,0}}{(\Delta R)^2} \right] \tag{3-143}$$

$$\frac{\rho_{j+1,0}^* U_{j+1,0} - \rho_{j,0}^* U_{j,0}}{\Delta Z} + \frac{2\rho_{j+1,0}^* V_{j+1,1}}{\Delta R} = 0 \tag{3-144}$$

and

$$\rho_{j,0}^* U_{j,0} \left(\frac{T_{j+1,0} - T_{j,0}}{\Delta Z} \right) = \frac{4k_{j,0}^*}{P_r} \left[\frac{T_{j+1,1} - T_{j+1,0}}{(\Delta R)^2} \right] \tag{3-145}$$

Equations (3-137) and (3-143) may be rewritten in more convenient forms. Equation (3-137), valid for $k > 0$, becomes

$$\begin{aligned}
 & \left[\frac{-\rho_{j,k}^* V_{j,k}}{2(\Delta R)} - \frac{\mu_{j,k}^*}{(\Delta R)^2} + \frac{\mu_{j,k}^*}{2(R_k)\Delta R} + \frac{\mu_{j,k+1}^* - \mu_{j,k-1}^*}{4(\Delta R)^2} \right] U_{j+1,k-1} \\
 & + \left[\frac{\rho_{j,k}^* U_{j,k}}{\Delta Z} + \frac{2\mu_{j,k}^*}{(\Delta R)^2} \right] U_{j+1,k} + \left[\frac{\rho_{j,k}^* V_{j,k}}{2(\Delta R)} - \frac{\mu_{j,k}^*}{(\Delta R)^2} \right. \\
 & \left. - \frac{\mu_{j,k}^*}{2(R_k)\Delta R} - \frac{\mu_{j,k+1}^* - \mu_{j,k-1}^*}{4(\Delta R)^2} \right] U_{j+1,k+1} = \frac{\rho_{j,k}^* U_{j,k}^2}{\Delta Z} \tag{3-146}
 \end{aligned}$$

and equation (3-143), valid for $k=0$, becomes

$$\begin{aligned}
 & + \left[\frac{\rho_{j,k}^* U_{j,k}}{\Delta Z} + \frac{2k_{j,k}^*}{Pr (\Delta R)^2} \right] T_{j+1,k} \\
 & + \left[\frac{\rho_{j,k}^* V_{j,k}}{2 (\Delta R)} - \frac{k_{j,k}^*}{Pr (\Delta R)^2} - \frac{k_{j,k}^*}{2R_k (\Delta R) Pr} - \frac{k_{j,k+1}^* - k_{j,k-1}^*}{4(Pr) (\Delta R)^2} \right] T_{j+1,k+1} \\
 & = \frac{U_{j,k}}{\Delta Z} + (\gamma - 1) M_\nu^2 \mu_{j,k}^* \left(\frac{U_{j+1,k+1} - U_{j+1,k-1}}{2(\Delta Y)} \right)^2 \quad (3-149)
 \end{aligned}$$

(The relationship $\rho_{j,k}^* T_{j,k} = 1$ has been employed in (3-149).) For $k=0$,

$$\begin{aligned}
 & \left[\frac{\rho_{j,0}^* U_{j,0}}{\Delta Z} + \frac{4k_{j,0}^*}{(Pr) (\Delta R)^2} \right] T_{j+1,0} \\
 & + \left[\frac{-4k_{j,0}^*}{Pr (\Delta R)^2} \right] T_{j+1,1} = \frac{\rho_{j,0}^* U_{j,0} T_{j,0}}{\Delta Z} = \frac{U_{j,0}}{\Delta Z} \quad (3-150)
 \end{aligned}$$

Equation (3-149) written for $k = 1(1)n$ and equation (3-150) for $k = 0$ are a complete set of linear equations in $T_{j+1,k}$. The set may be written in matrix form as

$$\begin{array}{|cccc|} \hline \beta'_0 & \frac{-4k_{j,0}^*}{Pr (\Delta R)^2} & & \\ \hline \alpha'_1 & \beta'_1 & \Omega'_1 & \\ & \alpha'_2 & \beta'_2 & \Omega'_2 \\ & & \text{---} & \text{---} \\ & & \text{---} & \text{---} \\ & & \text{---} & \text{---} \\ & & \alpha'_{n-1} & \beta'_{n-1} & \Omega'_{n-1} \\ & & & \alpha'_n & \beta'_n \\ \hline \end{array} \times \begin{array}{|c|} \hline T_{j+1,0} \\ \hline T_{j+1,1} \\ \hline T_{j+1,2} \\ \hline \text{---} \\ \hline \text{---} \\ \hline T_{j+1,n-1} \\ \hline T_{j+1,n} \\ \hline \end{array} = \begin{array}{|c|} \hline \phi'_0 \\ \hline \phi'_1 \\ \hline \phi'_2 \\ \hline \text{---} \\ \hline \text{---} \\ \hline \phi'_{n-1} \\ \hline \phi'_n - \Omega'_n (t_s/t_\nu) \\ \hline \end{array} \quad (3-151)$$

where

$$\begin{aligned}
 \alpha'_k & = \frac{-\rho_{j,k}^* V_{j,k}}{2(\Delta R)} - \frac{k_{j,k}^*}{(Pr) (\Delta R)^2} + \frac{k_{j,k}^*}{2R_k (Pr) (\Delta R)} + \frac{k_{j,k+1}^* - k_{j,k-1}^*}{4(Pr) (\Delta R)^2} \\
 \beta'_k & = \frac{\rho_{j,k}^* U_{j,k}}{\Delta Z} + \frac{2k_{j,k}^*}{Pr (\Delta R)^2} \quad (k > 0)
 \end{aligned}$$

$$\Omega'_k = \frac{\rho_{j,k}^* V_{j,k}}{2(\Delta R)} - \frac{k_{j,k}^*}{(Pr)(\Delta R)^2} - \frac{k_{j,k}^*}{2R_k(Pr)(\Delta R)} - \frac{k_{j,k+1}^* - k_{j,k-1}^*}{4(Pr)(\Delta R)^2}$$

$$\phi'_k = \frac{\rho_{j,k}^* U_{j,k} T_{j,k}}{\Delta Z} + (\gamma - 1) M_\mu^2 \mu_{j,k}^* \left[\frac{U_{j+1,k+1} - U_{j+1,k-1}}{2(\Delta y)} \right]^2$$

and

$$\beta'_0 = \frac{\rho_{j,0}^* U_{j,0}}{\Delta Z} + \frac{4k_{j,0}^*}{Pr(\Delta R)^2} \quad (k=0)$$

The set of equations (3-148) may now be solved for $U_{j+1,k}$ using the method of appendix A, and then the set (3-151) can be solved for $T_{j+1,k}$ using the same method.

From equation (3-140) the density may now be found:

$$\rho_{j+1,k}^* = \frac{1}{T_{j+1,k}} \quad (3-152)$$

The continuity equation is next solved for $V_{j+1,k+1}$. First, for $k=0$ from equation (3-144),

$$V_{j+1,1} = \frac{\Delta R}{2\Delta Z} \left[-U_{j+1,0} + \left(\frac{\rho_{j,0}^*}{\rho_{j+1,0}^*} \right) U_{j,0} \right] \quad (3-153)$$

and for $k=1(1)n$ from equation (3-138),

$$V_{j+1,k+1} = \left(\frac{\rho_{j+1,k}^* R_k}{\rho_{j+1,k+1}^* R_{k+1}} \right) V_{j+1,k} + \frac{\Delta R(R_k)}{\Delta Z(R_{k+1})} \left(\frac{\rho_{j,k}^* U_{j,k} - \rho_{j+1,k}^* U_{j+1,k}}{\rho_{j+1,k+1}^*} \right) \quad (3-154)$$

Finally, $\mu_{j+1,k}^*$ and $k_{j+1,k}^*$ may be found from equations (3-141) and (3-142). The solution may now be advanced downstream another step.

All forms of both the momentum and energy equations given in this section are universally stable except for $U < 0$ which presumably will not occur in the laminar jet flow situation.

The truncation error for both the momentum and energy equation difference representations is of $\mathcal{O}(\Delta R)^2$ and $\mathcal{O}(\Delta Z)$. The truncation error of the continuity equation is of $\mathcal{O}(\Delta R)$ and $\mathcal{O}(\Delta Z)$.

3.3 OTHER PROBLEMS WITH A SIMILAR FORMULATION

3.3.1 Jets With Body Forces

The basic formulations given in this chapter may be modified to include a body force of any type (for more details on the methods of solution when the body forces are electrical or magnetic in nature, see section 2.3.4). Body forces due to gravitational effects may also be readily included.

If the body force distribution is symmetric about the jet centerline in the main flow direction of the jet, symmetry is preserved. If this is not the case, the jet is no longer symmetric and it becomes necessary to determine the velocity distribution across the entire jet cross section at each axial step. In the case of the plane jet this means only that the full jet width must be considered instead of solving for velocities in only half of the jet width and then applying symmetry. If the body forces are sufficiently large, it may also become necessary to include the effects of momentum flux in the direction in which the body forces are applied. The formulations of this chapter may then no longer be directly applied. For the jet which has an initially circular cross section, body force distributions not axially symmetric and aligned with the main flow direction make the problem three dimensional and compound the complexity of a numerical solution enormously. The three-dimensional problem is not discussed here, but some idea of the difficulties involved and possible approaches to the problem may be found in later chapters of this book in connection with the discussion of flow in noncircular channels.

3.3.2 Jet Mixing When Primary and Secondary Streams Are Different Compressible Fluids

If a primary jet of gas issues into a secondary stream which is composed of a different gas, diffusion becomes one of the important mechanisms in the mixing process. The diffusion equation must then be included in the basic equations along with the proper equation of state, and the properties must be evaluated using the methods required for gas mixtures.

As an example of this type of problem, we shall consider the formulation for the plane mixing of a primary jet of gas with a moving or stationary secondary stream of a different gas at a different temperature. The configuration is shown in figure 3-5.

Pai (ref. 3) discusses the jet mixing of different gases, and the basic equations for diffusion may be found in Rohsenow and Choi (ref. 4) and Bird, Stewart, and Lightfoot (ref. 5). The equations given here are the result of the usual assumptions of the boundary layer type along with the assumption that the mass transfer due to diffusion involves a negligible momentum flux.

To the author's knowledge the finite difference formulation for this problem has not been previously available, although Pai presents a solution for the iso-

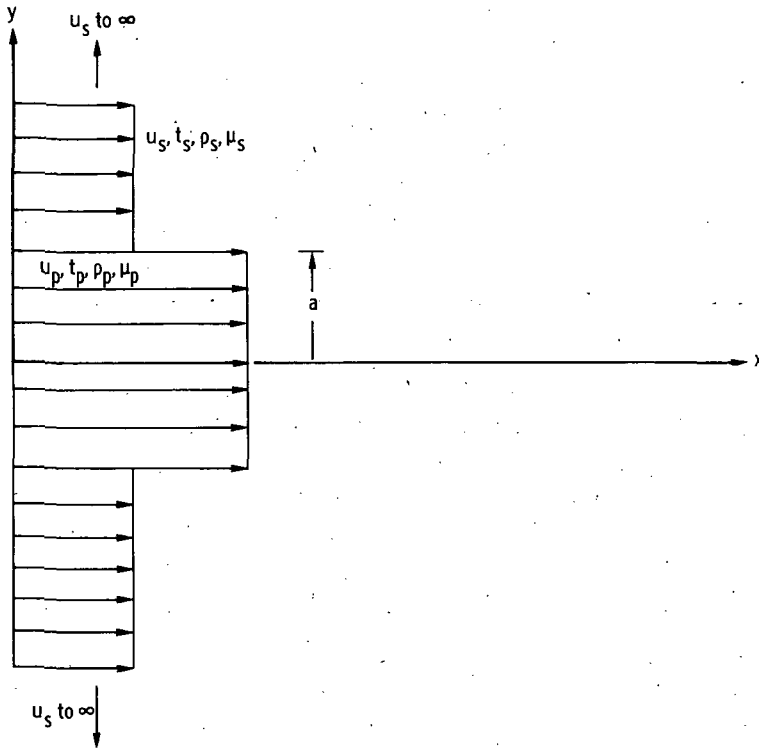


FIGURE 3-5. — Plane jet mixing of two different gases.

thermal case in which the basic equations are transformed into forms of the generalized heat conduction equation and then examined for several simplified cases (isothermal or isovelocity).

The equations of momentum, continuity, and energy may be written as

$$\rho \left(u \frac{\partial u}{\partial x} + v \frac{\partial u}{\partial y} \right) = \frac{\partial}{\partial y} \left(\mu \frac{\partial u}{\partial y} \right) \quad (3-155)$$

$$\frac{\partial(\rho u)}{\partial x} + \frac{\partial(\rho v)}{\partial y} = 0 \quad (3-156)$$

$$\rho \left(u \frac{\partial(c_p t)}{\partial x} + v \frac{\partial(c_p t)}{\partial y} \right) = \frac{\partial}{\partial y} \left(k \frac{\partial t}{\partial y} \right) + \mu \left(\frac{\partial u}{\partial y} \right)^2 \quad (3-157)$$

In our discussion of diffusion, we employ the subscript a for the primary gas and b for the secondary gas. We define

$$C_a^* = C_a / \rho \quad (3-158)$$

where C_a is the mass of component a per unit volume, ρ the mass of mixture per unit volume, and C_a^* the mass fraction of component a . In terms of C_a^* , the diffusion equation may be written as

$$\rho u \frac{\partial C_a^*}{\partial x} + \rho v \frac{\partial C_a^*}{\partial y} = D \frac{\partial}{\partial y} \left(\rho \frac{\partial C_a^*}{\partial y} \right) \quad (3-159)$$

where D is the diffusion coefficient. The D has been assumed constant which is an excellent approximation for most gases at constant pressure.

We now require an equation of state for the gas mixture in order to express ρ as a function of C_a^* , p , and t . We first express C_a^* as

$$C_a^* = C_a / \rho = \frac{N_a M_a}{N_a M_a + N_b M_b} \quad (3-160)$$

where N_a and N_b are, respectively, the number of moles of gas a and gas b per unit volume of the mixture, and M_a and M_b are the molecular weights of these gases. Since

$$N = N_a + N_b \quad (3-161)$$

where N is the total number of molecules in the gas mixture per unit volume, equation (3-160) may be rewritten as

$$C_a^* = \frac{N_a M_a}{N_a M_a + (N - N_a) M_b} \quad (3-162)$$

The equation of state for the mixture is

$$N = p / \mathcal{R} t \quad (3-163)$$

where \mathcal{R} is the universal gas constant and p is the total pressure of the gas mixture (constant in this case). Combining equations (3-162) and (3-163), and solving for N_a give

$$N_a = \frac{C_a^* N}{C_a^* + \eta (1 - C_a^*)} \quad (3-164)$$

where $\eta = M_a / M_b$. Equation (3-160) may now be written in the form

$$C_a^* = \frac{N_a M_a}{\rho} \quad (3-165)$$

Solving equation (3-165) for ρ and using equation (3-164) finally yield

$$\rho = \frac{pM_a}{(C_a^* + \eta(1 - C_a^*))\mathcal{R}t} \quad (3-166)$$

The transport properties are assumed to be functions of temperature and concentration only. An extensive literature has been devoted to the subject of the transport properties of gases and mixtures of gases and it does not seem worthwhile to present expressions here for these properties. The reader is referred to Hirschfelder, Curtis, and Bird (ref. 6) and Reid and Sherwood (ref. 7) for detailed discussions. For our purposes it is sufficient to state that the properties may be any desired function of concentration and temperature without complicating the actual solution in any way. We therefore simply state

$$c_p = c_p(t, C_a^*) \quad (3-167)$$

$$\mu = \mu(t, C_a^*) \quad (3-168)$$

$$k = k(t, C_a^*) \quad (3-169)$$

Equations (3-155) to (3-157), (3-159), and (3-166) to (3-169) now completely describe the problem.

The boundary conditions for this problem are

$$\left. \begin{aligned} u(0, y) &= u_p & y \leq a & \quad (\text{see appendix F}) \\ u(0, y) &= u_s & y > a \\ u(x, \infty) &= u_s \\ \frac{\partial u}{\partial y}(x, 0) &= 0 \\ v(x, 0) &= 0 \\ t(0, y) &= t_p & y \leq a \\ t(0, y) &= t_s & y > a \\ t(x, \infty) &= t_s \\ \frac{\partial t}{\partial y}(x, 0) &= 0 \\ C_a^*(0, y) &= 1 & y \leq a \\ C_a^*(0, y) &= 0 & y > a \\ C_a^*(x, \infty) &= 0 \\ \frac{\partial C_a^*}{\partial y}(x, 0) &= 0 \end{aligned} \right\} \quad (3-170)$$

The equations (3-155) to (3-157), (3-159), and (3-166) to (3-170) must now be expressed in dimensionless form. The following dimensionless variables are chosen:

$$\left. \begin{aligned} U &= u/u_p & Y &= y/a \\ V &= \frac{\rho_p v a}{\mu_p} & k^* &= k/k_p \\ T &= t/t_p & \mu^* &= \mu/\mu_p \\ N^* &= N/N_p & \rho^* &= \rho/\rho_p \\ X &= \frac{x\mu_p}{\rho_p \mu_p a^2} & c_p^* &= c_p/(c_p)_p \end{aligned} \right\} \quad (3-171)$$

The concentration C_a^* is already dimensionless. All reference values with subscript p are evaluated at the primary jet conditions at $X=0$.

Inserting these variables into the basic equations, the problem may be rewritten in dimensionless form as

$$\rho^* \left(U \frac{\partial U}{\partial X} + V \frac{\partial U}{\partial Y} \right) = \frac{\partial}{\partial Y} \left(\mu^* \frac{\partial U}{\partial Y} \right) \quad (3-172)$$

$$\frac{\partial(\rho^* U)}{\partial X} + \frac{\partial(\rho^* V)}{\partial Y} = 0 \quad (3-173)$$

$$\rho^* \left[U \frac{\partial(c_p^* T)}{\partial X} + V \frac{\partial(c_p^* T)}{\partial Y} \right] = \frac{1}{Pr} \frac{\partial}{\partial Y} \left(k^* \frac{\partial T}{\partial Y} \right) + (\gamma - 1) M_p^2 \mu^* \left(\frac{\partial U}{\partial Y} \right)^2 \quad (3-174)$$

$$\rho^* \left(U \frac{\partial C_a^*}{\partial X} + V \frac{\partial C_a^*}{\partial Y} \right) = \frac{1}{Sc} \frac{\partial}{\partial Y} \left(\rho^* \frac{\partial C_a^*}{\partial Y} \right) \quad (3-175)$$

$$\rho^* = \frac{1}{T[C_a^* + \eta(1 - C_a^*)]} \quad (3-176)$$

where

$$M_p = \frac{u_p}{\sqrt{\gamma \mathcal{R} t_p}}$$

$$Sc = \left(\frac{\mu}{\rho D} \right)_p$$

$$Pr = \left(\frac{\mu C_p}{k} \right)_p$$

are the Mach, Schmidt, and Prandtl numbers, respectively, evaluated at conditions in the primary stream at $X=0$.

The boundary conditions in dimensionless form are

$$\left. \begin{aligned}
 U(0, Y) &= 1 & Y \leq 1 \\
 U(0, Y) &= u_s/u_p & Y > 1 \\
 U(X, \infty) &= u_s/u_p \\
 \frac{\partial U}{\partial Y}(X, 0) &= 0 \\
 V(X, 0) &= 0 \\
 T(0, Y) &= 1 & Y \leq 1 \\
 T(0, Y) &= t_s/t_p & Y > 1 \\
 T(X, \infty) &= t_s/t_p \\
 \frac{\partial T}{\partial X}(X, 0) &= 0 \\
 C_a^*(0, Y) &= 1 & Y \leq 1 \\
 C_a^*(0, Y) &= 0 & Y > 1 \\
 C_a^*(X, \infty) &= 0 \\
 \frac{\partial C_a^*}{\partial Y}(X, 0) &= 0
 \end{aligned} \right\} \quad (3-177)$$

A finite difference form must now be selected for this problem. In order that the formulation be valid for all secondary velocities greater than or equal to zero, and to ensure accuracy in the evaluation of the properties, a nonlinear difference representation will be employed. The forms chosen for the momentum, continuity, and energy equations are essentially the same as those used in section 3.1.3. The complete finite difference representation for the problem is

$$\begin{aligned}
 \rho_{j+1,k}^* & \left[U_{j+1,k} \frac{U_{j+1,k} - U_{j,k}}{\Delta X} + V_{j+1,k} \frac{U_{j+1,k+1} - U_{j+1,k-1}}{2(\Delta Y)} \right] \\
 & = \mu_{j+1,k}^* \left[\frac{U_{j+1,k+1} - 2U_{j+1,k} + U_{j+1,k-1}}{(\Delta Y)^2} \right] +
 \end{aligned}$$

$$+ \left[\frac{\mu_{j+1,k+1}^* - \mu_{j+1,k-1}^*}{2(\Delta Y)} \right] \left[\frac{U_{j+1,k+1} - U_{j+1,k-1}}{2(\Delta Y)} \right] \quad (3-178)$$

$$\frac{\rho_{j+1,k}^* U_{j+1,k} - \rho_{j,k}^* U_{j,k}}{\Delta X} + \frac{\rho_{j+1,k+1}^* V_{j+1,k+1} - \rho_{j+1,k}^* V_{j+1,k}}{\Delta Y} = 0 \quad (3-179)$$

$$\begin{aligned} \rho_{j+1,k}^* & \left[U_{j+1,k} \frac{(c_p^*)_{j+1,k} T_{j+1,k} - (c_p^*)_{j,k} T_{j,k}}{\Delta X} \right. \\ & + V_{j+1,k} \frac{(c_p^*)_{j+1,k+1} T_{j+1,k+1} - (c_p^*)_{j+1,k-1} T_{j+1,k-1}}{2(\Delta Y)} \Big] \\ & = \frac{1}{P_r} \left\{ k_{j+1,k}^* \left[\frac{T_{j+1,k+1} - 2T_{j+1,k} + T_{j+1,k-1}}{(\Delta Y)^2} \right] \right. \\ & + \left. \left[\frac{k_{j+1,k+1}^* - k_{j+1,k-1}^*}{2(\Delta Y)} \right] \left[\frac{T_{j+1,k+1} - T_{j+1,k-1}}{2(\Delta Y)} \right] \right\} \\ & + (\gamma - 1) M_p^2 \mu_{j+1,k}^* \left[\frac{U_{j+1,k+1} - U_{j+1,k-1}}{2(\Delta Y)} \right]^2 \quad (3-180) \end{aligned}$$

$$\begin{aligned} \rho_{j+1,k}^* & \left[U_{j+1,k} \frac{(C_a^*)_{j+1,k} - (C_a^*)_{j,k}}{\Delta X} + V_{j+1,k} \frac{(C_a^*)_{j+1,k+1} - (C_a^*)_{j+1,k-1}}{2(\Delta Y)} \right] \\ & = \frac{1}{Sc} \left\{ \rho_{j+1,k}^* \left[\frac{(C_a^*)_{j+1,k+1} - 2(C_a^*)_{j+1,k} + (C_a^*)_{j+1,k-1}}{(\Delta Y)^2} \right] \right. \\ & + \left. \left[\frac{\rho_{j+1,k+1}^* - \rho_{j+1,k-1}^*}{2(\Delta Y)} \right] \left[\frac{(C_a^*)_{j+1,k+1} - (C_a^*)_{j+1,k-1}}{2(\Delta Y)} \right] \right\} \quad (3-181) \end{aligned}$$

$$\rho_{j+1,k}^* = \frac{1}{T_{j+1,k} ((C_a^*)_{j+1,k} + \eta(1 - (C_a^*)_{j+1,k}))} \quad (3-182)$$

$$(c_p^*)_{j+1,k} = (c_p^*)_{j+1,k}(T_{j+1,k}, C_{j+1,k}^*) \quad (3-183)$$

$$\mu_{j+1,k}^* = \mu_{j+1,k}^*(T_{j+1,k}, C_{j+1,k}^*) \quad (3-184)$$

$$k_{j+1,k}^* = k_{j+1,k}^*(T_{j+1,k}, C_{j+1,k}^*) \quad (3-185)$$

There is a very large number of possible iterative methods which might be applied to solve equations (3-178) to (3-185). The technique discussed here is very similar to that used in section 3.1.3 except for the presence of equation (3-181) (the diffusion equation) and the modified equation of state and property

relations. It should be noted that this iterative technique has not actually been applied by the author to this specific problem and, although there seems to be no reason why it should not work, the final proof must always be numbers on a sheet of computer output. Since the iterative method has been discussed in detail in sections 3.1.1 and 3.1.3, the presentation here is confined to the equations themselves. Equations (3-178), (3-180), and (3-181) are now reformulated slightly. The quantities with superscript (l) are from the iteration prior to the present one, while those with superscript $(l+1)$ are to be obtained in the present iteration. Equation (3-178) is rewritten as

$$\begin{aligned} \rho_{j+1,k}^{*(l)} & \left[U_{j+1,k}^{(l)} \frac{U_{j+1,k}^{(l+1)} - U_{j,k}^{(l+1)}}{\Delta X} + V_{j+1,k}^{(l)} \frac{U_{j+1,k+1}^{(l+1)} - U_{j+1,k-1}^{(l+1)}}{2(\Delta Y)} \right] \\ & = \mu_{j+1,k}^{*(l)} \left[\frac{U_{j+1,k+1}^{(l+1)} - 2U_{j+1,k}^{(l+1)} + U_{j+1,k-1}^{(l+1)}}{(\Delta Y)^2} \right] \\ & \quad + \left[\frac{\mu_{j+1,k+1}^{*(l)} - \mu_{j+1,k-1}^{*(l)}}{2(\Delta Y)} \right] \left[\frac{U_{j+1,k+1}^{(l+1)} - U_{j+1,k-1}^{(l+1)}}{2(\Delta Y)} \right] \end{aligned} \quad (3-186)$$

Equation (3-180) is rewritten as

$$\begin{aligned} \rho_{j+1,k}^{*(l)} & \left[U_{j+1,k}^{(l+1)} \frac{(c_p^*)_{j+1,k}^{(l)} T_{j+1,k}^{(l+1)} - (c_p^*)_{j,k} T_{j,k}}{\Delta X} \right. \\ & \quad \left. + V_{j+1,k}^{(l)} \frac{(c_p^*)_{j+1,k+1}^{(l)} T_{j+1,k+1}^{(l+1)} - (c_p^*)_{j+1,k-1}^{(l)} T_{j+1,k-1}^{(l+1)}}{2(\Delta Y)} \right] \\ & = \frac{1}{Pr} \left\{ k_{j+1,k}^{*(l)} \left[\frac{T_{j+1,k+1}^{(l+1)} - 2T_{j+1,k}^{(l+1)} + T_{j+1,k-1}^{(l+1)}}{(\Delta Y)^2} \right] \right. \\ & \quad \left. + \left[\frac{k_{j+1,k+1}^{*(l)} - k_{j+1,k-1}^{*(l)}}{2(\Delta Y)} \right] \left[\frac{T_{j+1,k+1}^{(l+1)} - T_{j+1,k-1}^{(l+1)}}{2(\Delta Y)} \right] \right\} \\ & \quad + (\gamma - 1) M_p^2 \mu_{j+1,k}^{*(l)} \left[\frac{U_{j+1,k+1}^{(l+1)} - U_{j+1,k-1}^{(l+1)}}{2(\Delta Y)} \right]^2 \end{aligned} \quad (3-187)$$

Finally, equation (3-181) is rewritten as

$$\rho_{j+1,k}^{*(l)} \left[U_{j+1,k}^{(l+1)} \frac{(C_a^*)_{j+1,k}^{(l+1)} - (C_a^*)_{j,k}}{\Delta X} + V_{j+1,k}^{(l)} \frac{(C_a^*)_{j+1,k+1}^{(l+1)} - (C_a^*)_{j+1,k-1}^{(l+1)}}{2(\Delta Y)} \right] =$$

$$= \frac{1}{Sc} \left\{ \rho_{j+1,k}^{*(l)} \left[\frac{(C_a^*)_{j+1,k+1}^{(l+1)} - 2(C_a^*)_{j+1,k}^{(l+1)} + (C_a^*)_{j+1,k-1}^{(l+1)}}{(\Delta Y)^2} \right] \right. \\ \left. + \left[\frac{\rho_{j+1,k+1}^{*(l)} - \rho_{j+1,k-1}^{*(l)}}{2(\Delta Y)} \right] \left[\frac{(C_a^*)_{j+1,k+1}^{(l+1)} - (C_a^*)_{j+1,k-1}^{(l+1)}}{2(\Delta Y)} \right] \right\} \quad (3-188)$$

Equation (3-186) written for $k=0(1)n$ now constitutes a set of $(n+1)$ linear equations in the $(n+1)$ unknowns $U_{j+1,k}^{(l+1)}$. Equations (3-187) and (3-188) written for $k=0(1)n$ constitute similar sets of equations for $T_{j+1,k}^{(l+1)}$ and $(C_a^*)_{j+1,k}^{(l+1)}$.

Equations (3-186) to (3-188) can be rearranged in the following more convenient forms:

$$\left[\frac{-\rho_{j+1,k}^{*(l)} V_{j+1,k}^{(l)} - \frac{\mu_{j+1,k}^{*(l)}}{(\Delta Y)^2} + \frac{\mu_{j+1,k+1}^{*(l)} - \mu_{j+1,k-1}^{*(l)}}{4(\Delta Y)^2} \right] U_{j+1,k-1}^{(l+1)} \\ + \left[\frac{\rho_{j+1,k}^{*(l)} U_{j+1,k}^{(l)}}{\Delta X} + \frac{2\mu_{j+1,k}^{*(l)}}{(\Delta Y)^2} \right] U_{j+1,k}^{(l+1)} \\ + \left[\frac{\rho_{j+1,k}^{*(l)} V_{j+1,k}^{(l)} - \frac{\mu_{j+1,k}^{*(l)}}{(\Delta Y)^2} - \frac{\mu_{j+1,k+1}^{*(l)} - \mu_{j+1,k-1}^{*(l)}}{4(\Delta Y)^2} \right] U_{j+1,k+1}^{(l+1)} \\ = \frac{\rho_{j+1,k}^{*(l)} U_{j+1,k}^{(l)} U_{j,k}}{\Delta X} \quad (3-189)$$

$$\left[\frac{-\rho_{j+1,k}^{*(l)} (c_p^*)_{j+1,k-1}^{(l)} V_{j+1,k}^{(l)} - \frac{k_{j+1,k}^{*(l)}}{Pr(\Delta Y)^2} + \frac{k_{j+1,k+1}^{*(l)} - k_{j+1,k-1}^{*(l)}}{4(Pr)(\Delta Y)^2} \right] T_{j+1,k-1}^{(l+1)} \\ + \left[\frac{\rho_{j+1,k}^{*(l)} (c_p^*)_{j+1,k}^{(l)} U_{j+1,k}^{(l+1)}}{\Delta X} + \frac{2k_{j+1,k}^{*(l)}}{Pr(\Delta Y)^2} \right] T_{j+1,k}^{(l+1)} \\ + \left[\frac{\rho_{j+1,k}^{*(l)} (c_p^*)_{j+1,k+1}^{(l)} V_{j+1,k}^{(l)} - \frac{k_{j+1,k}^{*(l)}}{Pr(\Delta Y)^2} - \frac{k_{j+1,k+1}^{*(l)} - k_{j+1,k-1}^{*(l)}}{4(Pr)(\Delta Y)^2} \right] T_{j+1,k+1}^{(l+1)} \\ = (\gamma - 1) M_p^2 \mu_{j+1,k}^{*(l)} \left(\frac{U_{j+1,k+1}^{(l+1)} - U_{j+1,k-1}^{(l+1)}}{2(\Delta Y)} \right)^2 + \frac{\rho_{j+1,k}^{*(l)} (c_p^*)_{j,k} U_{j+1,k}^{(l+1)} T_{j,k}}{\Delta X} \quad (3-190)$$

$$\begin{aligned}
 & \left[\frac{-\rho_{j+1,k}^{*(l)} V_{j+1,k}^{(l)}}{2(\Delta Y)} - \frac{\rho_{j+1,k}^{*(l)}}{Sc(\Delta Y)^2} + \frac{\rho_{j+1,k+1}^{*(l)} - \rho_{j+1,k-1}^{*(l)}}{4(Sc)(\Delta Y)^2} \right] (C_a^*)_{j+1,k-1}^{(l+1)} \\
 & + \left[\frac{\rho_{j+1,k}^{*(l)} U_{j+1,k}^{(l+1)}}{\Delta X} + \frac{2\rho_{j+1,k}^{*(l)}}{Sc(\Delta Y)^2} \right] (C_a^*)_{j+1,k}^{(l+1)} \\
 & + \left[\frac{\rho_{j+1,k}^{*(l)} V_{j+1,k}^{(l)}}{2(\Delta Y)} - \frac{\rho_{j+1,k}^{*(l)}}{Sc(\Delta Y)^2} - \frac{\rho_{j+1,k+1}^{*(l)} - \rho_{j+1,k-1}^{*(l)}}{4(Sc)(\Delta Y)^2} \right] (C_a^*)_{j+1,k+1}^{(l+1)} \\
 & = \frac{\rho_{j+1,k}^{*(l)} U_{j+1,k}^{(l+1)} (C_a^*)_{j,k}}{\Delta X} \quad (3-191)
 \end{aligned}$$

For each iteration the procedure is to solve the set of equations represented by (3-189) for $U_{j+1,k}^{(l+1)}$, the set represented by (3-190) for $T_{j+1,k}^{(l+1)}$, and finally the set represented by (3-191) for $(C_a^*)_{j+1,k}^{(l+1)}$. Equation (3-182) can now be solved for $\rho_{j+1,k}^{*(l+1)}$.

The values $V_{j+1,k+1}^{(l+1)}$ may now be solved for from continuity (eq. (3-179)):

$$V_{j+1,k+1}^{(l+1)} = V_{j+1,k}^{(l+1)} \left(\frac{\rho_{j+1,k}^{*(l+1)}}{\rho_{j+1,k+1}^{*(l+1)}} \right) - \frac{\Delta Y}{\Delta X} \left(\frac{\rho_{j+1,k}^{*(l+1)} U_{j+1,k}^{(l+1)} - \rho_{j,k}^* U_{j,k}}{\rho_{j+1,k+1}^{*(l+1)}} \right) \quad (3-192)$$

The properties c_p^* , μ^* , and k^* can be found from equations (3-183) to (3-185). The iteration $(l+1)$ is now complete. The iterative process may be repeated as many times as necessary until the values obtained on succeeding iterations agree to within any desired accuracy. Once the iterative process has converged, another step downstream may be taken and the solution obtained at that location using the same method. Over or under relaxation may be readily applied. (If there is difficulty in obtaining convergence, underrelaxation will probably be necessary.)

The matrix representations of equations (3-188), (3-190), and (3-191) are now written. Equation (3-189) in matrix form is

$$\begin{array}{|c|} \hline \beta_0^{(l)} \\ \hline \alpha_1^{(l)} \\ \hline \alpha_2^{(l)} \\ \hline \vdots \\ \hline \alpha_{n-1}^{(l)} \\ \hline \alpha_n^{(l)} \\ \hline \end{array} \begin{array}{|c|} \hline \frac{-2\mu_{j+1,0}^{*(l)}}{(\Delta Y)^2} \\ \hline \beta_1^{(l)} \\ \hline \beta_2^{(l)} \\ \hline \vdots \\ \hline \beta_{n-1}^{(l)} \\ \hline \beta_n^{(l)} \\ \hline \end{array} \begin{array}{|c|} \hline \Omega_1^{(l)} \\ \hline \Omega_2^{(l)} \\ \hline \vdots \\ \hline \Omega_{n-1}^{(l)} \\ \hline \Omega_n^{(l)} \\ \hline \end{array} \times \begin{array}{|c|} \hline U_{j+1,0}^{(l+1)} \\ \hline U_{j+1,1}^{(l+1)} \\ \hline U_{j+1,2}^{(l+1)} \\ \hline \vdots \\ \hline U_{j+1,n-1}^{(l+1)} \\ \hline U_{j+1,n}^{(l+1)} \\ \hline \end{array} = \begin{array}{|c|} \hline \phi_0^{(l)} \\ \hline \phi_1^{(l)} \\ \hline \phi_2^{(l)} \\ \hline \vdots \\ \hline \phi_{n-1}^{(l)} \\ \hline \phi_n^{(l)} - \Omega_n^{(l)} u_s / u_p \\ \hline \end{array} \quad (3-193)$$

where

$$\alpha_k^{(l)} = \frac{-\rho_{j+1,k}^{*(l)} V_{j+1,k}^{(l)}}{2(\Delta Y)} - \frac{\mu_{j+1,k}^{*(l)}}{(\Delta Y)^2} + \frac{\mu_{j+1,k+1}^{*(l)} - \mu_{j+1,k-1}^{*(l)}}{4(\Delta Y)^2}$$

$$\beta_k^{(l)} = \frac{\rho_{j+1,k}^{*(l)} U_{j+1,k}^{(l)}}{\Delta X} + \frac{2\mu_{j+1,k}^{*(l)}}{(\Delta Y)^2}$$

$$\Omega_k^{(l)} = \frac{\rho_{j+1,k}^{*(l)} V_{j+1,k}^{(l)}}{2(\Delta Y)} - \frac{\mu_{j+1,k}^{*(l)}}{(\Delta Y)^2} - \frac{\mu_{j+1,k+1}^{*(l)} - \mu_{j+1,k-1}^{*(l)}}{4(\Delta Y)^2}$$

$$\phi_k^{(l)} = \frac{\rho_{j+1,k}^{*(l)} U_{j+1,k}^{(l)} U_{j,k}}{\Delta X}$$

Equation (3-190) in matrix form is

$\beta_0'^{(l)}$	$\frac{-2k_{j+1,0}^{*(l)}}{Pr(\Delta Y)^2}$				$T_{j+1,0}^{(l+1)}$	$\phi_0'^{(l)}$
$\alpha_1'^{(l)}$	$\beta_1^{(l)}$	$\Omega_1^{(l)}$			$T_{j+1,1}^{(l+1)}$	$\phi_1'^{(l)}$
$\alpha_2'^{(l)}$	$\beta_2^{(l)}$	$\Omega_2^{(l)}$			$T_{j+1,2}^{(l+1)}$	$\phi_2'^{(l)}$

$$\phi_k^{(l)} = \frac{\rho_{j+1,k}^{*(l)} (c_p^*)_{j,k} U_{j+1,k}^{(l+1)} T_{j,k}}{\Delta X} + (\gamma - 1) M_p^2 \mu_{j+1,k}^{*(l)} \left[\frac{U_{j+1,k+1}^{(l+1)} - U_{j+1,k-1}^{(l+1)}}{2(\Delta Y)} \right]^2$$

Finally, equation (3-191) in matrix form is

$$\begin{array}{c|ccc|c|ccc} \beta_0^{''(l)} & \left(\frac{-2\rho_{j+1,0}^{*(l)}}{Sc(\Delta Y)^2} \right) & & & (C_a^*)_{j+1,0}^{(l+1)} & & \phi_0^{''(l)} \\ \alpha_1^{''(l)} & \beta_1^{''(l)} & \Omega_1^{''(l)} & & (C_a^*)_{j+1,1}^{(l+1)} & & \phi_1^{''(l)} \\ & \alpha_2^{''(l)} & \beta_2^{''(l)} & \Omega_2^{''(l)} & (C_a^*)_{j+1,2}^{(l+1)} & & \phi_2^{''(l)} \\ & & \text{---} & \text{---} & \text{---} & & \text{---} \\ & & & & \text{---} & & \text{---} \\ & & & & \text{---} & & \text{---} \\ & & & & (C_a^*)_{j+1,n-1}^{(l+1)} & & \phi_{n-1}^{''(l)} \\ & & & \alpha_{n-1}^{''(l)} & \beta_{n-1}^{''(l)} & \Omega_{n-1}^{''(l)} & \\ & & & & \alpha_n^{''(l)} & \beta_n^{''(l)} & \\ & & & & (C_a^*)_{j+1,n}^{(l+1)} & & \phi_n^{''(l)} \end{array} \times = \begin{array}{c} \phi_0^{''(l)} \\ \phi_1^{''(l)} \\ \phi_2^{''(l)} \\ \text{---} \\ \text{---} \\ \phi_{n-1}^{''(l)} \\ \phi_n^{''(l)} \end{array} \quad (3-195)$$

where

$$\alpha_k^{''(l)} = \frac{-\rho_{j+1,k}^{*(l)} V_{j+1,k}^{(l)}}{2(\Delta Y)} - \frac{\rho_{j+1,k}^{*(l)}}{Sc(\Delta Y)^2} + \frac{\rho_{j+1,k+1}^{*(l)} - \rho_{j+1,k-1}^{*(l)}}{4(Sc)(\Delta Y)^2}$$

$$\beta_k^{''(l)} = \frac{\rho_{j+1,k}^{*(l)} U_{j+1,k}^{(l+1)}}{\Delta X} + \frac{2\rho_{j+1,k}^{*(l)}}{Sc(\Delta Y)^2}$$

$$\Omega_k^{''(l)} = \frac{\rho_{j+1,k}^{*(l)} V_{j+1,k}^{(l)}}{2(\Delta Y)} - \frac{\rho_{j+1,k}^{*(l)}}{Sc(\Delta Y)^2} - \frac{\rho_{j+1,k+1}^{*(l)} - \rho_{j+1,k-1}^{*(l)}}{4(Sc)(\Delta Y)^2}$$

$$\phi_k^{''(l)} = \frac{\rho_{j+1,k}^{*(l)} U_{j+1,k}^{(l+1)} (C_a^*)_{j,k}}{\Delta X}$$

The truncation error of the momentum, energy, and diffusion equations is of $\mathcal{O}(\Delta X)$ and $\mathcal{O}(\Delta Y^2)$. The truncation error of the continuity equation is of $\mathcal{O}(\Delta X)$ and $\mathcal{O}(\Delta Y)$.

Although no stability analysis for this formulation has been carried out, it may be safely assumed from previous experience that the representation is stable for all $U \geq 0$.

3.4 EXAMPLE PROBLEM—TWO-DIMENSIONAL JET

As an illustration of the numerical technique, a solution has been carried out for a plane jet of fluid emerging from a finite slot with a parabolic velocity distribution into a stationary region of the same fluid (fig. 3-6). This problem differs only slightly from the problem formulated in section 3.1.1 for a uniform primary stream of velocity u_p . The formulation given in section 3.1.1 may be used for the present problem if the velocity u_p is used to represent the *maximum* velocity in the parabolic velocity distribution and if the boundary conditions (3-3) are modified to become

$$\left. \begin{aligned}
 u(0, y) &= u_p \left(1 - \frac{y^2}{a^2} \right) & y \leq a \\
 u(0, y) &= 0 & y > a \\
 u(x, \infty) &= 0 \\
 \frac{\partial u}{\partial y}(x, 0) &= 0 \\
 v(x, 0) &= 0
 \end{aligned} \right\} \quad (3-196)$$

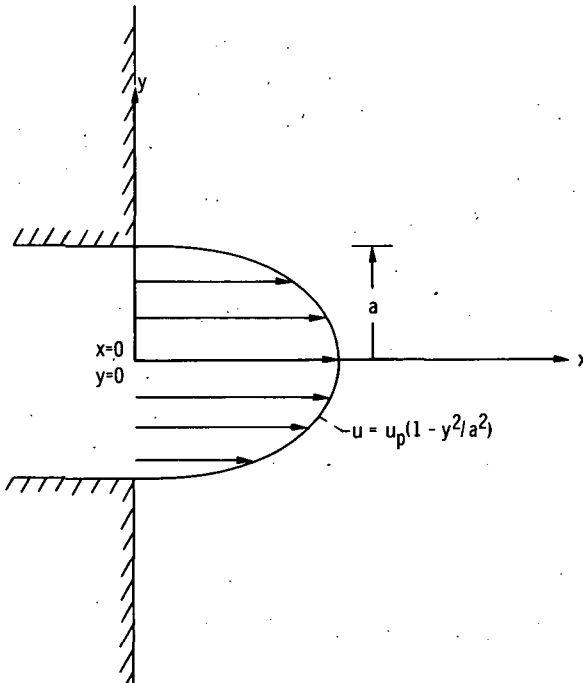


FIGURE 3-6.—Plane jet emerging from wall with parabolic velocity distribution into stationary fluid.

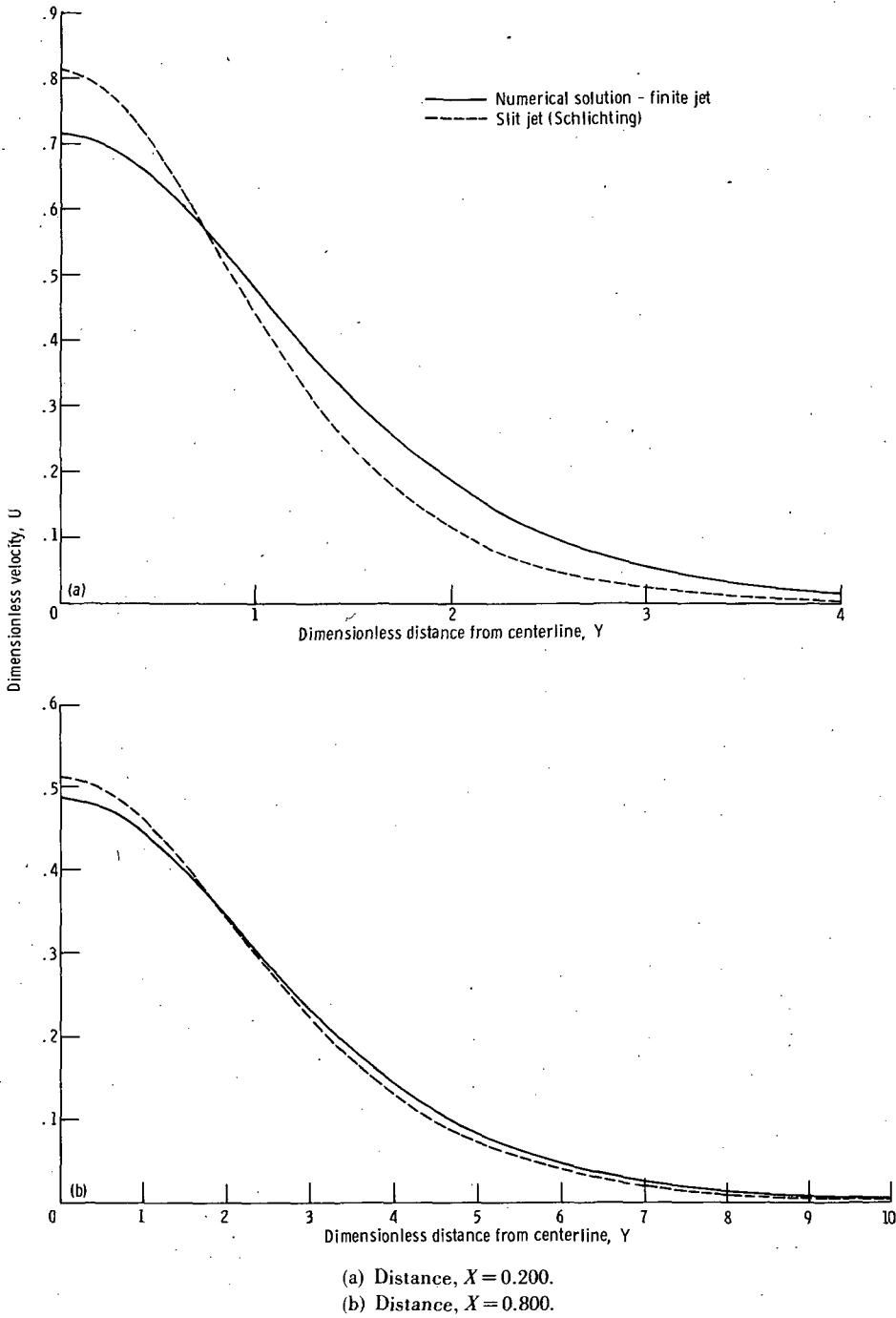
In dimensionless form, the conditions (3-196) become

$$\left. \begin{aligned}
 U(0, Y) &= 1 - Y^2 & Y \leq 1 \\
 U(0, Y) &= 0 & Y > 1 \\
 U(X, \infty) &= 0 \\
 \frac{\partial U}{\partial Y}(X, 0) &= 0 \\
 V(X, 0) &= 0
 \end{aligned} \right\} \quad (3-197)$$

The solution now proceeds exactly as outlined in section 3.1.1.

The numerical solution was carried out with mesh sizes of $\Delta X = 0.001$ and $\Delta Y = 0.05$ with $n = 300$. This large value of n made it unnecessary to expand the grid as the jet expanded, although clearly the number of mesh points in the Y -direction was much larger than was necessary for small X . It was found necessary to employ underrelaxation to obtain convergence of the iterative procedure. An underrelaxation factor of 0.3 was used.

Axial velocity U distributions obtained from the numerical solution are compared in figure 3-7 with the solution of Schlichting (ref. 8) for a plane jet emerging from a slit of infinitesimal height but with a finite momentum flux. The two solutions are compared on the basis of an equal momentum flux. The profiles at $X = 0.2$ shown in figure 3-7(a) indicate that the expansion of the jet is about the same for both solutions. However, the Schlichting solution gives a higher center-line velocity since the source of the jet is concentrated into an infinitesimal height while the jet in the numerical solution emerges from a finite source. Much farther downstream at $X = 0.8$, as shown in figure 3-7(b), the distribution of the source of the jet becomes much less important and the two solutions agree very well. A number of representative velocity profiles from the numerical solution are shown in figure 3-8.



(a) Distance, $X = 0.200$.
 (b) Distance, $X = 0.800$.
 FIGURE 3-7.—Comparison of velocity profiles for plane jet.

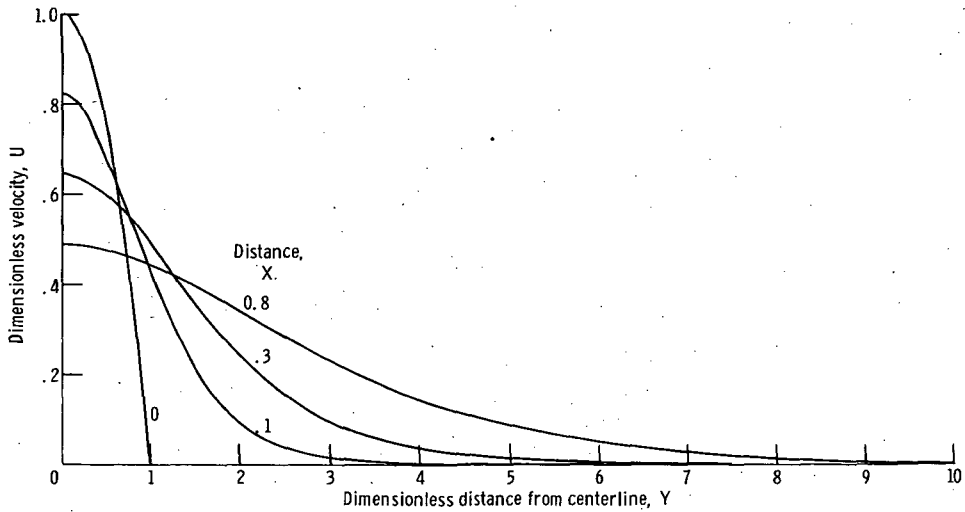


FIGURE 3-8. — Plane finite laminar jet velocity profiles — parabolic exit profile.

REFERENCES

1. CRANDALL, STEPHEN H.: *Engineering Analysis, A Survey of Numerical Procedures*. McGraw-Hill Book Co., Inc., 1956.
2. ROULEAU, WILFRED T.: *Finite Difference Methods for the Solution of Fluid Flow Problems Described by the Prandtl Equations*. Ph. D. Thesis, Carnegie Inst. Tech., 1954.
3. PAI, SHIH-I.: *Fluid Dynamics of Jets*. D. Van Nostrand Co., Inc., 1954.
4. ROHSENOW, WARREN M.; AND CHOI, HARRY Y.: *Heat, Mass, and Momentum Transfer*. Prentice-Hall, Inc., 1961.
5. BIRD, R. BYRON; STEWART, WARREN E.; AND LIGHTFOOT, EDWIN N.: *Transport Phenomena*. John Wiley & Sons, Inc., 1960.
6. HIRCHFELDER, JOSEPH O.; CURTISS, CHARLES F.; AND BIRD, R. BYRON: *Molecular Theory of Gases and Liquids*. John Wiley & Sons, Inc., 1954.
7. REID, ROBERT C.; AND SHERWOOD, THOMAS K.: *The Properties of Gases and Liquids*. McGraw-Hill Book Co., Inc., 1958.
8. SCHLICHTING, HERMANN (J. KESTIN, TRANS.): *Boundary Layer Theory*. Fourth ed., McGraw-Hill Book Co., Inc., 1960.

CHAPTER 4

FREE CONVECTION

Free convection (also called natural convection) results when a fluid in the presence of a gravity field undergoes density variations due to a nonuniform temperature distribution within the fluid. For almost all practical situations, the fluid can be considered as incompressible in the sense that variations in pressure do not significantly affect the density and that the effect of temperature variations on density can be adequately accounted for by using a coefficient of thermal expansion. Eshghy and Morrison (ref. 1) gives a complete discussion of the limitations of these assumptions. In addition, for large Grashoff numbers, a boundary layer model is acceptable for the free convection problem, and we shall employ such a model in this chapter.

4.1 FLOW ON A VERTICAL HEATED PLATE

The problem configuration considered first is shown in figure 4-1. The vertical plate is heated and the surrounding fluid is at rest.

4.1.1 Velocity and Temperature Solutions

The "incompressible" free convection equations (see ref. 1) may be written as

$$\rho \left(u \frac{\partial u}{\partial x} + v \frac{\partial u}{\partial y} \right) = \mu \frac{\partial^2 u}{\partial y^2} + \rho g_x B (t - t_\infty) \quad (4-1)$$

$$\frac{\partial u}{\partial x} + \frac{\partial v}{\partial y} = 0 \quad (4-2)$$

$$\rho c_p \left(u \frac{\partial t}{\partial x} + v \frac{\partial t}{\partial y} \right) = k \frac{\partial^2 t}{\partial y^2} \quad (4-3)$$

where g_x is the x -component (vertical) of the acceleration due to gravity and B is the thermal coefficient of volumetric expansion.

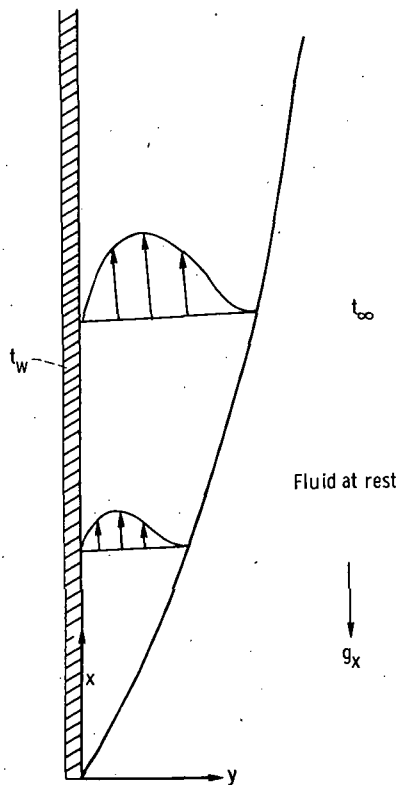


FIGURE 4-1.—Free convection flow on vertical heated plate.

The boundary conditions specified for the classical free convection problem are

$$\left. \begin{aligned} u(x, 0) &= 0 \\ u(x, \infty) &= 0 \\ u(0, y) &= 0 \\ v(x, 0) &= 0 \\ t(x, 0) &= t_w \\ t(x, \infty) &= t_\infty \\ t(0, y) &= t_\infty \end{aligned} \right\} \quad (4-4)$$

Other boundary conditions may be readily considered when the numerical technique is used as will be demonstrated in later sections of this chapter.

The equations (4-1) to (4-3) and boundary conditions (4-4) may now be put in dimensionless form by the proper choice of dimensionless variables. The

variables chosen are those used by Bodoia (ref. 2) for his investigation of confined free convection:

$$\left. \begin{aligned} U &= \frac{\nu}{L^2 g_x B (t_w - t_x)} u = \frac{uL}{\nu(Gr)} \\ V &= \frac{Lv}{\nu} \\ T &= \frac{t - t_x}{t_w - t_x} \\ X &= \frac{\nu^2}{g_x B (t_w - t_x) L^4} x = \frac{x}{L(Gr)} \\ Y &= \frac{y}{L} \end{aligned} \right\} \quad (4-5)$$

where $Gr = B(t_w - t_x)L^3 g_x / \nu^2$ is the Grashoff number and L is a characteristic length in the x -direction.

When these variables are inserted into equations (4-1) to (4-3), the basic equations become in dimensionless form

$$U \frac{\partial U}{\partial X} + V \frac{\partial U}{\partial Y} = \frac{\partial^2 U}{\partial Y^2} + T \quad (4-6)$$

$$\frac{\partial U}{\partial X} + \frac{\partial V}{\partial Y} = 0 \quad (4-7)$$

$$U \frac{\partial T}{\partial X} + V \frac{\partial T}{\partial Y} = \frac{1}{Pr} \frac{\partial^2 T}{\partial Y^2} \quad (4-8)$$

The boundary conditions (4-4) in dimensionless form become

$$\left. \begin{aligned} U(X, 0) &= 0 \\ U(X, \infty) &= 0 \\ U(0, Y) &= 0 \\ V(X, 0) &= 0 \\ T(X, 0) &= 1 \\ T(X, \infty) &= 0 \\ T(0, Y) &= 0 \end{aligned} \right\} \quad (4-9)$$

The only parameter appearing in the dimensionless problem is the Prandtl number.

A finite difference form for equations (4-6) to (4-8) must now be chosen. Essentially the same type of formulation is employed as was used for the jet with zero secondary velocity in section 3.1.1. This form is necessitated by the zero velocity free stream, which will result in the usual implicit formulations being inconsistent as discussed in section 3.1.1. The finite difference forms chosen for equations (4-6) to (4-8) are

$$U_{j+1,k} \frac{U_{j+1,k} - U_{j,k}}{\Delta X} + V_{j+1,k} \frac{U_{j+1,k+1} - U_{j+1,k-1}}{2(\Delta Y)} = \frac{U_{j+1,k+1} - 2U_{j+1,k} + U_{j+1,k-1}}{(\Delta Y)^2} + T_{j+1,k} \quad (4-10)$$

$$\frac{U_{j+1,k+1} - U_{j,k+1}}{\Delta X} + \frac{V_{j+1,k+1} - V_{j+1,k}}{\Delta Y} = 0 \quad (4-11)$$

$$U_{j+1,k} \frac{T_{j+1,k} - T_{j,k}}{\Delta X} + V_{j+1,k} \frac{T_{j+1,k+1} - T_{j+1,k-1}}{2(\Delta Y)} = \frac{1}{Pr} \frac{T_{j+1,k+1} - 2T_{j+1,k} + T_{j+1,k-1}}{(\Delta Y)^2} \quad (4-12)$$

Since the difference formulation given here is nonlinear, an iterative scheme is required to obtain a solution. The method used here is very similar to that employed in section 3.1.1. The difference equations (4-10) to (4-12) are first rewritten as

$$U_{j+1,k}^{(l)} \frac{U_{j+1,k}^{(l+1)} - U_{j,k}}{\Delta X} + V_{j+1,k}^{(l)} \frac{U_{j+1,k+1}^{(l+1)} - U_{j+1,k-1}^{(l+1)}}{2(\Delta Y)} = \frac{U_{j+1,k+1}^{(l+1)} - 2U_{j+1,k}^{(l+1)} + U_{j+1,k-1}^{(l+1)}}{(\Delta Y)^2} + T_{j+1,k}^{(l)} \quad (4-13)$$

$$\frac{U_{j+1,k+1}^{(l+1)} - U_{j,k+1}}{\Delta X} + \frac{V_{j+1,k+1}^{(l+1)} - V_{j+1,k}^{(l+1)}}{\Delta Y} = 0 \quad (4-14)$$

$$U_{j+1,k}^{(l+1)} \frac{T_{j+1,k}^{(l+1)} - T_{j,k}}{\Delta X} + V_{j+1,k}^{(l+1)} \frac{T_{j+1,k+1}^{(l+1)} - T_{j+1,k-1}^{(l+1)}}{2(\Delta Y)} = \frac{1}{Pr} \frac{T_{j+1,k+1}^{(l+1)} - 2T_{j+1,k}^{(l+1)} + T_{j+1,k-1}^{(l+1)}}{(\Delta Y)^2} \quad (4-15)$$

$$\Omega_k^{(l)} = \frac{-1}{(Pr)(\Delta Y)^2} + \frac{V_{j+1,k}^{(l+1)}}{2(\Delta Y)}$$

$$\phi_k^{(l)} = \frac{U_{j+1,k}^{(l+1)} T_{j,k}}{\Delta X}$$

As in the momentum equation solution, the method of appendix A may be used.

The iterative technique now consists of solving the sets of equations (4-17), (4-18) and (4-19) in that order repeatedly until the values obtained on a given iteration agree with those obtained on the previous iteration to within some predetermined accuracy.

Preliminary calculations by the author indicate that the iterative process may not converge unless some underrelaxation is employed. The relaxation procedure is discussed in detail in section 3.1.1. The underrelaxation factor found useful in the preliminary calculations was 0.3, but this should be determined for any given problem by experimental calculations.

The formulation given here is stable so long as $U \geq 0$. The truncation error is of $\mathcal{O}(\Delta X)$ and $\mathcal{O}(\Delta Y^2)$ for momentum and energy and $\mathcal{O}(\Delta X)$ and $\mathcal{O}(\Delta Y)$ for continuity.

4.1.2 Heat Transfer Solution

The local Nusselt number is given by

$$Nu_x = \frac{qx}{k(t_w - t_\infty)} \quad (4-21)$$

or

$$Nu_x = - \frac{\left. \frac{\partial t}{\partial y} \right|_{y=0} x}{(t_w - t_\infty)} \quad (4-22)$$

When the dimensionless variables (4-5) are used, equation (4-22) becomes

$$Nu_x = - \left. \frac{\partial T}{\partial Y} \right|_{Y=0} (X) (Gr) \quad (4-23)$$

where

$$Gr = \frac{g_x B (t_w - t_\infty) L^3}{\nu^2}$$

is the Grashoff number based on L . In difference form this can be written as

$$Nu_x = \left[\frac{3T_{j+1,0} - 4T_{j+1,1} + T_{j+1,2}}{2(\Delta Y)} \right] (X) (Gr) \quad (4-24)$$

(see appendix B, section B.1). The average Nusselt number is given by

$$Nu_m = \frac{1}{X} \int_0^X Nu_x dX \quad (4-25)$$

This equation can be readily evaluated using Simpson's rule (see section 2.1.3, eq. (2-31)).

4.2 OTHER PROBLEMS WITH SIMILAR FORMULATION

4.2.1 Combined Free and Forced Convection on a Vertical Heated Plate

This problem can be solved using the methods of this chapter, but only for so called "aiding" flow in which the free stream velocity is in the same direction as that induced by free convection. "Opposing" flow, in which the free stream is in the opposite direction, results in a flow reversal in the velocity field and instability of the finite difference technique. In order to approach this problem, it is necessary to solve the entire flow field simultaneously and to specify boundary conditions far above and far below the plate, an extremely difficult task which is beyond the scope of this book.

For aiding flow, only a few changes are necessary to the formulation in section 4.1.1. The boundary conditions (4-4) become

$$\left. \begin{aligned} u(x, 0) &= 0 \\ u(x, \infty) &= u_\infty \\ u(0, y) &= u_\infty \\ v(x, 0) &= 0 \\ t(x, 0) &= t_w \\ t(x, \infty) &= t_\infty \\ t(0, y) &= t_\infty \end{aligned} \right\} \quad (4-26)$$

In dimensionless form, the conditions (4-26) become

$$\left. \begin{aligned} U(X, 0) &= 0 \\ U(X, \infty) &= U_\infty \\ U(0, Y) &= U_\infty \\ V(X, 0) &= 0 \\ T(X, 0) &= 1 \\ T(X, \infty) &= 0 \\ T(0, Y) &= 0 \end{aligned} \right\} \quad (4-27)$$

where

$$U_x = \frac{\nu u_x}{L^2 g_x B (t_w - t_\infty)}$$

The matrix equation (4-17) is modified only in the last row of the right side column vector, where $\phi_n^{(l)}$ is replaced by $(\phi_n^{(l)} - \Omega_n^{(l)} U_x)$.

Even though the free stream velocity in the case now being considered is nonzero, it is strongly suggested that the difference forms (4-10) and (4-12) be retained, since preliminary calculations indicate that various numerical difficulties may be encountered if the usual implicit form is used when the free convection velocities become appreciably higher than those in the free stream.

It should be noted that the dimensionless variables may if desired be re-defined using U_x as a characteristic velocity, but this gains little, and the limiting case as $U_x \rightarrow 0$ cannot be readily considered.

The heat-transfer results may be obtained by using the formulation of section 4.1.2.

4.2.2 Free Convection With Wall Temperature or Wall Heat Flux a Function of Position

In the formulation given in section 4.1.1, it was assumed that the surface temperature of the plate is specified and is constant. If instead the surface temperature is a function of x , or if a heat flux (which may be a function of x) is specified, then the problem must be reformulated.

If the wall temperature is a function of x , then only minor changes are needed. The wall temperature t_{w0} at $x=0$ replaces t_w in the dimensionless variables (4-5). The boundary conditions (4-4) are then rewritten as

$$\left. \begin{aligned} U(X, 0) &= 0 \\ U(X, \infty) &= 0 \\ U(0, Y) &= 0 \\ V(X, 0) &= 0 \\ T(X, 0) &= T_w(X) = \frac{t_w(X) - t_\infty}{t_{w0} - t_\infty} \\ T(X, \infty) &= 0 \\ T(0, Y) &= 0 \end{aligned} \right\} \quad (4-28)$$

The matrix equation (4-20) must be slightly changed in that the first row of the right side column matrix, $(\phi_1^{(l)} - \alpha_1^{(l)})$ becomes $(\phi_1^{(l)} - \alpha_1^{(l)} T_w(X))$.

If a wall heat flux is specified (which in general may be a function of x), then the reformulation is more extensive. The boundary conditions (4-4) become

$$\left. \begin{aligned}
 u(x, 0) &= 0 \\
 u(x, \infty) &= 0 \\
 u(0, y) &= 0 \\
 v(x, 0) &= 0 \\
 -k \frac{\partial t}{\partial y}(x, 0) &= q(x) \\
 t(x, \infty) &= t_\infty \\
 t(0, y) &= t_\infty
 \end{aligned} \right\} \quad (4-29)$$

The new choice of dimensionless variables replacing (4-5) is

$$\left. \begin{aligned}
 U &= \frac{\nu k}{L^3 g_x B q_0} u \\
 V &= \frac{Lv}{\nu} \\
 T &= \frac{(t - t_\infty) k}{q_0 L} \\
 X &= \frac{\nu^2 k}{L^3 g_x B q_0} x \\
 Y &= \frac{y}{L}
 \end{aligned} \right\} \quad (4-30)$$

where q_0 is a reference heat flux (e.g., at the the leading edge of the plate). Using these variables, the basic equations (4-6) to (4-8) are unchanged.

The boundary conditions (4-29) become in dimensionless form

$$\left. \begin{aligned}
 U(X, 0) &= 0 \\
 U(X, \infty) &= 0 \\
 U(0, Y) &= 0 \\
 V(X, 0) &= 0 \\
 -\frac{\partial T}{\partial Y}(X, 0) &= \frac{q(X)}{q_0} \\
 T(X, \infty) &= 0 \\
 T(0, Y) &= 0
 \end{aligned} \right\} \quad (4-31)$$

The heat transfer solution for the local Nusselt number must be slightly reformulated from that given in section 4.1.2. The local Nusselt number is given by

$$Nu_x = \frac{qx}{k(t_w - t_x)} \quad (4-34)$$

which is, in dimensionless form,

$$Nu_x = \frac{X}{T_w} \left(\frac{L^4 g_x B q_0}{\nu^2 k} \right) \left[\frac{q(X)}{q_0} \right] \quad (4-35)$$

4.2.3 Free Convection With MHD or EHD Body Forces

The methods which may be used for this problem are virtually the same as those presented for the other problems in this chapter. The only change is the presence of an additional body force term in the momentum equation and if necessary the proper field equations. See section 2.3.4 for details of the method.

No difficulty is encountered if the additional body force aids the free convection flow, but if it opposes it, the solution cannot be carried beyond any point at which flow reversal occurs.

4.3 EXAMPLE PROBLEM—FREE CONVECTION FROM A HEATED VERTICAL PLATE

The problem chosen here as an example of the numerical technique is the vertical flat plate free convection problem formulated in section 4.1. The wall temperature is assumed constant and the fluid is assumed to be "incompressible" in the usual free convection sense. Similarity solutions for this problem have been obtained by Polhausen (ref. 3) for $Pr=0.73$ and by Ostrach (ref. 4) for a wide variety of Prandtl numbers.

The numerical solution was obtained for a Prandtl number of 1.0. The mesh sizes used were $\Delta X=0.0001$ and $\Delta Y=0.025$. The number of points employed in the Y -direction was $n=100$, which resulted in a value of $Y=2.5$ effectively representing infinity. This value of Y was sufficiently large for values of X up to about 0.01, which was as far as the present solution was carried. Larger values of X would necessitate expanding the mesh. Underrelaxation with a factor of 0.3 was necessary to obtain convergence of the iteration.

The results are shown in figures 4-2 and 4-3. The similarity solution of Ostrach (ref. 4) yields velocity and temperature profiles which may be represented as single curves if the similarity variables

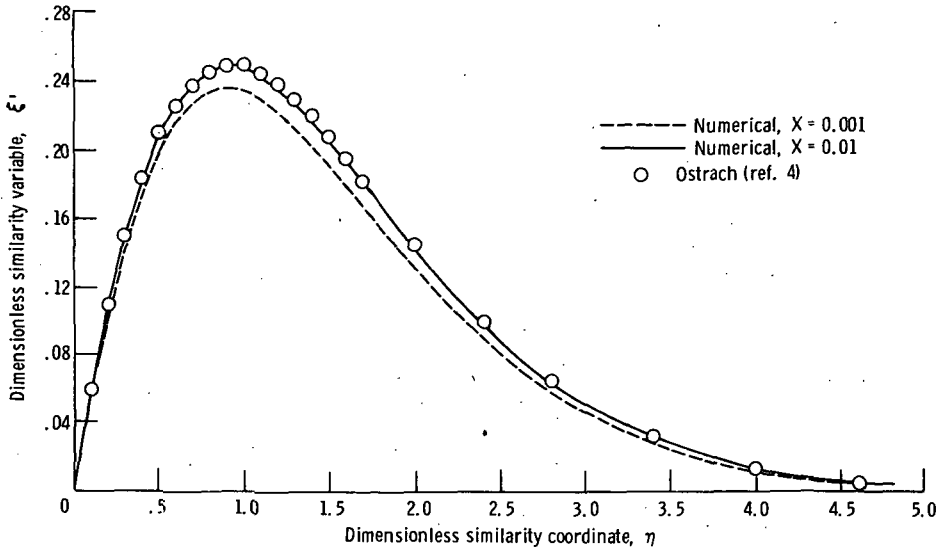


FIGURE 4-2.—Free convection velocity profiles for Prandtl number $Pr=1$.

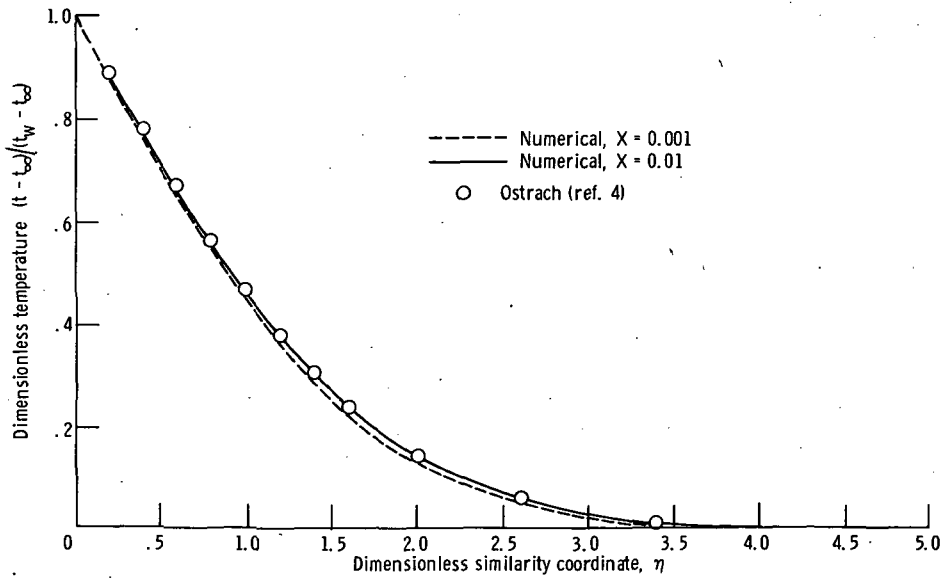


FIGURE 4-3.—Free convection temperature profiles for Prandtl number $Pr=1$.

and

$$\left. \begin{aligned} \xi' &= \frac{U}{2X^{1/2}} \\ \eta &= \frac{Y}{\sqrt{2}X^{1/4}} \end{aligned} \right\} \quad (4-36)$$

are employed. These results are shown in figures 4-2 and 4-3 along with the results obtained from the numerical solution after 10 steps downstream ($X=0.001$) and 100 steps downstream ($X=0.01$) from the leading edge. The numerical results have been transformed into the similarity variables ξ' and η . After 10 steps the velocity profile from the numerical solution agrees with the similarity solution to within a maximum error of less than 9 percent, while the temperature profile is very accurate. After 100 steps the numerical and similarity solutions yield virtually identical results for both the velocity and temperature distributions. The deviation of the velocity solution at $X=0.001$ (10 steps) from the similarity solution is due to the combined effects of the leading edge singularity and the small number of transverse mesh points within the boundary layer. The behavior of the numerical solution near the leading edge is thus qualitatively similar to that found for the boundary layer example in section 2.4. The effects of the leading edge singularity can be confined close to the leading edge by employing small ΔX steps in that region.

REFERENCES

1. ESHGHY, S.; AND MORRISON, F. A., JR.: Compressibility and Free Convection. Proc. Roy. Soc. (London), Ser. A, vol. 293, no. 1434, Aug. 9, 1966, pp. 395-407.
2. BODOIA, JOHN R.: The Finite Difference Analysis of Confined Viscous Flows. Ph.D. Thesis, Carnegie Inst. Tech., 1959.
3. POLHAUSEN, E.: D er W armeaustausch zwischen festen K orpern und Fl ussigkeiten mit kleiner Reibung and kleiner W armerleitung. Zeit. f. Angew. Math. Mech., vol. 1, no. 2, 1921, pp.115-121.
4. OSTRACH, SIMON: An Analysis of Laminar Free-Convection Flow and Heat Transfer About a Flat Plate Parallel to the Direction of the Generating Body Force. NACA TN-2635, 1952.

CHAPTER 5

TIME DEPENDENT BOUNDARY LAYERS

A considerable amount of work has been published recently on the numerical solution of time dependent viscous flows. Some typical examples of this work are references 1 and 2. However, these solutions have for the most part been concerned with problems which are spacewise elliptic, that is, problems such as flow over a cylinder or weir, or free convection in a closed cavity. These are, in general, problems in which all terms in the Navier-Stokes equations must be retained. It is not the purpose of this chapter to present techniques for problems such as this; rather, our attention is confined to transient problems describable by differential equations which in their spatially varying terms are similar to those discussed elsewhere in this book. Problems of this type include transient free convection on a flat plate (analyzed using finite difference methods by Hellums, ref. 3) and the flat plate boundary layer with an oscillating free stream (analyzed numerically by Farn and Arpaci, ref. 4).

5.1 PLANE TRANSIENT BOUNDARY LAYER

The problem presented here is that of the transient boundary layer on a flat plate when the free stream has an arbitrary motion in time parallel to the plate. Both incompressible and compressible formulations are presented, with the explicit incompressible velocity formulation essentially that of Farn and Arpaci (ref. 4) with some minor changes.

5.1.1 Incompressible Flow—Velocity Solution

The equations of motion for the incompressible case are

$$\rho \left(\frac{\partial u}{\partial \theta} + u \frac{\partial u}{\partial x} + v \frac{\partial u}{\partial y} \right) = -\frac{dp}{dx} + \mu \left(\frac{\partial^2 u}{\partial y^2} \right) \quad (5-1)$$

$$\frac{\partial u}{\partial x} + \frac{\partial v}{\partial y} = 0 \quad (5-2)$$

where θ is time, and the coordinate directions and velocities are as shown in figure 5-1.

The pressure gradient impressed on the plate can be found by writing the equation of motion for the inviscid free stream:

$$-\frac{1}{\rho} \frac{dp}{dx} = \frac{\partial u_\infty}{\partial \theta} + u_\infty \frac{\partial u_\infty}{\partial x} \quad (5-3)$$

When equation (5-3) is substituted into equation (5-1), the equation of motion in the boundary layer can be written as

$$\frac{\partial u}{\partial \theta} + u \frac{\partial u}{\partial x} + v \frac{\partial u}{\partial y} = \frac{\partial u_\infty}{\partial \theta} + u_\infty \frac{\partial u_\infty}{\partial x} + \nu \frac{\partial^2 u}{\partial y^2} \quad (5-4)$$

The initial and boundary conditions for the problem can be stated as

$$\left. \begin{aligned} u(x, y, 0) &= u_0(x, y) \\ v(x, y, 0) &= v_0(x, y) \\ u(0, y, \theta) &= u_\infty(0, \theta) \text{ (see appendix F)} \\ u(x, 0, \theta) &= 0 \\ u(x, \infty, \theta) &= u_\infty(x, \theta) \\ v(x, 0, \theta) &= 0 \end{aligned} \right\} \quad (5-5)$$

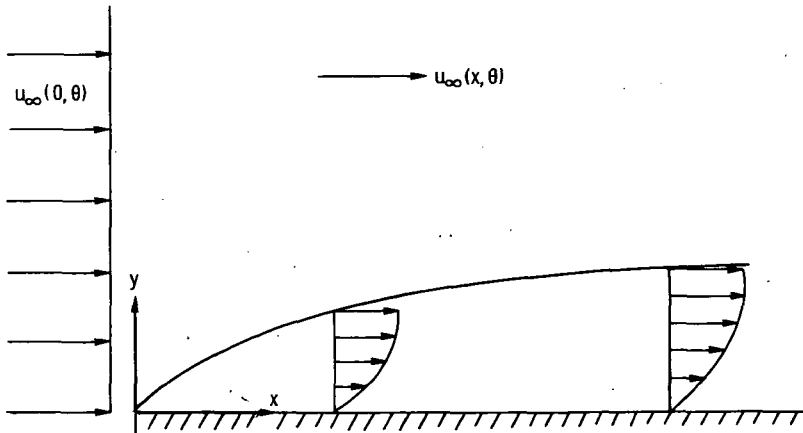


FIGURE 5-1.—Problem configuration for transient boundary layer on a flat plate.

Dimensionless variables must now be chosen. A characteristic velocity is needed and is specified here only as u_c since the one chosen depends on the problem being solved. The dimensionless variables are

$$\left. \begin{aligned} U &= u/u_c \\ V &= \frac{\rho v L}{\mu} \\ X &= \frac{x\mu}{L^2 \rho u_c} \\ Y &= y/L \\ \tau &= \frac{\mu \theta}{\rho L^2} \end{aligned} \right\} \quad (5-6)$$

As before, L is a characteristic length along the plate. When variables (5-6) are inserted into equations (5-4) and (5-2), the dimensionless equations of motion are

$$\frac{\partial U}{\partial \tau} + U \frac{\partial U}{\partial X} + V \frac{\partial U}{\partial Y} = \frac{\partial U_\infty}{\partial \tau} + U_\infty \frac{\partial U_\infty}{\partial X} + \frac{\partial^2 U}{\partial Y^2} \quad (5-7)$$

$$\frac{\partial U}{\partial X} + \frac{\partial V}{\partial Y} = 0 \quad (5-8)$$

where

$$U_\infty = u_\infty/u_c$$

The boundary conditions (5-5) become in dimensionless form

$$\left. \begin{aligned} U(X, Y, 0) &= U_0(X, Y) \\ V(X, Y, 0) &= V_0(X, Y) \\ U(0, Y, \tau) &= U_\infty(0, \tau) \\ U(X, 0, \tau) &= 0 \\ U(X, \infty, \tau) &= U_\infty(X, \tau) \\ V(X, 0, \tau) &= 0 \end{aligned} \right\} \quad (5-9)$$

A finite difference representation must now be chosen. To the author's knowledge, all such formulations appearing in the literature are explicit, but an implicit method would also appear to have its merits, so both are presented here.

5.1.1.1 Explicit representation.—The explicit representation of equation (5-7) is

$$\begin{aligned} & \frac{U_{j+1,k,i+1} - U_{j+1,k,i}}{\Delta\tau} + U_{j+1,k,i} \left(\frac{U_{j+1,k,i} - U_{j,k,i}}{\Delta X} \right) \\ & + V_{j+1,k,i} \left(\frac{U_{j+1,k+1,i} - U_{j+1,k-1,i}}{2(\Delta Y)} \right) = \left(\frac{\partial U_\infty}{\partial \tau} + U_\infty \frac{\partial U_\infty}{\partial X} \right)_{j+1,i} \\ & + \frac{U_{j+1,k+1,i} - 2U_{j+1,k,i} + U_{j+1,k-1,i}}{(\Delta Y)^2} \end{aligned} \quad (5-10)$$

The i subscript in equation (5-10) corresponds to the present (known) time step and $i+1$ to the future (unknown) time step. This representation is explicit in that equation (5-10) can be solved directly (explicitly) for $U_{j+1,k,i+1}$:

$$\begin{aligned} U_{j+1,k,i+1} = & U_{j+1,k,i} - \Delta\tau \left\{ U_{j+1,k,i} \left(\frac{U_{j+1,k,i} - U_{j,k,i}}{\Delta X} \right) \right. \\ & + V_{j+1,k,i} \left[\frac{U_{j+1,k+1,i} - U_{j+1,k-1,i}}{2(\Delta Y)} \right] - \left(\frac{\partial U_\infty}{\partial \tau} + U_\infty \frac{\partial U_\infty}{\partial X} \right)_{j+1,i} \\ & \left. + \frac{U_{j+1,k+1,i} - 2U_{j+1,k,i} + U_{j+1,k-1,i}}{(\Delta Y)^2} \right\} \end{aligned} \quad (5-11)$$

The values of U at each point in the flow field at the time step $i+1$ can thus be found in terms only of values at time step i .

After the U field has been determined at time step $i+1$, the V values at this time step may be found by writing equation (5-8) in difference form:

$$\frac{U_{j+1,k+1,i+1} - U_{j,k+1,i+1}}{\Delta X} + \frac{V_{j+1,k+1,i+1} - V_{j+1,k,i+1}}{\Delta Y} = 0 \quad (5-12)$$

Solving for $V_{j+1,k+1,i+1}$ yields

$$V_{j+1,k+1,i+1} = V_{j+1,k,i+1} - \frac{\Delta Y}{\Delta X} (U_{j+1,k+1,i+1} - U_{j,k+1,i+1}) \quad (5-13)$$

Equation (5-13) may be solved in a stepwise manner for each value of X , working from the plate to the free stream in the Y -direction.

The explicit procedure can now be summarized. The initial conditions on U and V are specified over the entire flow field at $\tau=0$. One time step $\Delta\tau$ is now taken with the subscript $i+1$ in equations (5-11) and (5-13) corresponding to values at this new time and the subscript i corresponding to the initial conditions. Starting at the leading edge, we can now use equation (5-11) to solve for the values of U at the new time, one step ΔX downstream, working outwards from the plate. Another step ΔX downstream can now be taken and the process continued until the values of U are known over the entire field at the new time

step. Equation (5-13) can now be used in exactly the same pattern until all values of V at the new time step are known. A new time step $\Delta\tau$ can now be taken and the process repeated.

Since the solution is explicit, it is to be expected that there are necessary conditions for stability. These conditions are given in reference 4 and are

$$\frac{1}{[U/\Delta X + 2/(\Delta Y)^2]} \geq \Delta\tau \quad (5-14)$$

$$\frac{2}{|V|} \geq \Delta Y \quad (5-15)$$

In order to keep $\Delta\tau$ positive, condition (5-14) also implies the same stability criterion on negative U velocities necessary in the implicit formulations for steady flow given in previous chapters, that is, if $U < 0$, then

$$|U| \leq \frac{2(\Delta X)}{(\Delta Y)^2} \quad (5-16)$$

which, in general, is satisfied only for very small values of $(-U)$. This means that only very small backflows are permissible and is an important restriction on the method, since large negative values of U_∞ also obviously cannot be permitted. Thus an oscillating component of the free stream flow can only be permitted if it is superimposed on a steady positive part of U_∞ sufficiently large so that U_∞ always remains positive.

The truncation error of the difference equations is of $\mathcal{O}(\Delta\tau)$, $\mathcal{O}((\Delta Y)^2)$, and $\mathcal{O}(\Delta X)$ for momentum and $\mathcal{O}(\Delta X)$ and $\mathcal{O}(\Delta Y)$ for continuity.

5.1.1.2 Implicit representation.—Despite the fact that the implicit formulation to be discussed here has apparently not been often employed, it has the great advantage of universal stability so long as $U \geq 0$. This means in particular that there is no restriction on the size of $\Delta\tau$. Very commonly, in using the explicit formulations, such small values of $\Delta\tau$ are required that computations can become extremely time consuming. Since the matrices encountered in the implicit formulation discussed here are tridiagonal, it would appear that the time required for a complete set of calculations at each time step will be approximately the same as that required for the explicit method, but the values of $\Delta\tau$ which may be used are very much larger than those permitted by the stability restrictions of the explicit method. As a result, it is likely that the implicit method would require less computer time than the explicit method to reach the same value of τ . As of this writing, apparently no such comparisons have been carried out, so the superiority of the implicit method remains to be proven.

There are many possible choices of implicit forms for equation (5-7). The one chosen here is

$$\alpha_k = \frac{-V_{j,k,i+1}}{2(\Delta Y)} - \frac{1}{(\Delta Y)^2}$$

$$\beta_k = \frac{U_{j,k,i+1}}{\Delta X} + \frac{2}{(\Delta Y)^2} + \frac{1}{\Delta \tau}$$

$$\Omega_k = \frac{V_{j,k,i+1}}{2(\Delta Y)} - \frac{1}{(\Delta Y)^2}$$

$$\phi_k = \left(\frac{\partial U_\infty}{\partial \tau} + U_\infty \frac{\partial U_\infty}{\partial X} \right)_{j+1,i+1} + \frac{U_{j+1,k,i}}{\Delta \tau} + \frac{U_{j,k,i+1}^2}{\Delta X}$$

The matrix of coefficients in equation (5-19) is tridiagonal and the method of appendix A may be used to obtain the values of $U_{j+1,k,i+1}$.

Continuity (eq. (5-8)) may be written in the same way as for the explicit solution (eq. (5-12)) and solved for $V_{j+1,k+1,i+1}$:

$$V_{j+1,k+1,i+1} = V_{j+1,k,i+1} - \frac{\Delta Y}{\Delta X} (U_{j+1,k+1,i+1} - U_{j,k+1,i+1}) \quad (5-20)$$

The V 's may be obtained from equation (5-20) in a stepwise manner working outward from the plate.

The implicit method can now be summarized. The initial conditions are first specified over the entire flow field. The flow field at $\tau = \Delta \tau$, one time step later, can now be found by starting from the leading edge and marching downstream. The solution at the leading edge is specified as a boundary condition, and the velocity distributions one step ΔX downstream are found by solving the matrix equation (5-19) for the U 's and equation (5-20) for the V 's. Another ΔX step may now be taken and the velocity distributions determined. This procedure is carried out in this manner until the entire flow field, as far downstream as desired, has been found at $\tau = \Delta \tau$. Another time step may now be taken and the entire flow field again solved for. The process may be repeated as many times as necessary to determine the solution for any given value of τ .

The method should be universally stable for all mesh sizes as long as $U \geq 0$. The truncation error is of $\mathcal{O}(\Delta X)$ and $\mathcal{O}((\Delta Y)^2)$ for momentum and $\mathcal{O}(\Delta X)$ and $\mathcal{O}(\Delta Y)$ for continuity.

5.1.2 Incompressible Flow—Temperature Solution

The energy equation for the transient incompressible boundary layer problem is

$$\rho c_p \left(\frac{\partial t}{\partial \theta} + u \frac{\partial t}{\partial x} + v \frac{\partial t}{\partial y} \right) = k \frac{\partial^2 t}{\partial y^2} \quad (5-21)$$

Two different thermal boundary conditions at the plate are considered in the present formulation—a constant wall temperature and a constant wall heat flux. These conditions are assumed to be independent of both position and time. Formulations for those cases where the boundary conditions may be functions of position and time are basically no different and are mentioned briefly in section 5.2.

The initial and boundary conditions considered here are

$$\begin{aligned}
 & t(x, y, 0) = t_0(x, y) \\
 & t(0, y, \theta) = t_x(0, \theta) \\
 & t(x, \infty, \theta) = t_\infty(x, \theta)
 \end{aligned}
 \quad \left. \begin{array}{l} \\ \\ \\ \text{and} \\ \\ \text{or} \end{array} \right\} \quad (5-22)$$

$$\begin{aligned}
 & t(x, 0, \theta) = t_w \quad (\text{constant wall temperature}) \\
 & -k \frac{\partial t}{\partial y} \Big|_{y=0} = q_w \quad (\text{constant wall heat flux})
 \end{aligned}$$

The problem can be restated in dimensionless form by using the following dimensionless variables:

$$\begin{aligned}
 U &= \frac{u}{u_c} & \tau &= \frac{\mu \theta}{\rho L^2} \\
 V &= \frac{\rho v L}{\mu} & X &= \frac{x \mu}{L^2 \rho u_c} \\
 & & Y &= \frac{y}{L}
 \end{aligned}
 \quad \left. \begin{array}{l} \\ \\ \\ \text{and} \end{array} \right\} \quad (5-23)$$

$$\begin{aligned}
 T &= \frac{t - t_w}{t_c - t_w} \quad (\text{constant wall temperature}) \\
 T &= \frac{k}{q_w L} (t - t_c) \quad (\text{constant wall heat flux})
 \end{aligned}$$

All quantities are as defined in the preceding velocity section, and t_c is a characteristic reference temperature chosen to suit the particular problem at hand.

Equation (5-21) may now be written in dimensionless form as

$$\frac{\partial T}{\partial \tau} + U \frac{\partial T}{\partial X} + V \frac{\partial T}{\partial Y} = \frac{1}{Pr} \frac{\partial^2 T}{\partial Y^2} \quad (5-24)$$

and the boundary conditions (5-22) become in dimensionless form for constant wall temperature

$$\left. \begin{aligned} T(X, Y, 0) &= \frac{t_0(X, Y) - t_w}{t_c - t_w} = T_0(X, Y) \\ T(0, Y, \tau) &= \frac{t_\infty(0, \tau) - t_w}{t_c - t_w} = T_\infty(0, \tau) \\ T(X, \infty, \tau) &= \frac{t_\infty(X, \tau) - t_w}{t_c - t_w} = T_\infty(X, \tau) \\ T(X, 0, \tau) &= 0 \end{aligned} \right\} \quad (5-25)$$

For constant wall heat flux,

$$\left. \begin{aligned} T(X, Y, 0) &= \frac{k}{q_w L} (t_0(X, Y) - t_c) = T_0(X, Y) \\ T(0, Y, \tau) &= \frac{k}{q_w L} (t_\infty(0, \tau) - t_c) = T_\infty(0, \tau) \\ T(X, \infty, \tau) &= \frac{k}{q_w L} (t_\infty(X, \tau) - t_c) = T_\infty(X, \tau) \\ \frac{\partial T}{\partial Y}(X, 0, \tau) &= -1 \end{aligned} \right\} \quad (5-26)$$

As was the case with the velocity solution, either an explicit or implicit finite difference representation can be chosen for equation (5-24). The representation chosen should be the same as that used for the velocity solution.

5.1.2.1 *Explicit representation.*—Equation (5-24) may be represented in explicit finite difference form as

$$\begin{aligned} \frac{T_{j+1, k, i+1} - T_{j+1, k, i}}{\Delta \tau} + U_{j+1, k, i} \left(\frac{T_{j+1, k, i} - T_{j, k, i}}{\Delta X} \right) \\ + V_{j+1, k, i} \left[\frac{T_{j+1, k+1, i} - T_{j+1, k-1, i}}{2(\Delta Y)} \right] \\ = \frac{1}{Pr} \left[\frac{T_{j+1, k+1, i} - 2T_{j+1, k, i} + T_{j+1, k-1, i}}{(\Delta Y)^2} \right] \end{aligned} \quad (5-27)$$

This explicit representation may be solved directly for $T_{j+1, k, i+1}$:

$$T_{j+1, k, i+1} = T_{j+1, k, i} - \Delta\tau \left\{ U_{j+1, k, i} \left(\frac{T_{j+1, k, i} - T_{j, k, i}}{\Delta X} \right) + V_{j+1, k, i} \left[\frac{T_{j+1, k+1, i} - T_{j+1, k-1, i}}{2(\Delta Y)} \right] - \frac{1}{Pr} \left[\frac{T_{j+1, k+1, i} - 2T_{j+1, k, i} + T_{j+1, k-1, i}}{(\Delta Y)^2} \right] \right\} \quad (5-28)$$

The values of T at time step $i+1$ can thus be found in terms of the values of U , V , and T only at time step i . These values of T at the new time may be found in any spacewise order desired. At each time step the velocity solution may be carried out first, and then the temperature solution. Another time step can then be taken and the process repeated.

To the author's knowledge, no stability analysis of (5-28) is available. However, by analogy with equation (5-11), the stability criterion can reasonably be expected to be

$$\frac{1}{U/\Delta X + \frac{2}{Pr(\Delta Y)^2}} \geq \Delta\tau \quad (5-29)$$

Whether the condition (5-28) or the conditions (5-14) and (5-15) are the determining factors in the choice of $\Delta\tau$ depends on whether Pr is greater or less than one. Similarly, the choice of ΔY is determined by the velocity solution for low and moderate Prandtl numbers, but high Prandtl numbers may require a very fine ΔY mesh for the temperature solution which as a matter of convenience would also be employed for the velocity solution.

The truncation error of the energy equation is of $\mathcal{O}(\Delta\tau)$, $\mathcal{O}(\Delta X)$ and $\mathcal{O}((\Delta Y)^2)$.

5.1.2.2 *Implicit representation.*—Equation (5-24) can be written in implicit finite difference form as

$$\begin{aligned} & \frac{T_{j+1, k, i+1} - T_{j+1, k, i}}{\Delta\tau} + U_{j, k, i+1} \left(\frac{T_{j+1, k, i+1} - T_{j, k, i+1}}{\Delta X} \right) \\ & + V_{j, k, i+1} \left[\frac{T_{j+1, k+1, i+1} - T_{j+1, k-1, i+1}}{2(\Delta Y)} \right] \\ & = \frac{1}{Pr} \left[\frac{T_{j+1, k+1, i+1} - 2T_{j+1, k, i+1} + T_{j+1, k-1, i+1}}{(\Delta Y)^2} \right] \quad (5-30) \end{aligned}$$

The method of solution for equation (5-30) is very similar to that employed for the implicit momentum equation (5-17) in section 5.1.2. Equation (5-30) is first rewritten in a more convenient form as

$$\frac{\partial \rho}{\partial \theta} + \frac{\partial(\rho u)}{\partial x} + \frac{\partial(\rho v)}{\partial y} = 0 \tag{5-36}$$

$$\rho c_p \left(\frac{\partial t}{\partial \theta} + u \frac{\partial t}{\partial x} + v \frac{\partial t}{\partial y} \right) = u \frac{dp}{dx} + \frac{\partial}{\partial y} \left(k \frac{\partial t}{\partial y} \right) + \mu \left(\frac{\partial u}{\partial y} \right)^2 \tag{5-37}$$

$$p = \rho \mathcal{R} t \tag{5-38}$$

$$\mu = \mu(t) \tag{5-39}$$

$$k = k(t) \tag{5-40}$$

The initial and boundary conditions for the problem are

$$\left. \begin{aligned} u(x, y, 0) &= u_0(x, y) \\ u(0, y, \theta) &= u_x(0, \theta) \quad (\text{see appendix F}) \\ u(x, 0, \theta) &= 0 \\ u(x, \infty, \theta) &= u_x(x, \theta) \\ v(x, y, 0) &= v_0(x, y) \\ v(x, 0, \theta) &= 0 \\ t(x, y, 0) &= t_0(x, y) \\ t(0, y, \theta) &= t_x(0, \theta) \\ t(x, \infty, \theta) &= t_x(x, \theta) \end{aligned} \right\} \tag{5-41}$$

and

$$t(x, 0, \theta) = t_w \quad (\text{constant wall temperature})$$

or

$$-k \frac{\partial t}{\partial y} \Big|_{y=0} = q_w \quad (\text{constant wall heat flux})$$

As in the incompressible case, we arbitrarily choose the representative constant wall temperature and constant wall heat flux cases for examination here.

In the compressible case, little would seem to be gained by replacing dp/dx by its relationship to other free stream quantities. Therefore, $u_x(x, \theta)$, $t_x(x, \theta)$ and $dp/dx(x, \theta)$ are presumed known from the free stream inviscid solution.

The dimensionless variables chosen for the problem are

$$\begin{aligned}
 U &= \frac{u}{u_c} & \tau &= \frac{\mu_c \theta}{\rho_c L^2} \\
 V &= \frac{\rho_c v L}{\mu_c} & \rho^* &= \frac{\rho}{\rho_c} \\
 T &= \frac{t}{t_c} & k^* &= \frac{k}{k_c} \\
 P &= \frac{p}{p_c} & \mu^* &= \frac{\mu}{\mu_c} \\
 X &= \frac{x \mu_c}{L^2 \rho_c u_c} \\
 Y &= \frac{y}{L}
 \end{aligned}
 \tag{5-42}$$

All quantities in (5-42) having subscript c are characteristic values of that quantity. These characteristic values can best be chosen when the form of the free stream variations are known in any specific case. When the dimensionless variables (5-42) are inserted in equations (5-35) to (5-37) the equations become

$$\rho^* \left(\frac{\partial U}{\partial \tau} + U \frac{\partial U}{\partial X} + V \frac{\partial U}{\partial Y} \right) = -\frac{1}{\gamma M_c^2} \frac{dP}{dX} + \frac{\partial}{\partial Y} \left(\mu^* \frac{\partial U}{\partial Y} \right) \tag{5-43}$$

$$\frac{\partial \rho^*}{\partial \tau} + \frac{\partial (\rho^* U)}{\partial X} + \frac{\partial (\rho^* V)}{\partial Y} = 0 \tag{5-44}$$

$$\begin{aligned}
 \rho^* \left(\frac{\partial T}{\partial \tau} + U \frac{\partial T}{\partial X} + V \frac{\partial T}{\partial Y} \right) &= \frac{\gamma - 1}{\gamma} U \frac{dP}{dX} \\
 &+ \frac{1}{Pr_c} \frac{\partial}{\partial Y} \left(k^* \frac{\partial T}{\partial Y} \right) + (\gamma - 1) M_c^2 \mu^* \left(\frac{\partial U}{\partial Y} \right)^2
 \end{aligned}
 \tag{5-45}$$

$$P = \rho^* T \tag{5-46}$$

$$\mu^* = T^f \tag{5-47}$$

$$k^* = T^g \tag{5-48}$$

In these equations, $M_c = U_c / \sqrt{\gamma \mathcal{R} t_c}$ and $Pr_c = \mu_c c_p / k_c$. In formulating equations (5-43) to (5-48), a perfect gas has been assumed and power law expressions have been assumed for the viscosity and thermal conductivity, based on t_c as a reference temperature.

The boundary and initial conditions (5-41) written in dimensionless form are

$$U(X, Y, 0) = \frac{u_0(X, Y)}{u_c} = U_0(X, Y)$$

$$U(0, Y, \tau) = \frac{u_\infty(0, \tau)}{u_c} = U_\infty(0, \tau)$$

$$U(x, 0, \tau) = 0$$

$$U(X, \infty, \tau) = \frac{u_\infty(X, \tau)}{u_c} = U_\infty(X, \tau)$$

$$V(X, Y, 0) = \frac{v_0(X, Y)\rho_c L}{\mu_c} = V_0(X, Y)$$

$$V(X, 0, \tau) = 0$$

$$T(X, Y, 0) = \frac{t_0(X, Y)}{t_c} = T_0(X, Y)$$

$$T(0, Y, \tau) = \frac{t_\infty(0, \tau)}{t_c} = T_\infty(0, \tau)$$

$$T(X, \infty, \tau) = \frac{t_\infty(X, \tau)}{t_c} = T_\infty(X, \tau)$$

$$T(X, 0, \tau) = t_w/t_c = T_w \quad (\text{constant wall temperature})$$

$$-k^* \frac{\partial T}{\partial Y} \Big|_{Y=0} = \frac{q_w L}{k_c t_c} \quad (\text{constant wall heat flux})$$

(5-49)

and

or

A finite difference formulation must now be chosen for the problem. To the best of the author's knowledge, no other difference formulation is presently available. The form chosen here is of the implicit type because of the inherent stability advantages of such a form. Equations (5-43) to (5-48) are written in difference form as

$$\begin{aligned}
\rho_{j,k,i+1}^* & \left\{ \left(\frac{U_{j+1,k,i+1} - U_{j+1,k,i}}{\Delta\tau} \right) + U_{j,k,i+1} \left(\frac{U_{j+1,k,i+1} - U_{j,k,i+1}}{\Delta X} \right) \right. \\
& \left. + V_{j,k,i+1} \left[\frac{U_{j+1,k+1,i+1} - U_{j+1,k-1,i+1}}{2(\Delta Y)} \right] \right\} = -\frac{1}{\gamma M_c^2} \left(\frac{P_{j+1,i+1} - P_{j,i+1}}{\Delta X} \right) \\
& + \mu_{j,k,i+1}^* \left[\frac{U_{j+1,k+1,i+1} - 2U_{j+1,k,i+1} + U_{j+1,k-1,i+1}}{(\Delta Y)^2} \right] \\
& + \left[\frac{\mu_{j,k+1,i+1}^* - \mu_{j,k-1,i+1}^*}{2(\Delta Y)} \right] \left[\frac{U_{j+1,k+1,i+1} - U_{j+1,k-1,i+1}}{2(\Delta Y)} \right] \quad (5-50)
\end{aligned}$$

$$\begin{aligned}
\frac{\rho_{j+1,k,i+1}^* - \rho_{j+1,k,i}^*}{\Delta\tau} + \frac{\rho_{j+1,k+1,i+1}^* U_{j+1,k+1,i+1}}{\Delta X} - \frac{\rho_{j,k+1,i+1}^* U_{j,k+1,i+1}}{\Delta X} \\
+ \frac{\rho_{j+1,k+1,i+1}^* V_{j+1,k+1,i+1} - \rho_{j+1,k,i+1}^* V_{j+1,k,i+1}}{\Delta Y} = 0 \quad (5-51)
\end{aligned}$$

$$\begin{aligned}
\rho_{j,k,i+1}^* & \left\{ \left(\frac{T_{j+1,k,i+1} - T_{j+1,k,i}}{\Delta\tau} \right) + U_{j,k,i+1} \left(\frac{T_{j+1,k,i+1} - T_{j,k,i+1}}{\Delta X} \right) \right. \\
& \left. + V_{j,k,i+1} \left[\frac{T_{j+1,k+1,i+1} - T_{j+1,k-1,i+1}}{2(\Delta Y)} \right] \right\} = \frac{\gamma-1}{\gamma} U_{j,k,i+1} \left(\frac{P_{j+1,i+1} - P_{j,i+1}}{\Delta X} \right) \\
& + \frac{1}{Pr_c} \left\{ k_{j,k,i+1}^* \left[\frac{T_{j+1,k+1,i+1} - 2T_{j+1,k,i+1} + T_{j+1,k-1,i+1}}{(\Delta Y)^2} \right] \right. \\
& \left. + \left[\frac{k_{j,k+1,i+1}^* - k_{j,k-1,i+1}^*}{2(\Delta Y)} \right] \left[\frac{T_{j+1,k+1,i+1} - T_{j+1,k-1,i+1}}{2(\Delta Y)} \right] \right\} \\
& + (\gamma-1) M_c^2 \mu_{j,k,i+1}^* \left[\frac{U_{j+1,k+1,i+1} - U_{j+1,k-1,i+1}}{2(\Delta Y)} \right]^2 \quad (5-52)
\end{aligned}$$

$$P_{j+1,i+1} = \rho_{j+1,k,i+1}^* T_{j+1,k,i+1} \quad (5-53)$$

$$\mu_{j+1,k,i+1}^* = (T_{j+1,k,i+1})^f \quad (5-54)$$

$$k_{j+1,k,i+1}^* = (T_{j+1,k,i+1})^g \quad (5-55)$$

Assuming that the entire field of U , V , T , and all properties are known at time step i , we now proceed to determine the flow field and properties at time step $i+1$ by starting at the leading edge of the plate and marching downstream.

Equation (5-50) is first rearranged in a more convenient form:

$$\begin{aligned}
 & \left[\frac{-\rho_{j,k,i+1}^* V_{j,k,i+1}}{2(\Delta Y)} - \frac{\mu_{j,k,i+1}^*}{(\Delta Y)^2} + \frac{\mu_{j,k+1,i+1}^* - \mu_{j,k-1,i+1}^*}{4(\Delta Y)^2} \right] U_{j+1,k-1,i+1} \\
 & + \left[\frac{\rho_{j,k,i+1}^*}{\Delta \tau} + \frac{\rho_{j,k,i+1}^* U_{j,k,i+1}}{\Delta X} + \frac{2\mu_{j,k,i+1}^*}{(\Delta Y)^2} \right] U_{j+1,k,i+1} \\
 & + \left[\frac{\rho_{j,k,i+1}^* V_{j,k,i+1}}{2(\Delta Y)} - \frac{\mu_{j,k,i+1}^*}{(\Delta Y)^2} - \frac{\mu_{j,k+1,i+1}^* - \mu_{j,k-1,i+1}^*}{4(\Delta Y)^2} \right] U_{j+1,k+1,i+1} \\
 & = \frac{\rho_{j,k,i+1}^* U_{j+1,k,i}}{\Delta \tau} + \frac{\rho_{j,k,i+1}^* U_{j,k,i+1}^2}{\Delta X} - \frac{1}{\gamma M_c^2} \left(\frac{P_{j+1,i+1} - P_{j,i+1}}{\Delta X} \right) \quad (5-56)
 \end{aligned}$$

Equation (5-56) written for $k = 1(1)n$ provides n equations in the unknowns $U_{j+1,k,i+1}$. This set may be written in matrix form as

$$\begin{array}{ccc|c|ccc}
 \beta_1 & \Omega_1 & & \times & U_{j+1,1,i+1} & = & \phi_1 \\
 \alpha_2 & \beta_2 & \Omega_2 & & U_{j+1,2,i+1} & & \phi_2 \\
 & \alpha_3 & \beta_3 & \Omega_3 & U_{j+1,3,i+1} & & \phi_3 \\
 & & - & - & - & & - \\
 & & - & - & - & & - \\
 & & - & - & - & & - \\
 & & & & \alpha_{n-1} & \beta_{n-1} & \Omega_{n-1} & U_{j+1,n-1,i+1} & \phi_{n-1} \\
 & & & & \alpha_n & \beta_n & & U_{j+1,n,i+1} & \phi_n - \Omega_n U_\infty
 \end{array} \quad (5-57)$$

where

$$\begin{aligned}
 \alpha_k &= \frac{-\rho_{j,k,i+1}^* V_{j,k,i+1}}{2(\Delta Y)} - \frac{\mu_{j,k,i+1}^*}{(\Delta Y)^2} + \frac{\mu_{j,k+1,i+1}^* - \mu_{j,k-1,i+1}^*}{4(\Delta Y)^2} \\
 \beta_k &= \frac{\rho_{j,k,i+1}^*}{\Delta \tau} + \frac{\rho_{j,k,i+1}^* U_{j,k,i+1}}{\Delta X} + \frac{2\mu_{j,k,i+1}^*}{(\Delta Y)^2} \\
 \Omega_k &= \frac{\rho_{j,k,i+1}^* V_{j,k,i+1}}{2(\Delta Y)} - \frac{\mu_{j,k,i+1}^*}{(\Delta Y)^2} - \frac{\mu_{j,k+1,i+1}^* - \mu_{j,k-1,i+1}^*}{4(\Delta Y)^2} \\
 \phi_k &= \frac{\rho_{j,k,i+1}^* U_{j+1,k,i}}{\Delta \tau} + \frac{\rho_{j,k,i+1}^* U_{j,k,i+1}^2}{\Delta X} - \frac{1}{\gamma M_c^2} \left(\frac{P_{j+1,i+1} - P_{j,i+1}}{\Delta X} \right)
 \end{aligned}$$

$$\alpha'_k = \frac{-\rho_{j,k,i+1}^* V_{j,k,i+1}}{2(\Delta Y)} - \frac{k_{j,k,i+1}^*}{Pr_c(\Delta Y)^2} + \frac{k_{j,k+1,i+1}^* - k_{j,k-1,i+1}^*}{4Pr_c(\Delta Y)^2}$$

$$\beta'_k = \frac{\rho_{j,k,i+1}^*}{\Delta \tau} + \frac{\rho_{j,k,i+1}^* U_{j,k,i+1}}{\Delta X} + \frac{2k_{j,k,i+1}^*}{Pr_c(\Delta Y)^2}$$

$$\Omega'_k = \frac{\rho_{j,k,i+1}^* V_{j,k,i+1}}{2(\Delta Y)} - \frac{k_{j,k,i+1}^*}{Pr_c(\Delta Y)^2} - \frac{k_{j,k+1,i+1}^* - k_{j,k-1,i+1}^*}{4Pr_c(\Delta Y)^2}$$

$$\phi'_k = \frac{\rho_{j,k,i+1}^* T_{j+1,k,i}}{\Delta \tau} + \frac{\rho_{j,k,i+1}^* U_{j,k,i+1} T_{j,k,i+1}}{\Delta X}$$

$$+ \frac{\gamma-1}{\gamma} U_{j,k,i+1} \left(\frac{P_{j+1,i+1} - P_{j,i+1}}{\Delta X} \right)$$

$$+ (\gamma-1) M_c^2 \mu_{j,k,i+1}^* \left[\frac{U_{j+1,k+1,i+1} - U_{j+1,k-1,i+1}}{2(\Delta Y)} \right]^2$$

The matrix of coefficients in (5-59) is tridiagonal and the method of appendix A may be used to solve for $T_{j+1,k,i+1}$.

If the constant wall heat flux case is to be considered, the wall temperature $T_{j+1,0,i+1}$ is an additional unknown. The necessary additional relationship comes from the heat flux boundary condition at the wall which may be expressed in finite-difference form as

$$-k_{j,0,i+1}^* \left[\frac{-3T_{j+1,0,i+1} + 4T_{j+1,1,i+1} - T_{j+1,2,i+1}}{2(\Delta Y)} \right] = \frac{q_w L}{k_{ctc}} \quad (5-60)$$

We are more or less forced to use $k_{j,0,i+1}^*$ in equation (5-60) to keep the equation linear in $T_{j+1,0,i+1}$; one possible alternative exists, and that is to use $k_{j+1,0,i}^*$. Assuming that relatively small mesh sizes are used, either should be acceptable, and only computational experience will indicate which is preferable. The additional row corresponding to equation (5-60) must be added to the matrix equation (5-59) along with a few other slight modifications. A more detailed description of the modifications necessary for dealing with constant heat flux cases is described in section 2.1.2.

Next, the dimensionless density ρ^* may be determined from the equation of state (5-53):

$$\rho_{j+1,k,i+1}^* = \frac{P_{j+1,i+1}}{T_{j+1,k,i+1}} \quad (5-61)$$

The continuity equation (5-51) may now be solved for $V_{j+1,k+1,i+1}$:

$$\begin{aligned}
 V_{j+1, k+1, i+1} = & \frac{\rho_{j+1, k, i+1}^*}{\rho_{j+1, k+1, i+1}^*} V_{j+1, k, i+1} \\
 & - \frac{\Delta Y}{\Delta X} \left(U_{j+1, k+1, i+1} - \frac{\rho_{j, k+1, i+1}^*}{\rho_{j+1, k+1, i+1}^*} U_{j, k+1, i+1} \right) \\
 & - \frac{\Delta Y}{\Delta \tau} \left(\frac{\rho_{j+1, k, i+1}^* - \rho_{j+1, k, i}^*}{\rho_{j+1, k+1, i+1}^*} \right) \quad (5-62)
 \end{aligned}$$

This equation may be solved in a stepwise manner, working outward from the plate. Finally, the properties are obtained from (5-54) and (5-55).

Another step ΔX downstream may now be taken and the process repeated. When the solution has been carried downstream as far as desired, another time step $\Delta \tau$ may be taken, and again starting at the leading edge, the solution is marched spacewise downstream. As the solution is obtained, only the quantities upstream of the point $j+1$ for time step $i+1$ and downstream of the point j for time step i need be retained.

Although no stability analysis has been undertaken, it is reasonable to assume that the implicit equations are stable for all $U \geq 0$. The truncation error is of $\mathcal{O}(\Delta X)$ and $\mathcal{O}((\Delta Y)^2)$ for momentum and energy and $\mathcal{O}(\Delta X)$ and $\mathcal{O}(\Delta Y)$ for continuity.

5.1.5 Compressible Flow—Heat Transfer Solution

The compressible flow transient heat transfer analysis is only slightly different from the steady state incompressible heat transfer analysis discussed in section 2.1.3. The only modifications to the incompressible steady analysis are in the use of a variable k^* in the heat flux equation (see eq. (5-60)) and in time averaging the Nusselt numbers by using Simpson's rule.

5.2 OTHER PROBLEMS WITH SIMILAR FORMULATIONS

Any of the additional variations and complications considered at the end of chapter 2 on steady state boundary layers can also be readily included for the transient case. No details are given here since most of the extensions are straightforward. Other problems which can be considered with little additional complication include those in which the wall temperature or heat flux is a function of space and time, suction or injection which is a function of space and time, and transient flows with MHD or EHD body forces.

5.3 EXAMPLE PROBLEM—OSCILLATING BOUNDARY LAYER ON A FLAT PLATE.

As an example of the use of the numerical technique for transient flows, the solution obtained by Farn and Arpaci (refs. 4 and 5) for the oscillating boundary layer on a flat plate is presented. The plate is assumed to be stationary and the free stream oscillates periodically about a constant mean value. The initial conditions are assumed to be those of steady Blasius flow. The general boundary conditions (eq. (5-5)) presented earlier can be rewritten for the present problem as

$$\left. \begin{aligned} u(x, y, 0) &= u_B(x, y) \\ v(x, y, 0) &= v_B(x, y) \\ u(0, y, \theta) &= u_m + \Delta u_\infty \sin \omega \theta \\ u(x, 0, \theta) &= 0 \\ u(x, \infty, \theta) &= u_m + \Delta u_\infty \sin \omega \theta \\ v(x, 0, \theta) &= 0 \end{aligned} \right\} \quad (5-63)$$

where $u_B(x, y)$ and $v_B(x, y)$ are the steady Blasius solution based on a constant free stream velocity of u_m . The constant mean velocity in the free stream is also u_m . The amplitude of the free stream oscillations is Δu_∞ and the frequency of these oscillations is ω . The dimensionless variables (eq. (5-6)) may now be defined with the characteristic velocity u_c equal to u_m . The boundary conditions (5-63) in dimensionless form are then

$$\left. \begin{aligned} U(X, Y, 0) &= U_B(X, Y) \\ V(X, Y, 0) &= V_B(X, Y) \\ U(0, Y, \tau) &= 1 + \Delta U_\infty \sin W\tau \\ U(X, 0, \tau) &= 0 \\ U(X, \infty, \tau) &= 1 + \Delta U_\infty \sin W\tau = U_\infty(\tau) \\ V(X, 0, \tau) &= 0 \end{aligned} \right\} \quad (5-64)$$

where $U_B(X, Y)$ and $V_B(X, Y)$ are the Blasius solution in dimensionless form, and

$$\Delta U_\infty = \Delta u_\infty / u_m$$

and

$$W = \frac{\omega L^2 \rho}{\mu}$$

The equations of motion in dimensionless form are equations (5-7) and (5-8). These equations of motion are represented in explicit finite difference form as equations (5-10) and (5-12).

The solution to these difference equations was carried out by Farn and Arpaci. Two cases were considered—high frequency and intermediate frequency. The values of the mesh sizes and parameters employed for these two cases are shown in table 5-1. Since the dimensionless variables used by Farn and Arpaci were different from those employed in this chapter, the numbers given in table 5-1 have been converted to the variables of this chapter.

TABLE 5-1.—MESH SIZES AND PARAMETERS EMPLOYED BY FARN AND ARPACI (REFS. 4 AND 5)

	Dimensionless mesh increment, ΔY		Range of dimensionless mesh increment, ΔX	Dimensionless time increment, $\Delta \tau$	Maximum dimensionless axial coordinate, X	Amplitude of free stream oscillations, ΔU_∞	Dimensionless frequency, W
	Near	Far					
High frequency	0.025	0.05	7×10^{-4} to $.3 \times 10^{-3}$	2×10^{-4}	0.082	0.05	$\pi \times 10^2$
Intermediate frequency	0.025	0.05	1.2×10^{-3} to 3×10^{-3}	3×10^{-4}	0.102	0.05	58.1776

The authors' primary interest in this solution was in the steady periodic behavior; in order to reach a steady periodic state, however, it was necessary to go through the transient. For both cases, five cycles were sufficient to attain steady periodic flow, but carrying the flow through this transient required considerable amounts of computer time.

Figures (5-2) and (5-3) show comparisons of the results of the numerical solution with those of Lin (ref. 6) for high frequencies and Hill and Stenning (ref. 7) for intermediate frequencies. Figure (5-2) shows the amplitude ratio $\Delta U/\Delta U_\infty$ for two different frequency parameters ($XW=9.0$ and $XW=25.8$) as functions of $Y\sqrt{W}/2$. These solutions agree very well with Lin's high frequency analytical solution which is a function of $Y\sqrt{W}/2$ only and hence yields a single curve. The phase angles of the velocity also agree well with Lin's solution for high frequencies (see ref. 5). Figure (5-3) compares the amplitude ratio obtained from the numerical solution with Hill and Stenning's approximate solution and experimental data for an intermediate frequency range. The agreement is again very good. For more detailed comparisons of both amplitude ratio and phase angle in the intermediate frequency range see reference 5.

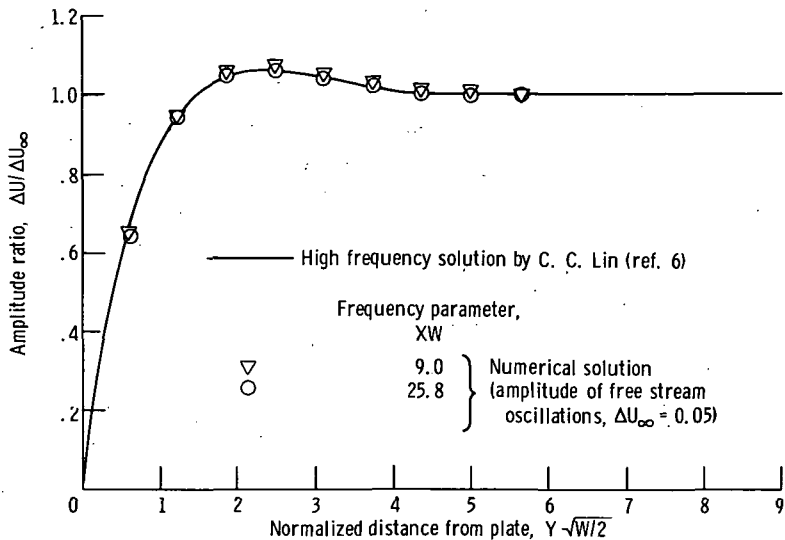


FIGURE 5-2. — Amplitude of high frequency oscillations in Blasius flow.

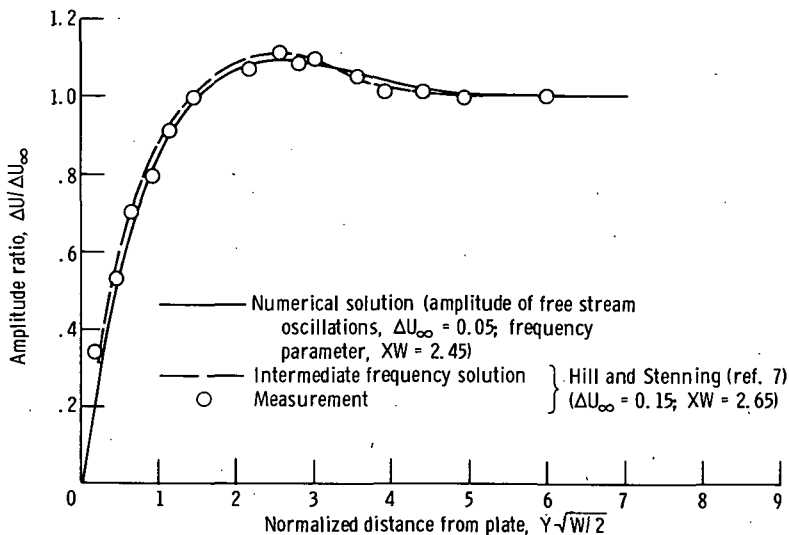


FIGURE 5-3. — Amplitude of intermediate frequency oscillations in Blasius flow ($XW = 2.45$).

REFERENCES

1. FROMM, J. E.: The Time Dependent Flow of an Incompressible Viscous Fluid. Fundamental Methods in Hydrodynamics. Vol. 3 of Methods in Computational Physics, Academic Press, 1964, pp. 346-382.
2. HARLOW, FRANCIS H.; AND FROMM, JACOB E.: Dynamics and Heat Transfer in the Von Kármán Wake of a Rectangular Cylinder. Phys. Fluids, vol. 7, no. 8, Aug. 1964, pp. 1147-1156.

3. HELLUMS, JESSE D.: Finite-Difference Computation of Natural Convection Heat Transfer. Ph. D. Thesis, Univ. Michigan, 1960.
4. FARN, CHARLES L. S.; AND ARPACI, VEDAT S.: On the Numerical Solution of Unsteady, Laminary Boundary Layers. AIAA J., vol. 4, no. 4, Apr. 1966, pp. 730-732.
5. FARN, CHARLES L. S.: A Finite Difference Method for Computing Unsteady, Incompressible, Laminary Boundary-Layer Flows. Ph. D. Thesis, Univ. Michigan, 1965.
6. LIN, C. C.: Motion in the Boundary Layer with a Rapidly Oscillating External Flow. Proceedings of the 9th International Congress on Applied Mechanics. Vol. 4. University of Brussels, 1957, pp. 155-167.
7. HILL, P. G.; AND STENNING, A. H.: Laminary Boundary Layers in Oscillatory Flow. J. Basic Eng., vol. 82, no. 3, Sept. 1960, pp. 593-608.

CHAPTER 6

PARALLEL PLATE CHANNEL

The treatment given for the parallel plate channel in the present chapter and that given for the circular tube in chapter 7 follow in many respects along similar lines. This similar treatment is due largely to the fact that both geometries are two-dimensional, although the effects of the cylindrical geometry in the circular tube case cause sufficiently significant differences between the formulations to warrant separate chapters for the two cases. In some situations, detailed and lengthy discussions for the parallel plate channel and circular tube would be identical or nearly so; for such situations, the detailed discussions are given in the present chapter and reference is made to these discussions in chapter 7.

6.1 ENTRANCE FLOW AND HEAT TRANSFER IN A PARALLEL PLATE CHANNEL

The first problems to be considered in our discussion of confined flows are those of entrance flow and heat transfer in a parallel plate channel. The parallel plate channel has been chosen for initial consideration because the formulation illustrates the techniques used for confined flows without the complicating geometrical and three-dimensional factors of other configurations. The parallel plate channel geometry is shown in figure 6-1. This channel is an approximation to a rectangular channel of high aspect ratio.

6.1.1 Incompressible Constant Property Flow — Velocity Solution

The development of laminar flow in the entrance of a channel bears considerable resemblance to boundary layer growth on a flat plate. Accordingly, the most commonly employed model for this problem is a boundary layer model near the channel walls with a potential core toward the center of the channel which accelerates as the boundary layers grow (see Schlichting, ref. 1). This model does an entirely adequate job in most respects; it is questionable only near the channel inlet where transverse momentum effects are important and

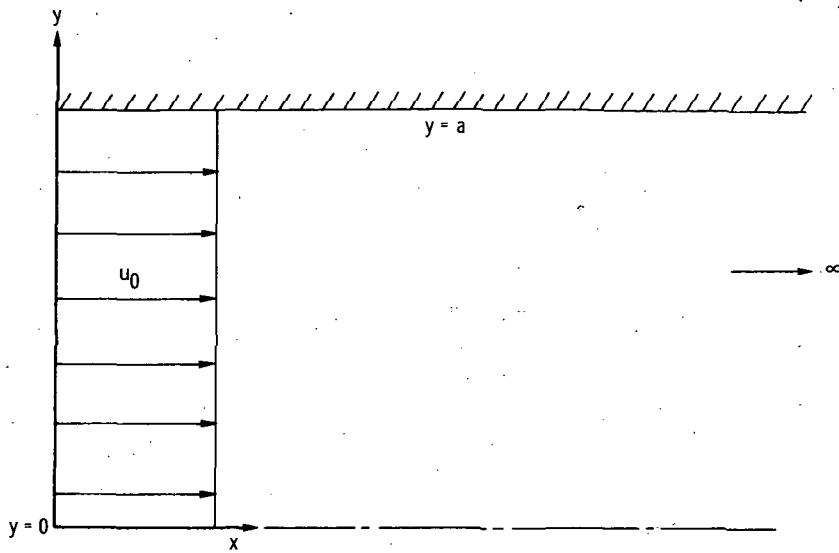


FIGURE 6-1. — Problem configuration and coordinate system for parallel plate channel.

hence the boundary layer model breaks down, and in the core region where viscous effects may actually be present. One other aspect of this type of model is that the velocity distribution at the inlet to the channel is assumed to be uniform. In actuality, the effect of the channel propagates upstream into the reservoir, causing the inlet profile to be rounded as shown in reference 2. In this reference Wang and Longwell obtained a numerical solution to the complete Navier-Stokes equations with all terms included for the two-dimensional problem of flow through an infinite stack of parallel plate channels. This upstream propagation effect did not influence the results strongly except for low Reynolds numbers (less than about 600).

The model for the velocity entrance region which we choose to employ here is the same as the one used by Bodoia and Osterle (ref. 3) and is very similar to the one discussed previously except that equations of the boundary layer type are assumed to apply over the entire flow field. This permits the viscous effects in the "core" region to be included. The transverse momentum effects which are important very near the inlet are again ignored, as are any upstream propagation effects. However, the velocity profile at the inlet to the channel may have any shape desired, including the uniform profile customarily employed.

The following formulation is based largely on the work of Bodoia and Osterle. The equations of motion are assumed to be

$$\rho \left(u \frac{\partial u}{\partial x} + v \frac{\partial u}{\partial y} \right) = - \frac{dp}{dx} + \mu \left(\frac{\partial^2 u}{\partial y^2} \right) \quad (6-1)$$

and

$$\frac{\partial u}{\partial x} + \frac{\partial v}{\partial y} = 0 \tag{6-2}$$

subject to the following boundary conditions:

$$\left. \begin{aligned} u(0, y) &= u_0 \text{ (assumed constant here, although a function of } y \text{)} \\ &\text{is also permissible; see also appendix F)} \\ u(x, a) &= 0 \\ \frac{\partial u}{\partial y}(x, 0) &= 0 \\ v(x, 0) &= 0 \\ v(x, a) &= 0 \\ p(0) &= p_0 \end{aligned} \right\} \tag{6-3}$$

The equations of motion may be made dimensionless by the following choice of dimensionless variables:

$$\left. \begin{aligned} U &= \frac{u}{u_0} & X &= \frac{x\mu}{a^2\rho u_0} \\ V &= \frac{\rho va}{\mu} & Y &= \frac{y}{a} \\ P &= \frac{(p - p_0)}{\rho u_0^2} \end{aligned} \right\} \tag{6-4}$$

Equations (3-1) and (3-2) written in dimensionless form become

$$U \frac{\partial U}{\partial X} + V \frac{\partial U}{\partial Y} = -\frac{dP}{dX} + \frac{\partial^2 U}{\partial Y^2} \tag{6-5}$$

and

$$\frac{\partial U}{\partial X} + \frac{\partial V}{\partial Y} = 0 \tag{6-6}$$

with the boundary conditions

$$\begin{aligned}
 U(0, Y) &= 1 \\
 U(X, 1) &= 0 \\
 \frac{\partial U}{\partial Y}(X, 0) &= 0 \\
 V(X, 0) &= 0 \\
 V(X, 1) &= 0 \\
 P(0) &= 0
 \end{aligned}
 \tag{6-7}$$

We must now choose a finite difference representation. The grid used is shown in figure 6-2. We employ the usual implicit form for equation (6-5).

$$U_{j,k} \frac{U_{j+1,k} - U_{j,k}}{\Delta X} + V_{j,k} \frac{U_{j+1,k+1} - U_{j+1,k-1}}{2(\Delta Y)} = - \frac{P_{j+1} - P_j}{\Delta X} + \frac{U_{j+1,k+1} - 2U_{j+1,k} + U_{j+1,k-1}}{(\Delta Y)^2}
 \tag{6-8}$$

A somewhat unusual representation of equation (6-6) is chosen for a reason which will become clear shortly. The form is

$$\frac{U_{j+1,k+1} - U_{j,k+1} + U_{j+1,k} - U_{j,k}}{2(\Delta X)} + \frac{V_{j+1,k+1} - V_{j+1,k}}{\Delta Y} = 0
 \tag{6-9}$$

Equations (6-8) and (6-9) written for $k=0(1)n$ constitute $2n+2$ equations in the $2n+2$ unknowns $U_{j+1,0}, \dots, U_{j+1,n}; V_{j+1,1}, \dots, V_{j+1,n};$ and P_{j+1} . The number of unknowns can be reduced materially by writing the continuity equation (6-9) for $k=0(1)n$ and adding together all of these equations. The resulting equation is

$$U_{j+1,0} + 2 \sum_{k=1}^n U_{j+1,k} = U_{j,0} + 2 \sum_{k=1}^n U_{j,k}
 \tag{6-10}$$

If both sides of equation (6-10) are multiplied by $\Delta Y/2$, it can be seen to be the trapezoidal rule integration form of the equation

$$\int_0^1 U dy \Big|_{j+1} = \int_0^1 U dy \Big|_j
 \tag{6-11}$$

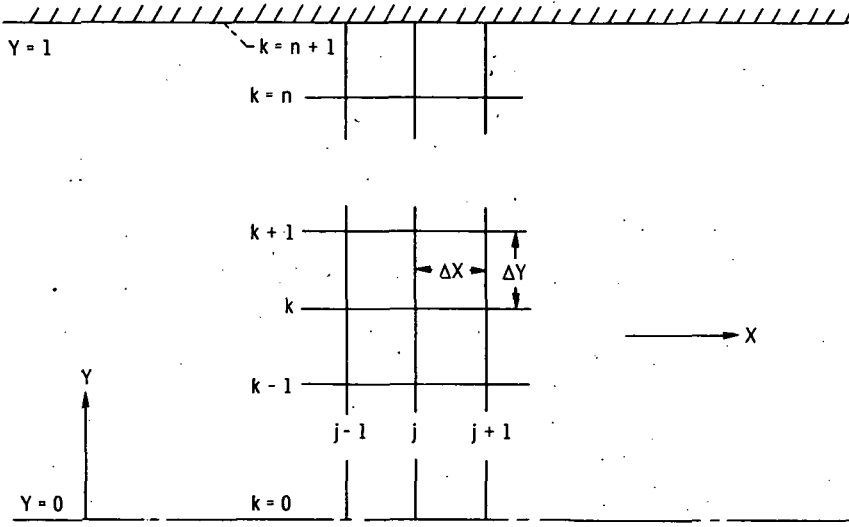


FIGURE 6-2. — Finite difference grid for parallel plate channel.

which is an integral form of the continuity equation. This equation is, of course, not independent of any of those already given, but simply incorporates the boundary conditions on V at the channel centerline and walls by requiring that the axial flow rate be a constant. The use of this equation to simplify the solution of confined flow problems was apparently first suggested by Bodoia (ref. 4) who called it an *equation of constraint*.

Since equation (6-10) does not involve V , equation (6-10) together with equation (6-8) written for $k=0(1)n$ now constitute $n+2$ equations in the $n+2$ unknowns $U_{j+1,0}, \dots, U_{j+1,n}$ and P_{j+1} . To aid in obtaining a solution, it is convenient to rewrite equation (6-8) as

$$\left[\frac{-V_{j,k}}{2(\Delta Y)} - \frac{1}{(\Delta Y)^2} \right] U_{j+1,k-1} + \left[\frac{U_{j,k}}{\Delta X} + \frac{2}{(\Delta Y)^2} \right] U_{j+1,k} + \left[\frac{V_{j,k}}{2(\Delta Y)} - \frac{1}{(\Delta Y)^2} \right] U_{j+1,k+1} + \left[\frac{1}{\Delta X} \right] P_{j+1} = \frac{U_{j,k}^2 + P_j}{\Delta X} \quad (6-12)$$

Equations (6-12) (written for $k=0(1)n$) and (6-10) may be written in matrix form as

1	2	2	2	2	—	—	2	2	0	$U_{j+1,0}$	S	
β_0	Ω_0								$\frac{1}{\Delta X}$	$U_{j+1,1}$	ϕ_0	
α_1	β_1	Ω_1							$\frac{1}{\Delta X}$	$U_{j+1,2}$	ϕ_1	
	α_2	β_2	Ω_2						$\frac{1}{\Delta X}$	$U_{j+1,3}$	ϕ_2	
		α_3	β_3	Ω_3					$\frac{1}{\Delta X}$	$U_{j+1,4}$	ϕ_3	
		—	—	—					—	—	—	
			—	—	—				—	—	—	
				—	—	—			—	—	—	
							α_{n-1}	β_{n-1}	Ω_{n-1}	$\frac{1}{\Delta X}$	$U_{j+1,n}$	ϕ_{n-1}
							α_n	β_n	$\frac{1}{\Delta X}$	P_{j+1}	ϕ_n	

(6-13)

where

$$\Omega_0 = -\frac{2}{(\Delta Y)^2} \text{ (incorporates symmetry at } Y = 0 \text{)}$$

$$S = U_{j,0} + 2 \sum_{k=1}^n U_{j,k}$$

and

$$\alpha_k = -\frac{V_{j,k}}{2(\Delta Y)} - \frac{1}{(\Delta Y)^2}$$

$$\beta_k = \frac{U_{j,k}}{\Delta X} + \frac{2}{(\Delta Y)^2}$$

$$\Omega_k = \frac{V_{j,k}}{2(\Delta Y)} - \frac{1}{(\Delta Y)^2} \quad (k > 0)$$

$$\phi_k = \frac{U_{j,k}^2 + P_j}{\Delta X}$$

The matrix of coefficients in equation (6-13) does not have the desirable tridiagonal character of the matrices encountered in the previous chapters on external flows. This matrix is, however, quite sparse. It would be possible to write a special computer program to solve the set (6-13) by taking full advantage of this sparseness. This would only be practical if a large number of production runs were contemplated and the savings in running time and storage space considered more important than the programming time required. As a general rule, it seems most practical to solve the set by using one of the standard routines for linear equations or matrix inversion which are available at any computer installation. A possible alternative is to solve the set by Gauss-Siedel iteration. This method will work effectively except for equation (6-10) (top row of eq. (6-13)), which must be drastically underrelaxed. (See chapter 3, section 3.1.1.1 for details of the relaxation process.)

After the set (6-13) has been solved for $U_{j+1,0}, \dots, U_{j+1,n}$ and P_{j+1} , equation (6-9) may be employed in the form

$$V_{j+1,k+1} = V_{j+1,k} - \frac{\Delta Y}{2(\Delta X)} (U_{j+1,k+1} - U_{j,k+1} + U_{j+1,k} - U_{j,k}) \quad (6-14)$$

which may be marched outward from the channel centerline to give the values of $V_{j+1,1}, \dots, V_{j+1,n}$.

Another step ΔX downstream may now be taken and the process repeated. This may be continued as many times as necessary.

The use of two different ΔY mesh sizes, coarse near the center of the channel and fine near the walls, will aid considerably in reducing the number of unknowns and hence the size of the matrix in equation (6-13). This technique is described in detail in appendix D.

The proper choice of the ΔX mesh size at and near the channel entrance is a very important factor in obtaining an accurate solution. This region represents difficulties of two kinds: first, the equations of the boundary layer type used in this chapter are not valid there because transverse (Y) momentum and axial (X) second derivatives become important; and second, the entrance itself represents a mathematical difficulty in that it behaves like a singularity. The breakdown of the equations is not discussed here except to say that the boundary layer equations provide an excellent model except in a very small region close to the inlet. The mathematical singularity may be dealt with in the manner described in chapter 2 for the leading edge in the boundary layer development problem, by keeping ΔX very small and hence taking a large number of steps in the region close to the entrance. As in the boundary layer case, the spread of the effect of the singularity downstream is primarily a function of how many steps are taken to reach

a given X position; if a large number of steps are taken to reach this value of X , then the effect of the singularity there tends to disappear. The effect of the singularity may thus be confined to a region arbitrarily close to the entrance. After this singularity has been taken care of, the ΔX mesh size may be increased considerably.

As usual, the only sure way to decide on final mesh sizes is to obtain solutions with succeeding smaller mesh sizes until the solutions obtained on two successive mesh reductions agree to within the desired accuracy.

The stability restrictions for this problem have been established by Bodoia (ref. 4) and are the same as those given in chapter 2 for the incompressible boundary layer problem. The formulation is universally stable for $U \geq 0$, and if $U < 0$, then

$$\frac{\Delta X}{|U|(\Delta Y)^2} \geq \frac{1}{2} \quad (6-15)$$

$$V \geq \sqrt{\frac{2|U|}{\Delta X}} \quad (6-16)$$

which are generally satisfied only for very small values of $|U|$.

The truncation error of the momentum equation is of $\mathcal{O}(\Delta X)$ and $\mathcal{O}((\Delta Y)^2)$ and that of continuity $\mathcal{O}(\Delta X)$ and $\mathcal{O}(\Delta Y)$.

Appendix C includes a discussion of inherent error in flow rate for confined flow problems of this type.

6.1.2 Incompressible Constant Property Flow – Temperature Solution

The energy equation for incompressible, constant property flow is uncoupled from the momentum equation once the velocity distribution is known. When viscous dissipation is neglected, the energy equation may be written as

$$\rho c_p \left(u \frac{\partial t}{\partial x} + v \frac{\partial t}{\partial y} \right) = k \frac{\partial^2 t}{\partial y^2} \quad (6-17)$$

The two most commonly considered thermal boundary conditions for confined flows are constant wall temperature and constant heat flux per unit length in the flow direction. Both of these conditions are considered in this formulation. The boundary conditions can be stated as

$$t(0, y) = t_0$$

$$\frac{\partial t}{\partial y}(x, 0) = 0$$

and

$$t(x, a) = t_w \text{ (constant wall temperature)}$$

or

$$k \frac{\partial t}{\partial y}(x, a) = q \text{ (constant wall heat flux)}$$

(6-18)

The choice of the dimensionless temperature variable is dependent on the thermal boundary condition which is to be considered. The remainder of the dimensionless variables are the same for both boundary conditions. The dimensionless variables chosen are

$$T = \frac{t - t_w}{t_0 - t_w} \text{ (constant wall temperature)}$$

or

$$T = \frac{k}{qa} (t - t_0) \text{ (constant wall heat flux)}$$

$$U = \frac{u}{u_0}$$

$$V = \frac{\rho va}{\mu}$$

$$X = \frac{x\mu}{\rho a^2 u_0}$$

$$Y = \frac{y}{a}$$

(6-19)

The temperature problem in dimensionless form now becomes

$$U \frac{\partial T}{\partial X} + V \frac{\partial T}{\partial Y} = \frac{1}{Pr} \frac{\partial^2 T}{\partial Y^2} \quad (6-20)$$

subject to

$$T(0, Y) = 1 \text{ (constant wall temperature)}$$

or

$$T(0, Y) = 0 \text{ (constant wall heat flux)}$$

$$\frac{\partial T}{\partial Y}(X, 0) = 0$$

and

$$T(X, 1) = 0 \text{ (constant wall temperature)}$$

or

$$\frac{\partial T}{\partial Y}(X, 1) = 1 \text{ (constant wall heat flux)}$$

(6-21)

Equation (6-20) may now be expressed in an implicit finite difference form similar to that used for the momentum equation in the preceding section. This difference form is

$$U_{j,k} \frac{T_{j+1,k} - T_{j,k}}{\Delta X} + V_{j,k} \frac{T_{j+1,k+1} - T_{j+1,k-1}}{2(\Delta Y)} = \frac{1}{Pr} \frac{T_{j+1,k+1} - 2T_{j+1,k} + T_{j+1,k-1}}{(\Delta Y)^2} \quad (6-22)$$

Equation (6-22) can be rewritten in a more useful form as

$$\left[\frac{-V_{j,k}}{2(\Delta Y)} - \frac{1}{Pr(\Delta Y)^2} \right] T_{j+1,k-1} + \left[\frac{U_{j,k}}{\Delta X} + \frac{2}{Pr(\Delta Y)^2} \right] T_{j+1,k} + \left[\frac{V_{j,k}}{2(\Delta Y)} - \frac{1}{Pr(\Delta Y)^2} \right] T_{j+1,k+1} = \frac{U_{j,k} T_{j,k}}{\Delta X} \quad (6-23)$$

Equation (6-23) written for $k=0(1)n$ forms a set of $n+1$ simultaneous linear equations in the values of $T_{j+1,k}$. If the wall temperature is known (constant wall temperature case), then these $n+1$ equations involve $n+1$ unknowns. The resulting matrix equation is

Prandtl numbers and by the temperature solution for large Prandtl numbers. Of course, numerical experimentation (including refining the originally chosen mesh size) is necessary to verify any choice of mesh size.

The solution can be carried downstream in the usual manner, solving first for the velocity distribution and then for the temperatures at each axial station.

6.1.3 Incompressible Constant Property Flow—Heat Transfer Solution

In order to solve for the heat transfer in confined flow situations, it is first necessary to find the bulk (mixed-mean) temperature. This quantity is defined for the parallel plate channel as

$$t_b \equiv \frac{\int_0^a u t dy}{\int_0^a u dy} \tag{6-28}$$

Inserting the dimensionless variables (6-19) into equation (6-28) gives

$$T_b = \frac{\int_0^1 UT dY}{\int_0^1 U dY} = \int_0^1 UT dY \tag{6-29}$$

The dimensionless bulk temperature T_b may be calculated numerically by employing Simpson's rule:

$$T_b|_{j+1} = \frac{\Delta Y}{3} \left(U_{j+1,0} T_{j+1,0} + 4 \sum_{k=1,3,5,7,\dots}^n U_{j+1,k} T_{j+1,k} + 2 \sum_{k=2,4,6,8,\dots}^{n-1} U_{j+1,k} T_{j+1,k} \right) \tag{6-30}$$

Equation (6-30) requires an even number of spaces across the half channel (n must be odd).

The local Nusselt number is given by

$$Nu_x = \frac{2ha}{k} \tag{6-31}$$

where

$$h(t_w - t_b) = k \left. \frac{\partial t}{\partial y} \right|_{y=a} \tag{6-32}$$

so

$$Nu_x = \frac{-2 \left. \frac{\partial t}{\partial y} \right|_{y=a}}{t_b - t_w} \quad (2a) \quad (6-33)$$

For isothermal walls, equation (6-33) may be written in dimensionless form as

$$Nu_x = \frac{-2 \left. \frac{\partial T}{\partial Y} \right|_{Y=1}}{T_b} \quad (6-34)$$

or, in finite difference form,

$$Nu_x = -2 \frac{(3T_{j+1, n+1} - 4T_{j+1, n} + T_{j+1, n-1})}{2(\Delta Y)T_b|_{j+1}} \quad (6-35)$$

For constant wall heat flux, the expression is

$$Nu_x = \frac{-2}{T_b - T_w} \quad (6-36)$$

or, in finite difference form,

$$Nu_x = \frac{-2}{T_b|_{j+1} - T_w|_{j+1}} \quad (6-37)$$

The mean Nusselt number is given by

$$Nu_m = \frac{1}{X} \int_0^X Nu_x dX \quad (6-38)$$

This may be computed by using Simpson's rule as

$$Nu_m|_{j+1} = \frac{1}{X_{j+1}} \left(Nu_x|_0 + 4 \sum_{i=1, 3, 5, 7, \dots}^{j-1} Nu_x|_i + 2 \sum_{i=2, 4, 6, 8, \dots}^{j-1} Nu_x|_i + Nu_x|_{j+1} \right) \frac{\Delta X}{3} \quad (6-39)$$

The calculation of $Nu_m|_{j+1}$ can only be done at every other ΔX step so that an even number of intervals from $X=0$ ($j=0$) will be involved.

6.1.4 Compressible Flow—Velocity and Temperature Solutions

For the viscous compressible flow in a parallel plate channel, no fully developed flow situation can exist in the usual sense. As the pressure changes along the channel, the density must also change, resulting in a velocity distribution which continually varies with axial position. The entire length of the channel, from entrance to exit, may thus be considered an "entrance" region. The same model is used for the compressible case as was employed earlier for the incompressible case; equations of the boundary layer type are assumed to apply over the entire flow field. The flow may be either subsonic at the entrance, as from a reservoir, or supersonic, as from a supersonic diffuser. In either case, if the flow approaches a Mach number of 1 in the channel, then considerable care in computation and interpretation is required. This is discussed in greater detail following the formulation.

The coupled equations of motion and energy are

$$\rho \left(u \frac{\partial u}{\partial x} + v \frac{\partial u}{\partial y} \right) = -\frac{dp}{dx} + \frac{\partial}{\partial y} \left(\mu \frac{\partial u}{\partial y} \right) \quad (6-40)$$

$$\frac{\partial(\rho u)}{\partial x} + \frac{\partial(\rho v)}{\partial y} = 0 \quad (6-41)$$

$$\rho c_p \left(u \frac{\partial t}{\partial x} + v \frac{\partial t}{\partial y} \right) = u \frac{dp}{dx} + \frac{\partial}{\partial y} \left(k \frac{\partial t}{\partial y} \right) + \mu \left(\frac{\partial u}{\partial y} \right)^2 \quad (6-42)$$

Assuming a perfect gas,

$$p = \rho \mathcal{R} t \quad (6-43)$$

and as in the external flow problems considered in previous chapters, we assume a power law relationship for the viscosity and thermal conductivity:

$$\mu = \mu_0 (t/t_0)^f \quad (6-44)$$

$$k = k_0 (t/t_0)^g \quad (6-45)$$

where the 0 subscripts represent reference values, here chosen as conditions at the channel entrance.

The velocity and pressure boundary conditions are

$$\left. \begin{aligned}
 u(0, y) &= u_0 \text{ (see appendix F)} \\
 u(x, a) &= 0 \\
 \frac{\partial u}{\partial y}(x, 0) &= 0 \\
 v(x, 0) &= 0 \\
 v(x, a) &= 0 \\
 p(0) &= p_0
 \end{aligned} \right\} (6-46)$$

The thermal boundary conditions considered include either a constant wall temperature or constant wall heat flux condition:

$$\left. \begin{aligned}
 t(0, y) &= t_0 \\
 \frac{\partial t}{\partial y}(x, 0) &= 0
 \end{aligned} \right\} (6-47)$$

and

$$t(x, a) = t_w \quad (\text{constant wall temperature})$$

or

$$k \frac{\partial t}{\partial y}(x, a) = q \quad (\text{constant wall heat flux})$$

The following dimensionless variables are chosen:

$$\left. \begin{aligned}
 U &= \frac{u}{u_0} & X &= \frac{x\mu_0}{\rho_0 u_0 a^2} \\
 V &= \frac{\rho_0 v a}{\mu_0} & Y &= \frac{y}{a} \\
 T &= \frac{t}{t_0} & k^* &= \frac{k}{k_0} \\
 P &= \frac{p}{p_0} & \mu^* &= \frac{\mu}{\mu_0} \\
 & & \rho^* &= \frac{\rho}{\rho_0}
 \end{aligned} \right\} (6-48)$$

The reference values, with subscript 0, correspond to the conditions at the entrance to the channel.

When the dimensionless variables (6-48) are inserted into equations (6-40) to (6-45), the problem may be restated in dimensionless form as

$$\rho^* \left(U \frac{\partial U}{\partial X} + V \frac{\partial U}{\partial Y} \right) = -\frac{1}{\gamma M_0^2} \frac{dP}{dX} + \frac{\partial}{\partial Y} \left(\mu^* \frac{\partial U}{\partial Y} \right) \quad (6-49)$$

$$\frac{\partial(\rho^*U)}{\partial X} + \frac{\partial(\rho^*V)}{\partial Y} = 0 \quad (6-50)$$

$$\rho^* \left(U \frac{\partial T}{\partial X} + V \frac{\partial T}{\partial Y} \right) = \frac{\gamma-1}{\gamma} U \frac{dP}{dX} + \frac{1}{Pr} \frac{\partial}{\partial Y} \left(k^* \frac{\partial T}{\partial Y} \right) + (\gamma-1) M_0^2 \mu^* \left(\frac{\partial U}{\partial Y} \right)^2 \quad (6-51)$$

$$P = \rho^* T \quad (6-52)$$

$$\mu^* = (T)^f \quad (6-53)$$

$$k^* = (T)^g \quad (6-54)$$

where $M_0 = u_0 / \sqrt{\gamma \mathcal{R} t}$ and $Pr = \mu_0 c_p / k_0$.

The boundary conditions (6-46) and (6-47) become, in dimensionless form,

$$\left. \begin{aligned} U(0, Y) &= 1 \\ U(X, 1) &= 0 \\ \frac{\partial U}{\partial Y}(X, 0) &= 0 \\ V(X, 0) &= 0 \\ V(X, 1) &= 0 \\ P(0) &= 1 \\ T(0, Y) &= 1 \\ \frac{\partial T}{\partial Y}(X, 0) &= 0 \end{aligned} \right\} \quad (6-55)$$

and $T(X, 1) = T_w$ (constant wall temperature)

or $k^* \frac{\partial T}{\partial Y}(X, 1) = \frac{qa}{k_0 t_0}$ (constant wall heat flux)

A finite difference representation must now be established for this problem. The finite difference form chosen here is based on the so-called "post-boundary-layer" equations of Walker (ref. 5) for the circular tube. The finite difference representations of equations (6-49) to (6-54) are

$$\begin{aligned}
 \rho_{j,k}^* & \left[U_{j,k} \frac{U_{j+1,k} - U_{j,k}}{\Delta X} + V_{j,k} \frac{U_{j+1,k+1} - U_{j+1,k-1}}{2(\Delta Y)} \right] \\
 & = \frac{-1}{\gamma M_0^2} \frac{P_{j+1} - P_j}{\Delta X} + \mu_{j,k}^* \left[\frac{U_{j+1,k+1} - 2U_{j+1,k} + U_{j+1,k-1}}{(\Delta Y)^2} \right] \\
 & \quad + \left[\frac{\mu_{j,k+1}^* - \mu_{j,k-1}^*}{2(\Delta Y)} \right] \left[\frac{U_{j+1,k+1} - U_{j+1,k-1}}{2(\Delta Y)} \right] \quad (6-56)
 \end{aligned}$$

$$\begin{aligned}
 \rho_{j,k+1}^* & \left[\frac{U_{j+1,k+1} - U_{j,k+1}}{2(\Delta X)} \right] + \rho_{j,k}^* \left[\frac{U_{j+1,k} - U_{j,k}}{2(\Delta X)} \right] \\
 & + \left(\frac{U_{j,k+1}}{T_{j,k+1}} + \frac{U_{j,k}}{T_{j,k}} \right) \left[\frac{P_{j+1} - P_j}{2(\Delta X)} \right] - \left(\frac{\rho_{j,k+1}^* U_{j,k+1}}{T_{j,k+1}} \right) \left[\frac{T_{j+1,k+1} - T_{j,k+1}}{2(\Delta X)} \right] \\
 & - \left(\frac{\rho_{j,k}^* U_{j,k}}{T_{j,k}} \right) \left[\frac{T_{j+1,k} - T_{j,k}}{2(\Delta X)} \right] + \frac{\rho_{j+1,k+1}^* V_{j+1,k+1} - \rho_{j+1,k}^* V_{j+1,k}}{\Delta Y} = 0 \quad (6-57)
 \end{aligned}$$

$$\begin{aligned}
 \rho_{j,k}^* & \left[U_{j,k} \frac{T_{j+1,k} - T_{j,k}}{\Delta X} + V_{j,k} \frac{T_{j+1,k+1} - T_{j+1,k-1}}{2(\Delta Y)} \right] \\
 & = \frac{\gamma - 1}{\gamma} U_{j,k} \frac{P_{j+1} - P_j}{\Delta X} + \frac{k_{j,k}^*}{Pr} \left[\frac{T_{j+1,k+1} - 2T_{j+1,k} + T_{j+1,k-1}}{(\Delta Y)^2} \right] \\
 & \quad + \frac{1}{Pr} \left[\frac{k_{j,k+1}^* - k_{j,k-1}^*}{2(\Delta Y)} \right] \left[\frac{T_{j+1,k+1} - T_{j+1,k-1}}{2(\Delta Y)} \right] \\
 & \quad + (\gamma - 1) M_0^2 \mu_{j,k}^* \left[\frac{U_{j,k+1} - U_{j,k-1}}{2(\Delta Y)} \right] \left[\frac{U_{j+1,k+1} - U_{j+1,k-1}}{2(\Delta Y)} \right] \quad (6-58)
 \end{aligned}$$

$$P_{j+1} = \rho_{j+1,k}^* T_{j+1,k} \quad (6-59)$$

$$\mu_{j+1,k}^* = (T_{j+1,k})^f \quad (6-60)$$

$$k_{j+1,k}^* = (T_{j+1,k})^q \quad (6-61)$$

Several comments are in order concerning this choice of difference representations. The unusual and somewhat lengthy representation of the continuity equation (eq. (6-57)) includes the perfect gas law and was chosen to keep the equation

linear and to avoid the necessity of an iterative type of solution. The form also has advantages in forming the integral representation of continuity, as will be seen later. The representation of the viscous dissipation term in equation (6-58) also serves to eliminate nonlinearities.

The finite differences forms of the momentum, continuity, and energy equations written for $k=0(1)n$ now constitute $3n+3$ simultaneous equations in the $3n+3$ or $3n+4$ unknowns $U_{j+1,k}$, $V_{j+1,k}$, $T_{j+1,k}$, and P_{j+1} , the number depending on whether the constant wall temperature or constant wall heat flux condition is desired. Note that, despite a considerable amount of effort devoted to that end, these equations are still not linear, due to the representation of the $\partial(\rho^*V)/\partial Y$ term in continuity (eq. (6-57)). In this last term in equation (6-57) both ρ^* and V are unknown and are multiplied together. The equations can be made linear and the number of equations substantially reduced, but first equations (6-56) and (6-58) are rearranged in a more convenient form. Equation (6-56) becomes

$$\begin{aligned} & \left[\frac{-\rho_{j,k}^* V_{j,k}}{2(\Delta Y)} - \frac{\mu_{j,k}^*}{(\Delta Y)^2} + \frac{\mu_{j,k+1}^* - \mu_{j,k-1}^*}{4(\Delta Y)^2} \right] U_{j+1,k-1} + \left[\frac{\rho_{j,k}^* U_{j,k}}{\Delta X} + \frac{2\mu_{j,k}^*}{(\Delta Y)^2} \right] U_{j+1,k} \\ & + \left[\frac{\rho_{j,k}^* V_{j,k}}{2(\Delta Y)} - \frac{\mu_{j,k}^*}{(\Delta Y)^2} - \frac{\mu_{j,k+1}^* - \mu_{j,k-1}^*}{4(\Delta Y)^2} \right] U_{j+1,k+1} + \left[\frac{1}{\gamma M_0^2 \Delta X} \right] P_{j+1} \\ & = \frac{\rho_{j,k}^* U_{j,k}^2}{\Delta X} + \frac{P_j}{\gamma M_0^2 \Delta X} \quad (6-62) \end{aligned}$$

and equation (6-58) becomes

$$\begin{aligned} & \left[\frac{-\rho_{j,k}^* V_{j,k}}{2(\Delta Y)} - \frac{1}{Pr} \frac{k_{j,k}^*}{(\Delta Y)^2} + \frac{1}{Pr} \frac{k_{j,k+1}^* - k_{j,k-1}^*}{4(\Delta Y)^2} \right] T_{j+1,k-1} \\ & + \left[\frac{\rho_{j,k}^* U_{j,k}}{\Delta X} + \frac{2}{Pr} \frac{k_{j,k}^*}{(\Delta Y)^2} \right] T_{j+1,k} + \left[\frac{\rho_{j,k}^* V_{j,k}}{2(\Delta Y)} - \frac{1}{Pr} \frac{k_{j,k}^*}{(\Delta Y)^2} \right. \\ & \left. - \frac{1}{Pr} \frac{k_{j,k+1}^* - k_{j,k-1}^*}{4(\Delta Y)^2} \right] T_{j+1,k+1} + \left\{ (\gamma - 1) M_0^2 \mu_{j,k}^* \left[\frac{U_{j,k+1} - U_{j,k-1}}{4(\Delta Y)^2} \right] \right\} U_{j+1,k-1} \\ & - \left\{ (\gamma - 1) M_0^2 \mu_{j,k}^* \left[\frac{U_{j,k+1} - U_{j,k-1}}{4(\Delta Y)^2} \right] \right\} U_{j+1,k+1} + \left[\frac{(1 - \gamma) U_{j,k}}{\gamma(\Delta X)} \right] P_{j+1} \\ & = \frac{(1 - \gamma) U_{j,k} P_j}{\gamma(\Delta X)} \quad (6-63) \end{aligned}$$

Equations (6-62) and (6-63) written for $k=0(1)n$ constitute $2n+2$ equations in the $2n+3$ unknowns $U_{j+1,k}$, $T_{j+1,k}$, and P_{j+1} . (This is for the constant wall

temperature case; if the constant wall heat flux case is considered, there are $2n+4$ unknowns.) The number of equations for the constant wall temperature case can be brought to $2n+3$ without adding any additional unknowns by adding together the continuity equation (6-57) for each value of $k=0(1)n$. This yields

$$\begin{aligned} \sum_{k=0}^n \left\{ \rho_{j,k+1}^* \left[\frac{U_{j+1,k+1} - U_{j,k+1}}{2(\Delta X)} \right] + \rho_{j,k}^* \left[\frac{U_{j+1,k} - U_{j,k}}{2(\Delta X)} \right] \right. \\ \left. + \left(\frac{U_{j,k+1}}{T_{j,k+1}} + \frac{U_{j,k}}{T_{j,k}} \right) \left[\frac{P_{j+1} - P_j}{2(\Delta X)} \right] \right. \\ \left. - \frac{\rho_{j,k+1}^* U_{j,k+1}}{T_{j,k+1}} \left[\frac{T_{j+1,k+1} - T_{j,k+1}}{2(\Delta X)} \right] \right. \\ \left. - \frac{\rho_{j,k}^* U_{j,k}}{T_{j,k}} \left[\frac{T_{j+1,k} - T_{j,k}}{2(\Delta X)} \right] \right\} = 0 \end{aligned} \quad (6-64)$$

Substituting the equation of state (6-59) as necessary and multiplying by (ΔX) (ΔY) , equation (6-64) can be rewritten as

$$\begin{aligned} \sum_{k=0}^n \left[\rho_{j,k+1}^* U_{j+1,k+1} + \rho_{j,k}^* U_{j+1,k} + \rho_{j,k+1}^* U_{j,k+1} \left(\frac{P_{j+1}}{P_j} - \frac{T_{j+1,k+1}}{T_{j,k+1}} \right) \right. \\ \left. + \rho_{j,k}^* U_{j,k} \left(\frac{P_{j+1}}{P_j} - \frac{T_{j+1,k}}{T_{j,k}} \right) \right] \frac{\Delta Y}{2} \\ = \sum_{k=0}^n \left(\rho_{j,k+1}^* U_{j,k+1} + \rho_{j,k}^* U_{j,k} \right) \frac{\Delta Y}{2} \end{aligned} \quad (6-65)$$

Note that the nonlinear term referred to earlier has vanished from equation (6-65) because of the repeated additions of terms with opposite sign.

Equation (6-65) along with equations (6-62) and (6-63) written for $k=0(1)n$ now constitute a complete set of $2n+3$ linear equations in the $2n+3$ unknowns $U_{j+1,k}$, $T_{j+1,k}$, and P_{j+1} for the constant wall temperature case. The set may be written in matrix form as

where

$$\Omega_0 = \frac{-2\mu_{j,k}^*}{(\Delta Y)^2}$$

$$\alpha_k = -\frac{\rho_{j,k}^* V_{j,k}}{2(\Delta Y)} - \frac{\mu_{j,k}^*}{(\Delta Y)^2} + \frac{\mu_{j,k+1}^* - \mu_{j,k-1}^*}{4(\Delta Y)^2}$$

$$\beta_k = \frac{\rho_{j,k}^* U_{j,k}}{\Delta X} + \frac{2\mu_{j,k}^*}{(\Delta Y)^2}$$

$$\Omega_k = \frac{\rho_{j,k}^* V_{j,k}}{2(\Delta Y)} - \frac{\mu_{j,k}^*}{(\Delta Y)^2} - \frac{\mu_{j,k+1}^* - \mu_{j,k-1}^*}{4(\Delta Y)^2} \quad (k > 0)$$

$$\phi_k = \frac{\rho_{j,k}^* U_{j,k}^2}{\Delta X} + \frac{P_j}{\gamma M_0^2(\Delta X)}$$

$$\eta_k = 1/\gamma M_0^2(\Delta X)$$

$$\alpha_k' = -\frac{\rho_{j,k}^* V_{j,k}}{2(\Delta Y)} - \frac{k_{j,k}^*}{Pr(\Delta Y)^2} + \frac{k_{j,k+1}^* - k_{j,k-1}^*}{4Pr(\Delta Y)^2}$$

$$\beta_k' = \frac{\rho_{j,k}^* U_{j,k}}{\Delta X} + \frac{2k_{j,k}^*}{Pr(\Delta Y)^2}$$

$$\Omega_k' = \frac{\rho_{j,k}^* V_{j,k}}{2(\Delta Y)} - \frac{k_{j,k}^*}{Pr(\Delta Y)^2} - \frac{k_{j,k+1}^* - k_{j,k-1}^*}{4Pr(\Delta Y)^2}$$

$$\psi_k = (\gamma - 1) M_0^2 \mu_{j,k}^* \left[\frac{U_{j,k+1} - U_{j,k-1}}{4(\Delta Y)^2} \right]$$

$$\eta_k' = \frac{(1-\gamma)U_{j,k}}{\gamma(\Delta X)}$$

$$\phi'_k = \frac{(1-\gamma)U_{j,k}P_j}{\gamma(\Delta X)}$$

$$E_0 = \rho_{j,0}^* \frac{(\Delta Y)}{2}$$

$$E_k = \rho_{j,k}^* (\Delta Y) \quad (k > 0)$$

$$E'_0 = \frac{-\rho_{j,0}^* U_{j,0} (\Delta Y)}{2(T_{j,0})}$$

$$E'_k = \frac{-\rho_{j,k}^* U_{j,k} (\Delta Y)}{T_{j,k}} \quad (k > 0)$$

$$G = \sum_{k=0}^n (\rho_{j,k+1}^* U_{j,k+1} + \rho_{j,k}^* U_{j,k}) \frac{(\Delta Y)}{2P_j}$$

$$S = \sum_{k=0}^n (\rho_{j,k+1}^* U_{j,k+1} + \rho_{j,k}^* U_{j,k}) \frac{\Delta Y}{2}$$

For the constant wall heat flux case, $T_{j+1,n+1}$ (the wall temperature) is also unknown. This adds one unknown to the set of equations. The additional necessary equation is the heat flux boundary condition in equation (6-55), which may be written in difference form as

$$k_{j,n+1}^* \left[\frac{T_{j+1,n-1} - 4T_{j+1,n} + 3T_{j+1,n+1}}{2(\Delta Y)} \right] = \frac{qa}{k_0 t_0} \quad (6-67)$$

or

$$T_{j+1,n-1} - 4T_{j+1,n} + 3T_{j+1,n+1} = \frac{2qa(\Delta Y)}{k_{j,n+1}^* k_0 t_0} \quad (6-68)$$

This representation, using $k_{j,n+1}^*$, is in the interests of maintaining linearity. Many other possible representations of the heat flux condition are possible, but since k^* is in general a function of T , it is difficult to envisage any other representation which would keep the equation linear in T . The additional equation (6-68) must be incorporated in the matrix form which will now have its dimension enlarged by one. The resulting matrix equation is

where all symbols are defined as in equation (6-66) and

$$Q = \frac{2qa(\Delta Y)}{k_{j,n+1}^* k_0 t_0}$$

The matrix equation (6-66) or (6-69) can be solved by any of the standard methods for linear equations such as that given in appendix E. The use of a refined mesh near the wall as discussed in appendix D is very useful in maintaining accuracy while keeping the size of the matrix to a minimum.

After this set has been solved, the density $\rho_{j+1,k}^*$ may be found by using the perfect gas law, equation (6-59), to yield

$$\rho_{j+1,k}^* = \frac{P_{j+1}}{T_{j+1,k}} \quad (6-70)$$

Continuity, equation (6-57), can now be solved in a stepwise fashion, working outward from the centerline, to yield

$$\begin{aligned} V_{j+1,k+1} = & \left(\frac{\rho_{j+1,k}^*}{\rho_{j+1,k+1}^*} \right) V_{j+1,k} - \left(\frac{\rho_{j,k+1}^*}{\rho_{j+1,k+1}^*} \right) \left[\frac{\Delta Y}{2(\Delta X)} \right] (U_{j+1,k+1} - U_{j,k+1}) \\ & - \left(\frac{\rho_{j,k}^*}{\rho_{j+1,k+1}^*} \right) \left(\frac{\Delta Y}{2(\Delta X)} \right) (U_{j+1,k} - U_{j,k}) \\ & - \left(\frac{\Delta Y}{2(\Delta X) \rho_{j+1,k+1}^*} \right) \left(\frac{U_{j,k+1}}{T_{j,k+1}} + \frac{U_{j,k}}{T_{j,k}} \right) (P_{j+1} - P_j) \\ & + \left(\frac{\rho_{j,k+1}^* U_{j,k+1}}{\rho_{j+1,k+1}^* T_{j,k+1}} \right) \left[\frac{\Delta Y}{2(\Delta X)} \right] (T_{j+1,k+1} - T_{j,k+1}) \\ & + \left(\frac{\rho_{j,k}^* U_{j,k}}{\rho_{j+1,k+1}^* T_{j,k}} \right) \left[\frac{\Delta Y}{2(\Delta X)} \right] (T_{j+1,k} - T_{j,k}) \quad (6-71) \end{aligned}$$

Finally, $\mu_{j+1,k}^*$ and $k_{j+1,k}^*$ may be found from equations (6-60) and (6-61).

Another step ΔX downstream may now be taken and the entire process repeated as desired.

For many wall heating and cooling conditions, the velocity of the compressible flow in a channel increases with increasing distance along the channel, primarily because of the decrease in density caused by the frictional pressure drop. The Mach number thus also tends to increase under these conditions. The marching procedure can be carried downstream until the local Mach number anywhere in the channel nears 1. At this point, certain difficulties develop which require some interpretation. This interpretation, based on the work of Walker (ref. 5), is now discussed.

One-dimensional compressible flow theory predicts that if the flow is subsonic at the inlet to a constant-area channel, then the Mach number cannot exceed 1 anywhere in the channel; and if a Mach number of 1 is reached in the channel, it must occur at the exit. The model employed in the present discussion has certain one-dimensional aspects in that only the axial momentum equation is included; however, it also has a two-dimensional character in that transverse velocities and transverse variations in the axial velocity profile are permitted. As a result of these two-dimensional aspects, the predictions of the one-dimensional theory on the behavior of the Mach number do not apply directly to the model considered here, but might reasonably be expected to apply to the Mach number averaged over the channel cross section. Walker (ref. 5), in his work on the circular tube, found this to be essentially true; for the adiabatic wall cases he considered, the Mach number increased along the tube until the average Mach number became very close to 1. At this point, the local Mach number on the centerline of the tube was greater than 1. Attempts to carry the solution past this point invariably resulted in numerical instabilities and a violation of the Second Law of Thermodynamics (the entropy generation became negative). This point was thus considered to be the exit of the channel. The fact that the model tells us the location of the end of the channel is not too surprising, in view of the fact that the parabolic equations considered here have no capability to "look ahead" and thus we are forced to specify both an inlet pressure *and* an inlet Mach number. In a real physical situation, the inlet Mach number would be a *result* of applying a certain pressure difference over a given length of channel. We have simply turned this around by specifying the inlet Mach number and finding the length of channel necessary to satisfy all conditions.

The previous discussion, while strictly applicable only to the circular tube, also should apply without qualification to the parallel plate channel.

Walker has also shown that difference representations of the type used here are stable for all $U \geq 0$ so long as the Mach number is not equal to 1. The stability at a Mach number of 1 could not be established.

The truncation error is of $\mathcal{O}(\Delta X)$ and $\mathcal{O}((\Delta Y)^2)$ for momentum and energy and of $\mathcal{O}(\Delta X)$ and $\mathcal{O}(\Delta Y)$ for continuity.

6.1.5 Compressible Flow—Heat Transfer Solution

As in the incompressible flow case discussed in section 6.1.3, the local Nusselt number is given by

$$Nu_x = \frac{2ha}{k} \quad (6-72)$$

Complications arise, however, in that for the compressible confined flow case, the choice of a reference temperature for h is somewhat involved. Due to the

presence of viscous dissipation, the bulk temperature is, by itself, no longer meaningful in this context. Shapiro (ref. 6), based on previous work by McAdams, Nicolai, and Keenan (ref. 7) and others, recommends that the adiabatic wall temperature be used for this reference temperature. The adiabatic wall temperature is defined as

$$t_{aw} \equiv t_m \left[1 + F \left(\frac{\gamma - 1}{2} \right) M_{ave}^2 \right] \quad (6-73)$$

where M_{ave} is taken as the local Mach number averaged over the channel cross section, t_m the mean temperature based on a one-dimensional model, and F is called a recovery factor. The value for F was found by McAdams, Nicolai, and Keenan (ref. 7) to average about 0.88 for air, and it has subsequently been suggested (e.g., Dorrance, ref. 8) that reasonable values for F can be obtained by using

$$F = \sqrt{Pr} \quad (6-74)$$

The two-dimensional analog of the one-dimensional mean temperature is the bulk temperature, so that we use

$$t_m = t_b = \frac{\int_0^a \rho u t \, dy}{\int_0^a \rho u \, dy} \quad (6-75)$$

In dimensionless form, the mean temperature is

$$T_m = T_b = \frac{\int_0^1 \rho^* U T \, dy}{\int_0^1 \rho^* U \, dy} = \int_0^1 \rho^* U T \, dy \quad (6-76)$$

The average Mach number is given by

$$M_{ave} = \frac{1}{a} \int_0^a \frac{u}{\sqrt{\gamma R t}} \, dy \quad (6-77)$$

or, in terms of dimensionless quantities,

$$M_{ave} = M_0 \int_0^1 \frac{U}{\sqrt{T}} \, dy \quad (6-78)$$

The dimensionless adiabatic wall temperature may now be formed, using equations (6-74), (6-76), and (6-78), as

$$T_{aw} = \left(\int_0^1 \rho^* U T dy \right) \left[1 + \sqrt{Pr} \left(\frac{\gamma-1}{2} \right) M_0^2 \left(\int_0^1 \frac{U}{\sqrt{T}} dy \right)^2 \right] \quad (6-79)$$

We are now prepared to define

$$h = \frac{k \frac{\partial t}{\partial y} \Big|_{y=a}}{t_w - t_{aw}} \quad (6-80)$$

From equation (6-72), the local Nusselt number is then given by

$$Nu_x = \frac{2a \frac{\partial t}{\partial y} \Big|_{y=a}}{t_w - t_{aw}} \quad (6-81)$$

In terms of dimensionless variables,

$$Nu_x = \frac{2 \frac{\partial T}{\partial Y} \Big|_{Y=1}}{T_w - T_{aw}} \quad (6-82)$$

Equation (6-82) may now be expressed in difference form as

$$Nu_x|_{j+1} = \frac{2(3T_{j+1,n+1} - 4T_{j+1,n} + T_{j+1,n-1})}{2(\Delta Y)(T_{j+1,n+1} - T_{aw}|_{j+1})} \quad (6-83)$$

where

$$\begin{aligned} T_{aw}|_{j+1} = & \left(\frac{\Delta Y}{3} \right) \left(\rho_{j+1,0}^* U_{j+1,0} T_{j+1,0} + 4 \sum_{k=1,3,5,7,\dots}^n \rho_{j+1,k}^* U_{j+1,k} T_{j+1,k} \right. \\ & + 2 \sum_{k=2,4,6,8,\dots}^{n-1} \rho_{j+1,k}^* U_{j+1,k} T_{j+1,k} \left. \right) \left\{ 1 + \frac{(\Delta Y)^2}{9} \sqrt{Pr} \left(\frac{\gamma-1}{2} \right) M_0^2 \left[\frac{U_{j+1,0}}{(T_{j+1,0})^{1/2}} \right. \right. \\ & \left. \left. + 4 \sum_{k=1,3,5,7,\dots}^n \frac{U_{j+1,k}}{(T_{j+1,k})^{1/2}} + 2 \sum_{k=2,4,6,8,\dots}^{n-1} \frac{U_{j+1,k}}{(T_{j+1,k})^{1/2}} \right]^2 \right\} \quad (6-84) \end{aligned}$$

Equation (6-84) uses Simpson's rule and requires n to be odd.

As in the incompressible case, the mean Nusselt number is given by

$$Nu_m = \frac{1}{X} \int_0^X Nu_x dX \quad (6-85)$$

or, in finite difference form,

$$Nu_m|_{j+1} = \frac{1}{X_{j+1}} \left(Nu_x|_0 + 4 \sum_{i=1,3,5,7,\dots}^j Nu_x|_i + 2 \sum_{i=2,4,6,8,\dots}^{j-1} Nu_x|_i + Nu_x|_{j+1} \right) \frac{\Delta X}{3} \tag{6-86}$$

This calculation may only be performed at every other ΔX step, so that an even number of ΔX intervals from $X=0$ ($j=0$) is involved.

6.2 OTHER PROBLEMS WITH A SIMILAR FORMULATION

6.2.1 Flow in Parallel Plate Channels With Porous Walls

In order to consider parallel plate channels with porous walls, the only modifications necessary to the formulations given earlier in this chapter are to the boundary conditions and equation of constraint (integral continuity). Bodoia (ref. 4) has briefly discussed this problem for the incompressible case, and essentially the same approach to that problem is presented here. The configuration is shown in figure 6-3, with the finite difference grid identical to that shown in figure 6-2.

For the incompressible case, the problem formulation is unchanged from that in section 6.1.1, except that the boundary conditions (6-3) become

$$\left. \begin{aligned} u(0, y) &= u_0 \text{ (see appendix F)} \\ u(x, a) &= 0 \\ \frac{\partial u}{\partial y}(x, 0) &= 0 \\ v(x, 0) &= 0 \\ v(x, a) &= v_w(x) \\ p(0) &= p_0 \end{aligned} \right\} \tag{6-87}$$

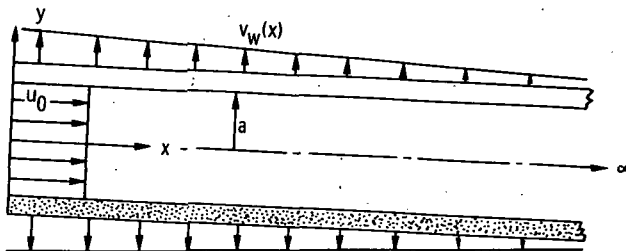


FIGURE 6-3. — Problem configuration and coordinate system for plane porous channel.

It should be noted that these boundary conditions correspond to a uniform inlet profile. Many other inlet profiles may be postulated and present no difficulties to the present method except for the choice of a reference velocity which would probably best be taken as \bar{u}_0 . It should also be noted that if the suction or injection velocity is constant with x and of the proper magnitude, it may be possible to get velocity profiles which are geometrically similar in a certain sense, but this is of little concern to us here. For details see Berman (ref. 9). Using the dimensionless variables (6-4), the boundary conditions (6-87) become

$$\left. \begin{aligned} U(0, Y) &= 1 \\ U(X, 1) &= 0 \\ \frac{\partial U}{\partial Y}(X, 0) &= 0 \\ V(X, 0) &= 0 \\ V(X, 1) &= V_w(X) \\ P(0) &= 0 \end{aligned} \right\} \quad (6-88)$$

The equation of constraint (integral continuity), equation (6-10), becomes

$$U_{j+1,0} + 2 \sum_{k=1}^n U_{j+1,k} = U_{j,0} + 2 \sum_{k=1}^n U_{j,k} - \frac{2V_w(X)\Delta X}{\Delta Y} \quad (6-89)$$

If $V_w(X)$ is known a priori, then no additional unknowns are introduced beyond those present in the impermeable wall case. The only modification to the matrix equation (6-13) is in the top element of the right column vector where S becomes

$$S = U_{j,0} + 2 \sum_{k=1}^n U_{j,k} - \frac{2V_w(X)\Delta X}{\Delta Y} \quad (6-90)$$

Another reasonable possibility is that the velocity through the wall may be a function of the pressure difference between the interior and the exterior of the channel. This might correspond to a relatively thin porous wall, across which Darcy's law (flow rate proportional to pressure gradient) may be applied. This model typically would yield a relationship of the form

$$V_w|_{j+1} = AP_{j+1} \quad (6-91)$$

where A is a constant.

When equation (6-91) is substituted into equation (6-89), the matrix equation becomes

1	2	2	2	-	-	-	2	2	$\frac{2A(\Delta X)}{\Delta Y}$	$U_{j+1,0}$	S	
β_0	Ω_0								$\frac{1}{\Delta X}$	$U_{j+1,1}$	ϕ_0	
α_1	β_1	Ω_1							$\frac{1}{\Delta X}$	$U_{j+1,2}$	ϕ_1	
	α_2	β_2	Ω_2						$\frac{1}{\Delta X}$	$U_{j+1,3}$	ϕ_2	
		α_3	β_3	Ω_3	-	-	-		$\frac{1}{\Delta X}$	$U_{j+1,4}$	ϕ_3	
					-	-	-		-	-	-	
									-	-	-	
							α_{n-1}	β_{n-1}	Ω_{n-1}	$\frac{1}{\Delta X}$	$U_{j+1,n}$	ϕ_{n-1}
								α_n	β_n	$\frac{1}{\Delta X}$	P_{j+1}	ϕ_n

(6-92)

where all symbols are as defined with equation (6-13). The computation of the V 's is not affected.

If the suction or injection is not the same on the top and bottom of the channel, then there is no symmetry at the channel centerline, and the finite difference equations must be written at each point across the entire channel. The changes in the matrix form are straightforward.

The compressible flow in a parallel plate channel with suction or injection has been presented in finite difference form by Buzzard (ref. 10). For the sake of unity of presentation, however, the discussion given here is based on section 6.1.4 rather than the work of Buzzard. The approach is fundamentally the same.

The modifications to the formulation of section 6.1.4 to account for the porous walls are again in the boundary conditions and equation of constraint. The formulation is unchanged except that the velocity and pressure boundary conditions (6-46) become

$$\left. \begin{aligned}
 u(0, y) &= u_0 \text{ (see appendix F)} \\
 u(x, a) &= 0 \\
 \frac{\partial u}{\partial y}(x, 0) &= 0 \\
 v(x, 0) &= 0 \\
 v(x, a) &= v_w(x) \\
 p(0) &= p_0
 \end{aligned} \right\} (6-93)$$

Using the dimensionless variables (6-48), the boundary conditions (6-93) become

$$\left. \begin{aligned}
 U(0, Y) &= 1 \\
 U(X, 1) &= 0 \\
 \frac{\partial U}{\partial Y}(X, 0) &= 0 \\
 V(X, 0) &= 0 \\
 V(X, 1) &= V_w(X) \\
 P(0) &= 1
 \end{aligned} \right\} (6-94)$$

The temperature boundary conditions are unchanged.

The equation of constraint (integral continuity), equation (6-64), becomes

$$\begin{aligned}
 \sum_{k=0}^n \rho_{j,k+1}^* \left[\frac{U_{j+1,k+1} - U_{j,k+1}}{2(\Delta X)} \right] + \rho_{j,k}^* \left[\frac{U_{j+1,k} - U_{j,k}}{2(\Delta X)} \right] \\
 + \left(\frac{U_{j,k+1}}{T_{j,k+1}} + \frac{U_{j,k}}{T_{j,k}} \right) \left[\frac{P_{j+1} - P_j}{2(\Delta X)} \right] - \frac{\rho_{j,k+1}^* U_{j,k+1}}{T_{j,k+1}} \left[\frac{T_{j+1,k+1} - T_{j,k+1}}{2(\Delta X)} \right] \\
 - \frac{\rho_{j,k}^* U_{j,k}}{T_{j,k}} \left[\frac{T_{j+1,k} - T_{j,k}}{2(\Delta X)} \right] + \frac{\rho_{j+1,n+1}^* V_{j+1,n+1}}{\Delta Y} = 0 \quad (6-95)
 \end{aligned}$$

Substituting the equation of state (6-59) as necessary and multiplying by (ΔX) (ΔY) , equation (6-95) may be rewritten as

$$\sum_{k=0}^n \left[\rho_{j,k+1}^* U_{j+1,k+1} + \rho_{j,k}^* U_{j+1,k} + \left(\rho_{j,k+1}^* U_{j,k+1} \right) \left(\frac{P_{j+1}}{P_j} - \frac{T_{j+1,k+1}}{T_{j,k+1}} \right) + \right.$$

$$\begin{aligned}
 & + \rho_{j,k}^* U_{j,k} \left(\frac{P_{j+1}}{P_j} - \frac{T_{j+1,k}}{T_{j,k}} \right) \left] \frac{\Delta Y}{2} + \frac{(\Delta X) V_{j+1,n+1} P_{j+1}}{T_{j+1,n+1}} \\
 & = \sum_{k=0}^n \left(\rho_{j,k+1}^* U_{j,k+1} + \rho_{j,k}^* U_{j,k} \right) \frac{\Delta Y}{2} \quad (6-96)
 \end{aligned}$$

This equation differs from equation (6-65) employed in section 6.1.4 by the addition of the term $(\Delta X) V_{j+1,n+1} P_{j+1} / T_{j+1,n+1}$. If the wall temperature $T_{j+1,n+1}$ and the suction or injection velocity at the wall $V_{j+1,n+1}$ are specified, then the term is merely an additional linear term in P_{j+1} and the procedure of solution employed in section 6.1.4 may be followed directly. If, however, the flow through the wall is proportional to pressure through Darcy's law, that is,

$$V_w|_{j+1} = AP_{j+1} \quad (6-97)$$

then the term becomes nonlinear (quadratic) in P_{j+1} and of the form $(\Delta X) AP_{j+1}^2 / T_{j+1,n+1}$. The only readily apparent approach to this problem is to linearize the term as $(\Delta X) (A) (P_j) (P_{j+1}) / T_{j+1,n+1}$ (assuming the wall temperature is specified) although this will obviously result in some loss of accuracy. The accuracy will of course improve with decreasing ΔX . If the wall temperature is not specified (as in the specified heat flux case) then a nonlinearity in $T_{j+1,n+1}$ is also introduced, which again would seem to be most readily resolved at the cost of accuracy by using $T_{j,n+1}$ instead. Of course, all of these nonlinearities may be accommodated without loss of accuracy, but only by employing an iterative method for the entire solution at a considerable cost in computer time.

For the specified wall temperature, specified suction or injection velocity case, the matrix equation (6-66) applies directly, with only the bottom right corner element of the coefficient matrix modified to become

$$G = \sum_{k=0}^n \left(\rho_{j,k+1}^* U_{j,k+1} + \rho_{j,k}^* U_{j,k} \right) \frac{(\Delta Y)}{2P_j} + \frac{(\Delta X) V_{j+1,n+1}}{T_{j+1,n+1}} \quad (6-98)$$

As in the incompressible case, the symmetry simplifications employed in the present discussion no longer apply if the suction or injection rates differ at the top and bottom of the channel and all quantities must be determined over the entire height of the channel.

6.2.2 Developing Confined Free Convection Flow Between Parallel Plates

The finite difference formulation and solution for developing free convection flow confined between parallel vertical plates has been obtained by Bodoia and Osterle (ref. 11), and the formulation given here is due to them.

Much of the development is similar to that presented in chapter 4 for unconfined free convection, and the emphasis here is on the changes due to the confined nature of the flow.

The configuration to be considered is shown in figure 6-4. The two vertical heated plates are held at a constant temperature, higher than the inlet temperature of the fluid. In the limit, as the plate spacing $2a$ becomes very large, the flow is essentially no longer confined, and the flow along each plate behaves as discussed in chapter 4. Bodoia and Osterle have assumed the velocity profile at the entrance to the channel formed by the plates to be uniform. This condition might be open to some conjecture, but the true inlet velocity profile could only be determined by solving the complete elliptic problem (most difficult indeed at the present state of the art). Since all of the flow must come from the $-x$ direction toward the $+x$ direction in order for the parabolic equations used here to apply, the uniform inlet profile seems the most logical choice. It is conceivable that the actual inlet profile might even involve backflow, but in the absence of other experimental or analytical evidence, we employ the uniform profile.

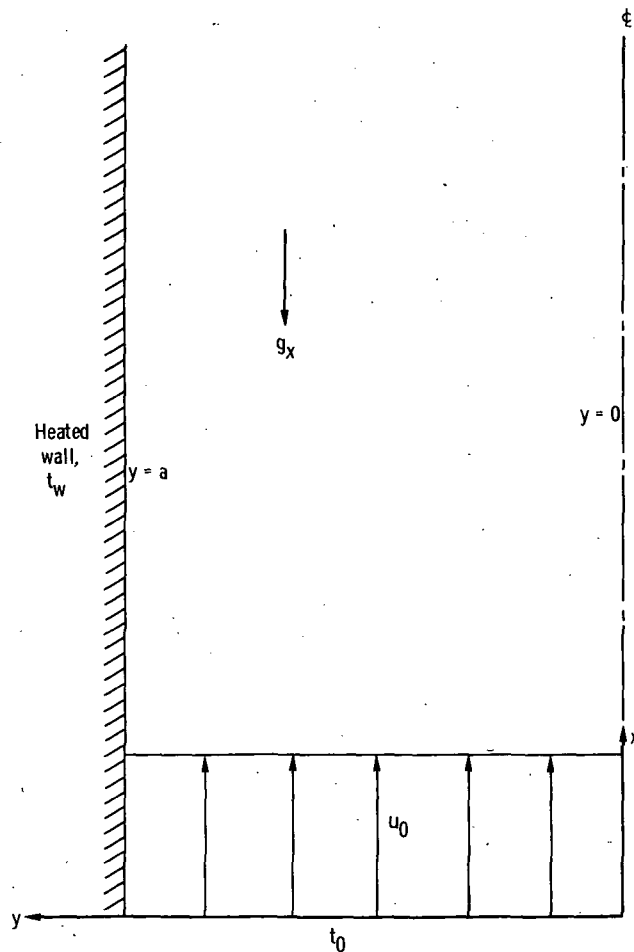


FIGURE 6-4.—Problem configuration and coordinate system for heated vertical parallel plate channel.

C³

The obvious difference between confined flows and the unconfined flows discussed in chapter 4 is the pressure gradient caused by the flow (or vice versa) in the confined channel. As is customary, we here define the pressure p as the difference between the actual pressure and the hydrostatic pressure which would exist if the entire fluid were at the inlet temperature:

$$p = p_{\text{actual}} - p_{\text{hydrostatic}} \quad (6-99)$$

The equations of motion for the confined flow case are thus modified from equations (4-1) to (4-3) for the unconfined case only by the addition of the pressure gradient term to the momentum equation. The basic equations are

$$\rho \left(u \frac{\partial u}{\partial x} + v \frac{\partial u}{\partial y} \right) = - \frac{dp}{dx} + \mu \frac{\partial^2 u}{\partial y^2} + \rho g_x B (t - t_0) \quad (6-100)$$

$$\frac{\partial u}{\partial x} + \frac{\partial v}{\partial y} = 0 \quad (6-101)$$

$$\rho c_p \left(u \frac{\partial t}{\partial x} + v \frac{\partial t}{\partial y} \right) = k \frac{\partial^2 t}{\partial y^2} \quad (6-102)$$

where symbols are defined as in equations (4-1) to (4-3).

The boundary conditions are

$$u(x, a) = 0$$

$$\frac{\partial u}{\partial y}(x, 0) = 0$$

$$u(0, y) = u_0 \text{ (see appendix F)}$$

$$v(x, 0) = 0$$

$$v(x, a) = 0$$

$$t(x, a) = t_w$$

$$t(0, y) = t_0$$

$$\frac{\partial t}{\partial y}(x, 0) = 0$$

$$p(0) = 0$$

(6-103)

We define the following dimensionless variables:

$$\left. \begin{aligned} U &= \frac{ua}{\nu(Gr)} \\ V &= \frac{va}{\nu} \\ P &= \frac{ppa^2}{\mu^2(Gr)^2} \\ T &= \frac{t - t_0}{t_w - t_0} \\ X &= \frac{x}{a(Gr)} \\ Y &= \frac{y}{a} \end{aligned} \right\} \quad (6-104)$$

where

$$Gr = \frac{a^3 g_x B (t_w - t_0)}{\nu^2}$$

The fundamental equations and boundary conditions (6-100) to (6-103) then become in dimensionless form,

$$U \frac{\partial U}{\partial X} + V \frac{\partial U}{\partial Y} = - \frac{dP}{dX} + \frac{\partial^2 U}{\partial Y^2} + T \quad (6-105)$$

$$\frac{\partial U}{\partial X} + \frac{\partial V}{\partial Y} = 0 \quad (6-106)$$

$$U \frac{\partial T}{\partial X} + V \frac{\partial T}{\partial Y} = \frac{1}{Pr} \frac{\partial^2 T}{\partial Y^2} \quad (6-107)$$

$$\begin{aligned}
 U(X, 1) &= 0 \\
 \frac{\partial U}{\partial Y}(X, 0) &= 0 \\
 U(0, Y) &= U_0 = \frac{u_0 a}{\nu(Gr)} \\
 V(X, 0) &= 0 \\
 V(X, 1) &= 0 \\
 T(X, 1) &= 1 \\
 T(0, Y) &= 0 \\
 \frac{\partial T}{\partial Y}(X, 0) &= 0 \\
 P(0) &= 0
 \end{aligned}
 \tag{6-108}$$

The parameters which appear in the problem are the dimensionless inlet velocity U_0 and the Prandtl number Pr . Since U_0 is a parameter, the question arises as to whether this formulation is also valid for combined free and forced convection. Indeed, this appears to be the case. In Bodoia and Osterle's original work, the solution was carried downstream until P again reached zero (until the pressure in the channel reached the external hydrostatic pressure which would exist at t_0). For each value of U_0 , a corresponding channel length was thus obtained which corresponded to free convection only. For any channel length different than this one, the problem is actually one in combined free and forced convection in which U_0 must be considered as composed of two components: the free convection component, which is just sufficient to cause P to reach zero at the specified channel length, and the forced component, which causes P at the exit to be either positive (opposing flow) or negative (aiding flow). The portions of U_0 due to each effect cannot be determined without separately solving the free convection problem for the specific channel length of interest, which would require a trial and error process to determine the inlet velocity which results in $P=0$ at the channel exit.

The difficulties encountered in chapter 4 which required a nonlinear difference representation are not present here, since the velocity throughout the

channel (except at the walls) is nonzero. We therefore employ conventional implicit difference representations similar to those used elsewhere in this chapter. The difference grid employed is identical to that shown in figure 6-2.

Equations (6-105), (6-106), and (6-107) become, in finite difference form,

$$U_{j,k} \frac{U_{j+1,k} - U_{j,k}}{\Delta X} + V_{j,k} \frac{U_{j+1,k+1} - U_{j+1,k-1}}{2(\Delta Y)} = - \frac{P_{j+1} - P_j}{\Delta X} + \frac{U_{j+1,k+1} - 2U_{j+1,k} + U_{j+1,k-1}}{(\Delta Y)^2} + T_{j+1,k} \quad (6-109)$$

$$\frac{U_{j+1,k+1} - U_{j,k+1} + U_{j+1,k} - U_{j,k}}{2(\Delta X)} + \frac{V_{j+1,k+1} - V_{j+1,k}}{\Delta Y} = 0 \quad (6-110)$$

$$U_{j,k} \frac{T_{j+1,k} - T_{j,k}}{\Delta X} + V_{j,k} \frac{T_{j+1,k+1} - T_{j+1,k-1}}{2(\Delta Y)} = \frac{1}{Pr} \frac{T_{j+1,k+1} - 2T_{j+1,k} + T_{j+1,k-1}}{(\Delta Y)^2} \quad (6-111)$$

The equation of constraint is unchanged from that employed in section 6.1.1:

$$U_{j+1,0} + 2 \sum_{k=1}^n U_{j+1,k} = U_{j,0} + 2 \sum_{k=1}^n U_{j,k} \quad (6-112)$$

Equations (6-109) and (6-111), written for $k=0(1)n$, along with equation (6-112) constitute $2n+3$ equations in the $2n+3$ unknowns $U_{j+1,0}, \dots, U_{j+1,n}$; $T_{j+1,0}, \dots, T_{j+1,n}$; and P_{j+1} .

Omitting the details and writing equations (6-109) and (6-111) directly in the most convenient form give

$$\left[-\frac{V_{j,k}}{2(\Delta Y)} - \frac{1}{(\Delta Y)^2} \right] U_{j+1,k-1} + \left[\frac{U_{j,k}}{\Delta X} + \frac{2}{(\Delta Y)^2} \right] U_{j+1,k} + \left[\frac{V_{j,k}}{2(\Delta Y)} - \frac{1}{(\Delta Y)^2} \right] U_{j+1,k+1} + \left(\frac{1}{\Delta X} \right) P_{j+1} = \frac{U_{j,k}^2 + P_j}{\Delta X} + T_{j+1,k} \quad (6-113)$$

$$\left[-\frac{V_{j,k}}{2(\Delta Y)} - \frac{1}{Pr(\Delta Y)^2} \right] T_{j+1,k-1} + \left[\frac{U_{j,k}}{\Delta X} + \frac{2}{Pr(\Delta Y)^2} \right] T_{j+1,k} + \left[\frac{V_{j,k}}{2(\Delta Y)} - \frac{1}{Pr(\Delta Y)^2} \right] T_{j+1,k+1} = \frac{U_{j,k} T_{j,k}}{\Delta X} \quad (6-114)$$

The energy equation (6-114) does not involve any unknown velocities at a given step and is therefore solved for T first at each step downstream. The matrix equation is identical to equation (6-24) and will not be repeated here.

The matrix form of equation (6-113) is solved next. This matrix equation is identical to equation (6-13) except for a redefinition of ϕ_k in the right column vector, which becomes

$$\phi_k = \frac{U_{j,k}^2 + P_j}{\Delta X} + T_{j+1,k} \quad (6-115)$$

The method of solution used to solve the matrix equation is discussed following equation (6-13).

After solving equation (6-110) for $V_{j+1,k+1}$ ($k=0(1)n$), another step downstream may be taken and the process repeated.

Bodoia and Osterle have shown the present formulation to be universally stable for all $U \geq 0$.

6.2.3 Flow in a Parallel Plate Channel With Body Forces

The analysis of flows involving body forces differs little in general from the formulations given earlier in this chapter. For most situations such as magneto-hydrodynamics or electrohydrodynamics, the only changes are the addition of constants or modifications to the coefficients of the various equations. For a few more details, see section 2.3.4.

The development region for a parallel plate channel in the presence of MHD and EHD body forces has been analyzed using finite difference methods by Shohet, Young, and Osterle (ref. 12).

6.3 EXAMPLE PROBLEM—INCOMPRESSIBLE ENTRANCE FLOW IN A PARALLEL PLATE CHANNEL

The finite difference analysis of the development region for incompressible flow in a parallel plate channel by Bodoia and Osterle (ref. 3) has been employed as a benchmark by a number of other investigators of this problem. The formulation was presented in section 6.1.1, and the results are given here as an example problem.

Details of the choice of mesh sizes used by Bodoia and Osterle are not available other than the statement that "Beyond a short distance from the mouth a 20 point mesh across the channel was used, but close to the mouth a larger number of mesh points was used to obtain better accuracy." However, personal communications with Bodoia and Osterle and attempts by the author to duplicate their results indicate that something on the order of 40 ΔY mesh spaces were used near the inlet, with the ΔX spacing increasing gradually from about $\Delta X = 2.5 \times 10^{-5}$

at the entrance to $\Delta X = 1.0 \times 10^{-3}$ far downstream. The calculations were performed on an IBM 650 digital computer.

Figure 6-5 shows the development of the dimensionless axial velocity U as a function of X for various transverse positions. Figure 6-6 shows the pressure development. The information in these two figures is also presented in table 6-I, abstracted from reference 4.

Figure 6-6 also compares the numerical solution with the solution presented by Schlichting (ref. 1). Schlichting's results were obtained by joining a power series expansion downstream to an asymptotic solution upstream, matching the velocities at $X = 0.004$. A rather sharp change in slope of the centerline velocity resulted. Schlichting's technique apparently resulted in an excessively rapid growth of the core velocity and a smaller pressure drop than that found by the numerical technique.

It is interesting to note that the numerical results, requiring many hours of computing time on a first generation machine, could be obtained in a few minutes on a modern third generation machine.

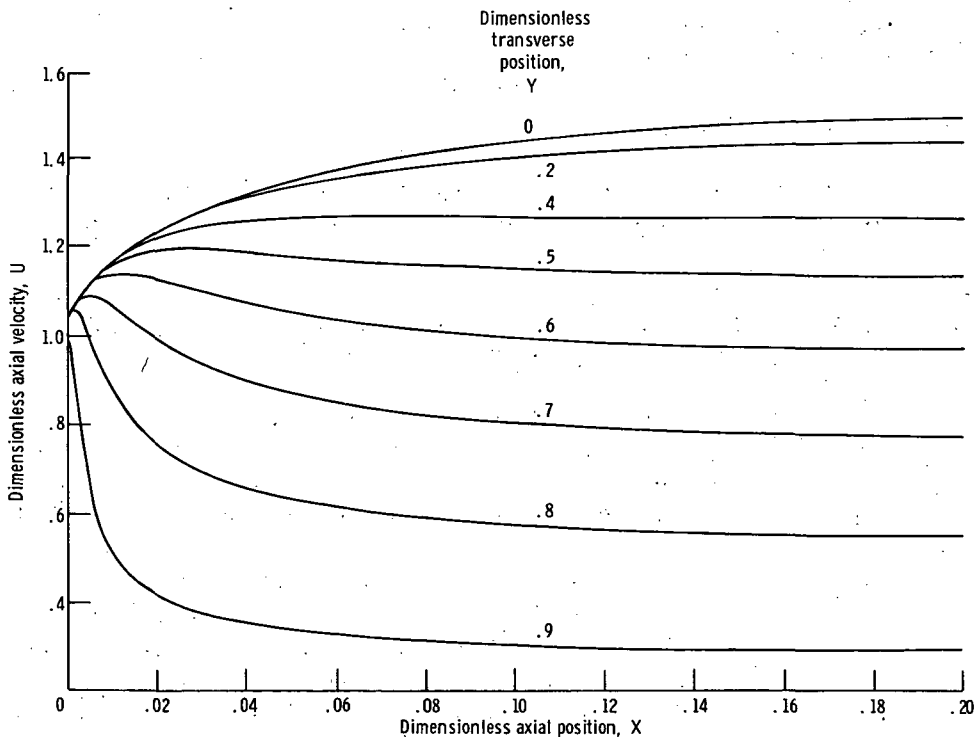


FIGURE 6-5.—Velocity variation in Poiseuille development.

TABLE 6-I.—POISEUILLE FLOW CALCULATION—DIMENSIONLESS VELOCITY AND PRESSURE

Dimensionless transverse position, <i>Y</i>	Dimensionless axial position, <i>X</i>						
	0.001	0.002	0.004	0.006	0.008	0.010	0.012
0	1.0615	1.0751	1.1013	1.1244	1.1443	1.1615	1.1767
.1	↓	↓	↓	↓	1.1443	1.1615	1.1767
.2					1.1443	1.1615	1.1766
.3					1.1442	1.1613	1.1763
.4			1.1012	1.1243	1.1438	1.1604	1.1745
.5			1.1010	1.1234	1.1414	1.1555	1.1665
.6		1.0750	1.0993	1.1176	1.1290	1.1351	1.1373
.7	1.0612	1.0725	1.0863	1.0874	1.0788	1.0655	1.0501
.8	1.0551	1.0485	1.0132	.9665	.9204	.8798	.8455
.9	.9587	.3655	.7194	.6204	.5567	.5136	.4832
1.0	.0000	.0000	.0000	.0000	.0000	.0000	.0000
- <i>P</i>	.06210	.07664	.10503	.13075	.15324	.17306	.19082

Dimensionless transverse position, <i>Y</i>	Dimensionless axial position, <i>X</i>						
	0.016	0.020	0.024	0.028	0.032	0.040	0.050
0	1.2031	1.2259	1.2463	1.2648	1.2818	1.3121	1.3441
.1	1.2030	1.2258	1.2460	1.2643	1.2811	1.3105	1.3412
.2	1.2028	1.2252	1.2448	1.2623	1.2778	1.3043	1.3306
.3	1.2017	1.2228	1.2406	1.2556	1.2684	1.2887	1.3067
.4	1.1972	1.2144	1.2275	1.2373	1.2447	1.2542	1.2601
.5	1.1813	1.1893	1.1928	1.1935	1.1923	1.1871	1.1786
.6	1.1339	1.1253	1.1144	1.1030	1.0918	1.0715	1.0504
.7	1.0185	.9896	.9644	.9429	.9246	.8950	.8677
.8	.7922	.7535	.7241	.7011	.6825	.6541	.6291
.9	.4427	.4162	.3971	.3825	.3708	.3534	.3383
1.0	.0000	.0000	.0000	.0000	.0000	.0000	.0000
- <i>P</i>	.22218	.24992	.27522	.29873	.32085	.36192	.40892

Dimensionless transverse position, <i>Y</i>	Dimensionless axial position, <i>X</i>					
	0.060	0.080	0.100	0.150	0.200	1.000
0	1.3707	1.4111	1.4388	1.4758	1.4903	1.499999
.1	1.3663	1.4039	1.4292	1.4629	1.4762	1.485000
.2	1.3511	1.3803	1.3993	1.4239	1.4336	1.440000
.3	1.3195	1.3357	1.3454	1.3573	1.3619	1.364000
.4	1.2626	1.2635	1.2628	1.2611	1.2604	1.260000
.5	1.1703	1.1565	1.1467	1.1336	1.1284	1.124999
.6	1.0337	1.0095	.9938	.9733	.9653	.969999
.7	.8475	.8197	.8022	.7796	.7708	.765000
.8	.6112	.5870	.5720	.5526	.5451	.540000
.9	.3275	.3132	.3042	.2926	.2880	.250000
1.0	.0000	.0000	.0000	.0000	.0000	.000000
- <i>P</i>	.45249	.53258	.60631	.77507	.93269	3.338018

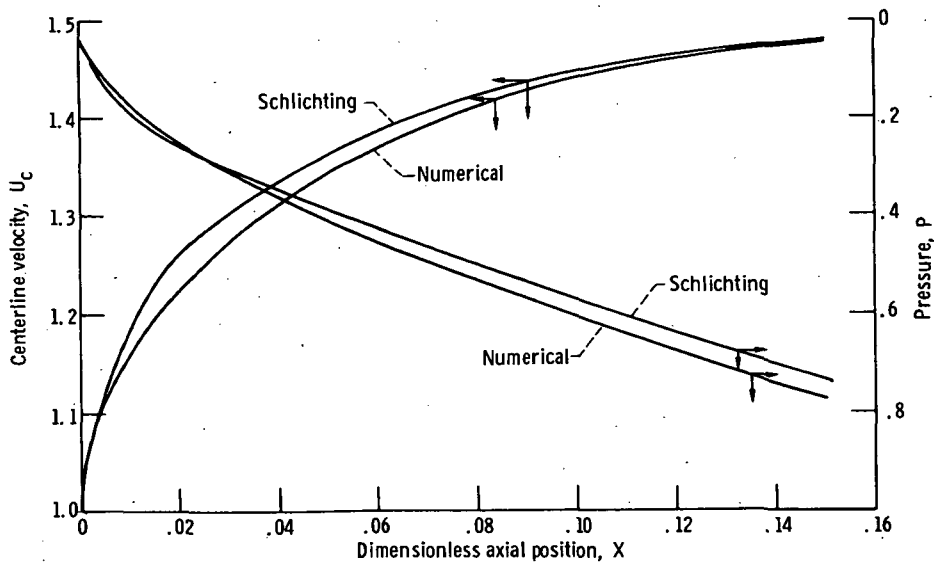


FIGURE 6-6.—Centerline velocity and pressure variation in Poiseuille development.

REFERENCES

1. SCHLICHTING, HERMANN (J. KESTIN, TRANS.): *Boundary Layer Theory*. Fourth ed., McGraw-Hill Book Co., Inc., 1960.
2. WANG, Y. L.; AND LONGWELL, P. A.: *Laminar Flow in the Inlet Section of Parallel Plates*. *AICHE J.*, vol. 10, no. 3, May 1964, pp. 323-329.
3. BODOIA, J. R.; AND OSTERLE, J. F.: *Finite Difference Analysis of Plane Poiseuille and Couette Flow Developments*. *Appl. Sci. Res.*, vol. A10, 1961, pp. 265-276.
4. BODOIA, JOHN R.: *The Finite Difference Analysis of Confined Viscous Flows*. Ph. D. Thesis, Carnegie Inst. Tech., 1959.
5. WALKER, M. L., JR.: *Laminar Compressible Flow in the Entrance Region of a Tube*. Ph. D. Thesis, Carnegie Inst. Tech., 1965.
6. SHAPIRO, ASCHER H.: *The Dynamics and Thermodynamics of Compressible Fluid Flow*. Vol. 2. Ronald Press Co., 1954.
7. MCADAMS, WILLIAM H.; NICOLAI, LLOYD A.; AND KEENAN, JOSEPH H.: *Measurements of Recovery Factors and Coefficients of Heat Transfer in a Tube for Subsonic Flow of Air*. *Trans. Am. In. Ch. En.*, vol. 42, 1946, pp. 907-925.
8. DORRANCE, WILLIAM H.: *Viscous Hypersonic Flow*. McGraw-Hill Book Co., Inc., 1962.
9. BERMAN, ABRAHAM S.: *Effects of Porous Boundaries on the Flow of Fluids in Systems with Various Geometries*. *Production of Nuclear Materials and Isotopes*. Vol. 4 of *Proceedings of the Second International Conference on the Peaceful Uses of Atomic Energy*. United Nations, 1958, pp. 351-358.
10. BUZZARD, GALE H., II: *Finite-Difference Analysis of the Compressible Inlet Problem in a Porous Plane Channel*. Ph.D. Thesis, North Carolina State Univ., 1966.
11. BODOIA, J. R.; AND OSTERLE, J. F.: *The Development of Free Convection Between Heated Vertical Plates*. *J. Heat Transfer*, vol. 84, no. 1, Feb. 1962, pp. 40-44.
12. SHOHEI, J. L.; OSTERLE, J. F.; AND YOUNG, F. J.: *Velocity and Temperature Profiles for Laminar Magnetohydrodynamic Flow in the Entrance Region of a Plane Channel*. *Phys. Fluids*, vol. 5, no. 5, May 1962, pp. 545-549.

CHAPTER 7

CIRCULAR TUBE

7.1 ENTRANCE FLOW AND HEAT TRANSFER IN A CIRCULAR TUBE

The flow and heat transfer in a tube of circular cross section have for some time been extremely popular subjects for analysis due to the enormous number of practical applications of this geometry. As in the parallel plate channel case discussed in the preceding chapter, the emphasis for the incompressible case is on the entrance region flow and heat transfer since the fully developed solutions are merely special cases of the formulations given; for the compressible cases, the entire flow is an "entrance" flow since no fully developed region can be defined. The problem configuration and coordinate system are shown in figure 7-1.

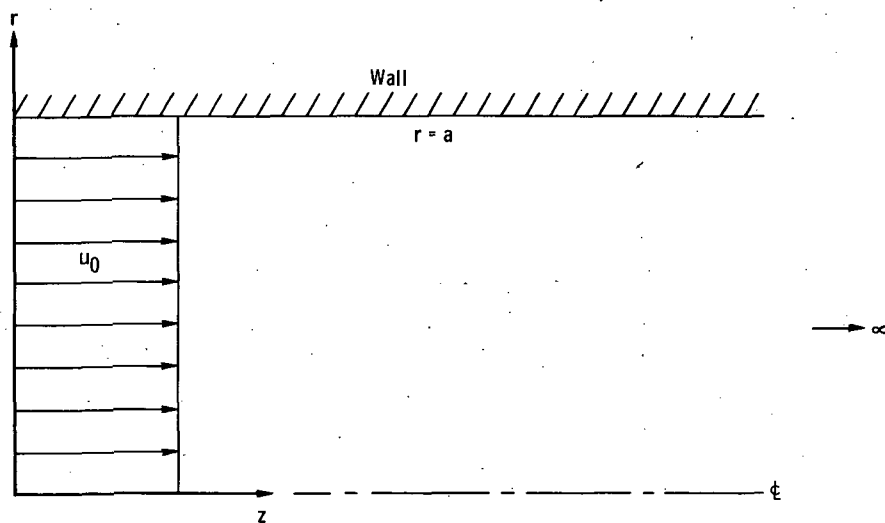


FIGURE 7-1. — Problem configuration and coordinate system for circular tube.

7.1.1 Incompressible Constant Property Flow – Velocity Solution

The model usually assumed for the entrance flow in a circular tube is the boundary layer model, which apparently provides a sufficiently accurate solution for engineering purposes. For the case of flow in the entrance of a porous circular tube, Hornbeck, Rouleau, and Osterle (ref. 1) have shown that a higher order of approximation, including radial momentum flux but not second derivatives in the axial direction, does not give significantly different results from the boundary layer type of model for Reynolds numbers greater than about 500. We shall limit the present discussion to the boundary layer model.

The equations of motion are

$$u \frac{\partial u}{\partial z} + v \frac{\partial u}{\partial r} = -\frac{1}{\rho} \frac{dp}{dz} + \nu \left(\frac{\partial^2 u}{\partial r^2} + \frac{1}{r} \frac{\partial u}{\partial r} \right) \quad (7-1)$$

and

$$r \frac{\partial u}{\partial z} + \frac{\partial(vr)}{\partial r} = 0 \quad (7-2)$$

The boundary conditions on velocity are

$$\left. \begin{aligned} u(r, 0) &= u_0 \text{ (see appendix F)} \\ u(a, z) &= 0 \\ \frac{\partial u}{\partial r}(0, z) &= 0 \\ v(a, z) &= 0 \\ v(0, z) &= 0 \\ p(0) &= p_0 \end{aligned} \right\} \quad (7-3)$$

where u_0 is the inlet profile (usually but not necessarily assumed constant).

The problem may now be restated in dimensionless form. The dimensionless variables chosen are

$$\left. \begin{aligned}
 U &= \frac{u}{u_0} \\
 V &= \frac{av}{\nu} \\
 P &= \frac{(p-p_0)}{\rho u_0^2} \\
 R &= \frac{r}{a} \\
 Z &= \frac{\nu z}{a^2 u_0}
 \end{aligned} \right\} \quad (7-4)$$

where u_0 is the mean velocity in the tube. In terms of these dimensionless variables, the problem may be rewritten as

$$U \frac{\partial U}{\partial Z} + V \frac{\partial U}{\partial R} = -\frac{dP}{dZ} + \frac{\partial^2 U}{\partial R^2} + \frac{1}{R} \frac{\partial U}{\partial R} \quad (7-5)$$

$$R \frac{\partial U}{\partial Z} + \frac{\partial(VR)}{\partial R} = 0 \quad (7-6)$$

subject to the boundary conditions

$$\left. \begin{aligned}
 U(R, 0) &= 1 \\
 U(1, Z) &= 0 \\
 \frac{\partial U}{\partial R}(0, Z) &= 0 \\
 V(1, Z) &= 0 \\
 V(0, Z) &= 0 \\
 P(0) &= 0
 \end{aligned} \right\} \quad (7-7)$$

The finite difference formulation to be presented here has been given in the literature by Hornbeck (ref. 2) and Hornbeck, Rouleau, and Osterle (ref. 3). The difference grid is shown in figure 7-2. Equations (7-5) and (7-6) are expressed in difference form as

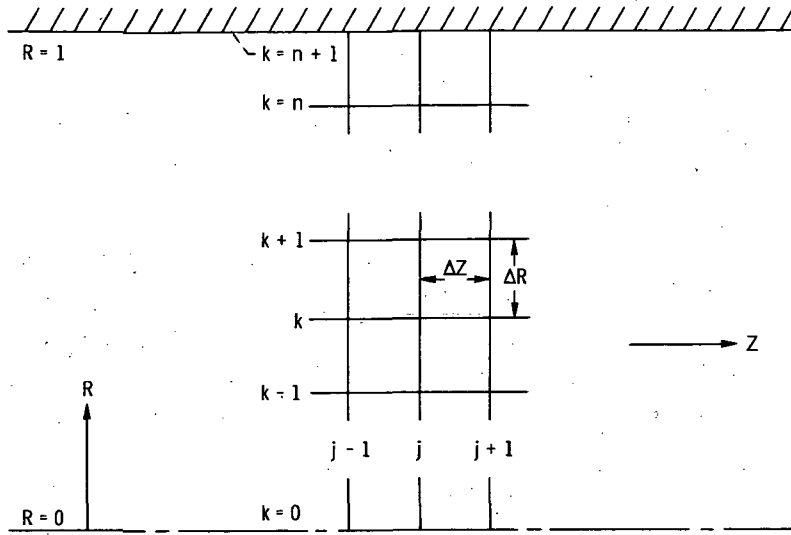


FIGURE 7-2.—Finite difference grid for circular tube.

$$U_{j,k} \frac{U_{j+1,k} - U_{j,k}}{\Delta Z} + V_{j,k} \frac{U_{j+1,k+1} - U_{j+1,k-1}}{2(\Delta R)} = -\frac{P_{j+1} - P_j}{\Delta Z} + \frac{U_{j+1,k+1} - 2U_{j+1,k} + U_{j+1,k-1}}{(\Delta R)^2} + \frac{1}{R_k} \frac{U_{j+1,k+1} - U_{j+1,k-1}}{2(\Delta R)} \quad (7-8)$$

and

$$\frac{R_k(U_{j+1,k} - U_{j,k})}{2(\Delta Z)} + \frac{R_{k+1}(U_{j+1,k+1} - U_{j,k+1})}{2(\Delta Z)} + \frac{V_{j+1,k+1}R_{k+1} - V_{j+1,k}R_k}{\Delta R} = 0 \quad (7-9)$$

As was found in chapter 3 for the centerline of the circular jet, it is necessary to give special attention to the equations at $R=0$ and to form a special version of the equations along the centerline. This may be accomplished by taking the limit of equations (7-5) and (7-6) as $R \rightarrow 0$. Applying L'Hôspital's rule, these equations may be written at $R=0$ as

$$U \frac{\partial U}{\partial Z} \Big|_{R=0} = -\frac{dP}{dZ} + 2 \frac{\partial^2 U}{\partial R^2} \Big|_{R=0} \quad (7-10)$$

and

$$\frac{\partial U}{\partial Z} \Big|_{R=0} + 2 \frac{\partial V}{\partial R} \Big|_{R=0} = 0 \quad (7-11)$$

Equations (7-10) and (7-11) can be written in finite difference form as

$$U_{j,0} \frac{U_{j+1,0} - U_{j,0}}{\Delta Z} = -\frac{P_{j+1} - P_j}{\Delta Z} + 4 \left[\frac{U_{j+1,1} - U_{j+1,0}}{(\Delta R)^2} \right] \quad (7-12)$$

and

$$\frac{U_{j+1,1} + U_{j+1,0} - U_{j,1} - U_{j,0}}{2(\Delta Z)} + \frac{2V_{j+1,1}}{\Delta R} = 0 \quad (7-13)$$

Equation (7-12) includes the symmetry boundary condition on U at $R = 0$ expressed in difference form as $U_{j+1,1} = U_{j+1,-1}$. Equation (7-13) includes the condition $V(0, Z) = 0$.

Equations (7-8) and (7-9) written for $k = 1(1)n$ and equations (7-12) and (7-13) for $k = 0$ together constitute $2n + 2$ equations in the $2n + 2$ unknowns $U_{j+1,k}$, $V_{j+1,k}$, and P_{j+1} .

The system of equations may be considerably reduced in size by using the integral continuity equation as discussed in the last chapter. Adding the continuity equation (7-9) for $k = 1(1)n$ and equation (7-13) for $k = 0$ together, the resulting equation can be written in the form

$$\Delta R \left(\frac{1}{4} U_{j+1,0} + \frac{3}{4} U_{j+1,1} \right) + \sum_{k=2}^n R_k U_{j+1,k} = \Delta R \left(\frac{1}{4} U_{j,0} + \frac{3}{4} U_{j,1} \right) + \sum_{k=2}^n R_k U_{j,k} \quad (7-14)$$

Equation (7-14) is the finite difference analog of

$$\int_0^1 UR dR = \text{a constant} \quad (7-15)$$

The use of this type of equation is discussed in more detail in section 6.1.1.

It is now convenient to rewrite equation (7-8) as

$$\left[-\frac{V_{j,k}}{2(\Delta R)} + \frac{1}{2R_k(\Delta R)} - \frac{1}{(\Delta R)^2} \right] U_{j+1,k-1} + \left[\frac{U_{j,k}}{\Delta Z} + \frac{2}{(\Delta R)^2} \right] U_{j+1,k} + \left[\frac{V_{j,k}}{2(\Delta R)} - \frac{1}{2R_k(\Delta R)} - \frac{1}{(\Delta R)^2} \right] U_{j+1,k+1} + \left(\frac{1}{\Delta Z} \right) P_{j+1} = \frac{U_{j,k}^2 + P_j}{\Delta Z} \quad (7-16)$$

and equation (7-12) as

$$\left[\frac{U_{j,0}}{\Delta Z} + \frac{4}{(\Delta R)^2} \right] U_{j+1,0} + \left[-\frac{4}{(\Delta R)^2} \right] U_{j+1,1} + \left(\frac{1}{\Delta Z} \right) P_{j+1} = \frac{U_{j,0}^2 + P_j}{\Delta Z} \quad (7-17)$$

Equation (7-16) written for $k = 1(1)n$, equation (7-17) for $k = 0$, and equation (7-14) now comprise $n+2$ linear algebraic equations in the $n+2$ unknowns $U_{j+1,k}$ and P_{j+1} .

This set of equations may be written in matrix form as

$$\begin{array}{cccccccccc|c|c}
 \frac{\Delta R}{4} & \frac{3\Delta R}{4} & R_2 & R_3 & - & - & - & R_{n-1} & R_n & 0 & U_{j+1,0} & S \\
 \beta_0 & \Omega_0 & & & & & & & & \frac{1}{\Delta Z} & U_{j+1,1} & \phi_0 \\
 \alpha_1 & \beta_1 & \Omega_1 & & & & & & & \frac{1}{\Delta Z} & U_{j+1,2} & \phi_1 \\
 & \alpha_2 & \beta_2 & \Omega_2 & & & & & & \frac{1}{\Delta Z} & U_{j+1,3} & \phi_2 \\
 & & \alpha_3 & \beta_3 & \Omega_3 & & & & & \frac{1}{\Delta Z} & U_{j+1,4} & \phi_3 \\
 & & & - & - & - & & & & - & - & - \\
 & & & & - & - & - & & & - & - & - \\
 & & & & & - & - & - & & - & - & - \\
 & & & & & & & \alpha_{n-1} & \beta_{n-1} & \Omega_{n-1} & \frac{1}{\Delta Z} & U_{j+1,n} & \phi_{n-1} \\
 & & & & & & & \alpha_n & \beta_n & \frac{1}{\Delta Z} & P_{j+1} & \phi_n
 \end{array} \times$$

(7-18)

where

$$\beta_0 = \frac{U_{j,0}}{\Delta Z} + \frac{4}{(\Delta R)^2}$$

$$\Omega_0 = -\frac{4}{(\Delta R)^2}$$

$$\phi_0 = \frac{\bar{U}_{j,0}^2 + P_j}{\Delta Z}$$

$$S = \frac{\Delta R}{4} U_{j,0} + \frac{3(\Delta R)}{4} U_{j,1} + \sum_{k=2}^n R_k U_{j,k}$$

and

$$\alpha_k = \frac{-V_{j,k}}{2(\Delta R)} + \frac{1}{2R_k(\Delta R)} - \frac{1}{(\Delta R)^2} \quad (k > 0)$$

$$\beta_k = \frac{U_{j,k}}{\Delta Z} + \frac{2}{(\Delta R)^2} \quad (k > 0)$$

$$\Omega_k = \frac{V_{j,k}}{2(\Delta R)} - \frac{1}{2R_k(\Delta R)} - \frac{1}{(\Delta R)^2} \quad (k > 0)$$

$$\phi_k = \frac{U_{j,k}^2 + P_j}{\Delta Z}$$

Since the matrix of coefficients of (7-18) is not tridiagonal, no unusually rapid method can be employed, and Gaussian (or Gauss-Jordan) elimination is suggested (see appendix E). Once the solution has been obtained, another step ΔZ may be taken.

It is strongly suggested that the variable mesh technique discussed in appendix D be employed in this problem, since by using a fine grid near the wall where it is needed and a large grid elsewhere, the number of equations to be solved can be reduced materially. More details of the application of this technique to pipe flow problems may be found in reference 4.

The representation given here has been shown to be stable for all $U \geq 0$ in reference 4. If $U < 0$ then the stability criteria which must be satisfied are

$$\left. \begin{aligned} \frac{\Delta Z}{|U|(\Delta R)^2} &\geq \frac{1}{2} \\ \left| V - \frac{1}{R} \right| &\geq \sqrt{\frac{2|U|}{\Delta Z}} \end{aligned} \right\} \quad (7-19)$$

These will, in general, be satisfied only for very small negative values of U .

The truncation error of the momentum equation is of $\mathcal{O}(\Delta Z)$ and $\mathcal{O}(\Delta R^2)$ and for continuity of $\mathcal{O}(\Delta Z)$ and $\mathcal{O}(\Delta R)$.

7.1.2 Incompressible Constant Property Flow – Temperature Solution

The energy equation for the problem considered here is

$$\rho c_p \left(u \frac{\partial t}{\partial z} + v \frac{\partial t}{\partial r} \right) = k \left(\frac{\partial^2 t}{\partial r^2} + \frac{1}{r} \frac{\partial t}{\partial r} \right) \quad (7-20)$$

Viscous dissipation has been neglected in equation (7-20) but could readily be included. Axial conduction has also been neglected.

We shall again consider two commonly used temperature boundary conditions, those of constant wall temperature and constant wall heat flux. The boundary conditions for the problem are

$$\left. \begin{aligned} t(r, 0) &= t_0 \text{ (assumed constant, although again not necessary)} \\ t(a, z) &= t_w \text{ (constant wall temperature)} \\ \text{or} \\ k \frac{\partial t}{\partial r}(a, z) &= q \text{ (constant wall heat flux)} \\ \text{and} \\ \frac{\partial t}{\partial r}(0, z) &= 0 \end{aligned} \right\} \quad (7-21)$$

The following dimensionless variables are now chosen

$$\left. \begin{aligned} T &= \frac{t - t_w}{t_0 - t_w} \text{ (constant wall temperature)} \\ \text{or} \\ T &= \frac{k}{qa} (t - t_0) \text{ (constant wall heat flux)} \\ \text{and} \\ U &= \frac{u}{u_0} \\ V &= \frac{va}{\nu} \\ Z &= \frac{z\mu}{\rho a^2 u_0} \\ R &= \frac{r}{a} \end{aligned} \right\} \quad (7-22)$$

The temperature problem in dimensionless form then becomes

$$U \frac{\partial T}{\partial Z} + V \frac{\partial T}{\partial R} = \frac{1}{Pr} \left(\frac{\partial^2 T}{\partial R^2} + \frac{1}{R} \frac{\partial T}{\partial R} \right) \quad (7-23)$$

subject to

$$T(R, 0) = 1 \text{ (constant wall temperature)}$$

or

$$T(R, 0) = 0 \text{ (constant wall heat flux)}$$

$$\frac{\partial T}{\partial R}(0, Z) = 0$$

and

$$T(1, Z) = 0 \text{ (constant wall temperature)}$$

or

$$\frac{\partial T}{\partial R}(1, Z) = 1 \text{ (constant wall heat flux)}$$

(7-24)

The finite difference formulation to be presented next is essentially that of Hornbeck (ref. 5) except for minor changes to conform with the representations employed throughout this book.

The difference form of equation (7-23) is

$$\begin{aligned} U_{j,k} \frac{T_{j+1,k} - T_{j,k}}{\Delta Z} + V_{j,k} \frac{T_{j+1,k+1} - T_{j+1,k-1}}{2(\Delta R)} \\ = \frac{1}{Pr} \left[\frac{T_{j+1,k+1} - 2T_{j+1,k} + T_{j+1,k-1}}{(\Delta R)^2} + \frac{1}{R_k} \frac{T_{j+1,k+1} - T_{j+1,k-1}}{2(\Delta R)} \right] \end{aligned} \quad (7-25)$$

This equation applies for $k = 1(1)n$.

For $R = 0$ it is again necessary to apply the limiting process as $R \rightarrow 0$ to equation (7-23), which results in

$$U \left. \frac{\partial T}{\partial Z} \right|_{R=0} = \frac{2}{Pr} \left. \frac{\partial^2 T}{\partial R^2} \right|_{R=0} \quad (7-26)$$

Expressing equation (7-26) in finite difference form yields

$$U_{j,0} \frac{T_{j+1,0} - T_{j,0}}{\Delta Z} = \frac{4}{Pr} \left[\frac{T_{j+1,1} - T_{j+1,0}}{(\Delta R)^2} \right] \quad (7-27)$$

Equation (7-27) includes the symmetry condition expressed as $T_{j+1,1} = T_{j+1,-1}$ at $R = 0$.

Equations (7-25) and (7-26) may be rewritten in more useful forms as

where all symbols are as defined in (7-30). Although the matrix of coefficients in (7-32) is not tridiagonal, it may be readily made tridiagonal as is discussed in section 6.1.2, and the method of appendix A may be used to obtain a solution.

After the solution has been obtained another step downstream may be taken and the process is repeated.

It is of course best to obtain the velocity and temperature solutions together, solving first at each step for the velocity and then for the temperature. If it is desired to solve a problem in which the temperature develops from the tube entrance but in which the velocity is already fully developed (i.e., the Graetz problem); then the velocity solution is, of course, bypassed.

The difference formulation for the energy equation is universally stable. The truncation error of the difference form of the energy equation is of $\mathcal{O}(\Delta Z)$ and $\mathcal{O}((\Delta R)^2)$.

7.1.3 Incompressible Constant Property Flow—Heat Transfer Solution

The bulk (mixed-mean) temperature for the circular tube is defined as

$$t_b = \frac{\int_0^a 2\pi r u t \, dr}{\int_0^a 2\pi r u \, dr} \quad (7-33)$$

which, in dimensionless form, is

$$T_b = 2 \int_0^1 U R T \, dR \quad (7-34)$$

This bulk temperature may be calculated numerically by applying Simpson's rule, which yields

$$T_b \Big|_{j+1} = \frac{2(\Delta R)}{3} \left(\sum_{k=1, 3, 5, 7, 9, \dots}^n 4U_{j+1, k} R_k T_{j+1, k} + \sum_{k=2, 4, 6, 8, \dots}^{n-1} 2U_{j+1, k} R_k T_{j+1, k} \right) \quad (7-35)$$

where n must be odd; that is, there must be an even number of spaces across the tube radius. If the variable mesh procedure mentioned earlier is used, then the integration will have to be done in two parts, each part covering the region of only one mesh size.

The local Nusselt number is given by

$$Nu_z = \frac{2ha}{k} \quad (7-36)$$

where

$$h(t_w - t_b) = k \left. \frac{\partial t}{\partial r} \right|_{r=a} \quad (7-37)$$

so

$$Nu_z = \frac{-\left. \frac{\partial t}{\partial r} \right|_{r=a} (2a)}{t_b - t_w} \quad (2a) \quad (7-38)$$

For constant wall temperature, equation (7-38) can be written in dimensionless difference form as

$$Nu_z \Big|_{j+1} = \left(\frac{-2 \left. \frac{\partial T}{\partial R} \right|_{R=1}}{T_b} \right)_{j+1} = \frac{-2 \left[\frac{3T_{j+1, n+1} - 4T_{j+1, n} + T_{j+1, n-1}}{2(\Delta R)} \right]}{T_b \Big|_{j+1}} \quad (7-39)$$

For constant wall heat flux,

$$h(t_w - t_b) = q \quad (7-40)$$

so

$$Nu_z = \frac{q(2a)}{k(t_b - t_w)} \quad (7-41)$$

which may be expressed in dimensionless difference form as

$$Nu_z \Big|_{j+1} = \left(\frac{2}{T_b - T_w} \right)_{j+1} \quad (7-42)$$

The mean Nusselt number is computed as

$$Nu_m = \frac{1}{Z} \int_0^Z Nu_z dZ \quad (7-43)$$

which may be evaluated using Simpson's rule as

$$Nu_m \Big|_{j+1} = \frac{1}{Z_{j+1}} \left(Nu_z \Big|_0 + 4 \sum_{i=1, 3, 5, 7, \dots}^j Nu_z \Big|_i + 2 \sum_{i=2, 4, 6, 8, \dots}^{j-1} Nu_z \Big|_i + Nu_z \Big|_{j+1} \right) \frac{\Delta Z}{3} \quad (7-44)$$

As discussed in chapter 6, the calculation of $Nu_m|_{j+1}$ can only be accomplished at every other ΔZ step so that an even number of intervals from $Z=0$ ($j=0$) is involved.

7.1.4 Compressible Flow—Velocity and Temperature Solutions

The coupled equations of motion, energy, state, and property relations for the compressible flow in a circular tube are assumed to be, for a perfect gas,

$$\rho \left(u \frac{\partial u}{\partial z} + v \frac{\partial u}{\partial r} \right) = - \frac{dp}{dz} + \frac{1}{r} \frac{\partial}{\partial r} \left(\mu r \frac{\partial u}{\partial r} \right) \quad (7-45)$$

$$\frac{\partial(\rho u)}{\partial z} + \frac{1}{r} \frac{\partial(\rho r v)}{\partial r} = 0 \quad (7-46)$$

$$\rho c_p \left(u \frac{\partial t}{\partial z} + v \frac{\partial t}{\partial r} \right) = u \frac{dp}{dz} + \frac{1}{r} \frac{\partial}{\partial r} \left(k r \frac{\partial t}{\partial r} \right) + \mu \left(\frac{\partial u}{\partial r} \right)^2 \quad (7-47)$$

$$p = \rho \mathcal{R} t \quad (7-48)$$

$$\mu = \mu(t) = \mu_0 \left(\frac{t}{t_0} \right)^f \quad (7-49)$$

$$k = k(t) = k_0 \left(\frac{t}{t_0} \right)^g \quad (7-50)$$

As before, we assume a power law relationship with temperature for μ and k . The velocity and pressure boundary conditions are

$$\left. \begin{aligned} u(a, z) &= 0 \\ u(r, 0) &= u_0 \text{ (again assumed constant, although a function of } r \text{ is} \\ &\quad \text{entirely permissible; see appendix F)} \\ \frac{\partial u}{\partial r}(0, z) &= 0 \\ v(a, z) &= 0 \\ v(0, z) &= 0 \\ p(0) &= p_0 \end{aligned} \right\} \quad (7-51)$$

The thermal boundary conditions to be considered are, as before, constant wall temperature and constant wall heat flux

$$\left. \begin{aligned}
 &t(r, 0) = t_0 \\
 &\frac{\partial t}{\partial r}(0, z) = 0 \\
 \text{and} \\
 &t(a, z) = t_w \text{ (constant wall temperature)} \\
 \text{or} \\
 &k \frac{\partial t}{\partial r}(a, z) = q \text{ (constant wall heat flux)}
 \end{aligned} \right\} \quad (7-52)$$

The dimensionless variables for this problem are

$$\left. \begin{aligned}
 Z &= \frac{z\mu_0}{\rho_0 u_0 a^2} \\
 U &= \frac{u}{u_0} & R &= \frac{r}{a} \\
 V &= \frac{\rho_0 v a}{\mu_0} & k^* &= \frac{k}{k_0} \\
 T &= \frac{t}{t_0} & \mu^* &= \frac{\mu}{\mu_0} \\
 P &= \frac{p}{p_0} & \rho^* &= \frac{\rho}{\rho_0}
 \end{aligned} \right\} \quad (7-53)$$

Employing these dimensionless variables, equations (7-45) to (7-50) may be written as

$$\rho^* \left(U \frac{\partial U}{\partial Z} + V \frac{\partial U}{\partial R} \right) = - \frac{1}{\gamma M_0^2} \frac{dP}{dZ} + \frac{1}{R} \frac{\partial}{\partial R} \left(\mu^* R \frac{\partial U}{\partial R} \right) \quad (7-54)$$

$$\frac{\partial(\rho^* U)}{\partial Z} + \frac{1}{R} \frac{\partial(\rho^* R V)}{\partial R} = 0 \quad (7-55)$$

$$\begin{aligned}
 \rho^* \left(U \frac{\partial T}{\partial Z} + V \frac{\partial T}{\partial R} \right) &= \frac{\gamma - 1}{\gamma} U \frac{dP}{dZ} + \frac{1}{(Pr)R} \frac{\partial}{\partial R} \left(k^* R \frac{\partial T}{\partial R} \right) \\
 &+ (\gamma - 1) M_0^2 \mu^* \left(\frac{\partial U}{\partial R} \right)^2 \quad (7-56)
 \end{aligned}$$

$$P = \rho^* T \quad (7-57)$$

$$\mu^* = (T)^f \quad (7-58)$$

$$k^* = (T)^y \quad (7-59)$$

where $M_0 = u_0/\sqrt{\gamma \mathcal{R} t_0}$ is the Mach number evaluated at t_0 , and $Pr = \mu_0 c_p/k_0$ is the Prandtl number evaluated at the same conditions (the inlet conditions).

The boundary conditions on velocity and pressure are, in dimensionless form.

$$\left. \begin{aligned} U(1, Z) &= 0 \\ U(R, 0) &= 1 \\ \frac{\partial U}{\partial R}(0, Z) &= 0 \\ V(1, Z) &= 0 \\ V(0, Z) &= 0 \\ P(0) &= 1 \end{aligned} \right\} \quad (7-60)$$

The dimensionless thermal boundary conditions are

$$\left. \begin{aligned} T(R, 0) &= 1 \\ \frac{\partial T}{\partial R}(0, Z) &= 0 \end{aligned} \right\} \quad (7-61)$$

and

$$T(1, Z) = \frac{t_w}{t_0} \text{ (constant wall temperature)}$$

or

$$k^* \frac{\partial T}{\partial R}(1, Z) = \frac{qa}{k_0 t_0} \text{ (constant wall heat flux)}$$

A finite difference representation to this problem must now be selected. The representation given here is based on that employed by Walker (ref. 6) for what he called the "post-boundary-layer region." The main difference from Walker's formulation is that, in his equations, the degree of implicitness is arbitrary; in the present formulation, the equations are fully implicit in an effort to be consistent with the representations given elsewhere in this book. The actual numbers generated should differ very little. The difference representations of equations (7-54) to (7-59) are

$$\rho_{j,k}^* \left[U_{j,k} \frac{U_{j+1,k} - U_{j,k}}{\Delta Z} + V_{j,k} \frac{U_{j+1,k+1} - U_{j+1,k-1}}{2(\Delta R)} \right] = -\frac{1}{\gamma M_0^2} \frac{P_{j+1} - P_j}{\Delta Z} +$$

$$\begin{aligned}
& + \mu_{j,k}^* \left[\frac{U_{j+1,k+1} - 2U_{j+1,k} + U_{j+1,k-1}}{(\Delta R)^2} + \frac{1}{R_k} \frac{U_{j+1,k+1} - U_{j+1,k-1}}{2(\Delta R)} \right] \\
& \quad + \left[\frac{\mu_{j,k+1}^* - \mu_{j,k-1}^*}{2(\Delta R)} \right] \left[\frac{U_{j+1,k+1} - U_{j+1,k-1}}{2(\Delta R)} \right] \quad (7-62)
\end{aligned}$$

$$\begin{aligned}
& \rho_{j,k+1}^* \left[\frac{U_{j+1,k+1} - U_{j,k+1}}{2(\Delta Z)} \right] + \rho_{j,k}^* \left[\frac{U_{j+1,k} - U_{j,k}}{2(\Delta Z)} \right] \\
& \quad + \left[\left(\frac{U_{j,k+1}}{T_{j,k+1}} \right) + \left(\frac{U_{j,k}}{T_{j,k}} \right) \right] \left[\frac{P_{j+1} - P_j}{2(\Delta Z)} \right] \\
& \quad - \left(\frac{\rho_{j,k+1}^* U_{j,k+1}}{T_{j,k+1}} \right) \left[\frac{T_{j+1,k+1} - T_{j,k+1}}{2(\Delta Z)} \right] \\
& \quad - \left(\frac{\rho_{j,k}^* U_{j,k}}{T_{j,k}} \right) \left[\frac{T_{j+1,k} - T_{j,k}}{2(\Delta Z)} \right] \\
& \quad + \left(\frac{2}{R_{k+1} + R_k} \right) \left(\frac{\rho_{j+1,k+1}^* R_{k+1} V_{j+1,k+1} - \rho_{j+1,k}^* R_k V_{j+1,k}}{\Delta R} \right) \\
& = 0 \quad (7-63)
\end{aligned}$$

$$\begin{aligned}
& \rho_{j,k}^* \left[U_{j,k} \frac{T_{j+1,k} - T_{j,k}}{\Delta Z} + V_{j,k} \frac{T_{j+1,k+1} - T_{j+1,k-1}}{2(\Delta R)} \right] = \frac{\gamma - 1}{\gamma} U_{j,k} \left(\frac{P_{j+1} - P_j}{\Delta Z} \right) \\
& \quad + \frac{1}{P_r} \left\{ k_{j,k}^* \left[\frac{T_{j+1,k+1} - 2T_{j+1,k} + T_{j+1,k-1}}{(\Delta R)^2} \right. \right. \\
& \quad + \left. \frac{1}{R_k} \frac{T_{j+1,k+1} - T_{j+1,k-1}}{2(\Delta R)} \right] + \left[\frac{k_{j,k+1}^* - k_{j,k-1}^*}{2(\Delta R)} \right] \\
& \quad \times \left. \left[\frac{T_{j+1,k+1} - T_{j+1,k-1}}{2(\Delta R)} \right] \right\} \\
& \quad + (\gamma - 1) M_0^2 \mu_{j,k}^* \left[\frac{U_{j,k+1} - U_{j,k-1}}{2(\Delta R)} \right] \left[\frac{U_{j+1,k+1} - U_{j+1,k-1}}{2(\Delta R)} \right] \quad (7-64)
\end{aligned}$$

$$P_{j+1} = \rho_{j+1,k}^* T_{j+1,k} \quad (7-65)$$

$$\mu_{j+1,k}^* = (T_{j+1,k})^f \quad (7-66)$$

$$k_{j+1,k}^* = (T_{j-1,k})^g \quad (7-67)$$

The complicated form of the continuity equation (eq. (7-63)) is required, as in the preceding chapter, in order to obtain a set of linear difference equations which can be solved without recourse to iteration.

Special forms of equations (7-62), (7-63), and (7-64) are required for $R=0$. These may be obtained by first taking the limit of equations (7-54), (7-55), and (7-56) as $R \rightarrow 0$. This procedure yields

$$\rho^* U \frac{\partial U}{\partial Z} \Big|_{R=0} = -\frac{1}{\gamma M_0^2} \frac{dP}{dZ} + 2\mu^* \frac{\partial^2 U}{\partial R^2} \Big|_{R=0} \quad (7-68)$$

$$\frac{\partial(\rho^* U)}{\partial Z} \Big|_{R=0} + 2 \frac{\partial(\rho^* V)}{\partial R} \Big|_{R=0} = 0 \quad (7-69)$$

$$\rho^* U \frac{\partial T}{\partial Z} \Big|_{R=0} = \frac{\gamma-1}{\gamma} U \frac{dP}{dZ} + \frac{2}{Pr} k^* \frac{\partial^2 T}{\partial R^2} \Big|_{R=0} \quad (7-70)$$

These equations in finite difference form are, for (7-68),

$$\rho_{j,0}^* U_{j,0} \frac{U_{j+1,0} - U_{j,0}}{\Delta Z} = -\frac{1}{\gamma M_0^2} \frac{P_{j+1} - P_j}{\Delta Z} + 4\mu_{j,0}^* \left[\frac{U_{j+1,1} - U_{j+1,0}}{(\Delta R)^2} \right] \quad (7-71)$$

Equation (7-63) gives the correct finite difference form for (7-69) when written for $k=0$. For equation (7-70), the difference form is

$$\rho_{j,0}^* U_{j,0} \frac{T_{j+1,0} - T_{j,0}}{\Delta Z} = \frac{\gamma-1}{\gamma} U_{j,0} \frac{P_{j+1} - P_j}{\Delta Z} + \frac{4}{Pr} k_{j,0}^* \left[\frac{T_{j+1,1} - T_{j+1,0}}{(\Delta R)^2} \right] \quad (7-72)$$

The finite difference forms of the momentum, continuity, and energy equations written for $k=0(1)n$ now include $3n+3$ or $3n+4$ unknowns $U_{j+1,k}$, $V_{j+1,k}$, $T_{j+1,k}$, and P_{j+1} , depending on whether the constant wall temperature or the constant wall heat flux condition is used. Before considering a possible reduction in this number, it is convenient to rewrite equations (7-62), (7-64), (7-71), and (7-72) in more useful forms. Equations (7-62) and (7-64) for $k=1(1)n$ become

$$\left[-\frac{\rho_{j,k}^* V_{j,k}}{2(\Delta R)} - \frac{\mu_{j,k}^*}{(\Delta R)^2} + \frac{\mu_{j,k}^*}{2(R_k)\Delta R} + \frac{\mu_{j,k+1}^* - \mu_{j,k-1}^*}{4(\Delta R)^2} \right] U_{j+1,k-1} + \left[\frac{\rho_{j,k}^* U_{j,k}}{\Delta Z} + \right.$$

$$\begin{aligned}
& + \frac{2\mu_{j,k}^*}{(\Delta R)^2} U_{j+1,k} + \left[\frac{\rho_{j,k}^* V_{j,k}}{2(\Delta R)} - \frac{\mu_{j,k}^*}{(\Delta R)^2} - \frac{\mu_{j,k}^*}{2(R_k)(\Delta R)} - \frac{\mu_{j,k+1}^* - \mu_{j,k-1}^*}{4(\Delta R)^2} \right] U_{j+1,k+1} \\
& + \left[\frac{1}{\gamma M_0^2(\Delta Z)} \right] P_{j+1} = \frac{P_j}{\gamma M_0^2(\Delta Z)} + \frac{\rho_{j,k}^* U_{j,k}^2}{\Delta Z} \quad (7-73)
\end{aligned}$$

$$\begin{aligned}
& \left[\frac{-\rho_{j,k}^* V_{j,k}}{2(\Delta R)} - \frac{k_{j,k}^*}{(Pr)(\Delta R)^2} + \frac{k_{j,k}^*}{2R_k(Pr)(\Delta R)} + \frac{k_{j,k+1}^* - k_{j,k-1}^*}{4(Pr)(\Delta R)^2} \right] T_{j+1,k-1} \\
& + \left[\frac{\rho_{j,k}^* U_{j,k}}{\Delta Z} + \frac{2k_{j,k}^*}{(Pr)(\Delta R)^2} \right] T_{j+1,k} \\
& + \left[\frac{\rho_{j,k}^* V_{j,k}}{2(\Delta R)} - \frac{k_{j,k}^*}{(Pr)(\Delta R)^2} - \frac{k_{j,k}^*}{2R_k(\Delta R)(Pr)} - \frac{k_{j,k+1}^* - k_{j,k-1}^*}{4(Pr)(\Delta R)^2} \right] T_{j+1,k+1} \\
& + \left\{ (\gamma - 1) M_0^2 \mu_{j,k}^* \left[\frac{U_{j,k+1} - U_{j,k-1}}{4(\Delta R)^2} \right] \right\} U_{j+1,k-1} \\
& + \left\{ (1 - \gamma) M_0^2 \mu_{j,k}^* \left[\frac{U_{j,k+1} - U_{j,k-1}}{4(\Delta R)^2} \right] \right\} U_{j+1,k+1} + \left[\frac{(1 - \gamma) U_{j,k}}{\gamma(\Delta Z)} \right] P_{j+1} \\
& = \frac{(1 - \gamma) U_{j,k}}{\gamma(\Delta Z)} P_j + \frac{\rho_{j,k}^* U_{j,k} T_{j,k}}{\Delta Z} \quad (7-74)
\end{aligned}$$

Equations (7-71) and (7-72) for $k=0$ become

$$\begin{aligned}
& \left[\frac{\rho_{j,0}^* U_{j,0}}{\Delta Z} + \frac{4\mu_{j,0}^*}{(\Delta R)^2} \right] U_{j+1,0} + \left[\frac{-4\mu_{j,0}^*}{(\Delta R)^2} \right] U_{j+1,1} + \left[\frac{1}{\gamma M_0^2 \Delta Z} \right] P_{j+1} \\
& = \frac{\rho_{j,0}^* U_{j,0}^2}{\Delta Z} + \frac{P_j}{\gamma M_0^2(\Delta Z)} \quad (7-75)
\end{aligned}$$

and

$$\begin{aligned}
& \left[\frac{\rho_{j,0}^* U_{j,0}}{\Delta Z} + \frac{4k_{j,0}^*}{(Pr)(\Delta R)^2} \right] T_{j+1,0} + \left[\frac{-4k_{j,0}^*}{(Pr)(\Delta R)^2} \right] T_{j+1,1} + \left[\frac{(1 - \gamma) U_{j,0}}{\gamma \Delta Z} \right] P_{j+1} \\
& = \frac{\rho_{j,0}^* U_{j,0} T_{j,0}}{\Delta Z} - \frac{P_j(\gamma - 1) U_{j,0}}{\gamma(\Delta Z)} \quad (7-76)
\end{aligned}$$

Equations (7-73) and (7-74) written for $k=1(1)n$ along with equations (7-75) and (7-76) for $k=0$ now comprise $2n+2$ equations in the $2n+3$ or $2n+4$ unknowns $U_{j+1,k}$, $T_{j+1,k}$, and P_{j+1} , depending again on which temperature bound-

any condition is considered. For the constant wall temperature condition, we are one equation short of having a complete set of equations. This additional equation may be obtained by adding together equation (7-63) written for all $k=0(1)n$. This results in the following:

$$\begin{aligned} \sum_{k=0}^n \left(\frac{R_{k+1} + R_k}{2} \right) & \left[\rho_{j,k+1}^* U_{j+1,k+1} + \rho_{j,k}^* U_{j+1,k} + \rho_{j,k+1}^* U_{j,k+1} \left(\frac{P_{j+1}}{P_j} - \frac{T_{j+1,k+1}}{T_{j,k+1}} \right) \right. \\ & \left. + \rho_{j,k}^* U_{j,k} \left(\frac{P_{j+1}}{P_j} - \frac{T_{j+1,k}}{T_{j,k}} \right) \right] \frac{\Delta R}{2} \\ & = \sum_{k=0}^n \left(\frac{R_{k+1} + R_k}{2} \right) (\rho_{j,k+1}^* U_{j,k+1} + \rho_{j,k}^* U_{j,k}) \frac{\Delta R}{2} \quad (7-77) \end{aligned}$$

Equation (7-77) along with equations (7-73) and (7-74) for $k=1(1)n$ plus equation (7-75) and (7-76) for $k=0$ now constitute a set of $2n+3$ equations in the $2n+3$ unknowns $U_{j+1,k}$, $T_{j+1,k}$, and P_{j+1} for the constant temperature case. This set may be expressed in matrix form as

(7-78)

β_0	Ω_0		η_0	$U_{j+1,0}$	ϕ_0
α_1	β_1	Ω_1	η_1	$U_{j+1,1}$	ϕ_1
α_2	β_2	Ω_2	η_2	$U_{j+1,2}$	ϕ_2
			—	—	—
			—	—	—
	α_{n-1}	β_{n-1}	Ω_{n-1}	$U_{j+1,n-1}$	ϕ_{n-1}
		α_n	β_n	$U_{j+1,n}$	ϕ_n
				$T_{j+1,0}$	ϕ'_0
Ψ_1	$-\Psi_1$			$T_{j+1,1}$	ϕ'_1
Ψ_2	$-\Psi_2$			$T_{j+1,2}$	ϕ'_2
				—	—
				—	—
	Ψ_{n-1}	$-\Psi_{n-1}$		$T_{j+1,n-1}$	ϕ'_{n-1}
		Ψ_n	0	$T_{j+1,n}$	ϕ'_n
E_0	E_1	E_2	E_0	P_{j+1}	S
			E_{n-1}		
			E_n		
			E'_0		
			E'_1		
			E'_2		
			—		
			E'_{n-1}		
			E'_n		
			G		

where

$$\beta_0 = \frac{\rho_{j,0}^* U_{j,0}}{\Delta Z} + \frac{4\mu_{j,0}^*}{(\Delta R)^2}$$

$$\Omega_0 = \frac{-4\mu_{j,0}^*}{(\Delta R)^2}$$

$$\alpha_k = \frac{-\rho_{j,k}^* V_{j,k}}{2(\Delta R)} - \frac{\mu_{j,k}^*}{(\Delta R)^2} + \frac{\mu_{j,k}^*}{2(R_k)(\Delta R)} + \frac{\mu_{j,k+1}^* - \mu_{j,k-1}^*}{4(\Delta R)^2}$$

$$\beta_k = \frac{\rho_{j,k}^* U_{j,k}}{\Delta Z} + \frac{2\mu_{j,k}^*}{(\Delta R)^2} \quad (k > 0)$$

$$\Omega_k = \frac{\rho_{j,k}^* V_{j,k}}{2(\Delta R)} - \frac{\mu_{j,k}^*}{(\Delta R)^2} - \frac{\mu_{j,k}^*}{2(R_k)(\Delta R)} - \frac{\mu_{j,k+1}^* - \mu_{j,k-1}^*}{4(\Delta R)^2} \quad (k > 0)$$

$$\eta_k = \frac{1}{\gamma M_0^2 (\Delta Z)}$$

$$\phi_k = \frac{P_j}{\gamma M_0^2 (\Delta Z)} + \frac{\rho_{j,k}^* U_{j,k}^2}{\Delta Z}$$

$$\beta'_0 = \frac{\rho_{j,0}^* U_{j,0}}{\Delta Z} + \frac{4k_{j,0}^*}{(Pr)(\Delta R)^2}$$

$$\Omega'_0 = \frac{-4k_{j,0}^*}{(Pr)(\Delta R)^2}$$

$$\alpha'_k = \frac{-\rho_{j,k}^* V_{j,k}}{2(\Delta R)} - \frac{k_{j,k}^*}{(Pr)(\Delta R)^2} + \frac{k_{j,k}^*}{2R'_k(\Delta R)(Pr)} + \frac{k_{j,k+1}^* - k_{j,k-1}^*}{4(Pr)(\Delta R)^2}$$

$$\beta'_k = \frac{\rho_{j,k}^* U_{j,k}}{\Delta Z} + \frac{2k_{j,k}^*}{Pr(\Delta R)^2} \quad (k > 0)$$

$$\Omega'_k = \frac{\rho_{j,k}^* V_{j,k}}{2(\Delta R)} - \frac{k_{j,k}^*}{(Pr)(\Delta R)^2} - \frac{k_{j,k}^*}{2R'_k(\Delta R)(Pr)} - \frac{k_{j,k+1}^* - k_{j,k-1}^*}{4(Pr)(\Delta R)^2} \quad (k > 0)$$

$$\Psi'_k = (1-\gamma)M_0^2 \mu_{j,k}^* \left[\frac{U_{j,k+1} - U_{j,k-1}}{4(\Delta R)^2} \right]$$

$$\eta'_k = \frac{(1-\gamma)U_{j,k}}{\gamma(\Delta Z)}$$

$$\phi'_k = \frac{(1-\gamma)U_{j,k}}{\gamma(\Delta Z)} + \frac{\rho_{j,k}^* U_{j,k} T_{j,k}}{\Delta Z}$$

$$E_0 = \frac{R_1 \rho_{j,0}^* (\Delta R)}{4}$$

$$E_k = \left(\frac{R_k + R_{k+1}}{2} \right) \rho_{j,k}^* (\Delta R) \quad (k > 0)$$

$$E'_0 = \frac{-R_1 \rho_{j,0}^* U_{j,0} (\Delta R)}{4(T_{j,0})}$$

$$E'_k = - \left(\frac{R_k + R_{k+1}}{2} \right) \frac{\rho_{j,k}^* U_{j,k} (\Delta R)}{T_{j,k}} \quad (k > 0)$$

$$G = \sum_{k=0}^n \left(\frac{R_k + R_{k+1}}{2} \right) (\rho_{j,k+1}^* U_{j,k+1} + \rho_{j,k}^* U_{j,k}) \frac{(\Delta R)}{2P_j}$$

$$S = \sum_{k=0}^n \left(\frac{R_k + R_{k+1}}{2} \right) (\rho_{j,k+1}^* U_{j,k+1} + \rho_{j,k}^* U_{j,k}) \frac{(\Delta R)}{2}$$

For the constant wall heat flux case, $T_{j+1, n+1}$ is also unknown. The necessary additional relationship is the heat flux condition at the wall. In finite difference form this is

$$k_{j, n+1}^* \left(\frac{3T_{j+1, n+1} - 4T_{j+1, n} + T_{j+1, n-1}}{2(\Delta R)} \right) = \frac{qa}{k_0 t_0} \quad (7-79)$$

As in the parallel plate channel case, the use of $k_{j, n+1}^*$ is to ensure linearity of the difference equations. The error induced should be relatively small if the mesh size in the Z -direction is kept small.

The equation (7-79) increases the size of the matrix equation by one, and the resulting matrix is

β_0	Ω_0	η_0	$U_{j+1,0}$	ϕ_0
α_1	β_1	η_1	$U_{j+1,1}$	ϕ_1
α_2	β_2	η_2	$U_{j+1,2}$	ϕ_2
		—	—	—
		—	—	—
	α_{n-1}	β_{n-1}	$U_{j+1,n-1}$	ϕ_{n-1}
		α_n	$U_{j+1,n}$	ϕ_n
			\times	$=$
Ψ_1	$-\Psi_1$	β'_0	$T_{j+1,0}$	ϕ'_0
		α'_1	$T_{j+1,1}$	ϕ'_1
Ψ_2	$-\Psi_2$	α'_2	$T_{j+1,2}$	ϕ'_2
		—	—	—
		—	—	—
	Ψ_{n-1}	$-\Psi_{n-1}$	$T_{j+1,n-1}$	ϕ'_{n-1}
		Ψ_n	$T_{j+1,n}$	ϕ'_n
E_0	E_1	E_2	$T_{j+1,n+1}$	Q
			P_{j+1}	S

(7-80)

where all symbols are as defined with equation (7-78) except

$$Q = \frac{2qa(\Delta R)}{k_{j, n+1}^* k_0 t_0}$$

Any standard matrix inversion or equation solving routine such as that given in appendix E may be used to solve the set (7-78) or (7-80). As mentioned many times before, a refined mesh near the wall is of considerable value (see appendix D).

As in the parallel plate channel case, difficulty will be encountered when the average Mach number in the channel nears 1. For a detailed discussion see section 6.1.4 and Walker (ref. 6). Walker has shown that these equations are stable for all $U \geq 0$ (except possibly $M = 1$) and for all mesh sizes.

The truncation error is of $\mathcal{O}(\Delta Z)$ and $\mathcal{O}((\Delta R)^2)$ for momentum and energy and of $\mathcal{O}(\Delta Z)$ and $\mathcal{O}(\Delta R)$ for continuity. For a discussion of the error inherent in flow rate for confined flow problems, see appendix C.

7.1.5 Compressible Flow—Heat Transfer Solution

The heat transfer formulation for the circular tube is virtually identical to that for the parallel plate channel presented in section 6.1.5, so only the differences and final results are presented here.

The bulk temperature in the cylindrical geometry is given by

$$t_b = \frac{\int_0^a 2\pi r \rho u t dr}{\int_0^a 2\pi r \rho u dr} \quad (7-81)$$

or, in dimensionless form,

$$T_b = 2 \int_0^1 \rho^* R U T dR \quad (7-82)$$

The average Mach number is given by

$$M_{ave} = \frac{1}{\pi a^2} \int_0^a 2\pi r \frac{u}{\sqrt{\gamma \mathcal{R} t}} dr \quad (7-83)$$

or, in terms of dimensionless quantities,

$$M_{ave} = 2M_0 \int_0^1 \frac{RU}{\sqrt{T}} dR \quad (7-84)$$

From section 6.1.5 it is recalled that the adiabatic wall temperature is given by

$$t_{aw} = t_b \left[1 + \sqrt{Pr} \left(\frac{\gamma - 1}{2} \right) M_{ave}^2 \right] \quad (7-85)$$

or, in dimensionless form,

$$T_{aw} = T_b \left[1 + \sqrt{Pr} \left(\frac{\gamma - 1}{2} \right) M_{ave}^2 \right] \quad (7-86)$$

The dimensionless adiabatic wall temperature can now be expressed for the cylindrical geometry as

$$T_{aw} = \left(2 \int_0^1 \rho^* R U T dR \right) \left[1 + 2 \sqrt{Pr} (\gamma - 1) M_0^2 \left(\int_0^1 \frac{R U}{\sqrt{T}} dR \right)^2 \right] \quad (7-87)$$

The same expression derived for the local Nusselt number in chapter 6 also applies here. It is

$$Nu_z = \frac{2 \left. \frac{\partial T}{\partial R} \right|_{R=1}}{T_w - T_{aw}} \quad (7-88)$$

The value T_w is specified for the constant wall temperature case and obtained from the temperature solution for the constant heat flux case.

The finite difference form of equation (7-88) is

$$Nu_z \Big|_{j+1} = \frac{2(3T_{j+1, n+1} - 4T_{j+1, n} + T_{j+1, n-1})}{2(\Delta R)(T_{j+1, n+1} - T_{aw}|_{j+1})} \quad (7-89)$$

where $T_{aw}|_{j+1}$, obtained by putting equation (7-87) in difference form, is

$$\begin{aligned} T_{aw} \Big|_{j+1} = & \left[\frac{2(\Delta R)}{3} \right] \left(4 \sum_{k=1, 3, 5, 7, \dots}^n \rho_{j+1, k}^* R_k U_{j+1, k} T_{j+1, k} \right. \\ & \left. + 2 \sum_{k=2, 4, 6, 8, \dots}^{n-1} \rho_{j+1, k}^* R_k U_{j+1, k} T_{j+1, k} \right) \left\{ 1 + \frac{2\sqrt{Pr} (\gamma - 1) M_0^2 (\Delta R)^2}{9} \right. \\ & \left. \times \left[4 \sum_{k=1, 3, 5, 7, \dots}^n \frac{R_k U_{j+1, k}}{(T_{j+1, k})^{1/2}} + 2 \sum_{k=2, 4, 6, 8, \dots}^{n-1} \frac{R_k U_{j+1, k}}{(T_{j+1, k})^{1/2}} \right]^2 \right\} \quad (7-90) \end{aligned}$$

In equation (7-90), n must be odd.

As in the incompressible case, the mean Nusselt number is given by

$$Nu_m = \frac{1}{Z} \int_0^Z Nu_z dZ \quad (7-91)$$

or, in difference form,

$$Nu_m \Big|_{j+1} = \frac{1}{Z_{j+1}} \left(Nu_z \Big|_0 + 4 \sum_{i=1,3,5,7,\dots}^j Nu_z \Big|_i + 2 \sum_{i=2,4,6,8,\dots}^{j-1} Nu_z \Big|_i + Nu_z \Big|_{j+1} \right) \frac{\Delta Z}{3} \quad (7-92)$$

where $Nu_m \Big|_{j+1}$ is evaluated at every other ΔZ step, starting from the inlet.

7.2. OTHER PROBLEMS WITH A SIMILAR FORMULATION

7.2.1 Flow in Circular Tubes With Porous Walls

In order to accommodate the consideration of porous walls in the circular tube, it is only necessary to alter the boundary conditions and equations of constraint from those presented for the impermeable wall cases earlier in this chapter. There are also, of course, marked similarities to the parallel plate channel porous wall cases presented in section 6.2.1. Only the differences from already presented formulations and the final results will be presented. The configuration is shown in figure 7-3. The finite difference grid is identical to that shown in figure 7-2.

Hornbeck (ref. 4) and Hornbeck, Rouleau, and Osterle (ref. 3) have presented detailed formulations and solutions for the incompressible flow problem, and the present formulation for the incompressible case is based on these investigations.

Considering first the incompressible case, the formulation is as given in section 7.1.1 except that the boundary conditions (7-3) become

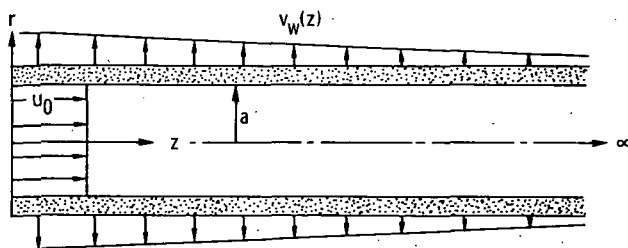


FIGURE 7-3.—Problem configuration and coordinate system for circular porous tube.

$$\left. \begin{aligned}
 u(r, 0) &= u_0 \text{ (see appendix F)} \\
 u(a, z) &= 0 \\
 \frac{\partial u}{\partial r}(0, z) &= 0 \\
 v(a, z) &= v_w(z) \\
 v(0, z) &= 0 \\
 p(0) &= p_0
 \end{aligned} \right\} \quad (7-93)$$

or, in dimensionless form,

$$\left. \begin{aligned}
 U(R, 0) &= 1 \\
 U(1, Z) &= 0 \\
 \frac{\partial U}{\partial R}(0, Z) &= 0 \\
 V(1, Z) &= V_w(Z) \\
 V(0, Z) &= 0
 \end{aligned} \right\} \quad (7-94)$$

The equation of constraint (7-14) in dimensionless finite difference form becomes, for the porous wall case,

$$\begin{aligned}
 \Delta R \left(\frac{1}{4} U_{j+1,0} + \frac{3}{4} U_{j+1,1} \right) + \sum_{k=2}^n R_k U_{j+1,k} &= \Delta R \left(\frac{1}{4} U_{j,0} + \frac{3}{4} U_{j,1} \right) \\
 &+ \sum_{k=2}^n R_k U_{j,k} - \frac{\Delta Z}{\Delta R} R_{n+1} V_{j+1,n+1} \quad (7-95)
 \end{aligned}$$

If $V_{j+1,n+1}$ is a specified function of Z , then the matrix equation (7-18) can be employed directly, with the only modification a redefinition of S in the right column vector to

$$S = \left(\frac{\Delta R}{4} \right) U_{j,0} + \frac{3(\Delta R)}{4} U_{j,1} + \sum_{k=2}^n R_k U_{j,k} - \frac{\Delta Z}{\Delta R} V_{j+1,n+1} \quad (7-96)$$

If $V_{j+1, n+1}$ is a function of pressure (e.g., through Darcy's law),

$$V_{j+1, n+1} = AP_{j+1} \tag{7-97}$$

then an additional coefficient must be added to the matrix in the upper right corner. The new matrix equation is

$\frac{\Delta R}{4}$	$\frac{3\Delta R}{4}$	R_2	R_3	—	—	—	R_{n-1}	R_n	$\frac{(\Delta Z)A}{\Delta R}$	$U_{j+1, 0}$	S	
β_0	Ω_0								$\frac{1}{\Delta Z}$	$U_{j+1, 1}$	ϕ_0	
α_1	β_1	Ω_1							$\frac{1}{\Delta Z}$	$U_{j+1, 2}$	ϕ_1	
	α_2	β_2	Ω_2						$\frac{1}{\Delta Z}$	$U_{j+1, 3}$	ϕ_2	
		α_3	β_3	Ω_3					$\frac{1}{\Delta Z}$	$U_{j+1, 4}$	ϕ_3	
			—	—	—				—	—	—	
				—	—	—			—	—	—	
					—	—			—	—	—	
							α_{n-1}	β_{n-1}	Ω_{n-1}	$\frac{1}{\Delta Z}$	$U_{j+1, n}$	ϕ_{n-1}
							α_n	β_n	$\frac{1}{\Delta Z}$	P_{j+1}	ϕ_n	

× $U_{j+1, 4} = \phi_3$

(7-98)

where all symbols are as defined with equation (7-18).
 The modifications to the compressible flow problem presented in section 7.1.4 are similar. The thermal boundary conditions are assumed unchanged, and the velocity and pressure boundary conditions (7-51) become

$$\left. \begin{aligned}
 \dot{u}(a, z) &= 0 \\
 u(r, 0) &= u_0 \\
 \frac{\partial u}{\partial r}(0, z) &= 0 \\
 v(a, z) &= v_w(z) \\
 v(0, z) &= 0 \\
 p(0) &= p_0
 \end{aligned} \right\} \quad (7-99)$$

or, in dimensionless form,

$$\left. \begin{aligned}
 U(1, z) &= 0 \\
 U(R, 0) &= 1 \\
 \frac{\partial U}{\partial R}(0, Z) &= 0 \\
 V(1, Z) &= V_w(Z) \\
 V(0, Z) &= 0 \\
 P(0) &= 1
 \end{aligned} \right\} \quad (7-100)$$

The equation of constraint (7-77), when modified to account for the porous wall effects, becomes

$$\begin{aligned}
 \sum_{k=0}^n \left(\frac{R_{k+1} + R_k}{2} \right) & \left[\rho_{j, k+1}^* U_{j+1, k+1} + \rho_{j, k}^* U_{j+1, k} + \rho_{j, k+1}^* U_{j, k+1} \left(\frac{P_{j+1}}{P_j} - \frac{T_{j+1, k+1}}{T_{j, k+1}} \right) \right. \\
 & \left. + \rho_{j, k}^* U_{j, k} \left(\frac{P_{j+1}}{P_j} - \frac{T_{j+1, k}}{T_{j, k}} \right) \right] \left(\frac{\Delta R}{2} \right) \\
 & + \frac{(\Delta Z) V_{j+1, n+1} P_{j+1}}{T_{j+1, n+1}} = \sum_{k=0}^n \left(\frac{R_{k+1} + R_k}{2} \right) \\
 & \times (\rho_{j, k+1}^* U_{j, k+1} + \rho_{j, k}^* U_{j, k}) \left(\frac{\Delta R}{2} \right) \quad (7-101)
 \end{aligned}$$

As was indicated in section 6.2.1, the only problem which can be readily considered here without sacrificing the linearity of the difference equations is the

specified suction or injection velocity and specified wall temperature case. For some suggestions on possible treatments of other boundary conditions, the reader is referred to that section. If $V_{j+1, n+1}(V_w(Z))$ and $T_{j+1, n+1}(T_w)$ are specified, then the only change in the formulation of section 7.1.4 is in the coefficient G in the matrix equation (7-78) which becomes

$$G = \left[\sum_{k=0}^n \left(\frac{R_k + R_{k+1}}{2} \right) (\rho_{j, k+1}^* U_{j, k+1} + \rho_{j, k}^* U_{j, k}) \right] \frac{\Delta R}{2P_j} + \frac{(\Delta Z)V_{j+1, n+1}}{T_{j+1, n+1}} \quad (7-102)$$

This completes the formulation for the porous wall case.

7.2.2 Developing Confined Free Convection Flow in a Circular Tube

The extensions of section 6.2.2 to a circular geometry are relatively straightforward. The problem configuration is shown in figure 7-4.

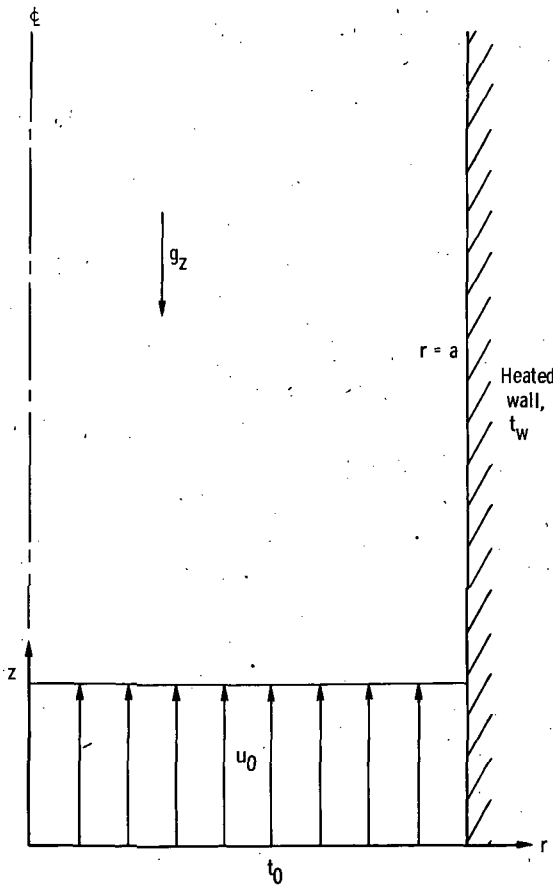


FIGURE 7-4. — Problem configuration and coordinate system for heated vertical circular tube.

The fundamental equations are

$$\rho \left(u \frac{\partial u}{\partial z} + v \frac{\partial u}{\partial r} \right) = \mu \left(\frac{\partial^2 u}{\partial r^2} + \frac{1}{r} \frac{\partial u}{\partial r} \right) - \frac{\partial p}{\partial x} + \rho g_z B (t - t_0) \quad (7-103)$$

$$\rho c_p \left(u \frac{\partial t}{\partial z} + v \frac{\partial t}{\partial r} \right) = k \left(\frac{\partial^2 t}{\partial r^2} + \frac{1}{r} \frac{\partial t}{\partial r} \right) \quad (7-104)$$

$$\frac{\partial u}{\partial z} + \frac{1}{r} \frac{\partial (vr)}{\partial r} = 0 \quad (7-105)$$

where p is the difference between true static and hydrostatic pressure, g_z the z -component of the acceleration due to gravity, and B the coefficient of volumetric expansion. The boundary conditions are

$$\left. \begin{aligned} u(r, 0) &= u_0 \\ u(a, z) &= 0 \\ \frac{\partial u}{\partial r}(0, z) &= 0 \\ v(0, z) &= 0 \\ v(a, z) &= 0 \\ t(a, z) &= t_w \\ t(r, 0) &= t_0 \\ \frac{\partial t}{\partial r}(0, z) &= 0 \\ p(0) &= 0 \end{aligned} \right\} \quad (7-106)$$

Using the dimensionless variables defined in (6-104) (of course substituting R for Y and Z for X), the fundamental equations and boundary conditions become in dimensionless form

$$U \frac{\partial U}{\partial Z} + V \frac{\partial U}{\partial R} = \frac{\partial^2 U}{\partial R^2} + \frac{1}{R} \frac{\partial U}{\partial R} - \frac{dP}{dZ} + T \quad (7-107)$$

$$U \frac{\partial T}{\partial Z} + V \frac{\partial T}{\partial R} = \frac{1}{Pr} \left(\frac{\partial^2 T}{\partial R^2} + \frac{1}{R} \frac{\partial T}{\partial R} \right) \quad (7-108)$$

$$\frac{\partial U}{\partial Z} + \frac{1}{R} \frac{\partial (VR)}{\partial R} = 0 \quad (7-109)$$

subject to

$$\left. \begin{aligned}
 U(R, 0) &= U_0 \\
 U(1, Z) &= 0 \\
 \frac{\partial U}{\partial R}(0, Z) &= 0 \\
 V(0, Z) &= 0 \\
 V(1, Z) &= 0 \\
 T(1, Z) &= 1 \\
 T(R, 0) &= 0 \\
 \frac{\partial T}{\partial R}(0, Z) &= 0 \\
 P(0) &= 0
 \end{aligned} \right\} \quad (7-110)$$

As in the parallel plate channel case the two parameters in the problem are the Prandtl number and U_0 . As indicated in section 6.2.2, this set of parameters actually results in a complete formulation for combined free and forced convection. The reader is referred to that section for details.

The finite difference grid employed is identical to that shown in figure 7-2. The finite difference form employed for equation (7-107) is

$$\begin{aligned}
 U_{j,k} \frac{U_{j+1,k} - U_{j,k}}{\Delta Z} + V_{j,k} \frac{U_{j+1,k+1} - U_{j+1,k-1}}{2(\Delta R)} \\
 = -\frac{P_{j+1} - P_j}{\Delta Z} + \frac{U_{j+1,k+1} - 2U_{j+1,k} + U_{j+1,k-1}}{(\Delta R)^2} \\
 + \frac{U_{j+1,k+1} - U_{j+1,k-1}}{2R_k(\Delta R)} + T_{j+1,k} \quad (k > 0) \quad (7-111)
 \end{aligned}$$

A separate form for $k=0$ may be readily obtained by letting $R \rightarrow 0$ in equation (7-107) and applying L'Hospital's rule as necessary. The resulting differential form is

$$U \left. \frac{\partial U}{\partial Z} \right|_{R=0} = -\frac{dP}{dZ} + 2 \left. \frac{\partial^2 U}{\partial R^2} \right|_{R=0} + T \left. \right|_{R=0} \quad (7-112)$$

or, in finite difference form, employing symmetry,

$$U_{j,0} \frac{U_{j+1,0} - U_{j,0}}{\Delta Z} = -\frac{P_{j+1} - P_j}{\Delta Z} + 4 \left(\frac{U_{j+1,1} - U_{j+1,0}}{(\Delta R)^2} \right) + T_{j+1,0} \quad (7-113)$$

The finite difference form for equation (7-108) is equation (7-25) for $k > 0$ and

equation (7-27) for $k=0$, while the finite difference form of equation (7-109) is (7-9) for $k > 0$ and (7-13) for $k=0$.

As indicated in the parallel plate channel discussion in section 6.2.2, the energy equation is solved first at each downstream step by solving the matrix equation (7-30), which is tridiagonal. The momentum equation is solved next. The matrix equation resulting from equation (7-111) written for $k=1(1)n$ and equation (7-113) for $k=0$, along with the equation of constraint (7-14), is identical to the matrix equation (7-18) except for the following change in the definition of ϕ_k :

$$\phi_k = \frac{U_{j,k}^2 + P_j}{\Delta Z} + T_{j+1,k} \quad (k \geq 0) \quad (7-114)$$

The continuity equation (7-9) for $k > 0$ and (7-13) for $k=0$ may now be solved for $V_{j+1,k+1}$ and another step taken downstream.

By analogy with section 6.2.2, it may be reasonably assumed that the solution is stable for all $U \geq 0$. The truncation error is the same as in all other confined flow cases considered in this chapter, $\mathcal{O}(\Delta Z)$ and $\mathcal{O}((\Delta R)^2)$ for momentum and energy and $\mathcal{O}(\Delta Z)$ and $\mathcal{O}(\Delta R)$ for continuity.

7.2.3 Flow in a Circular Tube With Body Forces

See section 6.2.3 and especially section 2.3.4 for discussions which apply equally well to the presently considered geometry.

7.2.4 Entrance Flow and Heat Transfer in a Concentric Annulus

In this section, we depart from the parallel treatment given the parallel plate channel and the circular tube through chapters 6 and 7. We consider a configuration unique to the circular geometry, the concentric annulus. The configuration is shown in figure 7-5.

Only the incompressible case is considered here, but the extension to compressible flow is straightforward, based on earlier sections of this chapter.

7.2.4.1 Incompressible constant property flow—velocity solution.—The fundamental equations are the same as those that apply to the circular tube (eqs. (7-1) and (7-2)). The boundary conditions are

$$\left. \begin{aligned} u(r, 0) &= u_0 \text{ (see appendix F)} \\ u(a, z) &= 0 \\ u(b, z) &= 0 \\ v(a, z) &= 0 \\ v(b, z) &= 0 \\ p(0) &= p_0 \end{aligned} \right\} \quad (7-115)$$

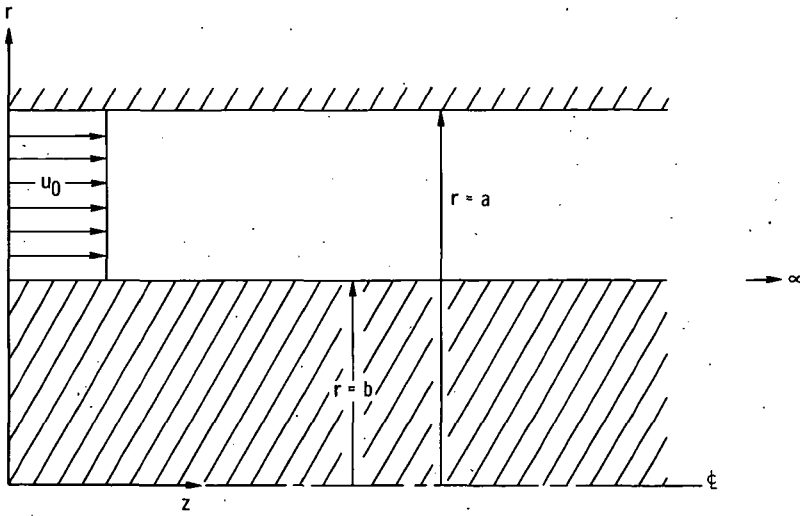


FIGURE 7-5.—Problem configuration and coordinate system for concentric annulus.

Employing the dimensionless variables (7-4), the complete problem may then be stated in dimensionless form as

$$U \frac{\partial U}{\partial Z} + V \frac{\partial U}{\partial R} = -\frac{dP}{dZ} + \frac{\partial^2 U}{\partial R^2} + \frac{1}{R} \frac{\partial U}{\partial R} \tag{7-116}$$

$$R \frac{\partial U}{\partial Z} + \frac{\partial(VR)}{\partial R} = 0. \tag{7-117}$$

$$\left. \begin{aligned} U(R, 0) &= 1 \\ U(1, Z) &= 0 \\ U\left(\frac{b}{a}, Z\right) &= 0 \\ V(1, Z) &= 0 \\ V\left(\frac{b}{a}, Z\right) &= 0 \\ P(0) &= 0 \end{aligned} \right\} \tag{7-118}$$

The finite difference grid employed is shown in figure 7-6.

The finite difference forms chosen for equations (7-116) and (7-117) are those used for the circular tube (eqs. (7-8) and (7-9)). No special version of the equations is necessary for $R=0$, since this point is never reached.

One unusual aspect of this problem is that the continuity equation (7-9) must be written at the inner wall ($k=0$) as well as at the interior points. It has not pre-

viously been necessary in our consideration of confined flow problems to write a difference equation at a solid-fluid interface. In all of these previous problems, however, there has been a line of symmetry at $k=0$, whereas the present problem possesses no such line of symmetry.

Adding together equation (7-9) written for $k=0(1)n$, we obtain the equation of constraint for this problem in the form

$$\sum_{k=1}^n R_k U_{j+1, k} = \sum_{k=1}^n R_k U_{j, k} \tag{7-119}$$

With finite difference equation (7-8) written for $k=1(1)n$ and the equation of constraint (7-119), we have a complete set of linear algebraic equations in

$$U_{j+1, 1}, \dots, U_{j+1, n} \text{ and } P_{j+1}.$$

The set may be written in matrix form as

$$\begin{pmatrix} R_1 & R_2 & R_3 & - & - & - & R_{n-1} & R_n & 0 \\ \beta_1 & \Omega_1 & & & & & & & \frac{1}{\Delta Z} \\ \alpha_2 & \beta_2 & \Omega_2 & & & & & & \frac{1}{\Delta Z} \\ & \alpha_3 & \beta_3 & \Omega_3 & & & & & \frac{1}{\Delta Z} \\ & & - & - & - & & & & \\ & & & - & - & - & & & \\ & & & & & & \alpha_{n-1} & \beta_{n-1} & \Omega_{n-1} & \frac{1}{\Delta Z} \\ & & & & & & \alpha_n & \beta_n & & \frac{1}{\Delta Z} \end{pmatrix} \times \begin{pmatrix} U_{j+1, 1} \\ U_{j+1, 2} \\ U_{j+1, 3} \\ U_{j+1, 4} \\ - \\ - \\ - \\ U_{j+1, n} \\ P_{j+1} \end{pmatrix} = \begin{pmatrix} S \\ \phi_1 \\ \phi_2 \\ \phi_3 \\ - \\ - \\ - \\ \phi_{n-1} \\ \phi_n \end{pmatrix} \tag{7-120}$$

where all symbols are as defined with the matrix equation (7-18), except that

$$S = \sum_{k=1}^n R_k U_{j, k}$$

Any standard method, such as that of appendix E, may be used to solve the set (7-119).

The difference form of the continuity equation (7-9) can now be used to find

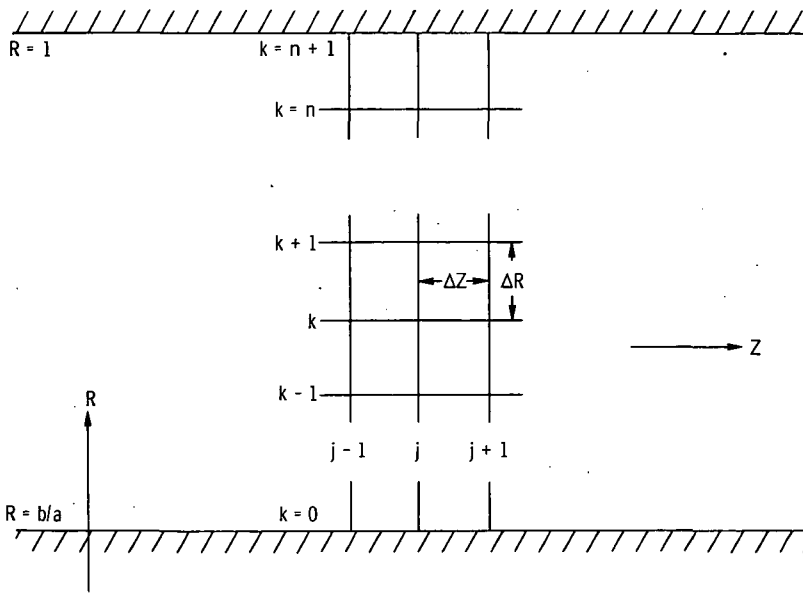


FIGURE 7-6.—Finite difference grid for concentric annulus.

$V_{j+1, k+1}$, working outward from the inside radius. Another step ΔZ downstream may now be taken and the process repeated.

It might be noted that since fine grid sizes are necessary near both walls, the complications introduced by changing mesh sizes twice in the radial direction may outweigh the gain in computing speed which using the variable mesh technique of appendix D usually provides. A uniform small mesh size over the entire radial span may thus be most convenient.

7.2.4.2 Incompressible constant property flow-temperature solution.—In order to avoid excessive complications because of the many combinations of thermal boundary conditions possible, we consider only the constant wall temperature case here, but allow the inner and outer walls to be at different temperatures, each also different from the inlet fluid temperature (assumed uniform). Other situations such as constant heat flux (possibly different on each wall), combinations of heat flux and temperature conditions, insulated walls, and variations involving axial dependence of the thermal conditions, all can be readily considered with a few minor changes.

The energy equation in the axially symmetric geometry is given by equation (7-20). The thermal boundary conditions are

$$\left. \begin{aligned} t(r, 0) &= t_0 \\ t(a, z) &= t_{ow} \\ t(b, z) &= t_{iw} \end{aligned} \right\} \quad (7-121)$$

We choose the following dimensionless variables:

and

$$\left. \begin{aligned} T &= \frac{t - t_0}{t_{0w} - t_0} \\ U &= \frac{u}{u_0} \\ V &= \frac{va}{\nu} \\ Z &= \frac{z\mu}{\rho a^2 u_0} \\ R &= \frac{r}{a} \end{aligned} \right\} \quad (7-122)$$

The complete problem in dimensionless form then becomes

$$U \frac{\partial T}{\partial Z} + V \frac{\partial T}{\partial R} = \frac{1}{Pr} \left(\frac{\partial^2 T}{\partial R^2} + \frac{1}{R} \frac{\partial T}{\partial R} \right) \quad (7-123)$$

$$T(R, 0) = 0$$

$$T(1, Z) = 1$$

$$T\left(\frac{b}{a}, Z\right) = \frac{t_{iw} - t_0}{t_{0w} - t_0} = T_{iw}$$

The finite difference form used for equation (7-123) is equation (7-25); and when equation (7-25) is written for $k=1(1)n$, the set becomes in matrix form

$$T_b \Big|_{j+1} = \frac{2(\Delta R)}{3[1 - (b/a)^2]} \left(\sum_{k=1, 3, 5, 7, 9, \dots}^n 4U_{j+1, k} R_k T_{j+1, k} + \sum_{k=2, 4, 6, 8, \dots}^{n-1} 2U_{j+1, k} R_k T_{j+1, k} \right) \quad (7-127)$$

where n must be odd.

The local heat transfer coefficient from the inside wall is

$$h_{iw}(t_{iw} - t_b) = -k \frac{\partial t}{\partial r} \Big|_{r=b} \quad (7-128)$$

and from the outside wall

$$h_{ow}(t_{ow} - t_b) = k \frac{\partial t}{\partial r} \Big|_{r=a} \quad (7-129)$$

The definition of local Nusselt numbers depends on the characteristic lengths chosen. Since the radius b is associated with the inside wall and a with the outside wall, we define the following:

$$Nu_{iz} = \frac{2h_{iw}b}{k} \quad (7-130)$$

and

$$Nu_{oz} = \frac{2h_{ow}a}{k} \quad (7-131)$$

Using the expressions (7-128) and (7-129), the Nusselt number expressions become

$$Nu_{iz} = \frac{-2 \frac{\partial t}{\partial r} \Big|_{r=b} (b)}{(t_{iw} - t_b)} \quad (7-132)$$

and

$$Nu_{oz} = \frac{2 \frac{\partial t}{\partial r} \Big|_{r=a} (a)}{(t_{ow} - t_b)} \quad (7-133)$$

or, in dimensionless terms,

$$Nu_{iz} = \frac{-2 \frac{b}{a} \frac{\partial T}{\partial R} \Big|_{R=b/a}}{T_{iw} - T_b} \quad (7-134)$$

and

$$Nu_{0z} = \frac{2 \frac{\partial T}{\partial R} \Big|_{R=1}}{T_{0w} - T_b} = \frac{2 \frac{\partial T}{\partial R} \Big|_{R=1}}{1 - T_b} \quad (7-135)$$

In finite difference form, these expressions are

$$Nu_{iz} \Big|_{j+1} = \frac{-2(b/a) \left[\frac{-3T_{j+1,0} + 4T_{j+1,1} - T_{j+1,2}}{2(\Delta R)} \right]}{T_{j+1,0} - T_b \Big|_{j+1}} \quad (7-136)$$

(note that $T_{j+1,0} = T_{iw}$) and

$$Nu_{0z} \Big|_{j+1} = \frac{2 \left[\frac{3T_{j+1,n+1} - 4T_{j+1,n} + T_{j+1,n-1}}{2(\Delta R)} \right]}{1 - T_b \Big|_{j+1}} \quad (7-137)$$

(note that $T_{j+1,n+1} = T_{0w} = 1$). The average values of these local Nusselt numbers may be readily obtained by using equation (7-44).

7.3 EXAMPLE PROBLEM—INCOMPRESSIBLE FLOW IN THE ENTRANCE REGION OF A CIRCULAR TUBE

The formulation of section 7.1.1 for the incompressible constant property velocity field has been solved by Hornbeck (ref. 2) and some of the results are presented here as an example.

The variable mesh technique discussed in appendix D was employed, with the radial mesh size $\Delta R = 0.1$ in the region $0 \leq R \leq 0.8$ and $\Delta R = 0.025$ for $0.8 < R \leq 1.0$. The axial mesh size was increased progressively from $\Delta Z = 2.5 \times 10^{-5}$ near the entrance to $\Delta Z = 1.0 \times 10^{-3}$ far downstream. The actual mesh sizes used in the various regions were $\Delta Z = 2.5 \times 10^{-5}$ in the region $0 \leq Z \leq 2.0 \times 10^{-4}$, $\Delta Z = 1.0 \times 10^{-4}$ in the region $2.0 \times 10^{-4} < Z \leq 1.0 \times 10^{-3}$, $\Delta Z = 5.0 \times 10^{-4}$ in the region $1.0 \times 10^{-3} < Z \leq 1.0 \times 10^{-2}$, and $\Delta Z = 1.0 \times 10^{-3}$ for $Z > 1.0 \times 10^{-2}$. These mesh sizes were established by extensive numerical experimentation.

Figure 7-7 shows the axial velocity development as a function of Z for various radial positions, and these results are presented in table 7-I.

In reference 2, comparisons of the numerical solution were made with the solutions of Campbell and Slattery (ref. 7) and Langhaar (ref. 8), both of which are solutions based essentially on integral techniques.

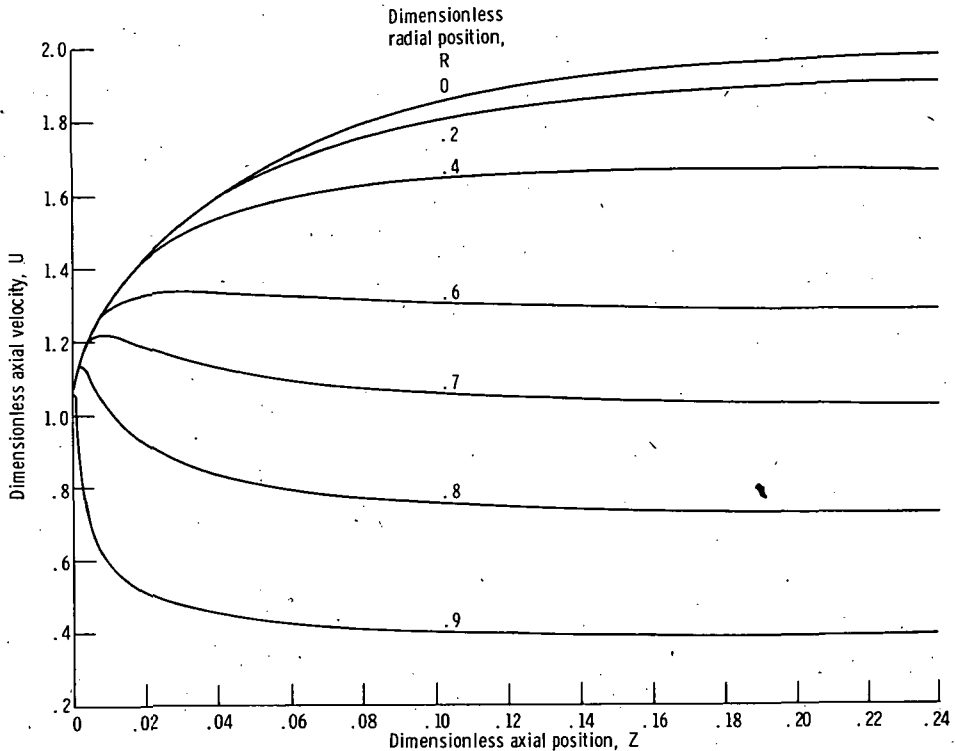


FIGURE 7-7.—Dimensionless axial velocity development for various dimensionless radial positions.

These comparisons are shown in figures 7-8 and 7-9. All three solutions yield virtually identical results for the pressure drop, shown in figure 7-8, but significant variations among the three solutions arise for the velocity results. The solution obtained by Langhaar was based on a linearized momentum equation, therefore the solution of Campbell and Slattery appears to be more accurate and is the main basis for comparison with the numerical solution. Almost all of the differences between the numerical solution and that of Campbell and Slattery can be attributed to the use of a two region model (flat central core and boundary layer) by Campbell and Slattery, whereas the present numerical solution uses a continuous model over the entire region. The two region model with a flat central core results in the centerline velocity (shown in fig. 7-9(a)) increasing less rapidly than the numerical solution, while for $R=0.6$ (shown in fig. 7-9(b)) the velocity increases more rapidly than the numerical result. At $R=0.9$ (shown in fig. 7-9(c)) the results are virtually identical since this radial position is within the boundary layer region of Campbell and Slattery's solution for almost the entire region.

TABLE 7-1. — DEVELOPMENT OF DIMENSIONLESS AXIAL VELOCITY FOR CIRCULAR TUBE

Dimensionless axial position, Z	Dimensionless radial position, R										Dimensionless pressure, P	
	0	0.1	0.2	0.3	0.4	0.5	0.6	0.7	0.8	0.9		1.0
	Dimensionless axial velocity, U											
0	1.0000	1.0000	1.0000	1.0000	1.0000	1.0000	1.0000	1.0000	1.0000	1.0000	1.0000	0
.002	1.1503	1.1503	1.1503	1.1503	1.1503	1.1503	1.1502	1.1485	1.1293	.8434	0	-.1610
.005	1.2269	1.2269	1.2269	1.2269	1.2268	1.2264	1.2230	1.2016	1.0950	.6893	0	-.2517
.010	1.3126	1.3126	1.3125	1.3124	1.3115	1.3068	1.2867	1.2144	1.0098	.5908	0	-.3602
.015	1.3782	1.3781	1.3779	1.3770	1.3733	1.3596	1.3160	1.2000	.9511	.5417	0	-.4480
.020	1.4332	1.4331	1.4324	1.4299	1.4214	1.3959	1.3292	1.1814	.9107	.5102	0	-.5253
.030	1.5239	1.5232	1.5204	1.5120	1.4902	1.4395	1.3349	1.1476	.8585	.4720	0	-.6606
.040	1.5977	1.5960	1.5893	1.5727	1.5358	1.4623	1.3308	1.1218	.8261	.4496	0	-.7805
.050	1.6595	1.6562	1.6448	1.6188	1.5675	1.4751	1.3245	1.1023	.8040	.4346	0	-.8911
.070	1.7555	1.7488	1.7269	1.6831	1.6073	1.4874	1.3125	1.0757	.7756	.4159	0	-1.0950
.090	1.8240	1.8142	1.7829	1.7244	1.6306	1.4927	1.3034	1.0588	.7584	.4047	0	-1.2846
.120	1.8920	1.8785	1.8366	1.7626	1.6509	1.4962	1.2943	1.0433	.7429	.3947	0	-1.5532
.160	1.9431	1.9266	1.8763	1.7901	1.6650	1.4981	1.2875	1.0321	.7319	.3877	0	-1.8947
.200	1.9698	1.9517	1.8969	1.8042	1.6721	1.4990	1.2840	1.0264	.7263	.3840	0	-2.2260
.250	1.9863	1.9672	1.9095	1.8128	1.6764	1.4996	1.2818	1.0229	.7229	.3818	0	-2.6344
∞	2.0000	1.9800	1.9200	1.8200	1.6800	1.5000	1.2800	1.0200	.7200	.3800	0

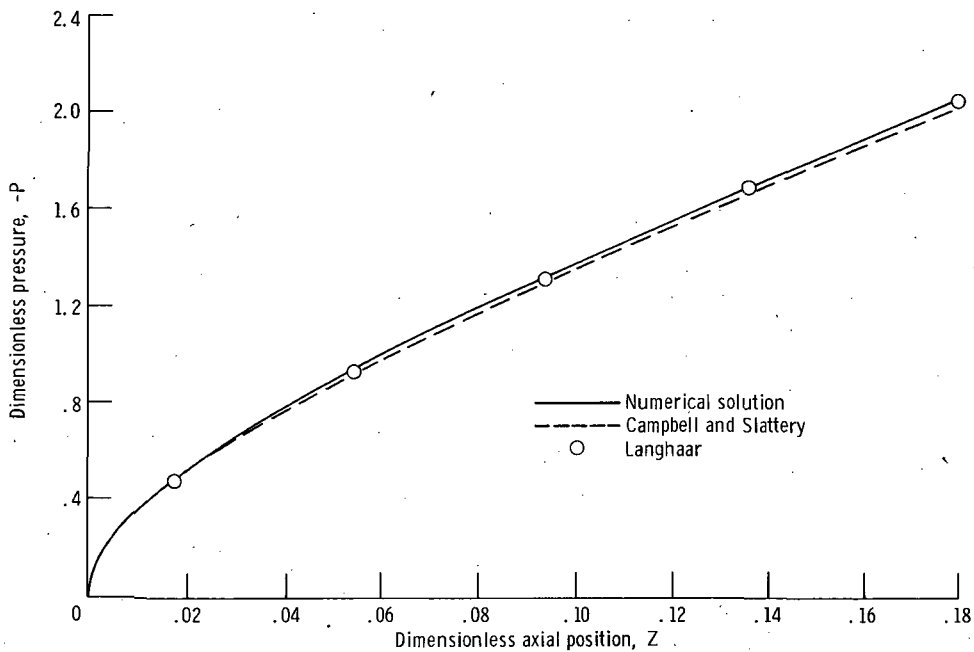
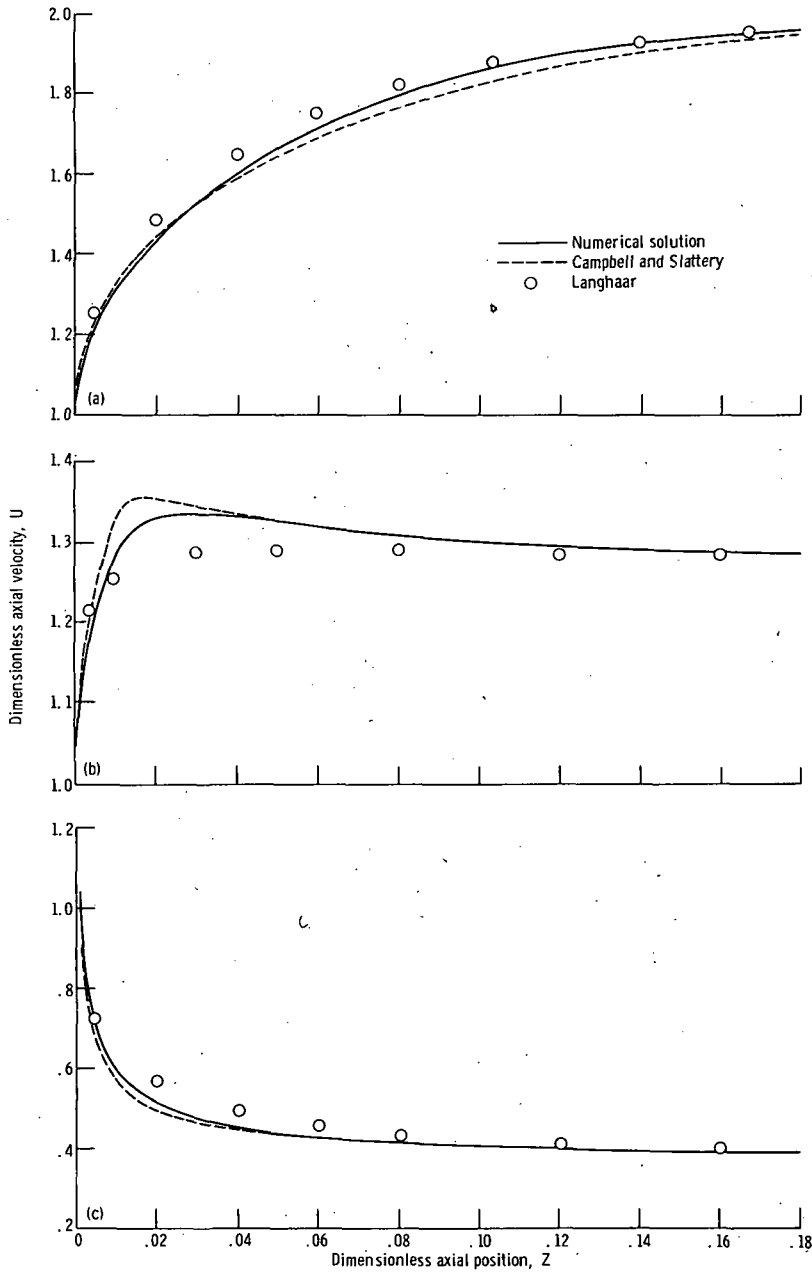


FIGURE 7-8.—Dimensionless pressure as function of dimensionless axial position.

Table 7-II shows a comparison of the results of all three solutions for the kinetic energy correction factor F_{ke} and the entrance length Z_e . The factor F_{ke} is defined as

$$F_{ke} = P_{fd} + \frac{1}{2} - 8Z \quad (7-138)$$

where P_{fd} is the dimensionless pressure sufficiently far downstream to assure that the flow is fully developed, and Z is the corresponding axial distance (see Goldstein, ref. 9). The entrance length Z_e is defined as the Z -coordinate at which the value of U on the tube centerline reaches 99 percent of its fully developed value of 2.0000. Despite the differences between the velocity profiles of Langhaar and the numerical solution shown in figure 7-9, the values of F_{ke} and Z_e for these two solutions are in excellent agreement. The longer development length found by Campbell and Slattery apparently reflects the slower velocity development at the centerline which results from the flat central core assumption.



(a) Radial position, $R = 0$.

(b) Radial position, $R = 0.6$.

(c) Radial position, $R = 0.9$.

FIGURE 7-9.—Dimensionless axial velocity as function of dimensionless axial position.

TABLE 7-II.—COMPARISONS OF DIMENSIONLESS ENTRANCE LENGTHS AND KINETIC ENERGY CORRECTION FACTORS FOR CIRCULAR TUBE

	Dimensionless entrance length, Z_e	Kinetic correction factor, F_{ke}
Numerical solution.....	0.226	1.140
Campbell and Slattery.....	.244	1.090
Langhaar.....	.227	1.140

REFERENCES

1. HORNBECK, ROBERT W.; ROULEAU, WILFRED T.; and OSTERLE, FLETCHER: Effect of Radial Momentum Flux on Flow in the Entrance of a Porous Tube. *J. Appl. Mech.*, vol. 32, no. 1, Mar. 1965, pp. 195-197.
2. HORNBECK, ROBERT W.: Laminar Flow in the Entrance Region of a Pipe. *Appl. Sci. Res., Sec. A*, vol. 13, 1963, pp. 224-232.
3. HORNBECK, ROBERT W.; ROULEAU, WILFRED T.; and OSTERLE, FLETCHER: Laminar Entry Problem in Porous Tubes. *Phys. Fluids*, vol. 6, no. 11, Nov. 1963, pp. 1649-1654.
4. HORNBECK, ROBERT W.: The Entry Problem in Pipes with Porous Walls. Ph.D. Thesis, Carnegie Inst. Tech., 1961.
5. HORNBECK, ROBERT W.: An All-Numerical Method for Heat Transfer in the Inlet of a Tube. Paper 65-WA/HT-36; ASME, Nov. 1965.
6. WALKER, M. L., Jr.: Laminar Compressible Flow in the Entrance Region of a Tube. Ph. D. Thesis. Carnegie Inst. Tech., 1965.
7. CAMPBELL, WILLIAM D.; and SLATTERY, JOHN C.: Flow in the Entrance of a Tube. *J. Basic Eng.*, vol. 85, no. 1, Mar. 1963, pp. 41-46.
8. LANGHAAR, HENRY L.: Steady Flow in the Transition Length of a Straight Tube. *J. Appl. Mech.*, vol. 9, no. 2, June 1942, pp. A55-A58.
9. GOLDSTEIN, SYDNEY, ED.: *Modern Developments in Fluid Dynamics*. Vol. 1. Dover Publ., 1965.

CHAPTER 8

RECTANGULAR CHANNEL

Flow and heat transfer in the entrance region of ducts of noncircular cross section presents a difficult three-dimensional problem. To the author's knowledge, only one entrance region fluid flow solution by finite difference methods is available, that of Carlson (ref. 1). This solution deals with the incompressible entrance flow in a square duct. A finite difference solution for the thermal entrance problem in rectangular ducts of arbitrary aspect ratio has been obtained by Montgomery and Wibuswas (ref. 2).

At present, to the best of the author's knowledge no solutions, by finite difference or otherwise, are available for the simultaneous development of velocity and temperature in the entrance of a noncircular channel (excepting of course the parallel plate channel). One of the most perplexing problems in the solution of noncircular channel entrance region problems is that the use of the usual order of magnitude analysis does not result in a usable and complete set of equations in the various unknowns. Since the available work on the rectangular channel illustrates these difficulties very well, we shall concentrate on this geometry in the present chapter.

8.1 ENTRANCE FLOW AND HEAT TRANSFER IN A RECTANGULAR CHANNEL

The channel configuration and coordinate system is shown in figure 8-1. Carlson (ref. 1) has shown that order of magnitude studies result in two distinct models for the fundamental equations of motion for the incompressible case. We shall first consider the formulations for these two models. It should be noted that actual results have been obtained only for the square channel, although the formulation for the arbitrary aspect ratio cases is discussed extensively.

Three representative heat transfer modes as suggested by Irvine (ref. 3) for the rectangular channel case are considered next, with the temperature formulations and then the heat transfer formulations given in that order for each of the three modes.

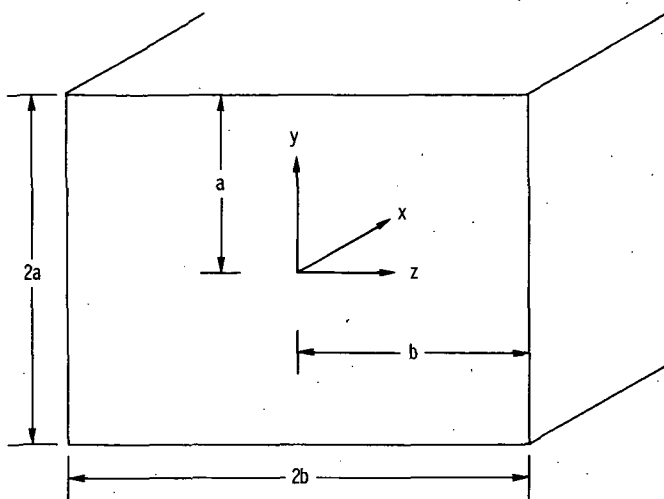


FIGURE 8-1.— Configuration and coordinate system for rectangular channel.

The final part of section 8.1 is devoted to a tentative formulation for the compressible flow in a rectangular channel.

8.1.1. Incompressible Constant Property Flow—Velocity Solution—First Model

The complete equations of motion for the rectangular channel, incorporating only the assumptions of laminar, incompressible, constant property flow, are as follows:

x—momentum:

$$\rho \left(u \frac{\partial u}{\partial x} + v \frac{\partial u}{\partial y} + w \frac{\partial u}{\partial z} \right) = - \frac{\partial p}{\partial x} + \mu \left(\frac{\partial^2 u}{\partial x^2} + \frac{\partial^2 u}{\partial y^2} + \frac{\partial^2 u}{\partial z^2} \right) \quad (8-1)$$

y—momentum:

$$\rho \left(u \frac{\partial v}{\partial x} + v \frac{\partial v}{\partial y} + w \frac{\partial v}{\partial z} \right) = - \frac{\partial p}{\partial y} + \mu \left(\frac{\partial^2 v}{\partial x^2} + \frac{\partial^2 v}{\partial y^2} + \frac{\partial^2 v}{\partial z^2} \right) \quad (8-2)$$

z—momentum:

$$\rho \left(u \frac{\partial w}{\partial x} + v \frac{\partial w}{\partial y} + w \frac{\partial w}{\partial z} \right) = - \frac{\partial p}{\partial z} + \mu \left(\frac{\partial^2 w}{\partial x^2} + \frac{\partial^2 w}{\partial y^2} + \frac{\partial^2 w}{\partial z^2} \right) \quad (8-3)$$

Continuity:

$$\frac{\partial u}{\partial x} + \frac{\partial v}{\partial y} + \frac{\partial w}{\partial z} = 0 \quad (8-4)$$

These equations are subject to the following complete boundary conditions:

$$u(x, a, z) = 0$$

$$u(x, y, b) = 0$$

$$\frac{\partial u}{\partial z}(x, y, 0) = 0$$

$$\frac{\partial u}{\partial y}(x, 0, z) = 0$$

$$v(x, y, b) = 0$$

$$v(x, a, z) = 0$$

$$\frac{\partial v}{\partial z}(x, y, 0) = 0$$

$$v(x, 0, z) = 0$$

$$w(x, a, z) = 0$$

$$w(x, y, b) = 0$$

$$\frac{\partial w}{\partial y}(x, 0, z) = 0$$

$$w(x, y, 0) = 0$$

$$\frac{\partial p}{\partial y}(x, 0, z) = 0$$

$$\frac{\partial p}{\partial z}(x, y, 0) = 0$$

$$u(0, y, z) = u_0$$

$$v(0, y, z) = 0 \text{ (see appendix F)}$$

$$w(0, y, z) = 0 \text{ (see appendix F)}$$

$$p(0, y, z) = p_0$$

(8-5)

An order of magnitude analysis, essentially that of Carlson (ref. 1), may now be applied to equations (8-1) to (8-4). If we denote l as the entrance length of the channel, then we assume the following orders of magnitude:

$$\left. \begin{aligned} x &= \mathcal{O}(l) \\ y &= \mathcal{O}(a) \\ z &= \mathcal{O}(b) \\ u &= \mathcal{O}(u_0) \end{aligned} \right\} \quad (8-6)$$

Applying these orders of magnitude to the continuity equation (8-4) gives

$$\mathcal{O}\left(\frac{u_0}{l}\right) + \mathcal{O}\left(\frac{v}{a}\right) + \mathcal{O}\left(\frac{w}{b}\right) = 0 \quad (8-7)$$

We now assume that $b = \mathcal{O}(a)$ —that is, that the duct has a finite aspect ratio and as a result $w = \mathcal{O}(v)$. Applying this information to (8-7) gives

$$\mathcal{O}(v) = \mathcal{O}\left(\frac{a}{l} u_0\right) \quad (8-8)$$

Inserting the relation (8-8) into the momentum equations (8-1) to (8-3), and indicating the order of magnitude of each term directly beneath that term, we obtain the following:

x-momentum:

$$\left. \begin{aligned} \rho \left(u \frac{\partial u}{\partial x} + v \frac{\partial u}{\partial y} + w \frac{\partial u}{\partial z} \right) &= -\frac{\partial p}{\partial x} + \mu \left(\frac{\partial^2 u}{\partial x^2} + \frac{\partial^2 u}{\partial y^2} + \frac{\partial^2 u}{\partial z^2} \right) \\ \mathcal{O}\left(\frac{\rho u_0^2}{l}\right) \mathcal{O}\left(\frac{\rho u_0^2}{l}\right) \mathcal{O}\left(\frac{\rho u_0^2}{l}\right) & \quad \mathcal{O}\left(\frac{\mu u_0}{l^2}\right) \mathcal{O}\left(\frac{\mu u_0}{a^2}\right) \mathcal{O}\left(\frac{\mu u_0}{a^2}\right) \end{aligned} \right\} \quad (8-9)$$

y-momentum:

$$\left. \begin{aligned} \rho \left(u \frac{\partial v}{\partial x} + v \frac{\partial v}{\partial y} + w \frac{\partial v}{\partial z} \right) &= -\frac{\partial p}{\partial y} + \mu \left(\frac{\partial^2 v}{\partial x^2} + \frac{\partial^2 v}{\partial y^2} + \frac{\partial^2 v}{\partial z^2} \right) \\ \mathcal{O}\left(\frac{\rho u_0^2 a}{l^2}\right) \mathcal{O}\left(\frac{\rho u_0^2 a}{l^2}\right) \mathcal{O}\left(\frac{\rho u_0^2 a}{l^2}\right) & \quad \mathcal{O}\left(\frac{\mu u_0 a}{l^3}\right) \mathcal{O}\left(\frac{\mu u_0}{al}\right) \mathcal{O}\left(\frac{\mu u_0}{al}\right) \end{aligned} \right\} \quad (8-10)$$

z -momentum:

$$\left. \begin{aligned} \rho \left(u \frac{\partial w}{\partial x} + v \frac{\partial w}{\partial y} + w \frac{\partial w}{\partial z} \right) &= -\frac{\partial p}{\partial z} + \mu \left(\frac{\partial^2 w}{\partial x^2} + \frac{\partial^2 w}{\partial y^2} + \frac{\partial^2 w}{\partial z^2} \right) \\ \mathcal{O} \left(\frac{\rho u_0^2 a}{l^2} \right) \mathcal{O} \left(\frac{\rho u_0^2 a}{l^2} \right) \mathcal{O} \left(\frac{\rho u_0^2 a}{l^2} \right) &\quad \mathcal{O} \left(\frac{\mu u_0 a}{l^3} \right) \mathcal{O} \left(\frac{\mu u_0}{al} \right) \mathcal{O} \left(\frac{\mu u_0}{al} \right) \end{aligned} \right\} \quad (8-11)$$

Assuming that we are considering the range of parameters where inertia effects are important ($\rho u_0 l / \mu \geq 1$) and that $(a/l) \ll 1$ which restricts the model to high Reynolds numbers, we note that all terms in equations (8-10) and (8-11) are $\mathcal{O}(a/l)$ or smaller compared to the terms in equation (8-9). Also, the term $\mu(\partial^2 u / \partial x^2)$ in equation (8-9) is of $\mathcal{O}(a^2/l^2)$ compared to the remainder of the terms in that equation. Neglecting all terms of $\mathcal{O}(a/l)$ or smaller compared to the terms of equation (8-9), we obtain

$$\rho \left(u \frac{\partial u}{\partial x} + v \frac{\partial u}{\partial y} + w \frac{\partial u}{\partial z} \right) = -\frac{dp}{dx} + \mu \left(\frac{\partial^2 u}{\partial y^2} + \frac{\partial^2 u}{\partial z^2} \right) \quad (8-12)$$

$$\frac{\partial u}{\partial x} + \frac{\partial v}{\partial y} + \frac{\partial w}{\partial z} = 0 \quad (8-13)$$

This model corresponds to the usual boundary layer assumptions that transverse momentum flux is small, that gradients in the x -direction are smaller than those in the y -direction, and the $p = p(x)$ only. This model has many advantages, but one serious drawback; it is incomplete. Equations (8-12) and (8-13) represent two equations in the three velocity components u , v , and w and are hence not solvable. (As in the parallel plate channel and circular tube cases considered in earlier chapters, p is not a true unknown in the same sense as u , v , and w since $p = p(x)$ only). An additional relation between v and w must be specified in order to have a complete set. Carlson (ref. 1) has proposed that for the square duct one possible choice is to assume that, at each point in the duct cross section, the transverse velocity vector is directed toward the duct centerline. Such a model must of course be verified, and this has also been done by Carlson by using a higher order approximation to equations (8-1) to (8-4) which does constitute a complete set. This higher order approximation is discussed in section 8.1.2.

The additional relation between v and w may be specified as

$$(v)(z) = (w)(y) \quad (8-14)$$

This relation guarantees that the transverse velocity vector will be directed toward the center of the duct. Although this relation has been verified only for the square duct, it is felt by the author that it may reasonably be extended to ducts of moderate

aspect ratio (say ≤ 4) although certainly not to large aspect ratios. A modification of this model may be possible which will be acceptable for large aspect ratios. Such a modification will be discussed after the present formulation is given.

Equations (8-1) to (8-4) may now be put in dimensionless form by employing the following dimensionless variables:

$$\begin{aligned} X &= \frac{\mu x}{\rho a^2 u_0} \\ Y &= \frac{y}{a} \\ Z &= \frac{z}{a} \\ U &= \frac{u}{u_0} \\ V &= \frac{\rho a v}{\mu} \\ W &= \frac{\rho a w}{\mu} \\ P &= \frac{(p - p_0)}{\rho u_0^2} \end{aligned} \quad (8-15)$$

Inserting these variables into equations (8-12) to (8-14) gives

$$U \frac{\partial U}{\partial X} + V \frac{\partial U}{\partial Y} + W \frac{\partial U}{\partial Z} = -\frac{dP}{dX} + \frac{\partial^2 U}{\partial Y^2} + \frac{\partial^2 U}{\partial Z^2} \quad (8-16)$$

$$\frac{\partial U}{\partial X} + \frac{\partial V}{\partial Y} + \frac{\partial W}{\partial Z} = 0 \quad (8-17)$$

$$VZ = WY \quad (8-18)$$

The boundary conditions from (8-5) in dimensionless form which apply to the present problem are

$$\begin{aligned}
 U(X, 1, Z) &= 0 \\
 U(X, Y, \sigma) &= 0 \\
 \frac{\partial U}{\partial Z}(X, Y, 0) &= 0 \\
 \frac{\partial U}{\partial Y}(X, 0, Z) &= 0 \\
 V(X, Y, \sigma) &= 0 \\
 V(X, 1, Z) &= 0 \\
 \frac{\partial V}{\partial Z}(X, Y, 0) &= 0 \\
 V(X, 0, Z) &= 0 \\
 W(X, 1, Z) &= 0 \\
 W(X, Y, \sigma) &= 0 \\
 \frac{\partial W}{\partial Y}(X, 0, Z) &= 0 \\
 W(X, Y, 0) &= 0 \\
 U(0, Y, Z) &= 1 \\
 P(0) &= 0
 \end{aligned} \tag{8-19}$$

where $\sigma = b/a$, the aspect ratio of the channel.

Before writing the basic equations in finite difference form, it is found advantageous, as in the other confined flow situations we have considered, to introduce the integral form of the continuity equation. In dimensional form this is

$$\int_0^b \int_0^a u \, dy \, dz = u_0 ab \tag{8-20}$$

or, in dimensionless form,

$$\int_0^\sigma \int_0^1 U \, dY \, dZ = \sigma \tag{8-21}$$

Equations (8-16) to (8-18) and equation (8-21) may now be written in finite difference form. The difference grid is shown in figure 8-2. We choose the following form:

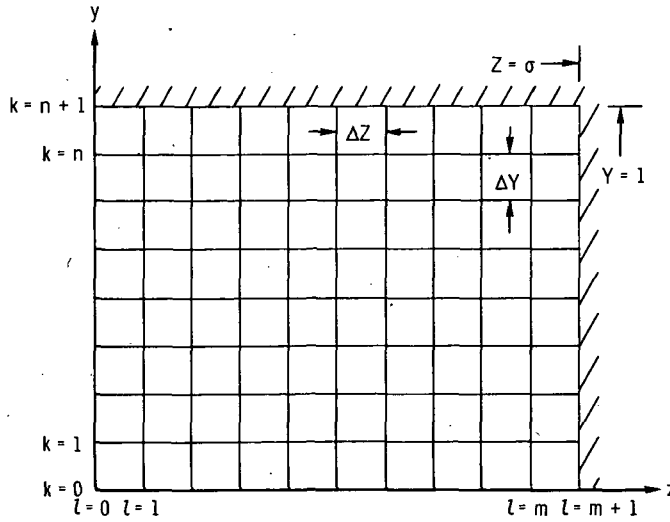


FIGURE 8-2.—Finite difference grid in rectangular channel cross section (for a constant value of j)

$$\begin{aligned}
 U_{j,k,l} \frac{U_{j+1,k,l} - U_{j,k,l}}{\Delta X} + V_{j,k,l} \frac{U_{j+1,k+1,l} - U_{j+1,k-1,l}}{2(\Delta Y)} \\
 + W_{j,k,l} \frac{U_{j+1,k,l+1} - U_{j+1,k,l-1}}{2(\Delta Z)} \\
 = -\frac{P_{j+1} - P_j}{\Delta X} + \frac{U_{j+1,k+1,l} - 2U_{j+1,k,l} + U_{j+1,k-1,l}}{(\Delta Y)^2} \\
 + \frac{U_{j+1,k,l+1} - 2U_{j+1,k,l} + U_{j+1,k,l-1}}{(\Delta Z)^2} \quad (8-22)
 \end{aligned}$$

$$\frac{U_{j+1,k,l} - U_{j,k,l}}{\Delta X} + \frac{V_{j+1,k+1,l} - V_{j+1,k,l}}{\Delta Y} + \frac{W_{j+1,k,l+1} - W_{j+1,k,l}}{\Delta Z} = 0 \quad (8-23)$$

$$V_{j+1,k,l} Z_l = W_{j+1,k,l} Y_k \quad (8-24)$$

and

$$\frac{4\sigma}{(\Delta Y)(\Delta Z)} = \sum_{k=1}^n \sum_{l=1}^m 4U_{j+1,k,l} + \sum_{l=1}^m 2U_{j+1,0,l} + \sum_{k=1}^n 2U_{j+1,k,0} + U_{j+1,0,0} \quad (8-25)$$

Equation (8-25) represents the application of the trapezoidal rule to equation (8-21).

Equations (8-22) to (8-24) written for $k = 0(1)n$ and $l = 0(1)m$ plus equation (8-25) now represent $(3mn + 1)$ equations in the $(3mn + 1)$ unknowns $U_{j+1,k,l}$, $V_{j+1,k,l}$, $W_{j+1,k,l}$, and P_{j+1} . For any reasonable grid size, the direct solution of

this set of equations' is out of the question because of the very large amounts of computer storage space and time required. For this reason, an iterative method, which is quite efficient, is employed. Equation (8-22) is solved for $U_{j+1,k,l}$ as

$$\begin{aligned}
 U_{j+1,k,l} = & \left\{ U_{j+1,k-1,l} \left[\frac{-V_{j,k,l}}{2(\Delta Y)} - \frac{1}{(\Delta Y)^2} \right] + U_{j+1,k+1,l} \left[\frac{V_{j,k,l}}{2(\Delta Y)} - \frac{1}{(\Delta Y)^2} \right] \right. \\
 & + U_{j+1,k,l-1} \left[\frac{-W_{j,k,l}}{2(\Delta Z)} - \frac{1}{(\Delta Z)^2} \right] + U_{j+1,k,l+1} \left[\frac{W_{j,k,l}}{2(\Delta Z)} - \frac{1}{(\Delta Z)^2} \right] \\
 & \left. + \frac{P_{j+1} - P_j - U_{j,k,l}^2}{\Delta X} \right\} / \left[\frac{-2}{(\Delta Z)^2} - \frac{2}{(\Delta Y)^2} - \frac{U_{j,k,l}}{\Delta X} \right] \quad (8-26)
 \end{aligned}$$

This equation is written for all $k=0(1)n$ and $l=0(1)m$ except $k=1, l=1$, where equation (8-22) is solved for P_{j+1} instead, yielding

$$\begin{aligned}
 P_{j+1} = & P_j + U_{j,1,1}^2 + \Delta X \left\{ U_{j+1,2,1} \left[-\frac{V_{j,1,1}}{2(\Delta Y)} + \frac{1}{(\Delta Y)^2} \right] \right. \\
 & + U_{j+1,0,1} \left[\frac{V_{j,1,1}}{2(\Delta Y)} + \frac{1}{(\Delta Y)^2} \right] \\
 & + U_{j+1,1,2} \left[\frac{-W_{j,1,1}}{2(\Delta Z)} + \frac{1}{(\Delta Z)^2} \right] \\
 & + U_{j+1,1,0} \left[\frac{W_{j,1,1}}{2(\Delta Z)} + \frac{1}{(\Delta Z)^2} \right] \\
 & \left. + U_{j+1,1,1} \left[\frac{-2}{(\Delta Z)^2} - \frac{2}{(\Delta Y)^2} - \frac{U_{j,1,1}}{\Delta X} \right] \right\} \quad (8-27)
 \end{aligned}$$

Equation (8-25) may now be solved for $U_{j+1,1,1}$ to yield

$$\begin{aligned}
 U_{j+1,1,1} = & \frac{\sigma}{(\Delta Y)(\Delta Z)} - \sum_{\substack{k=1 \\ (k \neq l \neq 1)}}^n \sum_{l=1}^m U_{j+1,k,l} \\
 & - \frac{1}{2} \sum_{l=1}^m U_{j+1,0,l} - \frac{1}{2} \sum_{k=1}^n U_{j+1,k,0} - \frac{1}{4} U_{j+1,0,0} \quad (8-28)
 \end{aligned}$$

Equations (8-26) to (8-28) now represent expressions for each value of $U_{j+1,k,l}$ in the cross section plus P_{j+1} . Guesses are now made for all of these quantities ($U_{j,k,l}$ and P_j usually provide excellent estimates), and they are then continuously recomputed in cyclic order over the entire cross section (Gauss-

Siedel iteration) until a sufficient degree of convergence is reached. This method of iteration converges only if equation (8-28) is drastically underrelaxed; a relaxation factor as small as $1/mn$ has been found necessary in practice.

Once the values of $U_{j+1,k,l}$ and P_{j+1} have been determined with sufficient accuracy, the transverse velocities must be found. The continuity equation (8-23) may first be solved for $V_{j+1,k,l}$. This is most easily accomplished by using equation (8-24) to find $W_{j+1,k,l}$ in terms of $V_{j+1,k,l}$ as

$$W_{j+1,k,l} = \frac{Z_l}{Y_k} V_{j+1,k,l} \quad (8-29)$$

Substituting this in continuity (eq. (8-23)) and solving for $V_{j+1,k,l}$ yield

$$V_{j+1,k,l} = \frac{\left[V_{j+1,k+1,l} + \frac{\Delta Y}{\Delta Z} W_{j+1,k,l+1} + \frac{\Delta Y}{\Delta X} (U_{j+1,k,l} - U_{j,k,l}) \right]}{\left(1 + \frac{(\Delta Y)Z_l}{(\Delta Z)Y_k} \right)} \quad (8-30)$$

This equation may now be employed in a stepwise manner, starting in the upper right corner ($Y=1, Z=\sigma$) and moving in the $-Z$ direction to $Z=0$, then moving down one step in the $-Y$ direction and repeating the process. As each new $V_{j+1,k,l}$ is computed, a $W_{j+1,k,l}$ may be found from equation (8-29). This procedure is carried down to and including $k=1$. For $k=0$ (the Z -axis), $V_{j+1,0,l}$ is zero, and continuity may be solved for $W_{j+1,0,l}$ to yield

$$W_{j+1,0,l} = W_{j+1,0,l+1} + \frac{\Delta Z}{\Delta Y} V_{j+1,1,l} + \frac{\Delta Z}{\Delta X} (U_{j+1,0,l} - U_{j,0,l}) \quad (8-31)$$

This equation can be solved in a stepwise manner starting at $l=m$ and moving in the $-Z$ direction. All transverse velocity components have now been computed, and the solution completed at the present value of X . An additional step downstream can now be taken and the process repeated.

It should be noted that the use of the variable mesh technique discussed in appendix D is highly recommended for this problem to cut down on the number of points in the cross section and still maintain reasonable accuracy. The technique is somewhat cumbersome (as shown in fig. 8-3), however, since four different regions with different mesh sizes are necessary and the corresponding difficulties with bridging the mesh size changes arise.

It was noted earlier in this chapter that a possible adaptation could be made to the present model to make it reasonably valid for high aspect ratios. In figure 8-4 is shown the cross section of a high aspect ratio channel with the direction (but not magnitude) of a postulated transverse velocity distribution indicated. The end effects are assumed to penetrate to one-half of the channel height, and the remainder of the channel is assumed to behave like a parallel plate channel, with

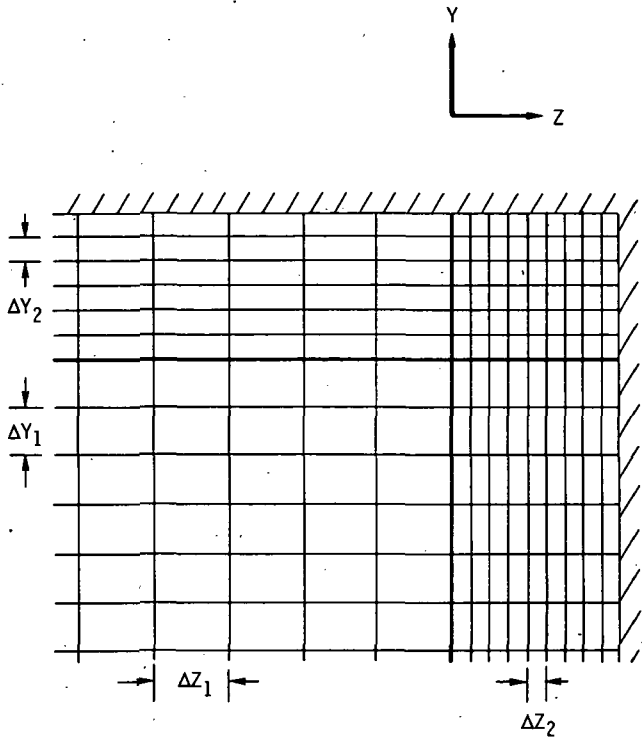


FIGURE 8-3.—Four regions which result when two different mesh sizes are employed in each of the two transverse directions.

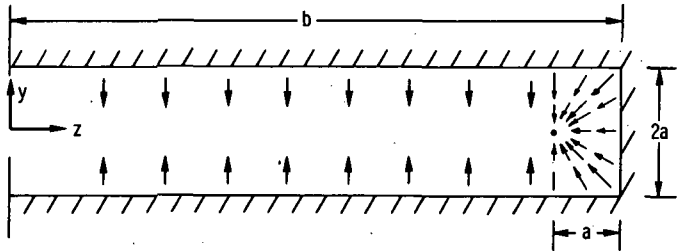


FIGURE 8-4.—Possible model for direction of transverse velocity vectors in a cross section for high aspect ratio channel.

the transverse velocity components in the Y -direction only. Near the sides of the channel, the transverse velocity vectors are assumed to be directed toward a point along the midplane of the channel and a distance a in from the sides. While such a transverse distribution seems to be reasonably plausible, such an assumption can only be verified by further analytical (including higher order approximations) or experimental verification. In defense of such a model, the influence of the transverse velocity distribution on the axial velocity distribution and pressure drop does appear to be relatively weak except very close to the channel entrance.

Carlson (ref. 1) found that for the square duct the incompressible equations are stable for all $U \geq 0$. This result also presumably applies to the rectangular duct of arbitrary aspect ratio.

The truncation error is of $\mathcal{O}(\Delta X)$, $\mathcal{O}((\Delta Y)^2)$, and $\mathcal{O}((\Delta Z)^2)$ for the momentum equation and of $\mathcal{O}(\Delta X)$, $\mathcal{O}(\Delta Y)$, and $\mathcal{O}(\Delta Z)$ for continuity.

8.1.2 Incompressible Constant Property Flow—Velocity Solution—Second Model

To obtain a higher order approximation to the fundamental equations for the rectangular channel, we consider again the orders of magnitude shown in equations (8-9) to (8-11). In the previous model, we neglected terms of $\mathcal{O}(a/l)$ compared to the terms of equation (8-9). Remembering that $a/l \ll 1$, we should obtain a higher order approximation by neglecting only terms of $\mathcal{O}(a^2/l^2)$ when compared to the terms in equation (8-9). Neglecting these terms gives

$$\rho \left(u \frac{\partial u}{\partial x} + v \frac{\partial u}{\partial y} + w \frac{\partial u}{\partial z} \right) = -\frac{\partial p}{\partial x} + \mu \left(\frac{\partial^2 u}{\partial y^2} + \frac{\partial^2 u}{\partial z^2} \right) \quad (8-32)$$

$$\rho \left(u \frac{\partial v}{\partial x} + v \frac{\partial v}{\partial y} + w \frac{\partial v}{\partial z} \right) = -\frac{\partial p}{\partial y} + \mu \left(\frac{\partial^2 v}{\partial y^2} + \frac{\partial^2 v}{\partial z^2} \right) \quad (8-33)$$

$$\rho \left(u \frac{\partial w}{\partial x} + v \frac{\partial w}{\partial y} + w \frac{\partial w}{\partial z} \right) = -\frac{\partial p}{\partial z} + \mu \left(\frac{\partial^2 w}{\partial y^2} + \frac{\partial^2 w}{\partial z^2} \right) \quad (8-34)$$

$$\frac{\partial u}{\partial x} + \frac{\partial v}{\partial y} + \frac{\partial w}{\partial z} = 0 \quad (8-35)$$

Note that only terms involving $\partial^2/\partial x^2$ are missing from these equations. The absence of these terms, however, is fortunately sufficient to maintain the parabolic character of the equations. The other fortunate aspect of this model is that equations (8-32) to (8-35) constitute a complete set of four differential equations in the four unknowns u , v , w , and p .

If the dimensionless variables (8-15) are employed, equations (8-32) to (8-35) become

$$U \frac{\partial U}{\partial X} + V \frac{\partial U}{\partial Y} + W \frac{\partial U}{\partial Z} = -\frac{\partial P}{\partial X} + \frac{\partial^2 U}{\partial Y^2} + \frac{\partial^2 U}{\partial Z^2} \quad (8-36)$$

$$U \frac{\partial V}{\partial X} + V \frac{\partial V}{\partial Y} + W \frac{\partial V}{\partial Z} = -\frac{\partial P}{\partial Y} (Re)^2 + \frac{\partial^2 V}{\partial Y^2} + \frac{\partial^2 V}{\partial Z^2} \quad (8-37)$$

$$U \frac{\partial W}{\partial X} + V \frac{\partial W}{\partial Y} + W \frac{\partial W}{\partial Z} = -\frac{\partial P}{\partial Z} (Re)^2 + \frac{\partial^2 W}{\partial Y^2} + \frac{\partial^2 W}{\partial Z^2} \quad (8-38)$$

$$\frac{\partial U}{\partial X} + \frac{\partial V}{\partial Y} + \frac{\partial W}{\partial Z} = 0 \quad (8-39)$$

where $Re = \rho au_0/\mu$. This additional parameter Re did not appear in the first model discussed in the previous section.

The difference representations chosen for equations (8-36) to (8-39) are

$$\begin{aligned}
 U_{j,k,l} \frac{U_{j+1,k,l} - U_{j,k,l}}{\Delta X} + V_{j,k,l} \frac{U_{j+1,k+1,l} - U_{j+1,k-1,l}}{2(\Delta Y)} \\
 + W_{j,k,l} \frac{U_{j+1,k,l+1} - U_{j+1,k,l-1}}{2(\Delta Z)} = - \frac{P_{j+1,k,l} - P_{j,k,l}}{\Delta X} \\
 + \frac{U_{j+1,k+1,l} - 2U_{j+1,k,l} + U_{j+1,k-1,l}}{(\Delta Y)^2} + \frac{U_{j+1,k,l+1} - 2U_{j+1,k,l} + U_{j+1,k,l-1}}{(\Delta Z)^2} \quad (8-40)
 \end{aligned}$$

$$\begin{aligned}
 U_{j,k,l} \frac{V_{j+1,k,l} - V_{j,k,l}}{\Delta X} + V_{j,k,l} \frac{V_{j+1,k+1,l} - V_{j+1,k-1,l}}{2(\Delta Y)} \\
 + W_{j,k,l} \frac{V_{j+1,k,l+1} - V_{j+1,k,l-1}}{2(\Delta Z)} = - (Re)^2 \frac{P_{j+1,k+1,l} + P_{j+1,k,l} - 2P_{j+1,k-1,l}}{3(\Delta Y)} \\
 + \frac{V_{j+1,k+1,l} - 2V_{j+1,k,l} + V_{j+1,k-1,l}}{(\Delta Y)^2} + \frac{V_{j+1,k,l+1} - 2V_{j+1,k,l} + V_{j+1,k,l-1}}{(\Delta Z)^2} \quad (8-41)
 \end{aligned}$$

$$\begin{aligned}
 U_{j,k,l} \frac{W_{j+1,k,l} - W_{j,k,l}}{\Delta X} + V_{j,k,l} \frac{W_{j+1,k+1,l} - W_{j+1,k-1,l}}{2(\Delta Y)} \\
 + W_{j,k,l} \frac{W_{j+1,k,l+1} - W_{j+1,k,l-1}}{2(\Delta Z)} = - (Re)^2 \frac{P_{j+1,k,l+1} + P_{j+1,k,l} - 2P_{j+1,k,l-1}}{3(\Delta Z)} \\
 + \frac{W_{j+1,k+1,l} - 2W_{j+1,k,l} + W_{j+1,k-1,l}}{(\Delta Y)^2} \\
 + \frac{W_{j+1,k,l+1} - 2W_{j+1,k,l} + W_{j+1,k,l-1}}{(\Delta Z)^2} \quad (8-42)
 \end{aligned}$$

$$\frac{U_{j+1,k,l} - U_{j,k,l}}{\Delta X} + \frac{V_{j+1,k+1,l} - V_{j+1,k,l}}{\Delta Y} + \frac{W_{j+1,k,l+1} - W_{j+1,k,l}}{\Delta Z} = 0 \quad (8-43)$$

The form chosen for $\partial P/\partial Y$ and $\partial P/\partial Z$ is dictated by the previous experience of the author with similar problems (ref. 4) in which it was found that the usual central difference representations could give sawtooth irregularities in the pressure profile unless very small mesh sizes were used. These irregularities are apparently due to the usual central difference representation not including the center point ($P_{j,k,l}$); therefore, when the difference equations are written there is only indirect coupling between the pressures at adjacent points, while there is direct coupling between pressures at alternate points. The form employed to overcome this difficulty consists simply of a biased average of forward and backward differences, one-third forward and two-thirds backward. This form has a truncation error

somewhat worse than a central difference representation, but it does bring the central point $P_{j,k,l}$ into the difference representations.

Along $k=0$, equation (8-37) reduces to

$$\frac{\partial P}{\partial Y} = 0 \quad (8-44)$$

which we chose to write in a high order difference form ($\mathcal{O}(\Delta Y)^2$) as

$$3P_{j+1,0,l} - 4P_{j+1,1,l} + P_{j+1,2,l} = 0 \quad (8-45)$$

Similarly, along $l=0$, equation (8-38) becomes

$$\frac{\partial P}{\partial Z} = 0 \quad (8-46)$$

which may be written in finite difference form as

$$3P_{j+1,k,0} - 4P_{j+1,k,1} + P_{j+1,k,2} = 0 \quad (8-47)$$

The X -momentum equation (8-40) written for all interior points $k=0(1)n$, $l=0(1)m$; the Y -momentum equation (8-41) written for $k=1(1)n$, $l=0(1)m$ with the special version (8-45) along the Z -axis $l=0(1)m$; the Z -momentum equation (8-42) written for $k=0(1)n$, $l=1(1)m$ with the special version (8-47) along the Y -axis $k=0(1)n$; and the continuity equation (8-43) written for all the interior points $k=0(1)n$, $l=0(1)m$ constitute a complete set of $4(m+1)(n+1)$ equations in the $4(m+1)(n+1)$ unknowns $U_{j+1,k,l}$, $V_{j+1,k,l}$, $W_{j+1,k,l}$, and $P_{j+1,k,l}$. The solution to such a large and varied set of equations must of necessity be more of an art than a science, and it will, therefore, involve considerable trial and error. Since to the author's knowledge this set of equations for an arbitrary aspect ratio has not been solved as yet, no direct advice can be given. However, the set of equations corresponding to a square duct has been solved (ref. 1) by taking advantage of the symmetry in the square duct. This solution should furnish information on the approach to the solution for a duct of arbitrary aspect ratio.

The solution for the square duct may be described briefly as follows: The $4(m+1)(n+1)$ equations become for the square duct $3(n+1)^2$ since equation (8-41) for $(j+1, k, l)$ is the same as equation (8-42) for $(j+1, l, k)$, and the number of unknowns is correspondingly reduced since $V_{j+1,k,l} = W_{j+1,l,k}$. Hence, equation (8-42) need not be written if $W_{j,k,l}$ and $W_{j+1,k,l}$ are replaced in the remaining equations by $V_{j,l,k}$ and $V_{j+1,l,k}$. Additional symmetry could be employed across the duct diagonal to reduce the number of $U_{j+1,k,l}$'s. However, specifying normal derivatives across the diagonal is somewhat cumbersome, and the fact that the $U_{j+1,k,l}$ profile as computed should be symmetric furnishes a "bootstrap" check.

The equations which are solved for the various unknowns are the following:

Equation (8-40) for $U_{j+1,k,l}$ for all k, l except $k=0$

Equation (8-43) for $U_{j+1,0,l}$ for all l

Equation (8-43) for $V_{j+1,k,l}$ for all k, l except $k=0$

Equation (8-41) for $P_{j+1,k+1,l}$ for all k, l

Equation (8-45) for $P_{j+1,0,l}$ for all l

All of these equations may be solved by Gauss-Siedel iteration except equation (8-43) for $V_{j+1,k,l}$. This equation must be severely underrelaxed. An alternative employed by Carlson was to determine the change in $V_{j+1,k,l}$ for each iteration by taking the average of the residuals of the equations at the four points surrounding $(j+1, k, l)$.

The use of a set of equations as complex as these is obviously a last resort; these equations should be employed only if a simpler model (perhaps similar to that suggested at the end of section 8.1.1) cannot be found which gives good results.

A complete stability analysis of such a set of equations is extremely difficult to obtain. The only information available is based on some "numerical experiments" by Carlson for the square duct. It is apparently impossible to simultaneously consider a small value of ΔX and a small value of Re . This means in practice that in general it is not possible to find accurate solutions for low values of Re (say less than about 500). For a Reynolds number $Re=650$, Carlson found that a value of $\Delta X=0.0025$ (quite coarse) was the minimum possible value which gave what appeared to be stable results.

The truncation error of the equations is of $\mathcal{O}(\Delta X)$, $\mathcal{O}((\Delta Y)^2)$, and $\mathcal{O}((\Delta Z)^2)$ for the three momentum equations (except for the pressure difference representations which are $\mathcal{O}(\Delta Y)$ and $\mathcal{O}(\Delta Z)$) and $\mathcal{O}(\Delta X)$, $\mathcal{O}(\Delta Y)$, and $\mathcal{O}(\Delta Z)$ for continuity.

8.1.3 Incompressible Constant Property Flow – Temperature and Heat Transfer Solutions

Once the velocity distributions have been determined, the energy equation can be considered. The constant property energy equation, neglecting axial conduction and viscous dissipation, is

$$\rho c_p \left(u \frac{\partial t}{\partial x} + v \frac{\partial t}{\partial y} + w \frac{\partial t}{\partial z} \right) = k \left(\frac{\partial^2 t}{\partial y^2} + \frac{\partial^2 t}{\partial z^2} \right) \quad (8-48)$$

The boundary conditions on the energy equation present something of a problem for noncircular ducts. In order that it not be necessary to solve a simultaneous problem in the wall and the fluid, including such wall properties as the thermal conductivity, certain assumptions must be made. Irvine (ref. 3) has suggested that for noncircular ducts it is reasonable to consider three cases:

- (1) Constant wall temperature both peripherally and axially (a high wall thermal conductivity assumption)

- (2) Constant heat input per unit axial distance and constant peripheral wall temperature at each axial position, with the wall temperature varying axially only (a high peripheral wall thermal conductivity assumption)
- (3) Constant heat input per unit axial distance and per unit peripheral distance (a low wall thermal conductivity assumption)

These cases would seem to represent the extremes of the real physical situation.

The boundary conditions for these three cases may then be given as follows:

Case 1:

$$\left. \begin{aligned} t(0, y, z) &= t_0 \\ t(x, a, z) &= t_w \\ t(x, y, b) &= t_w \\ \frac{\partial t}{\partial y}(x, 0, z) &= 0 \\ \frac{\partial t}{\partial z}(x, y, 0) &= 0 \end{aligned} \right\} \quad (8-49)$$

Case 2:

$$\left. \begin{aligned} t(0, y, z) &= t_0 \\ \int_0^a k \frac{\partial t}{\partial z} \Big|_b dy + \int_0^b k \frac{\partial t}{\partial y} \Big|_a dz &= q' \\ \frac{\partial t}{\partial y}(x, 0, z) &= 0 \\ \frac{\partial t}{\partial z}(x, y, 0) &= 0 \end{aligned} \right\} \quad (8-50)$$

where q' is the input heat flux per unit length through the walls of one quadrant of the channel.

Case 3:

$$\left. \begin{aligned} t(0, y, z) &= t_0 \\ k \frac{\partial t}{\partial y}(x, a, z) &= q'' \\ k \frac{\partial t}{\partial z}(x, y, b) &= q'' \\ \frac{\partial t}{\partial y}(x, 0, z) &= 0 \\ \frac{\partial t}{\partial z}(x, y, 0) &= 0 \end{aligned} \right\} \quad (8-51)$$

where q'' is the input heat flux per unit area through the channel wall.

Simple variations of these conditions could also easily be considered—for example, different heat fluxes through adjacent walls, an arbitrarily distributed heat flux along any wall, etc. The formulations for the cases given in equations (8-49) to (8-51) should demonstrate the techniques involved. The choice of dimensionless variables and solution method is dictated by the case considered. The dimensionless representation and solution are now discussed separately for each of the three cases.

8.1.3.1 *Case 1—constant wall temperature.*—The dimensionless variables chosen are

$$\left. \begin{aligned} T &= \frac{t_w - t}{t_w - t_0} \\ X &= \frac{xv}{a^2 u_0} \\ Y &= \frac{y}{a} \\ Z &= \frac{z}{a} \end{aligned} \right\} \quad (8-52)$$

Inserting these variables, the energy equation (8-48) becomes

$$U \frac{\partial T}{\partial X} + V \frac{\partial T}{\partial Y} + W \frac{\partial T}{\partial Z} = \frac{1}{Pr} \left(\frac{\partial^2 T}{\partial Y^2} + \frac{\partial^2 T}{\partial Z^2} \right) \quad (8-53)$$

subject to the dimensionless form of the boundary conditions (8-49):

$$\left. \begin{aligned} T(0, Y, Z) &= 1 \\ T(X, 1, Z) &= 0 \\ T(X, Y, \sigma) &= 0 \\ \frac{\partial T}{\partial Y}(X, 0, Z) &= 0 \\ \frac{\partial T}{\partial Z}(X, Y, 0) &= 0 \end{aligned} \right\} \quad (8-54)$$

Equation (8-53) may be expressed in difference form as

$$\begin{aligned}
 U_{j,k,l} \frac{T_{j+1,k,l} - T_{j,k,l}}{\Delta X} + V_{j,k,l} \frac{T_{j+1,k+1,l} - T_{j+1,k-1,l}}{2(\Delta Y)} \\
 + W_{j,k,l} \frac{T_{j+1,k,l+1} - T_{j+1,k,l-1}}{2(\Delta Z)} \\
 = \frac{1}{Pr} \left[\frac{T_{j+1,k+1,l} - 2T_{j+1,k,l} + T_{j+1,k-1,l}}{(\Delta Y)^2} \right. \\
 \left. + \frac{T_{j+1,k,l+1} - 2T_{j+1,k,l} + T_{j+1,k,l-1}}{(\Delta Z)^2} \right] \quad (8-55)
 \end{aligned}$$

The simplest method for the solution of equation (8-55) is Gauss-Siedel iteration. Solving for $T_{j+1,k,l}$ gives

$$\begin{aligned}
 T_{j+1,k,l} = & \left\{ T_{j+1,k+1,l} \left[\frac{-V_{j,k,l}}{2(\Delta Y)} + \frac{1}{Pr(\Delta Y)^2} \right] \right. \\
 & + T_{j+1,k-1,l} \left[\frac{V_{j,k,l}}{2(\Delta Y)} + \frac{1}{Pr(\Delta Y)^2} \right] + T_{j+1,k,l+1} \left[\frac{-W_{j,k,l}}{2(\Delta Z)} + \frac{1}{Pr(\Delta Z)^2} \right] \\
 & + T_{j+1,k,l-1} \left[\frac{W_{j,k,l}}{2(\Delta Z)} + \frac{1}{Pr(\Delta Z)^2} \right] \\
 & \left. + T_{j,k,l} \left(\frac{U_{j,k,l}}{\Delta X} \right) \right\} / \left[\frac{U_{j,k,l}}{\Delta X} + \frac{2}{Pr(\Delta Y)^2} + \frac{2}{Pr(\Delta Z)^2} \right] \quad (8-56)
 \end{aligned}$$

This equation may be used to solve for each value of $T_{j+1,k,l}$ in the field, repeating in some regular order until the values of $T_{j+1,k,l}$ on successive iterations agree to within any desired accuracy. A step ΔX downstream may then be taken and the process repeated. It is suggested that the velocity and temperature calculations be done on the same grid, with first the velocity calculations and then the temperature calculations performed at each ΔX step. This procedure will minimize the computer storage required.

If it is desired to solve some variety of the Graetz problem (fully developed velocity, developing temperature), then the fully developed velocity profile is used for $U_{j,k,l}$ and all transverse velocity components are zero.

We now calculate the heat transfer for the constant wall temperature case. Applying the first law of thermodynamics to a control volume of length ΔX along the channel and taking the limit as $\Delta X \rightarrow 0$ give

$$h4ab(t_w - t_b) = \frac{d}{dx} \int_{-b}^b \int_{-a}^a \rho c_p t \, dy \, dz \quad (8-57)$$

where the bulk temperature t_b is defined as

$$t_b \equiv \frac{\int_0^b \int_0^a u t dy dz}{\int_0^b \int_0^a u dy dz} \quad (8-58)$$

Solving for h gives

$$h = \frac{\rho c_p}{4(a+b)} \left(\frac{1}{t_w - t_b} \right) \frac{d}{dx} \int_{-b}^b \int_{-a}^a u t dy dz \quad (8-59)$$

The local Nusselt number is defined as

$$Nu_x = \frac{h D_h}{k} \quad (8-60)$$

where D_h , the hydraulic diameter, is defined as

$$D_h \equiv \frac{4(4ab)}{4a+4b} = \frac{4ab}{a+b} \quad (8-61)$$

Inserting the expression for h from equation (8-59) into equation (8-60), and expressing the results in terms of dimensionless variables gives

$$Nu_x = \frac{-4\sigma^2(Pr)}{(1+\sigma)^2} \frac{1}{T_b} \frac{dT_b}{dX} \quad (8-62)$$

where

$$T_b = \frac{\int_0^\sigma \int_0^1 TU dY dZ}{\int_0^\sigma \int_0^1 U dY dZ} = \frac{1}{\sigma} \int_0^\sigma \int_0^1 TU dY dZ \quad (8-63)$$

The integral in equation (8-63) can be evaluated by the use of the two-dimensional form of either the trapezoidal rule or Simpson's rule. The trapezoidal rule, which should be sufficiently accurate for most practical purposes, does not restrict m and n to be odd. The expression is

$$T_b \Big|_{j+1} = \frac{1}{\sigma} \left[\sum_{k=1}^n \sum_{l=1}^m 4T_{j+1, k, l} U_{j+1, k, l} + \sum_{l=1}^m 2T_{j+1, 0, l} U_{j+1, 0, l} \right. \\ \left. + \sum_{k=1}^n 2T_{j+1, k, 0} U_{j+1, k, 0} + T_{j+1, 0, 0} U_{j+1, 0, 0} \right] \left(\frac{\Delta Y \Delta Z}{2} \right) \quad (8-64)$$

The derivative $\frac{dT_b}{dX}$ may be readily evaluated as

$$\frac{dT_b}{dX} = \frac{T_b|_{j+1} - T_b|_j}{\Delta X} \quad (8-65)$$

The average Nusselt number is given by

$$Nu_m = \frac{1}{X} \int_0^X Nu_x dX \quad (8-66)$$

As usual, this expression may be evaluated at every other ΔX step, starting from the entrance ($j=0$) as

$$Nu_m|_{j+1} = \frac{\Delta X}{3} \left(Nu_x|_0 + 4 \sum_{i=1,3,5,7,\dots}^j Nu_x|_i + 2 \sum_{i=2,4,6,8,\dots}^{j-1} Nu_x|_i + Nu_x|_{j+1} \right) \left(\frac{1}{X_{j+1}} \right) \quad (8-67)$$

where $j+1$ must be even.

8.1.3.2 Case 2—constant heat input per unit length, uniform peripheral temperature.—The dimensionless variables chosen for this case are

$$\left. \begin{aligned} T &= \frac{t - t_0}{q' / k} \\ X &= \frac{x\nu}{a^2 u_0} \end{aligned} \right\} \quad (8-68)$$

$$\left. \begin{aligned} Y &= \frac{y}{a} \\ Z &= \frac{z}{a} \end{aligned} \right\} \quad (8-69)$$

Employing these variables, the energy equation (8-48) becomes

$$U \frac{\partial T}{\partial X} + V \frac{\partial T}{\partial Y} + W \frac{\partial T}{\partial Z} = \frac{1}{Pr} \left(\frac{\partial^2 T}{\partial Y^2} + \frac{\partial^2 T}{\partial Z^2} \right) \quad (8-70)$$

The boundary conditions (8-50) become

$$\left. \begin{aligned} T(0,Y,Z) &= 0 \\ \int_0^1 \frac{\partial T}{\partial Z} \Big|_{\sigma} dY + \int_0^{\sigma} \frac{\partial T}{\partial Y} \Big|_1 dZ &= 1 \\ \frac{\partial T}{\partial Y}(X,0,Z) &= 0 \\ \frac{\partial T}{\partial Z}(X,Y,0) &= 0 \end{aligned} \right\} \quad (8-71)$$

The finite difference form of the dimensionless energy equation (8-70) is identical to that used in the previous section for the constant wall temperature case and is given by equation (8-55). The finite difference form of the second boundary condition in (8-71) requires some explanation. Expressing only the gradients in difference form gives

$$\int_0^1 \frac{3T_{j+1,k,m+1} - 4T_{j+1,k,m} + T_{j+1,k,m-1}}{2(\Delta Z)} dY + \int_0^{\sigma} \frac{3T_{j+1,n+1,l} - 4T_{j+1,n,l} + T_{j+1,n-1,l}}{2(\Delta Y)} dZ = 1 \quad (8-72)$$

Now for this case, by assumption,

$$T_{j+1,k,m+1} = T_{j+1,n+1,l} = T_w|_{j+1} \quad (8-73)$$

where $T_w|_{j+1}$ is the dimensionless wall temperature, which will in general vary with X . Using this fact, equation (8-72) may be rewritten as

$$\begin{aligned} \frac{3T_w|_{j+1}}{2(\Delta Z)} \int_0^1 dY - \frac{2}{\Delta Z} \int_0^1 T_{j+1,k,m} dY + \frac{1}{2(\Delta Z)} \int_0^1 T_{j+1,k,m-1} dY \\ + \frac{3T_w|_{j+1}}{2(\Delta Y)} \int_0^{\sigma} dZ - \frac{2}{\Delta Y} \int_0^{\sigma} T_{j+1,n,l} dZ + \frac{1}{2(\Delta Y)} \int_0^{\sigma} T_{j+1,n-1,l} dZ = 1 \end{aligned} \quad (8-74)$$

or, when rearranging and solving for $T_w|_{j+1}$,

$$\begin{aligned} T_w|_{j+1} = \frac{2}{3} \left[1 + \frac{2}{\Delta Y} \int_0^{\sigma} T_{j+1,n,l} dZ + \frac{2}{\Delta Z} \int_0^1 T_{j+1,k,m} dY \right. \\ \left. - \frac{1}{2(\Delta Y)} \int_0^{\sigma} T_{j+1,n-1,l} dZ - \frac{1}{2(\Delta Z)} \int_0^1 T_{j+1,k,m-1} dY \right] / \left(\frac{\sigma}{\Delta Y} + \frac{1}{\Delta Z} \right) \end{aligned} \quad (8-75)$$

The integrals in (8-75) can be given in finite difference form using Simpson's rule:

$$\int_0^\sigma T_{j+1, n, l} dZ = \frac{\Delta Z}{3} \left[T_{j+1, n, 0} + 4 \sum_{i=1, 3, 5, 7, \dots}^m T_{j+1, n, i} + 2 \sum_{i=2, 4, 6, 8, \dots}^{m-1} T_{j+1, n, i} + T_{j+1, n, m+1} \right] \quad (8-76)$$

and

$$\int_0^1 T_{j+1, k, m} dY = \frac{\Delta Y}{3} \left[T_{j+1, 0, m} + 4 \sum_{i=1, 3, 5, 7, \dots}^n T_{j+1, i, m} + 2 \sum_{i=2, 4, 6, 8, \dots}^{n-1} T_{j+1, i, m} + T_{j+1, n+1, m} \right] \quad (8-77)$$

with exactly analogous expressions for the integrals of $T_{j+1, n-1, l}$ and $T_{j+1, k, m-1}$.

Note that the wall temperature has again appeared, since $T_{j+1, n, m+1}$ and $T_{j+1, n+1, m}$ (as well as $T_{j+1, n-1, m+1}$ and $T_{j+1, n+1, m-1}$ which appear in the integrals of $T_{j+1, n-1, l}$ and $T_{j+1, k, m-1}$) are all $T_w|_{j+1}$. After collecting all coefficients and solving for $T_w|_{j+1}$,

$$\begin{aligned} T_w|_{j+1} = & \frac{2}{3} \left\{ 1 + \frac{2(\Delta Z)}{3(\Delta Y)} \left[\left(T_{j+1, n, 0} - \frac{1}{4} T_{j+1, n-1, 0} \right) \right. \right. \\ & + 4 \sum_{i=1, 3, 5, 7, \dots}^m \left(T_{j+1, n, i} - \frac{1}{4} T_{j+1, n-1, i} \right) + 2 \sum_{i=2, 4, 6, 8, \dots}^{m-1} \left(T_{j+1, n, i} - \frac{1}{4} T_{j+1, n-1, i} \right) \left. \right] \\ & + \frac{2(\Delta Y)}{3(\Delta Z)} \left[\left(T_{j+1, 0, m} - \frac{1}{4} T_{j+1, 0, m-1} \right) + 4 \sum_{i=1, 3, 5, 7, \dots}^n \left(T_{j+1, i, m} - \frac{1}{4} T_{j+1, i, m-1} \right) \right. \\ & \left. \left. + 2 \sum_{i=2, 4, 6, 8, \dots}^{n-1} \left(T_{j+1, i, m} - \frac{1}{4} T_{j+1, i, m-1} \right) \right] \right\} / \left[\frac{\sigma}{\Delta Y} + \frac{1}{\Delta Z} - \frac{1}{3} \left(\frac{\Delta Z}{\Delta Y} + \frac{\Delta Y}{\Delta Z} \right) \right] \quad (8-78) \end{aligned}$$

The method of solution for this case can now be discussed. As in the previous section 8.1.3.1, the finite difference form of the energy equation is solved for $T_{j+1, k, l}$ and the result is given by equation (8-56). The method is now identical with that used for case 1, except that after each sweep through the field, the wall temperature must be recomputed using equation (8-78). Some numerical experiments by the author indicate that equation (8-78) must be rather severely underrelaxed in order to obtain convergence of the iterative process. Successive sweeps through

the cross section are taken until all values of $T_{j+1, k, l}$ change by less than some predetermined amount on two successive iterations. The solution is then considered converged and another ΔX step taken downstream.

We now proceed to the heat transfer analysis. The local heat transfer coefficient is defined from

$$h(a+b)(t_w - t_b) = q' \quad (8-79)$$

or

$$h = \frac{q'}{(a+b)(t_w - t_b)} \quad (8-80)$$

The local Nusselt number is defined as

$$Nu_x = \frac{hD_h}{k} \quad (8-81)$$

where

$$D_h = \frac{4ab}{a+b}$$

Inserting equation (8-80) into equation (8-81) gives

$$Nu_x = \frac{4q'ab}{k(a+b)^2(t_w - t_b)} \quad (8-82)$$

or, in dimensionless form,

$$Nu_x = \frac{4\sigma}{(1+\sigma)(T_w - T_b)} \quad (8-83)$$

Although for this case an analytical expression for T_b can be obtained, it is recommended for the sake of consistency that T_b be found from

$$T_b = \frac{\int_0^\sigma \int_0^1 TUdYdZ}{\int_0^\sigma \int_0^1 UdYdZ} \quad (8-84)$$

which is given in finite difference form in equation (8-64). The mean Nusselt number, if desired, may be found from the finite difference equation (8-67).

8.1.3.3 Case 3—constant heat input per unit area of duct surface.—The dimensionless variables chosen for this case are

$$\left. \begin{aligned} T &= \frac{t - t_0}{q'' a / k} \\ X &= \frac{xv}{a^2 u_0} \\ Y &= \frac{y}{a} \\ Z &= \frac{z}{a} \end{aligned} \right\} \quad (8-85)$$

Using these variables, the energy equation (8-48) becomes

$$U \frac{\partial T}{\partial X} + V \frac{\partial T}{\partial Y} + W \frac{\partial T}{\partial Z} = \frac{1}{Pr} \left(\frac{\partial^2 T}{\partial Y^2} + \frac{\partial^2 T}{\partial Z^2} \right) \quad (8-86)$$

which is identical with the form used for cases 1 and 2 in the two preceding sections. The boundary conditions (8-51) in dimensionless form are

$$\left. \begin{aligned} T(0, Y, Z) &= 0 \\ \frac{\partial T}{\partial Z}(X, Y, \sigma) &= 1 \\ \frac{\partial T}{\partial Y}(X, 1, Z) &= 1 \\ \frac{\partial T}{\partial Y}(X, 0, Z) &= 0 \\ \frac{\partial T}{\partial Z}(X, Y, 0) &= 0 \end{aligned} \right\} \quad (8-87)$$

The energy equation in finite difference form and the solution for $T_{j+1, k, l}$ are identical to the two previous cases (see eq. (8-56)). The difference forms of the second and third boundary conditions in (8-87) are

$$\frac{3T_{j+1, k, m+1} - 4T_{j+1, k, m} + T_{j+1, k, m-1}}{2(\Delta Z)} = 1 \quad (8-88)$$

and

$$\frac{3T_{j+1, n+1, l} - 4T_{j+1, n, l} + T_{j+1, n-1, l}}{2(\Delta Y)} = 1 \quad (8-89)$$

Equations (8-88) and (8-89) may now be solved for $T_{j+1, k, m+1}$ and $T_{j+1, n+1, l}$, respectively:

$$T_{j+1, k, m+1} = \frac{2}{3} \Delta Z + \frac{4}{3} T_{j+1, k, m} - \frac{1}{3} T_{j+1, k, m-1} \quad (8-90)$$

$$T_{j+1, n+1, l} = \frac{2}{3} \Delta Y + \frac{4}{3} T_{j+1, n, l} - \frac{1}{3} T_{j+1, n-1, l} \quad (8-91)$$

The problem is now similar to that of case 1 (section 8.1.3.1) except that the wall temperatures are unknown, along with the interior temperatures, and equations (8-90) and (8-91) must be solved along with equation (8-56) on each sweep through the cross section. Slight underrelaxation of equations (8-90) and (8-91) may be desirable.

We now consider the heat transfer for case 3. The definition of the heat transfer coefficient for this case may be found from

$$h(t_w - t_b) = q'' \quad (8-92)$$

so that

$$h = \frac{q''}{t_w - t_b} \quad (8-93)$$

The local Nusselt number is defined as

$$Nu_x \equiv \frac{hD_h}{k} \quad (8-94)$$

where

$$D_h = \frac{4ab}{a+b} \quad (8-95)$$

Inserting equations (8-93) and (8-95) into equation (8-94) gives

$$Nu_x = \frac{4q''ab}{k(a+b)(t_w - t_b)} \quad (8-96)$$

Expressing Nu_x in terms of dimensionless quantities gives

$$Nu_x = \frac{4\sigma}{(1+\sigma)(T_w - T_b)} \quad (8-97)$$

As in case 2, an analytical expression can be found for T_b , but it is suggested for internal consistency and accuracy that T_b be found from

$$T_b = \frac{\int_0^\sigma \int_0^1 TU \, dY \, dZ}{\int_0^\sigma \int_0^1 U \, dY \, dZ} \quad (8-98)$$

which is given in finite difference form in equation (8-64). The mean Nusselt number, if desired, may be found numerically from equation (8-67).

8.1.4 Compressible Flow in the Entrance of a Rectangular Channel – Proposed Velocity and Temperature Solutions

To the best of the author's knowledge, this problem has not previously been considered in its complete three-dimensional form anywhere in the literature. The methods used for the incompressible problem furnish a guide, but the formulation must necessarily be based largely on techniques and representations which have been successful for other geometries such as the circular tube (see Walker, ref. 5, and Deissler and Presler, ref. 6). The model employed is based on the first model for the incompressible case discussed in section 8.1.1 and consists of one momentum equation, the energy equation, continuity, the equation of state, and the additional relation that the transverse velocity in each cross section be directed toward the channel centerline. This restricts the formulation to moderate aspect ratios.

The configuration is identical to that considered in the earlier sections of this chapter and shown in figure 8-1. For simplicity, only one case is considered here – that of constant wall temperature. Other thermal boundary conditions may readily be considered using sections 8.1.3.2 and 8.1.3.3 as references.

The basic equations for the compressible flow are

$$\rho \left(u \frac{\partial u}{\partial x} + v \frac{\partial u}{\partial y} + w \frac{\partial u}{\partial z} \right) = -\frac{dp}{dx} + \left[\frac{\partial}{\partial y} \left(\mu \frac{\partial u}{\partial y} \right) + \frac{\partial}{\partial z} \left(\mu \frac{\partial u}{\partial z} \right) \right] \quad (8-99)$$

$$\frac{\partial(\rho u)}{\partial x} + \frac{\partial(\rho v)}{\partial y} + \frac{\partial(\rho w)}{\partial z} = 0 \quad (8-100)$$

$$vz = wy \quad (8-101)$$

$$\rho c_p \left(u \frac{\partial t}{\partial x} + v \frac{\partial t}{\partial y} + w \frac{\partial t}{\partial z} \right) =$$

$$= u \frac{dp}{dx} + \left[\frac{\partial}{\partial y} \left(k \frac{\partial t}{\partial y} \right) + \frac{\partial}{\partial z} \left(k \frac{\partial t}{\partial z} \right) \right] + \mu \left[\left(\frac{\partial u}{\partial y} \right)^2 + \left(\frac{\partial u}{\partial z} \right)^2 \right] \quad (8-102)$$

$$\frac{p}{\rho} = \mathcal{R}t \quad (8-103)$$

$$k = k(t) \quad (8-104)$$

$$\mu = \mu(t) \quad (8-105)$$

The boundary conditions are

$$u(x, a, z) = 0 \quad u(x, y, b) = 0$$

$$\frac{\partial u}{\partial z}(x, y, 0) = 0 \quad \frac{\partial u}{\partial y}(x, 0, z) = 0$$

$$v(x, a, z) = 0$$

$$v(x, y, b) = 0$$

$$v(x, 0, z) = 0$$

$$w(x, a, z) = 0$$

$$w(x, y, b) = 0$$

$$w(x, y, 0) = 0$$

$$t(x, a, z) = t_w$$

$$t(x, y, b) = t_w$$

$$\frac{\partial t}{\partial z}(x, y, 0) = 0 \quad \frac{\partial t}{\partial y}(x, 0, z) = 0$$

$$u(0, y, z) = u_0 \text{ (see appendix F)}$$

$$t(0, y, z) = t_0$$

$$p(0) = p_0$$

(8-106)

The dimensionless variables chosen are:

$$\left. \begin{aligned}
 U &= \frac{u}{u_0} \\
 V &= \frac{\rho_0 v a}{\mu_0} \\
 W &= \frac{\rho_0 w a}{\mu_0} \\
 T &= \frac{t}{t_0} \\
 P &= \frac{p}{p_0} \\
 X &= \frac{x \mu_0}{\rho_0 u_0 a^2} \\
 Y &= \frac{y}{a} \\
 Z &= \frac{z}{a} \\
 k^* &= \frac{k}{k_0} \\
 \mu^* &= \frac{\mu}{\mu_0} \\
 \rho^* &= \frac{\rho}{\rho_0}
 \end{aligned} \right\} \quad (8-107)$$

Inserting these variables into equations (8-99) to (8-103) yields

$$\rho^* \left(U \frac{\partial U}{\partial X} + V \frac{\partial U}{\partial Y} + W \frac{\partial U}{\partial Z} \right) = - \frac{1}{\gamma M_0^2} \frac{dP}{dX} + \frac{\partial}{\partial Y} \left(\mu^* \frac{\partial U}{\partial Y} \right) + \frac{\partial}{\partial Z} \left(\mu^* \frac{\partial U}{\partial Z} \right) \quad (8-108)$$

$$\frac{\partial(\rho^* U)}{\partial X} + \frac{\partial(\rho^* V)}{\partial Y} + \frac{\partial(\rho^* W)}{\partial Z} = 0 \quad (8-109)$$

$$VZ = WY$$

(8-110)

$$\rho^* \left(U \frac{\partial T}{\partial X} + V \frac{\partial T}{\partial Y} + W \frac{\partial T}{\partial Z} \right) = \frac{\gamma - 1}{\gamma} U \frac{dP}{dX}$$

$$+ \frac{1}{Pr} \left[\frac{\partial}{\partial Y} \left(k^* \frac{\partial T}{\partial Y} \right) + \frac{\partial}{\partial Z} \left(k^* \frac{\partial T}{\partial Z} \right) \right] + (\gamma - 1) M_0^2 \mu^* \left[\left(\frac{\partial U}{\partial Y} \right)^2 + \left(\frac{\partial U}{\partial Z} \right)^2 \right] \quad (8-111)$$

$$P = \rho^* T \quad (8-112)$$

where $M_0 = u_0 / \sqrt{\gamma \mathcal{R} t_0}$, the Mach number referred to the entrance conditions.

If the usual power law relations are assumed, equations (8-104) and (8-105) become in dimensionless form

$$\mu^* = (T)^f \quad (8-113)$$

$$k^* = (T)^g \quad (8-114)$$

The boundary conditions (8-1) in dimensionless form are

$$\left. \begin{aligned} U(X, 1, Z) = 0 & \quad U(X, Y, \sigma) = 0 \\ \frac{\partial U}{\partial Z}(X, Y, 0) = 0 & \quad \frac{\partial U}{\partial Y}(X, 0, Z) = 0 \\ V(X, 1, Z) = 0 \\ V(X, Y, \sigma) = 0 \\ V(X, 0, Z) = 0 \\ W(X, 1, Z) = 0 \\ W(X, Y, \sigma) = 0 \\ W(X, 0, Z) = 0 \\ T(X, 1, Z) = T_w = \frac{t_w}{t_0} \\ T(X, Y, \sigma) = T_w \\ \frac{\partial T}{\partial Z}(X, Y, 0) = 0 & \quad \frac{\partial T}{\partial Y}(X, 0, Z) = 0 \\ U(0, Y, Z) = 1 \\ T(0, Y, Z) = 1 \\ P(0) = 1 \end{aligned} \right\} \quad (8-115)$$

The basic equations can now be represented in difference form. Since an iterative scheme must be used, no effort is made to keep the difference equations linear. Equations (8-108) to (8-114) become

$$\begin{aligned} \rho_{j,k,l}^* & \left[U_{j,k,l} \frac{U_{j+1,k,l} - U_{j,k,l}}{\Delta X} + V_{j,k,l} \frac{U_{j+1,k+1,l} - U_{j+1,k-1,l}}{2(\Delta Y)} \right. \\ & \quad \left. + W_{j,k,l} \frac{U_{j+1,k,l+1} - U_{j+1,k,l-1}}{2(\Delta Z)} \right] \\ & = -\frac{1}{\gamma M_0^2} \frac{P_{j+1} - P_j}{\Delta Z} + \mu_{j+1,k,l}^* \left[\frac{U_{j+1,k+1,l} - 2U_{j+1,k,l} + U_{j+1,k-1,l}}{(\Delta Y)^2} \right] \\ & \quad + \left[\frac{\mu_{j+1,k+1,l}^* - \mu_{j+1,k-1,l}^*}{2(\Delta Y)} \right] \left[\frac{U_{j+1,k+1,l} - U_{j+1,k-1,l}}{2(\Delta Y)} \right] \\ & \quad + \mu_{j+1,k,l}^* \left[\frac{U_{j+1,k,l+1} - 2U_{j+1,k,l} + U_{j+1,k,l-1}}{(\Delta Z)^2} \right] \\ & \quad + \left[\frac{\mu_{j+1,k,l+1}^* - \mu_{j+1,k,l-1}^*}{2(\Delta Z)} \right] \left[\frac{U_{j+1,k,l+1} - U_{j+1,k,l-1}}{2(\Delta Z)} \right] \quad (8-116) \end{aligned}$$

$$\begin{aligned} \frac{\rho_{j+1,k,l}^* U_{j+1,k,l} - \rho_{j,k,l}^* U_{j,k,l}}{\Delta X} & + \frac{\rho_{j+1,k+1,l}^* V_{j+1,k+1,l} - \rho_{j+1,k,l}^* V_{j+1,k,l}}{\Delta Y} \\ & + \frac{\rho_{j+1,k,l+1}^* W_{j+1,k,l+1} - \rho_{j+1,k,l}^* W_{j+1,k,l}}{\Delta Z} = 0 \quad (8-117) \end{aligned}$$

$$V_{j+1,k,l} Z_l = W_{j+1,k,l} Y_k \quad (8-118)$$

$$\begin{aligned} \rho_{j,k,l}^* & \left[U_{j,k,l} \frac{T_{j+1,k,l} - T_{j,k,l}}{\Delta X} + V_{j,k,l} \frac{T_{j+1,k+1,l} - T_{j+1,k-1,l}}{2(\Delta Y)} \right. \\ & \quad \left. + W_{j,k,l} \frac{T_{j+1,k,l+1} - T_{j+1,k,l-1}}{2(\Delta Z)} \right] = \frac{\gamma-1}{\gamma} \bar{U}_{j,k,l} \frac{P_{j+1} - P_j}{\Delta X} \\ & \quad + \frac{1}{Pr} \left\{ k_{j+1,k,l}^* \left[\frac{T_{j+1,k+1,l} - 2T_{j+1,k,l} + T_{j+1,k-1,l}}{(\Delta Y)^2} \right] \right. \\ & \quad + \left[\frac{k_{j+1,k+1,l}^* - k_{j+1,k-1,l}^*}{2(\Delta Y)} \right] \left[\frac{T_{j+1,k+1,l} - T_{j+1,k-1,l}}{2(\Delta Y)} \right] \\ & \quad + k_{j+1,k,l}^* \left[\frac{T_{j+1,k,l+1} - 2T_{j+1,k,l} + T_{j+1,k,l-1}}{(\Delta Z)^2} \right] \\ & \quad \left. + \left[\frac{k_{j+1,k,l+1}^* - k_{j+1,k,l-1}^*}{2(\Delta Z)} \right] \left[\frac{T_{j+1,k,l+1} - T_{j+1,k,l-1}}{2(\Delta Z)} \right] \right\} + \end{aligned}$$

$$+ (\gamma - 1) M_0^2 \mu_{j+1,k,l}^* \left\{ \left[\frac{U_{j+1,k+1,l} - U_{j+1,k-1,l}}{2 (\Delta Y)} \right]^2 + \left[\frac{U_{j+1,k,l+1} - U_{j+1,k,l-1}}{2 (\Delta Z)} \right]^2 \right\} \quad (8-119)$$

$$P_{j+1} = \rho_{j+1,k,l}^* T_{j+1,k,l} \quad (8-120)$$

$$\mu_{j+1,k,l}^* = T_{j+1,k,l}^y \quad (8-121)$$

$$k_{j+1,k,l}^* = T_{j+1,k,l}^y \quad (8-122)$$

Very little concrete advice can be given on the solution of these equations, since to the best of the author's knowledge it has not yet been attempted. Certainly an iterative scheme is required, and in general, equation (8-116) should be solved for the $U_{j+1,k}$'s, equations (8-117) and (8-118) for the $V_{j+1,k}$'s and $W_{j+1,k}$'s, and equation (8-119) for the $T_{j+1,k}$'s; beyond these broad statements, little detail can be specified. There will certainly be difficulty in obtaining a converged solution.

It would be presumptuous to discuss the heat transfer formulation for this problem without any proven solution method for the velocities, temperatures, and properties. Therefore, the reader is referred to sections 6.1.5 and 7.1.5 for discussions of compressible flow heat transfer in parallel plate channels and circular tubes, respectively. These discussions certainly will have some application to the present problem, once the difficulties of obtaining a converged solution to the difference equations have been overcome.

8.2 OTHER PROBLEMS WITH A SIMILAR FORMULATION

8.2.1 Flow in Rectangular Channels With Porous Walls

If a specified suction or injection velocity is applied to the walls of the channel, some small modifications must be made to the formulations of this chapter. As usual, we shall only present the changes to the already given formulations.

We limit our discussion here to incompressible flow, because of the obvious uncertainties in the compressible flow formulation. If the first model, discussed in section 8.1.1, is employed, then modifications must be made to integral continuity and to the boundary conditions. Assuming the suction or injection velocity to be uniform around the periphery of the channel (although it may vary with axial distance in a specified manner), the following modifications must be made to the boundary conditions (8-5):

$$\left. \begin{aligned} v(x, a, z) &= v_w(x) \\ w(x, y, b) &= v_w(x) \end{aligned} \right\} \quad (8-123)$$

or, in dimensionless form,

$$\left. \begin{aligned} V(X, 1, Z) &= V_w(X) \\ W(X, Y, \sigma) &= V_w(X) \end{aligned} \right\} \quad (8-124)$$

The difference form of integral continuity, equation (8-25), becomes

$$\begin{aligned} \frac{4}{(\Delta Y)(\Delta Z)} \left[\sigma - V_w \Big|_{j+1} (1 + \sigma) \Delta X \right] &= \sum_{k=1}^n \sum_{l=1}^m 4U_{j+1, k, l} \\ &+ \sum_{l=1}^m 2U_{j+1, 0, l} + \sum_{k=1}^n 2U_{j+1, k, 0} + U_{j+1, 0, 0} \end{aligned} \quad (8-125)$$

The solution can now be carried out exactly as detailed in section 8.1.1. Solving equation (8-125) for $U_{j+1, 1, 1}$ yields

$$\begin{aligned} U_{j+1, 1, 1} &= \frac{\sigma - V_w \Big|_{j+1} (1 + \sigma) \Delta X}{(\Delta Y)(\Delta Z)} - \sum_{\substack{k=1 \\ (k, l \neq 1 \text{ if } k=l)}}^n \sum_{l=1}^m U_{j+1, k, l} \\ &- \frac{1}{2} \sum_{l=1}^m U_{j+1, 0, l} - \frac{1}{2} \sum_{k=1}^n U_{j+1, k, 0} - \frac{1}{4} U_{j+1, 0, 0} \end{aligned} \quad (8-126)$$

This expression can be used in place of equation (8-28).

If the problem of specified wall suction or injection velocity is to be considered using the second model (section 8.1.2), then only the boundary conditions need be changed to the form (8-124). These conditions are then automatically brought into the solution when the finite difference forms of the various equations are written adjacent to the walls.

If the suction or injection velocity is related to the pressure at the wall (e.g., through Darcy's Law), then additional modifications to the original formulations are necessary.

When the first model of section 8.1.1 is used, since pressure is a function only of X , a typical relation between velocity through the wall and pressure might be

$$V_w \Big|_{j+1} = AP_{j+1} \quad (8-127)$$

Equation (8-127) can now be introduced into the iterative scheme of solution of the first model immediately following the solution of equation (8-27) for P_{j+1} and preceding the solution of equation (8-126) for $U_{j+1, 1, 1}$. Equation (8-126) must of course be used here since it allows for flow through the wall. Underrelaxation of (8-127) may be required if A is large.

If it is desired to use the second model of section 8.1.2, then since the pressure can vary peripherally around the channel, so can the velocity through the wall, which might be typically expressed as

$$W_{j+1, k, m+1} = AP_{j+1, k, m+1} \quad (8-128)$$

and

$$V_{j+1, n+1, l} = AP_{j+1, n+1, l} \quad (8-129)$$

Equations (8-128) and (8-129) may now be introduced into the iterative scheme of the second model, probably immediately preceding the solution for $P_{j+1, k, l}$. However, this has not been tried, and the usual difficulties in obtaining convergence can be expected. Again, underrelaxation of (8-128) and (8-129) may be necessary for large A .

8.2.2 Entrance Flow in Channels With Cross Sections Composed of Rectangular Elements

If we wish to consider flow in channels with cross sections composed of rectangular elements such as the L -shaped channel, the rectangular channel with a rectangular plug (a "rectangular annulus"), and other similar shapes as shown in figure 8-5, the formulations given in this chapter for the second model (section 8.1.2) apply directly when the boundary conditions are properly applied at the channel walls. The advantage of such channels over channels of arbitrary cross section is that since all boundaries are straight lines and all angles are right angles, rectangular finite difference grids are directly applicable. It should be noted, however, that different grid sizes may be necessary in different regions in order for an integral number of grid spaces to exactly span the region. The usual difficulties can be expected in trying to obtain a converged solution with the second model.

The first model (section 8.1.1) cannot be employed here unless some educated guess can be made about a relation between the transverse velocities at a given cross section (a rather difficult task in such complex configurations).

8.2.3 Flows With Body Forces in Rectangular Channels

The rectangular channel has been a source of considerable interest to workers in the MHD field since it represents the configuration of many MHD generators. To the author's knowledge as of this time, however, no numerical work has been done on the entrance flows in such channels incorporating the effects of the body forces. Including these effects in the formulation of the first model (section 8.1.1) would seem to introduce few practical difficulties. However, the assumption that the transverse velocity vector is directed toward the center of the channel may no longer be valid because of the presence of the body forces. Including the effects

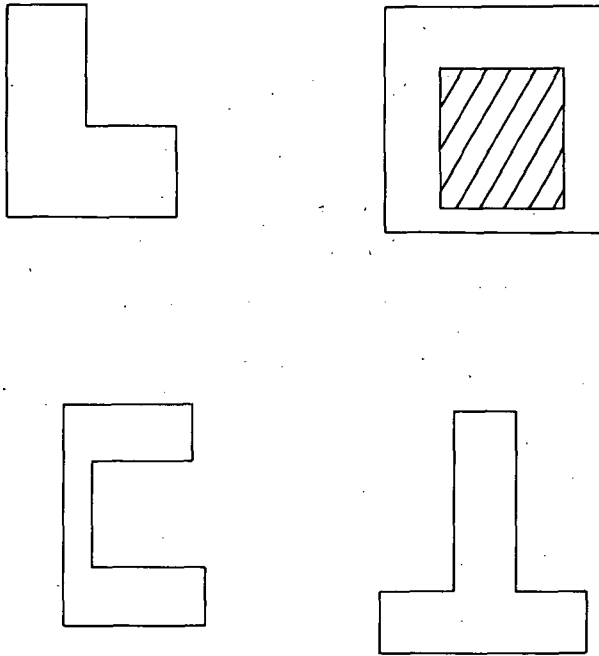


FIGURE 8-5.—Examples of channels composed of rectangular elements.

of body forces in the second model (section 8.1.2) would undoubtedly cause additional problems in obtaining convergence, and since these problems already seem very large indeed, this approach will undoubtedly require a great deal of work.

The reader is referred to section 2.3.4 for a generally applicable discussion of the effects of including body forces on the numerical techniques employed in this book.

8.2.4 Confined Free Convection in a Vertical Rectangular Channel

This problem has apparently not been previously considered in the literature. The modifications to both the first and second models in order to accommodate the buoyancy effects are not very extensive and are briefly discussed here. The treatment here parallels that given in section 6.2.2 for the parallel plate channel and 7.2.2 for the circular tube and draws heavily on those sections. The geometry is shown in figure 8-1, with g_x in the $-X$ direction.

Consider the first model of section 8.1.1 with the modified basic equations

$$\rho \left(u \frac{\partial u}{\partial x} + v \frac{\partial u}{\partial y} + w \frac{\partial u}{\partial z} \right) = - \frac{dp}{dx} + \mu \left(\frac{\partial^2 u}{\partial y^2} + \frac{\partial^2 u}{\partial z^2} \right) + \rho g_x B(t - t_0). \quad (8-130)$$

$$\rho c_p \left(u \frac{\partial t}{\partial x} + v \frac{\partial t}{\partial y} + w \frac{\partial t}{\partial z} \right) = k \left(\frac{\partial^2 t}{\partial y^2} + \frac{\partial^2 t}{\partial z^2} \right) \quad (8-131)$$

$$\frac{\partial u}{\partial x} + \frac{\partial v}{\partial y} + \frac{\partial w}{\partial z} = 0 \quad (8-132)$$

$$vz = wy \quad (8-133)$$

where p is the difference between the static pressure and the hydrostatic pressure, g_x the x -component of the acceleration due to gravity, B the thermal coefficient of volumetric expansion, and t_0 the fluid temperature at the channel inlet. The velocity and pressure boundary conditions are unchanged from those of section 8.1.1 and the temperature boundary conditions are (8-49) of the constant wall temperature case (case 1).

The choice of dimensionless variables is based on those used in section 6.2.2, equations (6-104):

$$\left. \begin{aligned} U &= \frac{ua}{\nu(Gr)} \\ V &= \frac{va}{\nu} \\ W &= \frac{wa}{\nu} \\ P &= \frac{p\rho a^2}{\mu^2(Gr)^2} \\ T &= \frac{t - t_0}{t_w - t_0} \\ X &= \frac{x}{a(Gr)} \\ Y &= \frac{y}{a} \\ Z &= \frac{z}{a} \\ Gr &= \frac{a^3 g_x B (t_w - t_0)}{\nu^2} \end{aligned} \right\} \quad (8-134)$$

where

Equations (8-130) to (8-133) may now be written in dimensionless form as

$$U \frac{\partial U}{\partial X} + V \frac{\partial U}{\partial Y} + W \frac{\partial U}{\partial Z} = -\frac{dP}{dX} + \frac{\partial^2 U}{\partial Y^2} + \frac{\partial^2 U}{\partial Z^2} + T \quad (8-135)$$

$$U \frac{\partial T}{\partial X} + V \frac{\partial T}{\partial Y} + W \frac{\partial T}{\partial Z} = \frac{1}{Pr} \left(\frac{\partial^2 T}{\partial Y^2} + \frac{\partial^2 T}{\partial Z^2} \right) \quad (8-136)$$

$$\frac{\partial U}{\partial X} + \frac{\partial V}{\partial Y} + \frac{\partial W}{\partial Z} = 0 \quad (8-137)$$

$$VZ = WY \quad (8-138)$$

with the dimensionless boundary conditions (8-19) on velocity and pressure, except that

$$U(0, Y, Z) = U_0 = \frac{u_0 a}{\nu(Gr)} \quad (8-139)$$

and with the constant temperature boundary conditions in dimensionless form, which are

$$\left. \begin{aligned} T(0, Y, Z) &= 0 \\ T(X, 1, Z) &= 1 \\ T(X, Y, \sigma) &= 1 \\ \frac{\partial T}{\partial Y}(X, 0, Z) &= 0 \\ \frac{\partial T}{\partial Z}(X, Y, 0) &= 0 \end{aligned} \right\} \quad (8-140)$$

The finite difference representation of (8-135) is identical to (8-22) with the additional term added to the right side ($+T_{j+1, k, l}$). The finite difference forms of equations (8-136) to (8-138) are unchanged from their earlier versions which are (8-55), (8-23), and (8-24), respectively.

The procedure for solution is then to solve the temperature problem first at each time step. This is just the content of section 8.1.3.1 but using the boundary conditions (8-140).

8.3 EXAMPLE PROBLEM—LAMINAR INCOMPRESSIBLE ENTRANCE FLOW IN A SQUARE DUCT

As an example of the techniques employed for the rectangular channel, we present the solutions of Carlson (ref. 1) for the laminar incompressible entrance flow in a square duct. Both the first model, discussed in section 8.1.1, and the second model, discussed in section 8.1.2, were employed in these investigations.

Since the square duct was considered, symmetry about the duct diagonal was employed to reduce the number of unknowns.

For the first model, the axial (X) mesh sizes used varied from $\Delta X = 2.5 \times 10^{-5}$ near the inlet to $\Delta X = 4 \times 10^{-3}$ far downstream. Solutions were obtained for transverse mesh sizes of $\Delta Y = \Delta Z = 1/12$ and for $\Delta Y = \Delta Z = 1/24$. The velocity distributions obtained were not significantly different for the two different mesh sizes, but the pressure results varied sufficiently so it was felt the most accurate results could be obtained by extrapolation of the solutions for the two mesh sizes to zero mesh size (see ref. 1 for details).

For the second model, there were practical limitations on both the axial and transverse mesh sizes. There is an apparent stability restriction on the difference representation of the second model which places lower bounds on the values of ΔX and the Reynolds number Re . Although a stability analysis is most difficult for the second model, Hornbeck (ref. 4) has carried out a numerical stability analysis for a similar (although only two-dimensional) model employed for the circular tube entrance flow problem. This analysis indicated that there might be a lower limit for stability on a product of ΔX and Re , perhaps of the form $(\Delta X)(Re)^2$. All numerical experiments on the second model showed that a similar restriction applied to the use of this model for the square duct. The second model was first successfully solved using $Re = 2000$ and $\Delta X = 6.25 \times 10^{-4}$. In order to consider the effect of Reynolds number on the flow pattern, the second model was also solved for $Re = 1000, 750, 650,$ and 500 . For these Reynolds numbers, an initial ΔX of 2.5×10^{-3} (quite coarse) was as small as could be considered. The transverse mesh size employed for all cases was $\Delta Y = \Delta Z = 1/12$. The large amounts of computer time required for each case precluded the use of any smaller values for ΔY and ΔZ .

The numerical results from these two models are now presented and compared with each other and with the analytical solution of Han (ref. 7), which is based on an integral technique using a linearized form of the axial momentum equation. Experimental data obtained by Goldstein and Kreid (ref. 8) using a Laser-Doppler flowmeter is also available for entrance flow in a square duct and is included in the comparisons.

Figures 8-6 and 8-7 show axial velocities as functions of X at two different transverse locations—the duct centerline ($Y=0, Z=0$) in figure 8-6, and the centerline of one-fourth of the duct ($Y=0.5, Z=0.5$) in figure 8-7. The second model results are for $Re = 2000$. At the duct centerline, all mathematical models and the experimental points agree very well. At $Y = 0.5, Z = 0.5$, the numerical solutions show a sharp rise and dropoff with a peak around $X = 0.02$. The rise is due to this transverse position being in the relatively flat "core" for $X < 0.02$, and this core is accelerating as the boundary layer grows. After about $X = 0.02$, the boundary layer reaches this transverse position and the velocity begins to decrease. The experimental points of Goldstein and Kreid clearly exhibit a similar behavior not shown by Han's results.

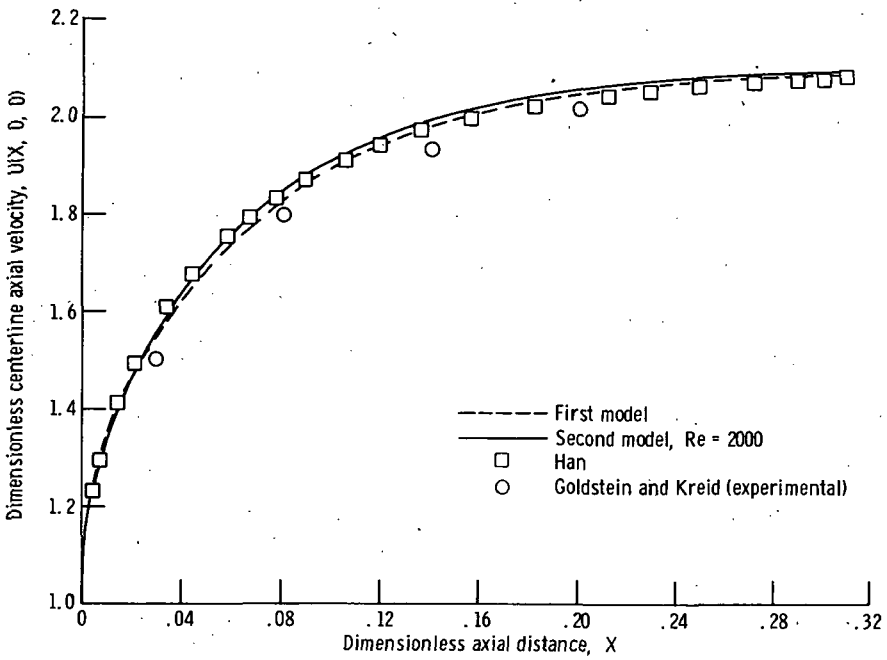


FIGURE 8-6.—Axial velocity at centerline of rectangular duct.

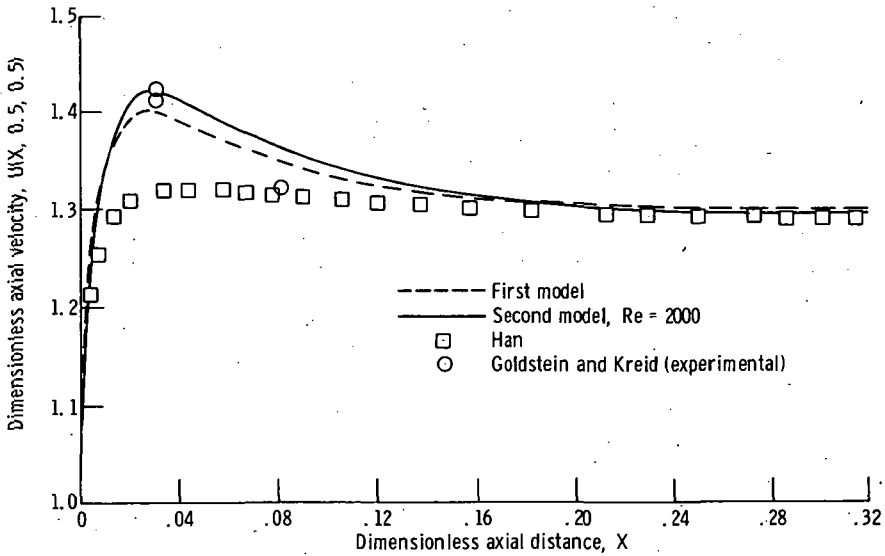
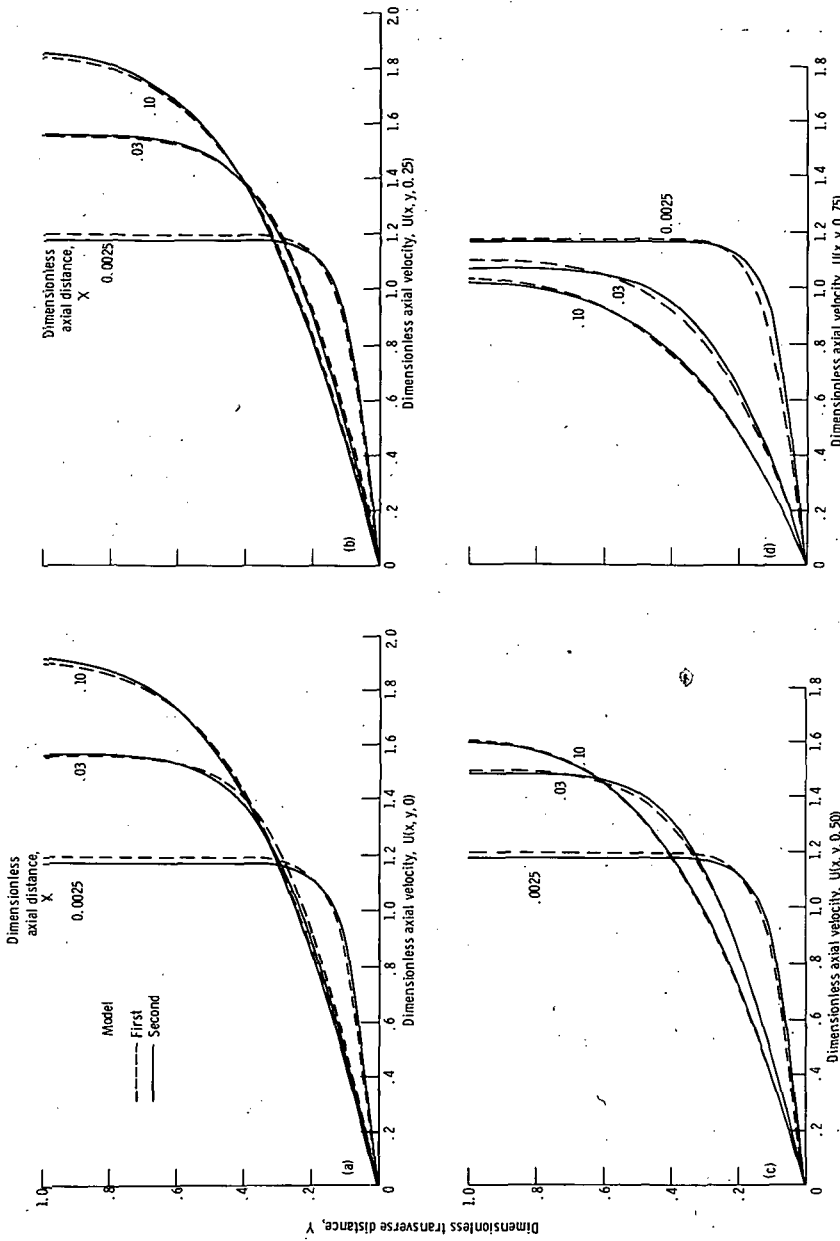


FIGURE 8-7.—Axial velocity at $Y=0.5, Z=0.5$ in rectangular duct.

Figure 8-8 shows axial velocity profiles from the first model and from the second model for $Re = 2000$ at various values of X . Results from the second model



(a) On centerplane $Z = 0$.
 (b) On the plane $Z = 0.25$.
 (d) On the plane $Z = 0.75$.

FIGURE 8-8. — Axial velocity profiles in a square duct for Reynolds number, Re , of 2000.

for $Re = 1000$, 750, and 650 differed only slightly from these profiles, and then only very close to the duct inlet. By $X = 0.02$, the velocity distributions obtained from the second model for all Reynolds numbers agreed to within 5 percent. An exception to this was found for $Re = 500$, but since considerable numerical difficulty was encountered for this Reynolds number, the results are not felt sufficiently reliable to report here.

Figure 8-9 compares the axial pressure distribution for various theoretical solutions. The two numerical models give results which fall below those of Han. The results for the second model are for $Re = 2000$, although the curve is virtually identical for all $Re \geq 650$ if $X > 0.02$. Since the second model does not explicitly employ integral continuity, there is a certain tendency for the flow rate to drift slightly because of roundoff error. The author therefore feels that the pressure distribution from the first model (which has been extrapolated to zero transverse mesh size) gives the most accurate pressure results.

Table 8-I shows the results of several investigators for the entrance length X_e , defined as the dimensionless axial position at which the centerline velocity reaches 99 percent of its fully developed value, and the kinetic energy correction factor F_{ke} , defined as

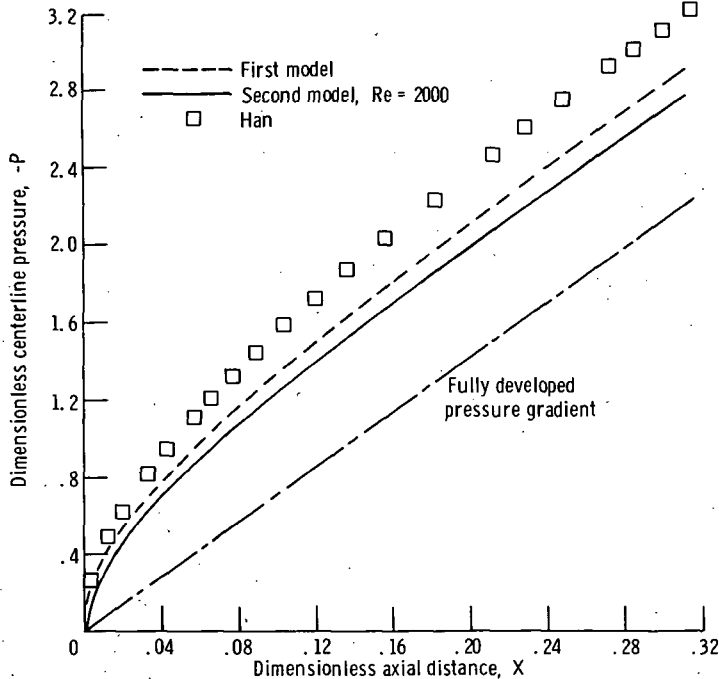


FIGURE 8-9.—Centerline pressure as function of axial position for various investigations.

TABLE 8-I.—ENTRANCE LENGTH AND KINETIC ENERGY CORRECTION FACTOR FOR SQUARE CHANNEL

Investigation	Dimensionless entrance length, X_e	Kinetic energy correction factor, F_{ke}
Han (ref. 8).....	0.301	1.51
Goldstein and Kreid (ref. 9) (experimental).....	.360
Lundgren, Sparrow and Starr (ref. 10).....	1.275
Present numerical solution:		
First model.....	.278	1.215
Second model.....	.266	1.073

$$F_{ke} = -P_{fd} + \left(\frac{dP}{dX} \right)_{fd} X + \frac{1}{2} \quad (8-141)$$

where P_{fd} is the dimensionless pressure evaluated at an X sufficiently large to be in the fully developed region and X is this position (see Goldstein, ref. 9). The analysis of Lundgren, Sparrow, and Starr (ref. 10) yields entrance pressure defects, but not velocity distributions, for arbitrary shaped ducts. The results shown are of course for the square duct. The large discrepancies in the entrance lengths among the various investigations were not unexpected, since this quantity is extremely sensitive to small variations in velocity and, as indicated by Goldstein and Kreid, can vary widely. With respect to the kinetic energy correction factor, it is worth noting that Sparrow, Hixon, and Shavit (ref. 11) carried out experiments on rectangular ducts, and although a square duct was not included, F_{ke} was considerably lower for other aspect ratios than previous theory (refs. 8 and 10) predicted. The results of the present numerical investigation for the square duct also show this trend.

Finally, we note that the results from the first model appear to be entirely adequate as compared to the more complex second model, at least for $Re \geq 650$. One additional point of interest is to examine the assumption employed in the first model that the transverse velocities are directed toward the duct centerline. The second model does not force this condition, but instead employs the two transverse momentum equations. Figure 8-10 shows the direction (but not the magnitude) of the local transverse velocity vectors in the cross section for the second model, $Re = 2000$, $X = 0.005$. With the exception of the immediate region of the corner, the assumption that the transverse velocities are directed toward the duct centerline seems to be satisfied very well. The validity of such an assumption, or variations thereof, for other aspect ratios remains to be proven.

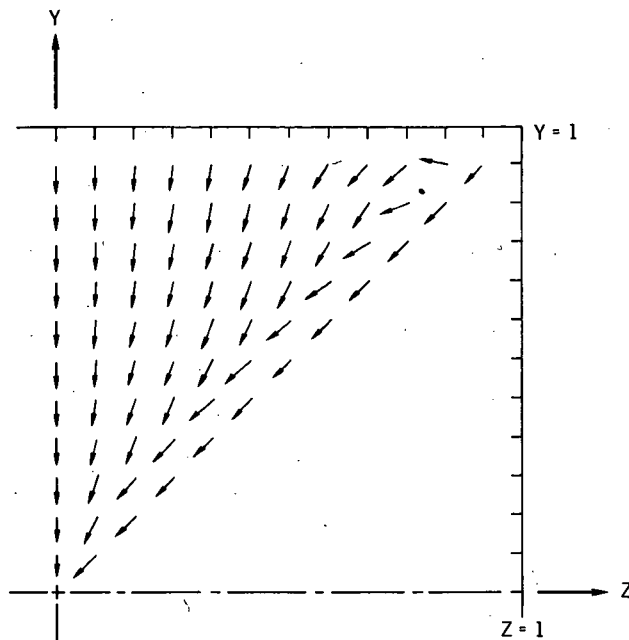


FIGURE 8-10.—Direction of local transverse velocity vectors for second model. Reynolds number, $Re = 2000$; dimensionless axial distance, $X = 0.005$.

REFERENCES

1. CARLSON, G. A.: Laminar Entrance Flow in a Square Duct. Ph. D. Thesis, Carnegie Inst. Tech., 1966.
2. MONTGOMERY, S. R.; AND WIBULSWAS, P.: Laminar Flow Heat-Transfer in Ducts of Rectangular Cross-Section. Proceedings of the Third International Heat Transfer Conference. Vol. 1. AIChE, 1966, pp. 104-112.
3. IRVINE, THOMAS F., JR.: Noncircular Duct Convective Heat Transfer. Modern Developments in Heat Transfer. Warren Shele, ed., Academic Press, 1963, pp. 1-17.
4. HORNBECK, ROBERT W.: The Entry Problem in Pipes with Porous Walls. Ph. D. Thesis, Carnegie Inst. Tech., 1961.
5. WALKER, M. L., JR.: Laminar Compressible Flow in the Entrance Region of a Tube. Ph. D. Thesis, Carnegie Inst. Tech., 1965.
6. DEISSLER, ROBERT G.; AND PRESLER, ALDEN F.: Analysis of Developing Laminar Flow and Heat Transfer in a Tube for a Gas with Variable Properties. Proceedings of the Third International Heat Transfer Conference. Vol. 1. AIChE, 1966, pp. 250-256.
7. HAN, L. S.: Hydrodynamic Entrance Lengths for Incompressible Laminar Flow in Rectangular Ducts. J. Appl. Mech., vol. 27, no. 3, Sept. 1960, pp. 403-409.
8. GOLDSTEIN, R. J.; AND KREID, D. K.: Measurement of Laminar Flow Development in a Square Duct Using a Laser-Doppler Flowmeter. J. Appl. Mech., vol. 34, no. 4, Dec. 1967, pp. 813-818.
9. GOLDSTEIN, SYDNEY, ED.: Modern Developments in Fluid Dynamics. Dover Publ., 1965.
10. LUNDGREN, T. S.; SPARROW, E. M.; AND STARR, J. B.: Pressure Drop Due to the Entrance Region in Ducts of Arbitrary Cross Section. J. Basic Eng., vol. 86, no. 3, Sept. 1964, pp. 620-626.
11. SPARROW, E. M.; HIXON, C. W.; AND SHAVIT, G.: Experiments on Laminar Flow Development in Rectangular Ducts. J. Basic Eng., vol. 89, no. 1, Mar. 1967, pp. 116-124.

CHAPTER 9

OTHER NONCIRCULAR AND VARYING AREA CHANNELS

The discussions to be presented in this chapter are concerned primarily with entrance flow and heat transfer problems. This is true for several reasons. If channels with varying cross-sectional areas are considered, then there is in general no fully developed solution; this is also true of compressible flow in any channel. Incompressible flow in constant area channels does eventually reach a fully developed flow situation, but this may be considered as a special case of the entrance flow. More important, fully developed flow in constant area channels is mathematically represented by a two-dimensional form of Poisson's equation, and very powerful and sophisticated techniques outside the scope of this book may, and indeed should, be employed if only the fully developed solution is required. Some of these techniques may also be useful in obtaining the entrance region solutions discussed later in this chapter.

9.1 NONCIRCULAR CHANNELS OF CONSTANT AREA

The solutions of problems of flow and heat transfer in channels having other than circular or rectangular cross sections present a variety of difficulties. The first obstacle is in the selection of the proper equations of motion. For certain geometries, a relation such as that specified between the transverse velocity components in the first model for the rectangular channel (section 8.1.1) may be useful. Other possibilities might include neglecting the inertia terms in the transverse momentum equations, specifying the axial component of the vorticity as zero, etc. While these stratagems have little physical foundation, the saving feature of problems of this type is that, at least based on the experience of Carlson (see ref. 1 and chapter 8) for the square channel, almost any relation between transverse velocities will give at least adequate results. This is probably due to the fact that as long as the region very close to the entrance is not considered, any

relation between transverse velocities will be of second order, as may be seen from an order of magnitude analysis of the fundamental equations (see section 8.1). In any case, some approximate relation between transverse velocity components is highly recommended in preference to solving the complete set of three momentum equations.

Another problem which may be encountered is the difficulty of dealing with irregular boundaries, or with boundaries not directly compatible with a rectangular or cylindrical finite difference grid. This problem has been discussed extensively by Forsythe and Wasow (ref. 2) and Allen (ref. 3) and can be a source of considerable difficulty in carrying out the details of a numerical solution. In some cases, it is possible to transform the problem to a coordinate system where a rectangular or cylindrical grid can be employed. If this is feasible, it is highly desirable because, although the equations of motion may be highly complicated in the new coordinate system, the finite difference approach is straightforward. It is also worthwhile to note at this point that finite difference representations can also be based on equilateral triangular, parallelogram, and hexagonal grids (see Allen, ref. 3). Although relatively little use is usually made of such grids, these grid shapes could be particularly useful for cross sections of similar shapes. The reader must be cautioned, however, that in employing such grid shapes he is largely on his own.

9.1.1 Alternating Direction Implicit (ADI) Techniques

An advantage available to investigators attempting to solve channel flow problems numerically is the large amount of work which has been done on the solution of elliptic problems involving second order differential equations such as Laplace's or Poisson's equation. Much of this work can be heuristically extended to the solution of channel flow problems, which at each step downstream have the appearance of an elliptic problem in the transverse directions. As mentioned before, if only the fully developed solution is desired, then these methods may be applied directly. Techniques such as the alternating direction implicit (ADI) methods have apparently not as yet been applied to any great extent to entrance flow problems, but they appear to show great promise for noncircular channels. Forsythe and Wasow (ref. 2) and Carnahan, Luther, and Wilkes (ref. 4) have excellent discussions of these techniques and their use in solving elliptic problems, and it would seem of little value to repeat the complete treatment here. However, a brief description might be in order.

ADI methods actually have two uses. They may be employed to solve problems such as the transient two-dimensional conduction equation, in which a solution for temperatures must be marched out in time while the spatially varying temperature field must be found at each time step. In addition, ADI methods may be used as effective iterative schemes for effectively solving spacewise elliptic problems such as Laplace's equation. Both of these capabilities are of interest to

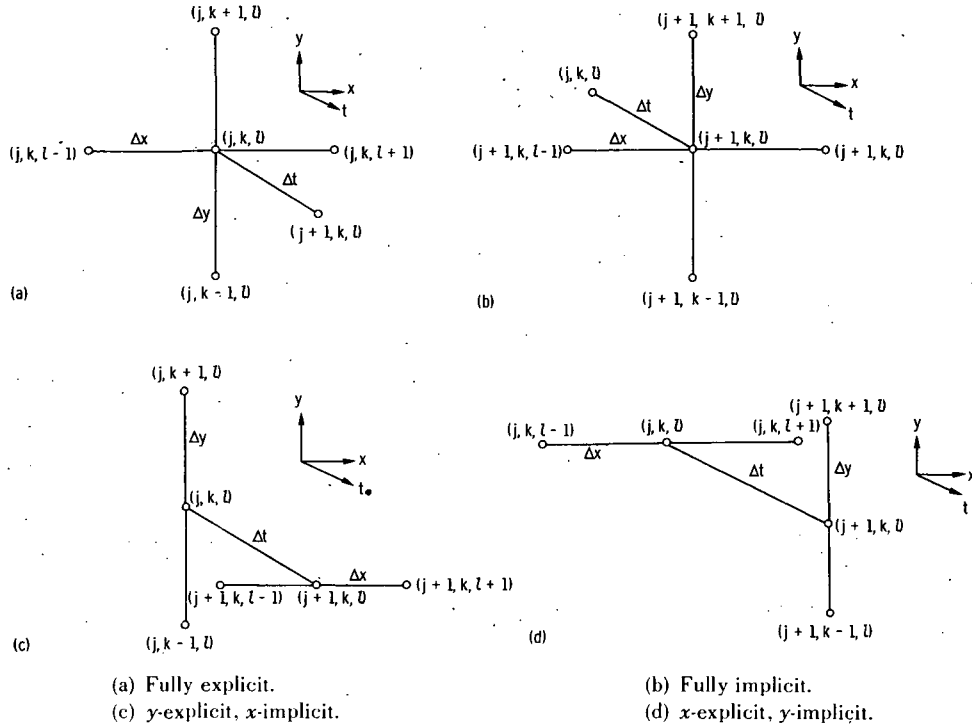


FIGURE 9-1. - Representation of two-dimensional transient conduction equation.

us in attempting to solve fluid flow and heat transfer problems in noncircular channels.

Consider first problems of the type represented by the two-dimensional transient conduction equation. There are two classical methods for solving this type of problem and both have serious drawbacks.

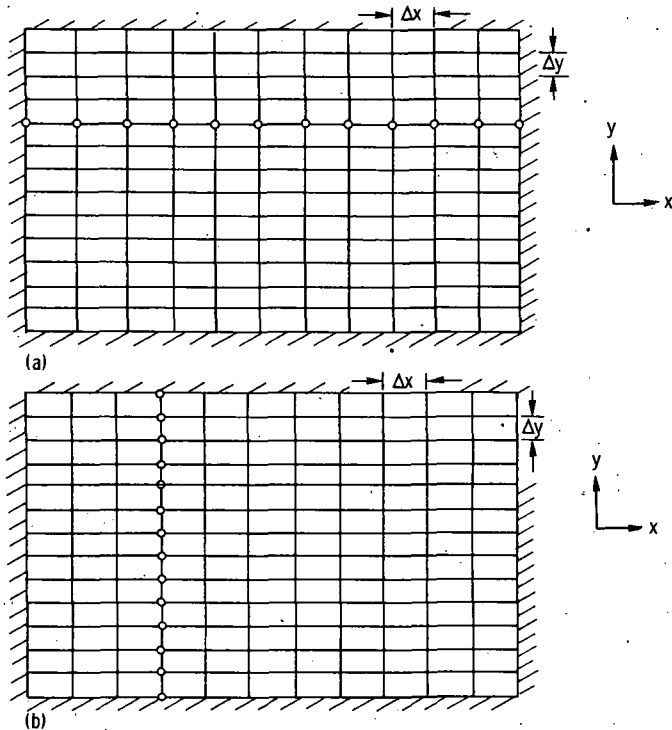
One of the methods is the fully explicit method which is shown in figure 9-1(a). In this method, all spatial derivatives are represented at the known time step j and the time derivative is represented as a forward difference, which brings in the value of the function at the unknown $j+1$ time step. This value may then be solved for directly (explicitly). When all the points in the space field at $j+1$ have been solved for, another time step may taken. The value of this method is that the amount of computer time per time step is very small. The drawback of the method is that stability restrictions force very small time steps, generally much smaller than necessary to obtain reasonable accuracy. As a result, many time steps are required and the computer time required increases correspondingly.

The other classical method is the fully implicit method, shown in figure 9-1(b), in which the spatial derivatives are expressed at the unknown $j+1$ time step and the time derivative as a backward difference. This method results in a

set of simultaneous linear algebraic equations in the values of the unknown function at $j+1$ equal in number to the number of points in the space grid. This set of equations can be quite time consuming to solve since, in general, it will be very large and iterative techniques must often be employed. The method has the advantage of universal stability, however, and any time step size consistent with accuracy may be used.

Obviously it would be advantageous to combine the best features of the explicit and implicit methods, and this is precisely what the alternating direction implicit methods accomplish.

The representations used in the Peaceman-Rachford method, a typical ADI method, are shown in figures 9-1(c) and (d). At one time step the y space difference is written at the known j time step and the x space difference is written at the unknown $j+1$ time step as shown in figure 9-1(c). When such an equation is written for every space point at $j+1$, instead of having a set of equations involving all values at all points in the space mesh, there results an independent set of linear



- (a) y -explicit, x -implicit form results in set of algebraic equations for each value of y , involving only unknowns along a single line as shown.
- (b) x -explicit, y -implicit form results in set of algebraic equations for each value of x , involving only unknowns along a single line as shown.

FIGURE 9-2.—Unknowns resulting from each of the alternating direction implicit forms.

algebraic equations involving *only* points along a given y -position, with a different independent set for each y -position as shown in figure 9-2(a). Each of these sets can be solved separately, and, very significantly, each of the sets has a matrix of coefficients which is *tridiagonal*. Thus, the very rapid method of appendix A may be used for each set and, as it turns out, no more computer time is required to solve the entire space field at a given time step than would be required by the fully explicit method. Once the entire space field has been solved for this time step, the difference representation is changed to that shown in figure 9-1(d). Another time step is then taken; and this time the result is a set of simultaneous tridiagonal linear algebraic equations for each value of x , as shown in figure 9-2(b), which may be solved as before. The procedure is thus to alternate at each new time step from the representation shown in figure 9-1(c) to that shown in figure 9-1(d) and back again. Because of the tridiagonal nature of the equations, no more computer time per time step is required than with the fully explicit method, but the procedure is *universally stable* so that the size of the time steps, as in the fully implicit method, is limited only by truncation error.

The use of the ADI methods to provide an iterative technique for the solution of elliptic problems such as Laplace's equation now follows directly. The values obtained on each iteration simply take the place of the values obtained at each time step in the preceding discussion. The representation is thus implicit in the values to be obtained on the present iteration and explicit in the known values from the last iteration. The resulting sets of tridiagonal equations are solved, the new values assume the role of the known values, the representation is alternated in direction, and the process repeated until convergence is obtained. ADI iterative techniques are among the most efficient iterative methods presently known for solving Laplace's and similar equations numerically, particularly when suitable relaxation factors are used.

9.1.2 Irregular Boundaries

If the techniques of coordinate transformation or the use of unusual mesh shapes as discussed earlier in this chapter do not make the boundaries compatible with the mesh used, then it becomes necessary to use a conventional rectangular or cylindrical grid and let the boundaries intersect the grid lines between grid points. Several methods may be used to treat these boundaries.

The first and simplest method is to use as fine a mesh as possible and to let the grid points fall where they may. Then, choose those points nearest the boundary as boundary points and the functions evaluated at these points as boundary values (see fig. 9-3). This method can work surprisingly well if a sufficiently fine mesh is employed. This has been called *interpolation of degree zero* by Forsythe and Wasow (ref. 2) in an excellent discussion of irregular boundaries.

An alternative which is not only aesthetically considerably more satisfying but which also gives much better results than interpolation of degree zero for the same mesh size, is to use central difference representations near the boundaries

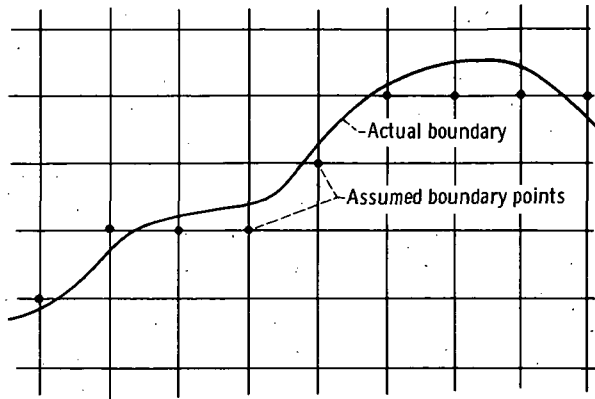


FIGURE 9-3. — “Zero degree interpolation” to represent irregular boundary.

that have unequal spacings between the grid points. These representations have been called *irregular stars* by Southwell (see Allen, ref. 3).

The discussion given here is based on the method of interpolation used in appendix D for unequal mesh sizes.

If a first central difference at the point k would span a boundary as shown in figure 9-4, then the difference may be expressed in terms of the boundary value as

$$\left. \frac{\partial f}{\partial y} \right|_k = \frac{f_B - f_k(1 - \theta^2) - f_{k-1}(\theta^2)}{\theta(1 + \theta)\Delta y} \quad (9-1)$$

If a second central difference at the point k would span the boundary as shown in figure 9-4, then the difference may be expressed as

$$\left. \frac{\partial^2 f}{\partial y^2} \right|_k = 2 \left[\frac{f_B - (1 + \theta)f_k + (\theta)f_{k-1}}{(1 + \theta)\theta(\Delta y)^2} \right] \quad (9-2)$$

These representations involve second degree interpolation. If the representations (9-1) and (9-2) near the boundary are used along with the usual second-degree symmetrical central difference representations in the interior, the equations

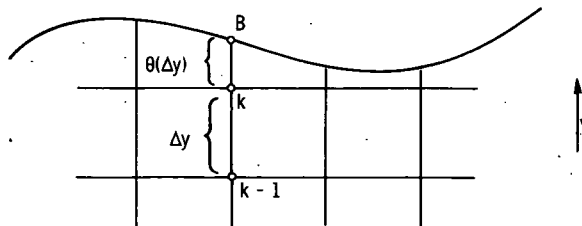


FIGURE 9-4. — Uneven mesh spacing near boundary.

of fluid motion and the energy equation can be written anywhere in an irregularly shaped field. Linear interpolation could also have been used to obtain formulas similar to equations (9-1) and (9-2); but the representations given here are more accurate, just about as simple to apply, and, most important, have the same error order as the usual central difference representations used elsewhere in this book.

The real difficulty of using such techniques as these at a boundary is in the amount of programming and computer time they require. With irregular boundaries one must continually check in the course of sweeps of the field to see if the boundary has been reached; if the boundary has been reached, special computations must be performed.

9.1.3 Normal Gradient Boundary Conditions

In the context of the problems discussed in this book, normal gradient boundary conditions will usually arise as heat flux conditions at a surface. If there are grid lines normal to the boundary at the desired point, then the normal gradient conditions may be expressed in the conventional manner used throughout this book. If, however, the boundaries are curved or irregular, then there may be great difficulty in expressing such conditions in difference form.

Although Forsythe and Wasow (ref. 2) indicate that it is far from clear how best to deal with this problem, they do present one possible approach which will be outlined here. Shaw (ref. 5) gives a similar discussion. It is assumed in this discussion that there are no corners on the boundary (i.e., that the boundary consists only of curves with no discontinuity in slope). The problem is illustrated in figure 9-5. Through each exterior grid point closest to the boundary, a perpendicular to the boundary is drawn and extended to the interior region of the cross section until it intersects a grid line. Thus, a line is drawn through P and perpendicular to S until it reaches point Q . The value of the function $f(Q)$ may be found in terms of $f(A)$ and $f(B)$ by linear interpolation. The value $f(P)$ will usually be unknown and will result from the solution of the problem. Then the normal gradient

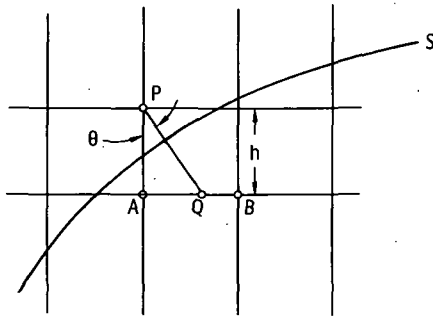


FIGURE 9-5.—Method for representing normal gradient boundary conditions.

$\partial f/\partial n$ is represented as

$$\frac{\partial f}{\partial n} = \frac{f(P) - f(Q)}{h/\cos \theta} \quad (9-3)$$

One such equation may be written for each of the grid points adjacent to the boundary. Equation (9-3) is not as accurate as the usual central difference representation to the differential equations involved and may be more compatible with the *extrapolation of degree zero* method of dealing with irregular boundaries than with any other more accurate method. In practice, it is apparently feasible to handle corners using this technique if the interior angle of the corner is not too small and if the mesh sizes are made sufficiently small, at least in the region of the corner.

9.1.4 General Remarks

The foregoing discussion should indicate clearly that the method of approach to the general problem of entrance flow and heat transfer in constant area noncircular channels is far from well defined. It is thus necessary, once a specific problem has been adequately mathematically formulated, to use to a considerable extent a "cut and try" technique. While this approach may be offensive to some formalists, there appears to be no substitute for it in the practical numerical analysis of a new (and usually nonlinear) engineering situation. If one generalization about the fluid flow problem can be made, it is that the use of an integral form of the continuity equation in finite difference form will almost invariably result in a reduction of the number of equations which it is necessary to solve. However, even this statement is true only when some simplified model for the flow has been chosen as opposed to solving the complete Navier-Stokes equations with only the axial second derivatives neglected.

9.2 CHANNELS OF VARYING CROSS-SECTIONAL AREA

Flow and heat transfer in channels of varying cross-sectional area present the additional complication to a finite difference analysis that the total number of transverse mesh points and/or the transverse mesh size will not remain constant as each axial step is taken.

Since the fundamental equations in such flows are identical to those for constant area channels (assuming that the area changes with axial position are not so severe that separation occurs or that the second axial derivatives of velocity and temperature can no longer be neglected), our concern is with the mechanics of varying the number of mesh points or size of the mesh as necessary.

Three possible approaches to the problem are the following:

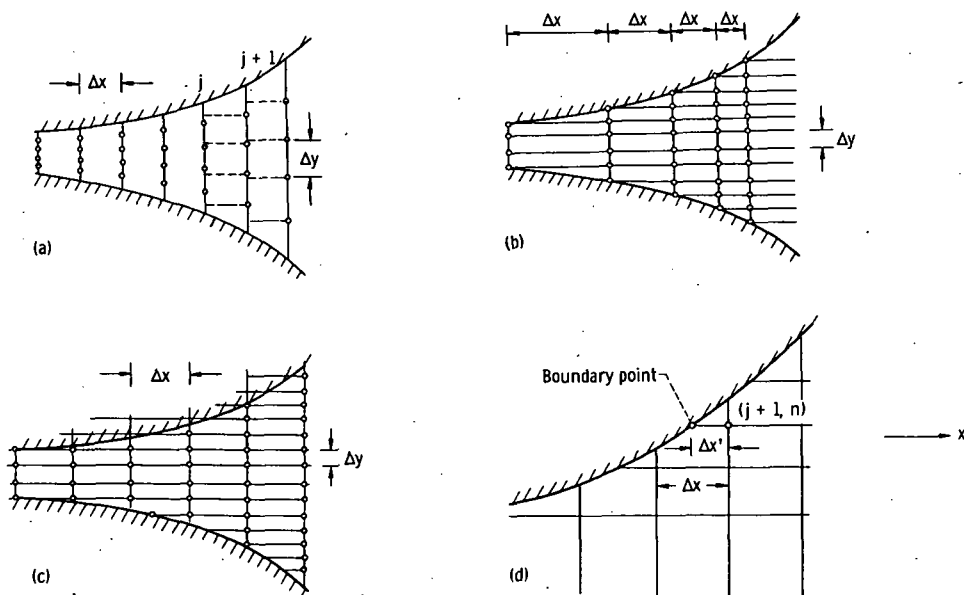
- (1) Adjust the transverse grid size with each axial step so that the total number

of transverse grid points remains constant. This technique (illustrated in fig. 9-6(a)) results in difficulties in the evaluation of backward differences. Since the values of the function are not available exactly at the points desired, it is necessary to interpolate for these values.

(2) Adjust the axial step size so that exactly one transverse grid point is added (or subtracted) while maintaining the same transverse grid size (see fig. 9-6(b)).

(3) Maintain the transverse grid size as constant and let the boundary fall where it may, then adjust the difference representation that spans the boundary (see fig. 9-6(c)).

We shall now discuss briefly the use, advantages, and disadvantages of these three approaches. Method (1) (fig. 9-6(a)) requires interpolation at location j so that the values of the function at these points may be used in evaluating backward differences. It would appear that accuracy is not sacrificed in this process, providing that the interpolation is of such an order as to provide error no greater than the difference equations themselves (usually interpolation on a second-degree polynomial will be sufficient). Some extra computational time is required to do the necessary interpolation after each axial step. This technique of interpolation has been used successfully by Beus (ref. 6) in his numerical investigation of



(a) Number of transverse grid points held constant.

(b) Axial step size adjusted to add one transverse point on each side of channel at each axial step.

(c) Axial and transverse step sizes held constant and boundary allowed to cross grid at any point.

(d) Evaluation of backward differences for method (3) in diverging section.

FIGURE 9-6. — Methods of handling grid structure in channels of varying area.

compressible flow in varying area channels, which is discussed in section 9.3 as an example problem.

Method (2) (fig. 9-6(b)) has the advantage that backward differences may be evaluated directly. However, if the channel area changes very slowly, the axial step size may be larger than desired; if the transverse mesh is reasonably coarse, the effect will be exaggerated. One reasonable course of action with this method is to employ the variable mesh technique discussed in appendix D. By employing this technique, the transverse mesh size in the region immediately adjacent to the wall can be made as small as desired and, correspondingly, the axial mesh size can be held to a moderate level. A potential difficulty with this method is that in a diverging section (e.g., a diffuser) if the transverse mesh size is held constant, then the number of grid points may become too large. This difficulty may be countered by using the same approach employed for the free flows discussed in chapters 2 to 5—that is, by doubling the transverse grid size and halving the number of points at some axial station and then proceeding as before.

Method (3) (fig. 9-6(c)) appears to overcome most of the shortcomings of the other two methods, but this may be only the result of the fact that the author has had personal experience with using the first two methods but not with the third. This method allows the direct computation of backward differences except for the points adjacent to the boundary in a diverging section, and it allows an arbitrary choice of axial step size. Those transverse differences which span the boundary may be evaluated by the use of equations (9-1) and (9-2). For the points adjacent to the boundary in a diverging section, as shown in figure 9-6(d), the backward differences may be evaluated as

$$\left. \frac{\partial f}{\partial x} \right|_{j+1, n} = \frac{f_{j+1, n} - f(\text{evaluated at boundary})}{\Delta x'} \quad (9-4)$$

The evaluation of equation (9-4) requires no auxiliary computation since the value of f (boundary) is known.

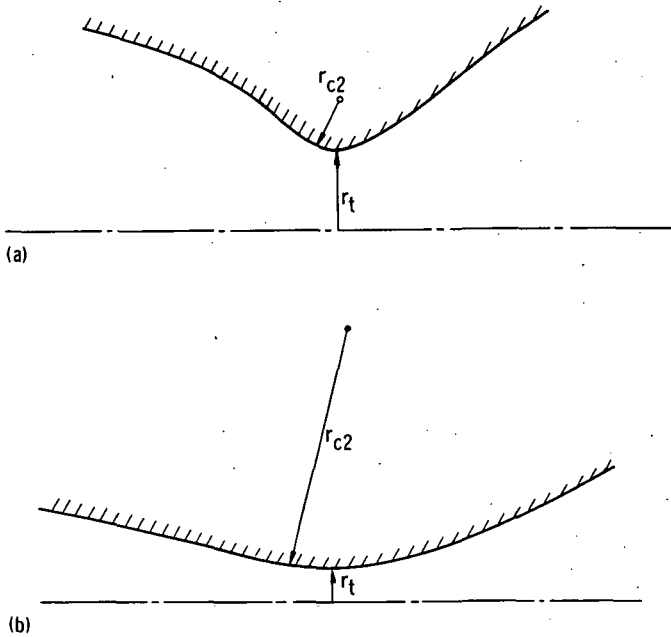
No matter which method is used, it may be necessary to use very small mesh sizes in a converging section or at a throat, since the boundary layer thicknesses can become very small in these regions and the gradients very high. If it becomes necessary to shift from a coarse transverse mesh to a finer one as the solution is carried downstream, then some type of interpolation such as that indicated in method 1 will have to be employed, at least at the one axial position in the channel where the transverse mesh size change takes place.

As in all channel flows, the use of integral continuity in difference form will help to reduce the number of simultaneous equations to be solved.

Flow and heat transfer in noncircular channels of varying cross-sectional area and arbitrary cross section would appear to present a monumental challenge to the numerical analyst, and to the author's knowledge, no information in these areas is available.

9.3 EXAMPLE PROBLEM—COMPRESSIBLE FLOW IN VARYING AREA CHANNELS

The example given here is the solution presented by Beus (ref. 6) for the compressible flow in axisymmetric channels of varying area, with particular application to converging-diverging nozzles. A single set of equations of the boundary layer type is applied to the entire flow field and numerical techniques are employed which are adapted from those discussed in section 7.1.4 for the constant area tube. The use of the boundary layer model over the entire flow field allows the consideration of the effect of the growth of the boundary layer on the flow rate through the nozzle. This effect is neglected in the usual nozzle analysis, in which the boundary layer is ignored in computing the inviscid flow in the nozzle, and the resulting pressure gradient is imposed on the wall boundary layer. The latter approach is entirely adequate and, in fact, necessary for nozzles which are relatively short and of large diameter with a relatively small radius of curvature at the throat (see fig. 9-7(a)). This approach is not sufficient, however, for long slender nozzles (fig. 9-7(b)) which are of increasing importance in fluidics applications. For long slender nozzles, the boundary layer model considered here properly includes the viscous effects on nozzle flow rate.



(a) Small throat radius of curvature, large throat radius.
(b) Slender nozzle.

FIGURE 9-7.—Nozzle geometry.

The fundamental equations of viscous compressible flow employed by Beus are equations (7-45) to (7-50) of section 7.1.4, with the following boundary conditions:

$$u(r_w, z) = 0$$

$$u(r, 0) = u_0(r) \text{ where various boundary layer thicknesses are specified at the nozzle inlet (see appendix F)}$$

$$\frac{\partial u}{\partial r}(0, z) = 0$$

$$v(r_w, z) = 0$$

$$v(0, z) = 0$$

$$p(0) = p_0$$

$$t(r, 0) = t_0$$

$$\frac{\partial t}{\partial r}(0, z) = 0$$

(9-5)

and

$$t(r_w, z) = t_w \text{ (constant wall temperature)}$$

or

$$\frac{\partial t}{\partial r}(r_w, z) = 0 \text{ (adiabatic wall)}$$

The dimensionless variables employed are (7-53) of section 7.1.4 with a representing a characteristic radius of the nozzle (Beus employed the inlet radius) and u_0 replaced by any characteristic velocity chosen as convenient. The resulting dimensionless equations are (7-54) to (7-59) with the following dimensionless boundary conditions:

$$\begin{aligned}
 U(R_w, Z) &= 0 \\
 U(R, 0) &= U_0(R) \\
 \frac{\partial U}{\partial R}(0, Z) &= 0 \\
 V(R_w, Z) &= 0 \\
 V(0, Z) &= 0 \\
 P(0) &= 1 \\
 T(R, 0) &= 1 \\
 \frac{\partial T}{\partial R}(0, Z) &= 0 \\
 \text{and} \\
 T(R_w, Z) &= T_w \text{ (constant wall temperature)} \\
 \text{or} \\
 \frac{\partial T}{\partial R}(R_w, Z) &= 0 \text{ (adiabatic wall)}
 \end{aligned}
 \tag{9-6}$$

Because the boundary layers in the throat area are quite thin, some type of variable mesh procedure was indicated. Rather than employ the method of appendix D, which would be somewhat unwieldy in a variable area channel, Beus chose to make the following transformation of the radial coordinate:

$$Y = R_w^s - R^s \left\{ \begin{array}{l} s \geq 1 \\ 0 \leq R \leq R_w \\ R_w^s \geq Y \geq 0 \end{array} \right. \tag{9-7}$$

where $R_w(z)$ is the local radius of the duct. Equally spaced Y -coordinate points may now result in unequally spaced points in the R -coordinate. Larger values of s result in a bunching of points close to the wall in the R -coordinate, exactly the effect desired to accommodate the high velocity gradients in the boundary layer. The resulting differential equations and finite difference forms chosen are much too lengthy to repeat here, and the reader is referred to reference 6 for details.

One particular difficulty which arises due to the area variation is worth noting—mainly to indicate the difficulties which may arise in the type of problem discussed in this chapter. For various reasons, it is more useful in the compressible nozzle flow problem to write integral continuity in the form

$$\int_0^{r_w} \frac{\partial}{\partial z} (\rho u) r \, dr = 0 \tag{9-8}$$

rather than in the usual form

$$\int_0^{r_w} \rho u r dr = \text{constant} \quad (9-9)$$

For a constant area duct, equations (9-8) and (9-9) are actually identical equations when written in finite difference form, both simply stating that

$$\int_0^{r_w} \rho u r dr \Big|_j = \int_0^{r_w} \rho u r dr \Big|_{j+1} \quad (9-10)$$

However, if r_w is a function of z , the finite difference forms of equations (9-8) and (9-9) are not identical due to different truncation errors involved in their difference representations. In practice, since equation (9-8) does not explicitly hold the flow rate constant when written in difference form, a certain amount of cumulative drift tended to occur in the flow rate as the solution was carried downstream. This was corrected by an iterative procedure carried out at each step involving the difference forms of both equations (9-8) and (9-9) (in dimensionless form, of course). To obtain convergence it was necessary to underrelax the difference form of equation (9-9). The amount of underrelaxation varied, depending on whether a converging or diverging section was being considered. Some difficulty was encountered with convergence at the throat as will be discussed later.

The parameters which must be considered in the problem include the geometry, the Prandtl number, and the inlet Mach number. For a given geometry and Prandtl number, if a low inlet Mach number is specified, then as the solution is marched downstream, the flow is subsonic through the converging section, subsonic in the throat, and subsonic in the diffuser. As the inlet Mach number is raised, a point is eventually reached where the flow becomes almost sonic at the throat, before it drops back down subsonically through the diffuser. The nozzle is then running slightly below what must be considered as design conditions for that geometry. If the inlet Mach number is increased by a significant amount, a violent numerical instability results immediately beyond the throat. If, instead, the inlet Mach number is increased by increments as small as of the order of $\Delta M_0 = 0.00001$, then an inlet Mach number can be found which results in the flow at the throat passing smoothly through the transonic region and accelerating supersonically out through the diffuser. The nozzle is then running at its design conditions. The design pressure ratio is simply the dimensionless exit pressure of the diffuser. (Any desired point in the diffuser may be considered as the exit, since the nozzle can be cut off at any point in the diffuser without disturbing the upstream flow as long as the flow is supersonic). This calculation is obviously very sensitive to the inlet Mach number and the search for the correct value can be quite time consuming. The iterative procedure on integral continuity mentioned earlier must be suspended for a few steps through the transonic region at the throat since it is not possible to obtain convergence in this region. Fortunately, the flow rate varies little in this region because of the small area variation, and the results are not significantly affected.

Now that some of the considerable difficulties of the technique have been discussed (again demonstrating the amount of art necessary in such calculations), we turn to some representative results. These results were obtained with basic mesh sizes of $0.02 \leq \Delta Y \leq 0.05$ and $\Delta Z = 0.0001$, although ΔZ was reduced whenever the area varied rapidly or when $1.25 > M > 0.75$, and values of ΔY as small as $\Delta Y = 0.005$ were used for checking purposes. The transformation exponent s in equation (9-7) was varied between 2 and 6 as required to provide sufficient mesh points within the velocity and thermal boundary layers. Different relaxation factors for the iterative scheme on integral continuity were necessary in different regions of the nozzle. Details may be found in reference 6. The equations and programs were verified by comparing results with existing solutions for straight tubes, both compressible and incompressible, and with varying area incompressible flow solutions.

Figure 9-8 shows a comparison of the pressure distribution obtained from the numerical solution with the classical one-dimensional isentropic nozzle solution

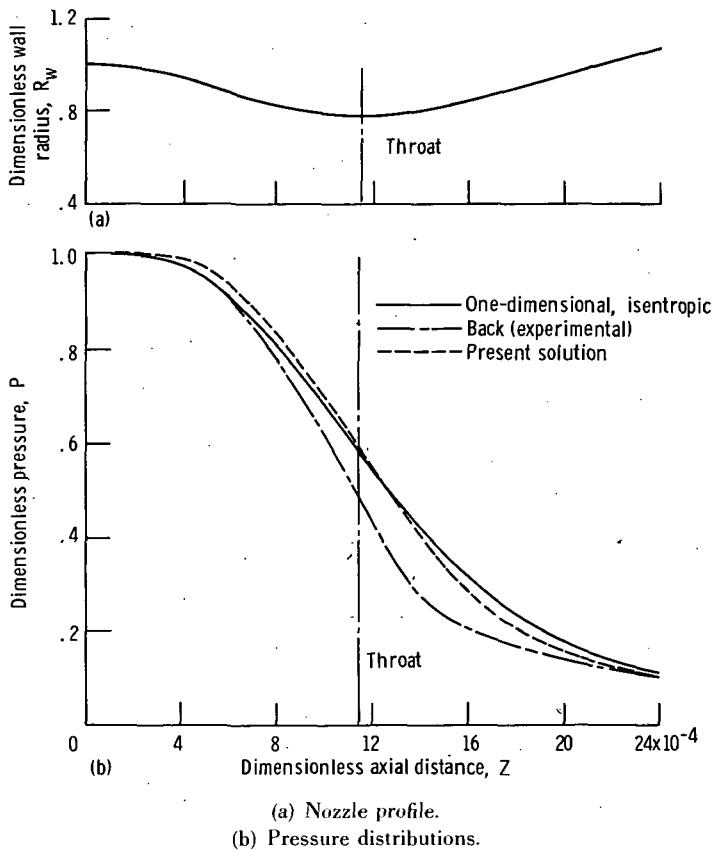


FIGURE 9-8.—Nozzle profile and pressure distributions in a nonslender nozzle.

and with the experimental distribution of Back, Massier, and Gier (ref. 7) for a subsonic-supersonic nozzle. This nozzle is not actually sufficiently slender to expect either the numerical solution or the one-dimensional isentropic solutions to be particularly accurate, but the nature of the numerical solution, particularly in its slope near the throat, indicates that at least some of the two-dimensional and viscous effects not included in the one-dimensional solution have been accounted for.

Figure 9-9 is representative of most of the results of this investigation. It shows the velocity distributions for a typical slender nozzle with a thick boundary layer ($\delta/r_w = 0.8$) at the nozzle inlet. The boundary layer is obviously sufficiently thick through the entire nozzle that the effect of the boundary layer thickness on the flow rate cannot be neglected.

Table 9-1 shows the effect of the boundary layer on flow rate for several adiabatic nozzles. The W_r is defined as the ratio of the flow rate obtained from the numerical solution to the flow rate obtained from a one-dimensional isentropic solution for the same pressure ratio across the nozzle. The largest flow rate decrease, about 25 percent, occurs for the nozzle with the largest inlet boundary layer thickness ratio, case 3. For a fixed inlet boundary layer thickness ratio (cases 1, 2 and 4), the flow rate decreases with increasing slenderness of the nozzle (increasing throat ratio) because of the thicker boundary layers in the interior of the more slender nozzles.

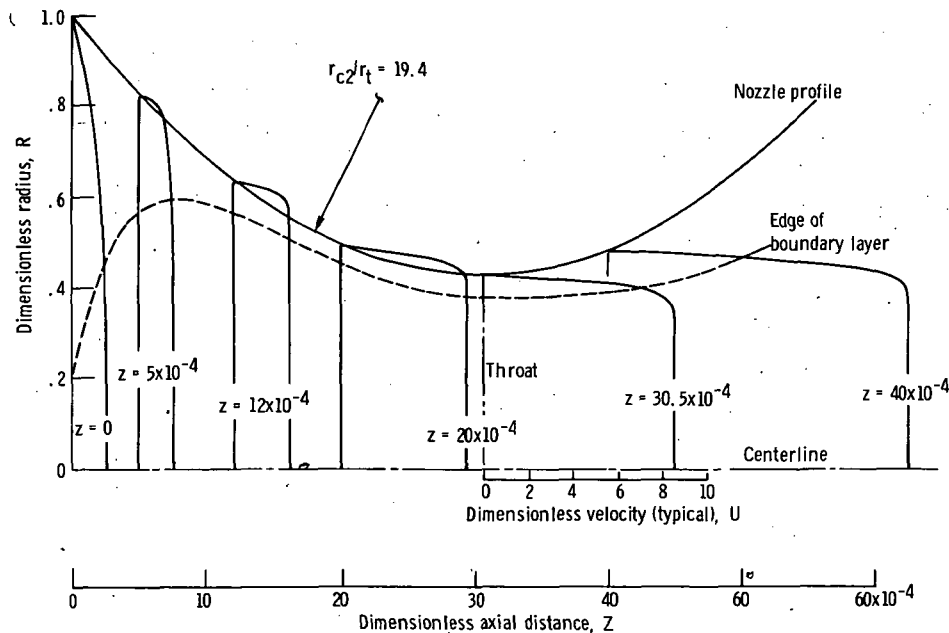


FIGURE 9-9. — Velocity profiles for typical nozzle ($\delta/r_w)_0 = 0.80$.

TABLE 9-I.—FLOW RATE RATIO COMPARISON

Case	Throat ratio, r_c/r_t	Inlet boundary layer thickness, $(\delta/r_w)_0$	Flow rate ratio, W_r
1	2.0	0.30	0.947
2	19.4	.30	.918
3	19.4	.80	.744
4	200.0	.30	.885

REFERENCES

1. CARLSON, G. A.: Laminar Entrance Flow in a Square Duct. Ph.D. Thesis, Carnegie Inst. Tech., 1966.
2. FORSYTHE, GEORGE E.; AND WASOW, WOLFGANG R.: Finite-Difference Methods for Partial Differential Equations. John Wiley & Sons, Inc., 1960.
3. ALLEN, DERYCK N. DE G.: Relaxation Methods in Engineering and Science. McGraw-Hill Book Co., Inc., 1954.
4. CARNAHAN, BRICE; LUTHER, H. A.; AND WILKES, JAMES O.: Applied Numerical Methods. John Wiley & Sons, Inc., 1969.
5. SHAW, FREDERICK S.: An Introduction to Relaxation Methods. Dover Publ., 1953.
6. BEUS, S. G.: Compressible Viscous Flow in Varying-Area Ducts. Ph. D. Thesis, Carnegie-Mellon Univ., 1968.
7. BACK, L. H.; MASSIER, P. F.; AND GIER, H. L.: Comparison of Measured and Predicted Flows Through Conical Supersonic Nozzles, with Emphasis on the Transonic Region. AIAA J., vol. 3, no. 9, Sept. 1965, pp. 1606-1614.

tions of multiplying or dividing any equation by a constant and adding or subtracting any equation from any other equation. This upper triangular set has the form

$$\begin{array}{cccccccc|c|c|c}
 D_{11} & D_{12} & D_{13} & \cdots & \cdots & \cdots & D_{1n} & & Y_1 & & S_1 \\
 & D_{22} & D_{23} & \cdots & \cdots & \cdots & D_{2n} & & Y_2 & & S_2 \\
 & & D_{33} & \cdots & \cdots & \cdots & D_{3n} & & Y_3 & & S_3 \\
 & & & \cdots & \cdots & \cdots & \cdots & & \times & = & \cdots \\
 & & & & \cdots & \cdots & \cdots & & & & \cdots \\
 & & & & & D_{(n-1)(n-1)} & D_{(n-1)n} & & & & Y_{n-1} & S_{n-1} \\
 & & & & & & D_{nn} & & & & Y_n & S_n
 \end{array} \quad (A-2)$$

The last equation may then be solved directly for Y_n , the next to the last for Y_{n-1} once Y_n has been found, etc., continuing the back substitution until the top equation is finally solved for Y_1 . A variation of this method, called Gauss-Jordan elimination, is presented in appendix E.

Equations of the form (A-1) are particularly easy to put into the form (A-2). A number of the necessary operations will be performed on equation (A-1) to illustrate the method and then generalized to a recurrence scheme highly suitable for a digital computer. First, the top equation in (A-1) is divided by B_1 :

$$\begin{array}{cccc|c|c|c}
 1 & \frac{C_1}{B_1} & & & X_1 & & \frac{R_1}{B_1} \\
 A_2 & B_2 & C_2 & & \times X_2 & = & R_2 \\
 A_3 & B_3 & C_3 & & X_3 & & R_3
 \end{array} \quad (A-3)$$

The top equation is now multiplied by A_2 and subtracted from the second equation:

$$\begin{array}{cccc|c|c|c}
 1 & \frac{C_1}{B_1} & & & X_1 & & \frac{R_1}{B_1} \\
 \left(B_2 - \frac{C_1 A_2}{B_1}\right) & C_2 & & & \times X_2 & = & \left(R_2 - \frac{R_1}{B_1} A_2\right) \\
 A_3 & B_3 & C_3 & & X_3 & & R_3
 \end{array} \quad (A-4)$$

With the relatively well-conditioned sets of equations which result from finite difference representations, sets of equations with n of the order of several hundred may be readily and accurately handled using this method.

The method may now be presented in the form of an algorithm. We employ the usual computer notation in which the equal sign means *replaced by*. The elements of the matrix equation (A-1) are modified as follows:

$$\begin{array}{l}
 C_1 = \frac{C_1}{B_1} \\
 R_1 = \frac{R_1}{B_1} \\
 B_1 = 1 \\
 k = 2(1)n \quad \left\{ \begin{array}{l} B_k = B_k - C_{k-1}A_k \\ C_k = \frac{C_k}{B_k} \\ R_k = R_k - R_{k-1}A_k \end{array} \right. \\
 X_n = R_n \\
 k = n(-1)2 \quad \{ X_{k-1} = -X_k C_{k-1} + R_{k-1} \}
 \end{array} \quad (A-8)$$

To complete this discussion, we now present a FORTRAN IV subprogram which accomplishes the solution discussed in this appendix. The symbols are those used in equation (A-1). For simplicity, the dimensions used in the dimension statement on A , B , C , X , and R have been shown as 120. It is suggested that the value of n be inserted in this dimension statement whenever the routine is employed; more sophisticated dimensioning procedures are possible but depend on the particular FORTRAN compiler used and will not be discussed here.

C PROGRAM FOR SOLVING SET OF TRIDIAGONAL EQUATIONS

```
SUBROUTINE TRIDI(A, B, C, X, R, N)
```

```
  DIMENSION A(120), B(120), C(120), X(120), R(120)
```

```
  A(N) = A(N)/B(N)
```

```
  R(N) = R(N)/B(N)
```

```
DO 1100 I=2, N
  II=-I+N+2
  BN=1./(B(II-1)-A(II)*C(II-1))
  A(II-1)=A(II-1)*BN
1100 R(II-1)=(R(II-1)-C(II-1)*R(II))*BN
  X(1)=R(1)
  DO 1101 I=2, N
1101 X(I)=R(I)-A(I)*X(I-1)
  RETURN
END
```

The routine is called from the main program by the statement

```
CALL TRIDI(A, B, C, X, R, N)
```

The results are left in the vector X and A, B, C, and R are destroyed.

APPENDIX B—FINITE DIFFERENCE REPRESENTATIONS, TRUNCATION ERROR ANALYSIS, AND STABILITY ANALYSIS

B.1 FINITE DIFFERENCE REPRESENTATIONS

The foundation of all numerical analysis, and particularly of finite difference methods, is the Taylor series. A function $H(x)$ may be expanded in a Taylor series near $x = x_0$ if H and all of its derivatives exist and are finite near $x = x_0$. The infinite series expression is

$$H(x) = H(x_0) + (x - x_0) \left. \frac{dH}{dx} \right|_{x=x_0} + \frac{(x - x_0)^2}{2!} \left. \frac{d^2H}{dx^2} \right|_{x=x_0} + \frac{(x - x_0)^3}{3!} \left. \frac{d^3H}{dx^3} \right|_{x=x_0} + \dots \quad (\text{B-1})$$

For the present discussion, we limit ourselves to functions of a single independent variable arbitrarily called x , but the results may be directly extended to functions of many variables. We employ the following notation:

$$\left. \begin{aligned} x - x_0 &= \Delta x \\ H(x) &= H(x_0 + \Delta x) = H_{j+1} \\ H(x_0) &= H_j \\ \left. \frac{dH}{dx} \right|_{x_0} &= \left. \frac{dH}{dx} \right|_j, \text{ etc.} \end{aligned} \right\} \quad (\text{B-2})$$

Equation (B-1) may then be rewritten as

$$H_{j+1} = H_j + \Delta x \left. \frac{dH}{dx} \right|_j + \frac{(\Delta x)^2}{2!} \left. \frac{d^2H}{dx^2} \right|_j + \frac{(\Delta x)^3}{3!} \left. \frac{d^3H}{dx^3} \right|_j + \dots \quad (\text{B-3})$$

We may obtain an expression for $\left. \frac{dH}{dx} \right|_j$ by solving equation (B-3) for this quantity:

$$\left. \frac{dH}{dx} \right|_j = \frac{H_{j+1} - H_j}{\Delta x} - \frac{\Delta x}{2!} \left. \frac{d^2H}{dx^2} \right|_j - \frac{(\Delta x)^2}{3!} \left. \frac{d^3H}{dx^3} \right|_j + \dots \quad (\text{B-4})$$

If only values of H are known, but not any of its derivatives, then equation (B-4) provides an approximation to $\left. \frac{dH}{dx} \right|_j$ if we neglect all terms involving higher derivatives of H . Since Δx is small and the derivatives of H are finite (but unknown), the dominant error term in equation (B-4) will presumably be $\left. \frac{\Delta x}{2} \frac{d^2H}{dx^2} \right|_j$. Since the only part of the term which is under our control is Δx , we say that

$$\left. \frac{dH}{dx} \right|_j = \frac{H_{j+1} - H_j}{\Delta x} + \mathcal{O}(\Delta x) \quad (\text{B-5})$$

where $\mathcal{O}(\Delta x)$ is interpreted as *of order* Δx . The term $(H_{j+1} - H_j)/\Delta x$ is called a *forward difference representation of* $\left. \frac{dH}{dx} \right|_j$ *of error order* Δx .

If we define

$$H_{j-1} = H(x_0 - \Delta x) \quad (\text{B-6})$$

and express H_{j-1} by a Taylor series expansion around x_0 , we obtain

$$H_{j-1} = H_j - \Delta x \left. \frac{dH}{dx} \right|_j + \frac{(\Delta x)^2}{2!} \left. \frac{d^2H}{dx^2} \right|_j - \frac{(\Delta x)^3}{3!} \left. \frac{d^3H}{dx^3} \right|_j + \dots \quad (\text{B-7})$$

Solving this equation for $\left. \frac{dH}{dx} \right|_j$ gives

$$\left. \frac{dH}{dx} \right|_j = \frac{H_j - H_{j-1}}{\Delta x} + \frac{\Delta x}{2!} \left. \frac{d^2H}{dx^2} \right|_j - \frac{(\Delta x)^2}{3!} \left. \frac{d^3H}{dx^3} \right|_j + \dots \quad (\text{B-8})$$

or

$$\left. \frac{dH}{dx} \right|_j = \frac{H_j - H_{j-1}}{\Delta x} + \mathcal{O}(\Delta x) \quad (\text{B-9})$$

The expression $(H_j - H_{j-1})/\Delta x$ is called the *backward difference expression of error order* Δx for $\left. \frac{dH}{dx} \right|_j$.

If equation (B-7) is subtracted from equation (B-3), we obtain

$$H_{j+1} - H_{j-1} = 2(\Delta x) \left. \frac{dH}{dx} \right|_j + \frac{2(\Delta x)^3}{3!} \left. \frac{d^3H}{dx^3} \right|_j + \dots \quad (\text{B-10})$$

Solving for $\left. \frac{dH}{dx} \right|_j$,

$$\left. \frac{dH}{dx} \right|_j = \frac{H_{j+1} - H_{j-1}}{2(\Delta x)} - \frac{(\Delta x)^2}{3!} \left. \frac{d^3H}{dx^3} \right|_j - \frac{(\Delta x)^4}{5!} \left. \frac{d^5H}{dx^5} \right|_j + \dots \quad (\text{B-11})$$

or

$$\left. \frac{dH}{dx} \right|_j = \frac{H_{j+1} - H_{j-1}}{2(\Delta x)} + \mathcal{O}((\Delta x)^2) \quad (\text{B-12})$$

The expression $(H_{j+1} - H_{j-1})/2(\Delta x)$ is called a *central difference expression of error order* $(\Delta x)^2$ for $\left. \frac{dH}{dx} \right|_j$. Since Δx is small, the central difference expression (B-12) is more accurate than either the forward (B-5) or backward (B-8) difference expressions for $\left. \frac{dH}{dx} \right|_j$, assuming a fixed Δx .

We shall require only one type of difference expression for the second derivative. This may be found by equating the expressions for $\left. \frac{dH}{dx} \right|_j$ from equations (B-4) and (B-8):

$$\begin{aligned} \frac{H_{j+1} - H_j}{\Delta x} - \frac{\Delta x}{2!} \left. \frac{d^2H}{dx^2} \right|_j - \frac{(\Delta x)^2}{3!} \left. \frac{d^3H}{dx^3} \right|_j - \frac{(\Delta x)^3}{4!} \left. \frac{d^4H}{dx^4} \right|_j + \dots \\ = \frac{H_j - H_{j-1}}{\Delta x} + \frac{\Delta x}{2!} \left. \frac{d^2H}{dx^2} \right|_j - \frac{(\Delta x)^2}{3!} \left. \frac{d^3H}{dx^3} \right|_j + \frac{(\Delta x)^3}{4!} \left. \frac{d^4H}{dx^4} \right|_j + \dots \end{aligned} \quad (\text{B-13})$$

Solving for $\left. \frac{d^2H}{dx^2} \right|_j$ gives

$$\left. \frac{d^2H}{dx^2} \right|_j = \frac{H_{j+1} - 2H_j + H_{j-1}}{(\Delta x)^2} - \frac{(\Delta x)^2}{12} \left. \frac{d^4H}{dx^4} \right|_j + \dots + \mathcal{O}(\Delta x)^4 \quad (\text{B-14})$$

or

$$\left. \frac{d^2H}{dx^2} \right|_j = \frac{H_{j+1} - 2H_j + H_{j-1}}{(\Delta x)^2} + \mathcal{O}((\Delta x)^2) \quad (\text{B-15})$$

The expression $(H_{j+1} - 2H_j + H_{j-1})/(\Delta x)^2$ is called a *second central difference expression of error order* $(\Delta x)^2$ for $\left. \frac{d^2 H}{dx^2} \right|_j$.

Wherever possible in this book we have employed central difference expressions for derivatives in the transverse (nonmarching) directions. (This was usually not possible for the continuity equation.) When boundary conditions are required on the first transverse derivative of a function (as in heat flux problems), it is important that the error order in the expression for the gradient at the boundary be the same as that of the central difference expressions used in the interior of the region. Since the central differences discussed here are of error order $(\Delta x)^2$, it is necessary that the derivative expressions at the boundary also be of order $(\Delta x)^2$. Central differences cannot be directly applied at the boundary, since a point outside the region of interest would have to be employed. An imaginary point exterior to the region can be utilized, but it is generally the author's preference to employ forward or backward differences of order $(\Delta x)^2$ and thus express the derivatives entirely in terms of points interior to the region of interest and the boundary points.

We first consider forward differences. We find $H(x_0 + 2(\Delta x)) = H_{j+2}$ by a Taylor Series expansion around x_0 :

$$H_{j+2} = H_j + 2(\Delta x) \left. \frac{dH}{dx} \right|_j + 2(\Delta x)^2 \left. \frac{d^2 H}{dx^2} \right|_j + \frac{4(\Delta x)^3}{3} \left. \frac{d^3 H}{dx^3} \right|_j + \dots \quad (\text{B-16})$$

Now multiply equation (B-3) by 4 and subtract equation (B-16):

$$4H_{j+1} - H_{j+2} = 3H_j + 2(\Delta x) \left. \frac{dH}{dx} \right|_j - \frac{2}{3} (\Delta x)^3 \left. \frac{d^3 H}{dx^3} \right|_j + \dots \quad (\text{B-17})$$

Solving for $\left. \frac{dH}{dx} \right|_j$ gives

$$\left. \frac{dH}{dx} \right|_j = \frac{-H_{j+2} + 4H_{j+1} - 3H_j}{2(\Delta x)} + \frac{(\Delta x)^2}{3} \left. \frac{d^3 H}{dx^3} \right|_j + \dots \quad (\text{B-18})$$

or

$$\left. \frac{dH}{dx} \right|_j = \frac{-H_{j+2} + 4H_{j+1} - 3H_j}{2(\Delta x)} + \mathcal{O}((\Delta x)^2) \quad (\text{B-19})$$

The expression $(-H_{j+2} + 4H_{j+1} - 3H_j)/2(\Delta x)$ is called a *forward difference representation of error order* $(\Delta x)^2$ for $\left. \frac{dH}{dx} \right|_j$.

In an entirely analogous way, we may find H_{j-2} by a Taylor series expansion and proceed to find

$$\left. \frac{dH}{dx} \right|_j = \frac{3H_j - 4H_{j-1} + H_{j-2}}{2(\Delta x)} + \mathcal{O}((\Delta x)^2) \quad (\text{B-20})$$

where the expression $(3H_j - 4H_{j-1} + H_{j-2})/2(\Delta x)$ is called a *backward difference representation of error order* $(\Delta x)^2$ for $\left. \frac{dH}{dx} \right|_j$.

We may now summarize the results obtained thus far:

Derivative	Difference representation	Type	Error order
$\left. \frac{dH}{dx} \right _j$	$\frac{H_{j+1} - H_j}{\Delta x}$	Forward	(Δx)
$\left. \frac{dH}{dx} \right _j$	$\frac{H_j - H_{j-1}}{\Delta x}$	Backward	(Δx)
$\left. \frac{dH}{dx} \right _j$	$\frac{H_{j+1} - H_{j-1}}{2(\Delta x)}$	Central	$(\Delta x)^2$
$\left. \frac{dH}{dx} \right _j$	$\frac{-H_{j+2} + 4H_{j+1} - 3H_j}{2(\Delta x)}$	Forward	$(\Delta x)^2$
$\left. \frac{dH}{dx} \right _j$	$\frac{3H_j - 4H_{j-1} + H_{j-2}}{2(\Delta x)}$	Backward	$(\Delta x)^2$
$\left. \frac{d^2H}{dx^2} \right _j$	$\frac{H_{j+1} - 2H_j + H_{j-1}}{(\Delta x)^2}$	Central	$(\Delta x)^2$

B.2 TRUNCATION ERROR AND A SAMPLE TRUNCATION ERROR ANALYSIS

In the context of this book, we define the truncation error in a difference representation of a partial differential equation as the error made *in the equation* at a point by replacing the differential operators by difference operators. A much more useful quantity to know, and one which is also often called truncation or discretization error, would be the error in the velocities or pressures made by solving the difference equation rather than the differential equation. However, determining this error is essentially equivalent to knowing the exact solution to the differential problem. Forsythe and Wasow (ref. 1) distinguish between these two types of error by calling the error made *in the equation* by replacing differential operators by difference operators, the *formal discretization error at a point*. This is the quantity which we will estimate in this section. There is no guarantee that the order of magnitude of this error will be the same as the order of magnitude of the errors in velocities or pressures, but there is obviously an advantage in keeping the error in the equation itself as small as possible.

As an example, we consider the truncation error at a point for the difference representations of the incompressible boundary layer equations discussed in section 2.1.1. For the momentum equation, the truncation error is

$$E_t = \left(\frac{\partial^2 U}{\partial Y^2} - \frac{dP}{dX} - U \frac{dU}{dX} - V \frac{dU}{dY} \right) - \left[\frac{U_{j+1, k+1} - 2U_{j+1, k} + U_{j+1, k-1}}{(\Delta Y)^2} - \frac{P_{j+1} - P_j}{\Delta X} - U_{j, k} \frac{U_{j+1, k} - U_{j, k}}{\Delta X} - V_{j, k} \frac{U_{j+1, k+1} - U_{j+1, k-1}}{2(\Delta Y)} \right] \quad (B-21)$$

Using the expressions (B-4), (B-11), and (B-14), we obtain

$$E_t = -\frac{(\Delta Y)^2}{12} \frac{\partial^4 U}{\partial Y^4} \Big|_{j+1, k} + \mathcal{O}((\Delta Y)^4) + \frac{\Delta X}{2} \frac{\partial^2 P}{\partial X^2} \Big|_{j+1, k} + \mathcal{O}((\Delta X)^2) + U \left[\frac{\Delta X}{2} \frac{\partial^2 U}{\partial X^2} \Big|_{j+1, k} + \mathcal{O}((\Delta X)^2) \right] + V \left[\frac{(\Delta Y)^2}{6} \frac{\partial^3 U}{\partial Y^3} \Big|_{j+1, k} + \mathcal{O}((\Delta Y)^4) \right] \quad (B-22)$$

Since all functions are assumed analytic in the neighborhood of the point $(j+1, k)$, their derivatives must be bounded. We may therefore write

$$E_t = \mathcal{O}((\Delta Y)^2) + \mathcal{O}(\Delta X) \quad (B-23)$$

The truncation error analysis for the continuity equation proceeds in a similar manner;

$$E_t = \left(\frac{\partial U}{\partial X} + \frac{\partial V}{\partial Y} \right) - \left(\frac{U_{j+1, k} - U_{j, k}}{\Delta X} + \frac{V_{j+1, k} - V_{j+1, k-1}}{\Delta Y} \right) \quad (B-24)$$

Employing expressions (B-4) and (B-8) gives E_t as

$$E_t = \frac{\Delta X}{2} \frac{\partial^2 U}{\partial X^2} \Big|_{j+1, k} + \mathcal{O}((\Delta X)^2) - \frac{\Delta Y}{2} \frac{\partial^2 V}{\partial Y^2} \Big|_{j+1, k} + \mathcal{O}((\Delta Y)^2) \quad (B-25)$$

or

$$E_t = \mathcal{O}(\Delta X) + \mathcal{O}(\Delta Y) \quad (B-26)$$

B.3 A GENERAL METHOD OF STABILITY ANALYSIS

Various methods of stability analysis have been used to obtain stability criteria for difference representations of the type presented in this book. These

include the work of Rouleau (ref. 2), which is based on a paper by Hyman, O'Brien, and Kaplan (ref. 3), and that of Bodoia (ref. 4), which is based on the work of Lax (ref. 5). Of the two, it would appear that the approach of Lax would have the most general application, particularly to systems of simultaneous differential equations. The stability analysis given here will thus be based on the work of Lax, and will rely heavily on the excellent description of this work given by Bodoia, with additional comments added to aid in interpretation.

The Lax method of stability analysis given here requires that the difference equations be linear with constant coefficients. Since this is not the case for any problem in which we are interested, it will be necessary to make a heuristic extension of the method to the actual problems to be analyzed. This extension will be made after the method has been presented.

The set of discrete variables $U_{j,k}^1, U_{j,k}^2, \dots, U_{j,k}^p, \dots, U_{j,k}^s$ is assumed to be described on a finite difference grid at a point (j, k) by a set of difference equations which may be arranged in the form

$$\sum_{p=1}^s \sum_{l=-1}^{+1} E_{l,p}^q U_{j+1,k+l}^p = \sum_{p=1}^s \sum_{l=-1}^{+1} F_{l,p}^q U_{j,k+l}^p \quad q=1,2,\dots,s \quad (\text{B-27})$$

There are s such equations. Some interpretation may be helpful at this point. The set of variables $U_{j,k}^1, \dots, U_{j,k}^s$ represents the different variables such as $U_{j,k}, V_{j,k}$, and $P_{j,k}$ (for this case $s=3$). Generally speaking, if there are s different discrete variables at each point, then there should be s independent difference equations written at each point, corresponding to the s equations of the type (B-27). Each of these equations will have different coefficients, as denoted by the superscript q on the coefficients in (B-27). Since, in general, all variables may appear in any given equation, it is necessary to sum over all variables (the summation on p). The summation on l goes only from -1 to $+1$ since it is assumed that only equations of second order and lower will be encountered in the transverse (non-marching) direction, and a second central difference involves the variables only at $k+1, k$, and $k-1$. The rearrangement into essentially the form of equation (B-27) has been regularly done in the discussion of almost every difference equation presented in this book. It is important to note that the variables $U_{j,k}^p$ represent the *exact* solution to the difference equations, which is only theoretically obtainable, since in practice roundoff error will always be present, regardless of how many decimal places are carried in the computations.

We now introduce $\delta_{j,k}^p$ as the error due to roundoff at the point (j, k) for the variable $U_{j,k}^p$, and define in a similar manner $\delta_{j+1,k}^p$. In the actual computations which we are performing, roundoff error will be present, and equation (B-27) must assume the form

$$\sum_{p=1}^s \sum_{l=-1}^{+1} E_{l,p}^q \left(U_{j+1,k+l}^p + \delta_{j+1,k+l}^p \right) = \sum_{p=1}^s \sum_{l=-1}^{+1} F_{l,p}^q \left(U_{j,k+l}^p + \delta_{j,k+l}^p \right) \quad (\text{B-28})$$

Equation (B-27) may now be subtracted from equation (B-28) leaving

$$\sum_{\nu=1}^s \sum_{l=-1}^{+1} E_{l,\nu}^q \delta_{j+1,k+1}^\nu = \sum_{\nu=1}^s \sum_{l=-1}^{+1} F_{l,\nu}^q \delta_{j,k+1}^\nu \quad (\text{B-29})$$

We now search for a solution to equation (B-29) for $\delta_{j+1,k+1}^\nu$. Consider the errors at $j=0$ (chosen arbitrarily but without loss of generality). This line of errors corresponding to the variable $U_{0,k}^\nu$ may be expressed as the complex Fourier series

$$\delta_{0,k}^\nu = \sum_{\substack{m=0 \\ k=0(1)n}}^n A_m^\nu e^{(im\pi/n)k} \quad (\text{B-30})$$

where n , as usual, represents the last point in the field for which the difference equation is written. The only solution to equation (B-29) which will reduce to the form (B-30) for $j=0$ will have terms of the form

$$[\xi_\beta^\nu]^j e^{i\beta_m k} \quad (\text{B-31})$$

where $\beta_m = \frac{m\pi}{n}$; this form represents a product solution of a function of j and a function of k .

The function of j , $[\xi_\beta^\nu]^j$, is interpreted as ξ_β^ν raised to the power j , where ξ_β^ν is a function of the coefficients of equation (B-29), E and F , as well as β_m . There is one ξ_β^ν for each value of ν , (i.e., one for each variable U^ν). We need consider only one term of the Fourier series by superposition. We substitute a term of the form (B-31) for $\delta_{j,k}^\nu$ in equation (B-29), which yields

$$\sum_{\nu=1}^s \sum_{l=-1}^{+1} E_{l,\nu}^q [\xi_\beta^\nu]^{j+1} e^{i\beta_m(k+l)} = \sum_{\nu=1}^s \sum_{l=-1}^{+1} F_{l,\nu}^q [\xi_\beta^\nu]^{j+1} e^{i\beta_m(k+l)} \quad (\text{B-32})$$

There are s such equations, one for each value of $q=1(1)s$. The set of equations (B-32) represents a set of simultaneous equations in the unknowns

$$[\xi_\beta^1]^{j+1}, \dots, [\xi_\beta^s]^{j+1}$$

on the left side and

$$[\xi_\beta^1]^j, \dots, [\xi_\beta^s]^j$$

on the right side. This set of equations may be written in matrix form as

$$H_1 \Xi_\beta^{j+1} = H_0 \Xi_\beta^j \quad (\text{B-33})$$

where Ξ_{β}^{j+1} and Ξ_{β}^j are the column vectors of the unknowns $[\xi_{\beta}^1]^{j+1}, \dots, [\xi_{\beta}^s]^{j+1}$ and $[\xi_{\beta}^1]^j, \dots, [\xi_{\beta}^s]^j$, and H_1 and H_0 are square matrices of order s with elements given by

$$(H_1)_{r,c} = \sum_{l=-1}^{+1} E_{l,c}^r e^{i\beta_m(k+l)} \quad (\text{B-34})$$

and

$$(H_0)_{r,c} = \sum_{l=-1}^{+1} F_{l,c}^r e^{i\beta_m(k+l)} \quad (\text{B-35})$$

where the subscript r denotes row location and c column location. The elements of H_1 and H_0 are thus functions only of the coefficients of the difference equations (B-27) and β_m .

Equation (B-33) is now premultiplied by the inverse of H_1, H_1^{-1} , to yield

$$\Xi_{\beta}^{j+1} = (H_1^{-1}) (H_0) \Xi_{\beta}^j \quad (\text{B-36})$$

or

$$\Xi_{\beta}^{j+1} = G \Xi_{\beta}^j \quad (\text{B-37})$$

where $G = H_1^{-1} H_0$. The matrix G may now be seen to transform the vector $[\xi_{\beta}^1]^j, \dots, [\xi_{\beta}^s]^j$ into the vector $[\xi_{\beta}^1]^{j+1}, \dots, [\xi_{\beta}^s]^{j+1}$. A nonrigorous explanation of stability might then be that if G causes an "amplification" of Ξ_{β}^j , then the representation is unstable; and if it does not, then the representation is stable. Lax (ref. 5) termed G the *amplification matrix* and defined as stability the requirement that G must be a bounded function of j . We may alternatively define stability in terms of the so-called von Neumann condition (see Bodoia, ref. 4) by stating that if λ^p denotes one of the $\lambda^1, \lambda^2, \dots, \lambda^p, \dots, \lambda^s$ eigenvalues of G , then it is necessary and sufficient for stability that all of the eigenvalues of G be bounded for all β_m , and that, with the possible exception of one eigenvalue, they satisfy

$$|\lambda^p| \leq 1 \quad (\text{B-38})$$

If one eigenvalue does not satisfy (B-38), then that eigenvalue must satisfy

$$|\lambda^p| \leq 1 + \mathcal{O}(\Delta X) \quad (\text{B-39})$$

where ΔX is the mesh size in the marching direction.

The heuristic extension to coefficients which are nonconstant, (i.e., which

vary with k) may be justified if it is assumed that instability develops locally and then propagates throughout the field. Under this assumption, it is reasonable to treat the coefficients as constant over a small region and to apply the stability analysis as discussed here.

B.4 SAMPLE STABILITY ANALYSIS

We chose for a sample stability analysis the simplest set of difference equations which adequately illustrate all of the features of such an analysis: the difference form of the incompressible two-dimensional boundary layer equations discussed in section 2.1.1. These are the same equations for which a truncation error analysis was performed in section B.2. These equations are

$$U_{j,k} \frac{U_{j+1,k} - U_{j,k}}{\Delta X} + V_{j,k} \frac{U_{j+1,k+1} - U_{j+1,k-1}}{2(\Delta Y)} = -\frac{P_{j+1} - P_j}{\Delta X} + \frac{U_{j+1,k+1} - 2U_{j+1,k} + U_{j+1,k-1}}{(\Delta Y)^2} \quad (\text{B-40})$$

and

$$\frac{U_{j+1,k+1} - U_{j,k+1}}{\Delta X} + \frac{V_{j+1,k+1} - V_{j+1,k}}{\Delta Y} = 0 \quad (\text{B-41})$$

This set of equations differs from the set analyzed by Bodoia (ref. 4) only in the form of continuity (B-41), and the analysis is quite similar to his.

Equations (B-40) and (B-41) must first be rearranged into the form (B-27). This rearrangement results in the following equations:

$$\left[\frac{-V_{j,k}}{2(\Delta Y)} - \frac{1}{(\Delta Y)^2} \right] U_{j+1,k-1} + \left[\frac{U_{j,k}}{\Delta X} + \frac{2}{(\Delta Y)^2} \right] U_{j+1,k} + \left[\frac{V_{j,k}}{2(\Delta Y)} - \frac{1}{(\Delta Y)^2} \right] U_{j+1,k+1} = \frac{P_j - P_{j+1}}{\Delta X} + \left[\frac{U_{j,k}}{\Delta X} \right] U_{j,k} \quad (\text{B-42})$$

and

$$\left[\frac{1}{\Delta X} \right] U_{j+1,k+1} + \left[\frac{1}{\Delta Y} \right] V_{j+1,k+1} - \left[\frac{1}{\Delta Y} \right] V_{j+1,k} = \left[\frac{1}{\Delta X} \right] U_{j,k+1} \quad (\text{B-43})$$

For this problem, $s=2$ since U and V are the only discrete variables to be considered, and P is not a variable since it is specified for the boundary layer problem.

The actual computed values of U and V are $U + \delta^1$ and $V + \delta^2$ where δ is the roundoff error in each variable. Thus, the actual equations we have solved are

$$\begin{aligned} & \left[\frac{-V_{j,k}}{2(\Delta Y)} - \frac{1}{(\Delta Y)^2} \right] (U_{j+1,k-1} + \delta_{j+1,k-1}^1) + \left[\frac{U_{j,k}}{\Delta X} + \frac{2}{(\Delta Y)^2} \right] (U_{j+1,k} + \delta_{j+1,k}^1) \\ & + \left[\frac{V_{j,k}}{2(\Delta Y)} - \frac{1}{(\Delta Y)^2} \right] (U_{j+1,k+1} + \delta_{j+1,k+1}^1) = \frac{P_j - P_{j+1}}{\Delta X} + \left(\frac{U_{j,k}}{\Delta X} \right) (U_{j,k} + \delta_{j,k}^1) \end{aligned} \quad (\text{B-44})$$

and

$$\begin{aligned} & \left(\frac{1}{\Delta X} \right) (U_{j+1,k+1} + \delta_{j+1,k+1}^1) + \left(\frac{1}{\Delta Y} \right) (V_{j+1,k+1} + \delta_{j+1,k+1}^2) \\ & - \left(\frac{1}{\Delta Y} \right) (V_{j+1,k} + \delta_{j+1,k}^2) = \left(\frac{1}{\Delta X} \right) (U_{j,k+1} + \delta_{j,k+1}^1) \end{aligned} \quad (\text{B-45})$$

Subtracting equation (B-42) from (B-44) and equation (B-43) from (B-45), we obtain

$$\begin{aligned} & \left[-\frac{V}{2(\Delta Y)} - \frac{1}{(\Delta Y)^2} \right] \delta_{j+1,k-1}^1 + \left[\frac{U}{\Delta X} + \frac{2}{(\Delta Y)^2} \right] \delta_{j+1,k}^1 \\ & + \left[\frac{V}{2(\Delta Y)} - \frac{1}{(\Delta Y)^2} \right] \delta_{j+1,k+1}^1 = \left(\frac{U}{\Delta X} \right) \delta_{j,k}^1 \end{aligned} \quad (\text{B-46})$$

and

$$\left(\frac{1}{\Delta X} \right) \delta_{j+1,k+1}^1 + \left(\frac{1}{\Delta Y} \right) \delta_{j+1,k+1}^2 - \left(\frac{1}{\Delta Y} \right) \delta_{j+1,k}^2 = \left(\frac{1}{\Delta X} \right) \delta_{j,k+1}^1 \quad (\text{B-47})$$

Note that we have dropped the subscripts from the quantities in the coefficients of the δ 's since we assume these coefficients constant in a small region.

These two equations, (B-46) and (B-47), correspond to equation (B-33) when written in the form

$$H_1 \Xi_B^{j+1} = H_0 \Xi_B^j. \quad (\text{B-48})$$

The matrices H_1 and H_0 can now be formed by using the relations (B-34) and (B-35). The matrix H_1 is given by

$$H_1 = \begin{bmatrix} J & 0 \\ K & L \end{bmatrix} \quad (\text{B-49})$$

where

$$J = \left[\frac{-V}{2(\Delta Y)} - \frac{1}{(\Delta Y)^2} \right] e^{i\beta_m(k-1)} + \left[\frac{U}{\Delta X} + \frac{2}{(\Delta Y)^2} \right] e^{i\beta_m(k)} + \left[\frac{V}{2(\Delta Y)} - \frac{1}{(\Delta Y)^2} \right] e^{i\beta_m(k+1)}$$

$$K = \left(\frac{1}{\Delta X} \right) e^{i\beta_m(k+1)}$$

$$L = \left(\frac{1}{\Delta Y} \right) e^{i\beta_m(k+1)} - \left(\frac{1}{\Delta Y} \right) e^{i\beta_m(k)}$$

and H_0 is given by

$$H_0 = \begin{bmatrix} M & 0 \\ N & 0 \end{bmatrix} \quad (\text{B-50})$$

where

$$M = \left(\frac{U}{\Delta X} \right) e^{i\beta_m k}$$

and

$$N = \left(\frac{1}{\Delta X} \right) e^{i\beta_m(k+1)}$$

After dividing both sides of equation (B-48) by

$$e^{i\beta_m k} \left[\frac{(\Delta Y)^2}{\Delta X} \right]$$

and using the identity

$$e^{\pm i\beta_m} = \cos \beta_m \pm i \sin \beta_m$$

the matrices H_1 and H_0 may be rewritten, after some manipulation, as

$$H_1 = \begin{bmatrix} \frac{1}{s} - A & 0 \\ l(e^{i\beta_m}) & (e^{i\beta_m} - 1) \end{bmatrix} \quad (\text{B-51})$$

$$H_0 = \begin{bmatrix} \frac{1}{s} & 0 \\ l(e^{i\beta_m}) & 0 \end{bmatrix} \quad (\text{B-52})$$

where

$$s = \frac{\Delta X}{U(\Delta Y)^2}$$

$$A = 2(\cos \beta_m - 1) - iV(\Delta Y) \sin \beta_m$$

$$l = \frac{\Delta Y}{\Delta X}$$

Now the amplification matrix G is defined as

$$G = H_1^{-1}H_0 \quad (\text{B-53})$$

and

$$H_1^{-1} = \begin{bmatrix} \frac{s}{1-sA} & 0 \\ \frac{-ls(e^{i\beta_m})}{(1-sA)(e^{i\beta_m}-1)} & \frac{1}{(e^{i\beta_m}-1)} \end{bmatrix} \quad (\text{B-54})$$

so that

$$G = \begin{bmatrix} \frac{1}{1-sA} & 0 \\ \frac{-lsA(e^{i\beta_m})}{(1-sA)(e^{i\beta_m}-1)} & 0 \end{bmatrix} \quad (\text{B-55})$$

One of the eigenvalues of G is zero. The other is $1/(1-sA)$. According to our requirements for stability, it is necessary that

$$\left| \frac{1}{1-sA} \right| \leq 1 + \mathcal{O}(\Delta X) \quad (\text{B-56})$$

This is the identical criterion found by Bodoia for the same set of differential equations, but employing a different continuity difference representation. This is undoubtedly caused by the very weak linkage between momentum and continuity in the boundary layer difference equations. The elements of G satisfy the criterion that they are bounded for all β_m except $\beta_m = 0$. At $\beta_m = 0$, $(G)_{21}$ is unbounded. Returning to the Fourier series expression for the error at $j=0$, equation (B-30), we note that $\beta_m = m\pi/n = 0$ must correspond to a zero error frequency. As mentioned in reference 4, a zero error frequency may only appear if the boundary conditions are of the nonfixed type. This means that for the flat plate problem since the boundary conditions are fixed, $\beta_m = 0$ is not possible and our condition (B-56) is sufficient. For problems of the wake type such as in section 2.3.1 where a symmetry condition is used at the centerline, theoretically $\beta_m = 0$ is possible but to the author's knowledge has not been noted in practice. For our purposes then, the condition (B-56) may be considered sufficient.

We will now interpret the stability condition (B-56). The term sA is

$$sA = \frac{\Delta X}{U(\Delta Y)^2} \left[2(\cos \beta_m - 1) - iV(\Delta Y) \sin \beta_m \right] \quad (\text{B-57})$$

or

$$sA = \left[\frac{2(\Delta X)}{U(\Delta Y)^2} (\cos \beta_m - 1) \right] - i \left[\frac{V(\Delta X)}{U(\Delta Y)} \sin \beta_m \right] \quad (\text{B-58})$$

The locus of $-sA$ is shown in figure B-1, and that of $(1-sA)$ and $1/(1-sA)$ in figure B-2. The solid curve is for $U > 0$, and the dashed curve for $U < 0$. For $U > 0$, $|1-sA| \geq 1$ and therefore

$$|\lambda| = \frac{1}{|1-sA|} \leq 1 \quad (\text{B-59})$$

The representation is therefore stable for $U > 0$. For $U < 0$ we examine

$$\frac{1}{1-sA} = \frac{\left[1 - \frac{2(\Delta X)}{U(\Delta Y)^2} (\cos \beta_m - 1) \right] - i \left[\frac{V(\Delta X)}{U(\Delta Y)} \sin \beta_m \right]}{\left[1 - \frac{2(\Delta X)}{U(\Delta Y)^2} (\cos \beta_m - 1) \right]^2 + \left[\frac{V(\Delta X)}{U(\Delta Y)} \sin \beta_m \right]^2} \quad (\text{B-60})$$

Now we let

$$C = 1 - \frac{2(\Delta X)}{U(\Delta Y)^2} (\cos \beta_m - 1) \quad (\text{B-61})$$

and

$$D = \frac{V(\Delta X)}{U(\Delta Y)} \sin \beta_m \quad (\text{B-62})$$

so that

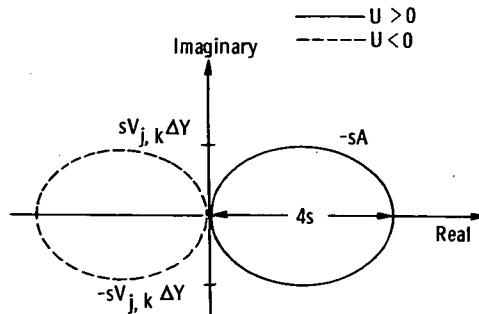


FIGURE B-1.—Plot of $-sA$.

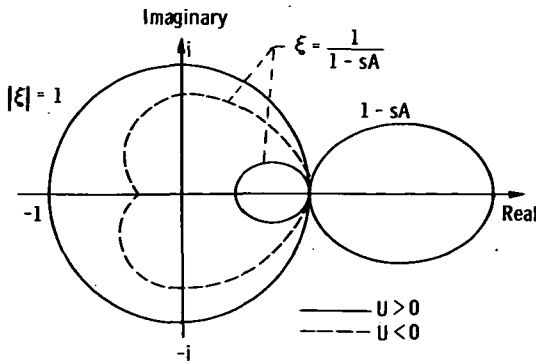


FIGURE B-2. — Plot of $\xi = \frac{1}{1-sA}$.

$$\frac{1}{1-sA} = \frac{C - iD}{C^2 + D^2} \tag{B-63}$$

and

$$\left| \frac{1}{1-sA} \right| = \frac{\sqrt{C^2 + D^2}}{C^2 + D^2} = \frac{1}{\sqrt{C^2 + D^2}} \tag{B-64}$$

Now

$$\left| \frac{1}{1-sA} \right| \leq 1 \text{ only if } C^2 + D^2 \geq 1 \tag{B-65}$$

or,

$$\left[1 - \frac{2(\Delta X)}{U(\Delta Y)^2} (\cos \beta_m - 1) \right]^2 + \frac{V^2(\Delta X)^2}{U^2(\Delta Y)^2} \sin^2 \beta_m \geq 1 \tag{B-66}$$

This inequality will be satisfied if

$$\frac{\Delta X}{|U|(\Delta Y)^2} \geq \frac{1}{2} \tag{B-67}$$

and

$$V \geq \sqrt{\frac{2|U|}{\Delta X}} \tag{B-68}$$

These are the stability criteria.

REFERENCES

1. FORSYTHE, GEORGE E.: AND WASOW, W. R.: Finite-Difference Methods for Partial Differential Equations. John Wiley & Sons, Inc., 1960.
2. ROULEAU, W. T.: Finite Difference Methods for the Solution of Fluid Flow Problems Described by the Prandtl Equations. Ph.D. Thesis, Carnegie Inst. Tech., 1954.

3. O'BRIEN, GEORGE G.; HYMAN, MORTON A.; AND KAPLAN, SIDNEY: A Study of the Numerical Solution of Partial Differential Equations. *J. Math. Phys.*, vol. 29, 1950, pp. 223-251.
4. BODOIA, J. R.: *The Finite Difference Analysis of Confined Viscous Flows*. Ph.D. Thesis. Carnegie Inst. Tech., 1959.
5. LAX, P. D.: *Difference Approximation to Solution of Linear Differential Equations—An Operator Theoretical Approach*. Lecture Series of the Symposium on Partial Differential Equations. University of Kansas Press, 1957.

APPENDIX C—ANALYSIS AND CORRECTION OF INHERENT ERROR IN FLOW RATE FOR CONFINED FLOW PROBLEMS IN CHANNELS OF CONSTANT AREA

When a continuous velocity distribution must be represented by a discrete set of values on a finite difference grid, some error will necessarily be incurred when an operation such as differentiation or integration of that distribution must be performed. In finding the flow rate in a channel, a transverse integration of the axial velocity distribution must be performed, and it is the purpose of this appendix to analyze and to help correct the error in such a flow rate calculation.

This error correction can be of considerable importance, since a flow rate calculation is performed, either explicitly or implicitly, in every confined flow analysis discussed in this book. Errors in the channel flow rate will thus result in errors in both the axial pressure distribution and the local velocity distributions.

The effects of flow rate errors on the axial pressure distribution and local velocity distributions occur through relatively subtle mechanisms and, except in the fully developed region, are very difficult to evaluate. In fact, many possible definitions of flow rate error are possible. The definition of flow rate error and the corresponding correction technique discussed in this appendix, while nonunique, seem logical. Most important, the error correction technique works in the sense that when it is used results are obtained which are more accurate for both velocity distributions and pressure gradients. This improvement in accuracy has been verified by comparing the results with those obtained by using much finer mesh sizes.

The use of finite difference forms of the continuity equation which involve only first-order forward and backward transverse spacewise differences, as has been common practice throughout this book, restricts the numerical approximation of the flow rate to that of a trapezoidal rule integration over the mesh. This is evident from the forms of equations (6-10) and (7-14) which are the difference forms of integral continuity for the parallel plate channel and the circular tube, respectively, and which result directly from adding together the finite difference representations of differential continuity obtained at all transverse mesh points. Even in those cases where the integral continuity equation is not directly applied

(e.g., the second model for flow in a rectangular channel, section 8.1.2), the trapezoidal rule integral is implied as may be seen by adding together the continuity difference equations written for all transverse mesh points. The actual error in flow rate in such cases is greater than the error in trapezoidal rule integration, since without the actual use of integral continuity the flow rate tends to drift because of roundoff error.

The details of error analysis and error correction will be carried out here for the simplest case, that of the parallel plate channel, but they may be extended readily to a constant area channel of any shape. To the best of the author's knowledge, no information on error analysis and correction in flow rate is available for varying area channels, and any general error analysis would be very difficult to obtain since the results would be highly geometry dependent.

We first examine the entrance flow problem discussed in section 6.1.1. In the following discussion we assume the existence of a known exact solution to the fundamental differential equations of the problem which yields continuous velocity distributions over the entire region of interest. We then apply the discrete form of integral continuity to these continuous velocity distributions in order to examine the error involved in the discrete approximations.

Using the variables of section 6.1.1, the exact continuous solution gives

$$U_{0,k} = U_{e_k} = 1 \quad (\text{C-1})$$

A trapezoidal rule integration for the dimensionless flow rate over the discrete grid yields

$$Q_d = \left(U_{0,0} + 2 \sum_{k=1}^n U_{0,k} \right) \frac{\Delta Y}{2} \quad (\text{C-2})$$

or, using (C-1) and since $\sum_{k=1}^n (1) = n$,

$$Q_d = (1 + 2n) \frac{\Delta Y}{2} \quad (\text{C-3})$$

For a uniform mesh,

$$\frac{1}{n+1} = \Delta Y \quad (\text{C-4})$$

so that (C-3) becomes

$$Q_d = 1 - \frac{\Delta Y}{2} \quad (\text{C-5})$$

The exact flow rate from a continuous profile would be

$$Q_e = 1 \quad (\text{C-6})$$

We define the inherent error in flow rate due to discretization as

$$\epsilon_Q \equiv Q_e - Q_d \quad (\text{C-7})$$

Using equations (C-5) and (C-6) gives

$$\epsilon_Q = \frac{\Delta Y}{2} \quad (\text{C-8})$$

This is the error in flow rate made at the inlet by replacing the continuous inlet profile by a discrete set of values having the same magnitude as the continuous profile at each point.

The error ϵ_Q evaluated from equation (C-7) will be different at different axial positions as the solution is carried downstream since Q_d as evaluated from equation (C-2) does not remain constant as the exact solution velocity profile changes. (The expressions for Q_d in equation (C-5) and ϵ_Q in equation (C-8) apply only at the inlet.) It is instructive to compute the error ϵ_Q for fully developed flow. For the present geometry, the exact continuous fully developed velocity distribution is given in dimensionless form by

$$U_e = 1.5(1 - Y^2) \quad (\text{C-9})$$

At the grid points, assuming a uniform grid,

$$U_{e_k} = 1.5[1 - k^2(\Delta Y)^2] \quad (\text{C-10})$$

Employing the trapezoidal rule gives

$$Q_d = \left(U_{e_0} + 2 \sum_{k=1}^n U_{e_k} \right) \frac{\Delta Y}{2} \quad (\text{C-11})$$

or when using equation (C-10),

$$Q_d = 1.5 \left\{ 1 + 2 \sum_{k=1}^n [1 - k^2(\Delta Y)^2] \right\} \frac{\Delta Y}{2} \quad (\text{C-12})$$

Now, since

$$\sum_{k=1}^n k^2 = \frac{n(n+1)(2n+1)}{6} \quad (\text{C-13})$$

we may rewrite equation (C-12) as

$$Q_d = 1.5 \left\{ 1 + \frac{2(1 - \Delta Y)}{\Delta Y} - 2(\Delta Y)^2 \left[\frac{n(n+1)(2n+1)}{6} \right] \right\} \frac{\Delta Y}{2} \quad (\text{C-14})$$

or, since

$$\frac{1}{n+1} = \Delta Y \quad (\text{C-15})$$

we find after some manipulation that

$$Q_d = 1 - \frac{(\Delta Y)^2}{4} \quad (\text{C-16})$$

or, since $Q_e = 1$,

$$\epsilon_Q = Q_e - Q_d = \frac{(\Delta Y)^2}{4} \quad (\text{C-17})$$

The error in flow rate made by replacing the continuous profile from the exact solution with discrete points bearing the same velocity values is thus much smaller in the fully developed region ($(\Delta Y)^2/4$) than that in the entrance region ($\Delta Y/2$). Either of these errors will of course be reduced in magnitude if the mesh size ΔY is reduced. If the variable mesh size technique of appendix D is applied, the error expressions given by equations (C-8) and (C-17) still apply, with $\Delta Y = \Delta Y_2$, the small mesh size used near the channel wall.

In actually obtaining a numerical solution, the value of Q_d is set by the values of $U_{0,k}$ used for the inlet profile through the trapezoidal rule integral for the flow rate (the equation of constraint) which states that

$$Q_d = \left(U_{0,0} + 2 \sum_{k=1}^n U_{0,k} \right) \frac{\Delta Y}{2} = \left(U_{j+1,k} + 2 \sum_{k=1}^n U_{j+1,k} \right) \frac{\Delta Y}{2} = \text{constant} \quad (\text{C-18})$$

The Q_d then remains constant over the entire length of the channel. By proper choice of the values of $U_{0,k}$, the inherent error in flow rate defined by equation (C-7) may be compensated for either at the inlet or in the fully developed region (but not both).

If the flow rate error is to be compensated for in the fully developed region, the inlet profile may be multiplied by $1/\{1 - [(\Delta Y)^2/4]\}$. For example,

$$U_{0,k} = \frac{1}{1 - \frac{(\Delta Y)^2}{4}} \quad (\text{C-19})$$

based on the error term (C-17). In the particular case under consideration here, when the flow rate is corrected by (C-19), then the fully developed velocities at each point ($U_{j,k}$) and the fully developed pressure gradient $(P_{j+1} - P_j)/\Delta X$ obtained from the finite difference solution are exactly those of the analytical solution. This

is largely a fortuitous circumstance, mainly because the exact fully developed velocity distribution is a parabola and because the central differences used for transverse velocity gradients are exact for parabolas. In general, the results of the error correction technique will be good, but not perfect. The error correction (C-19) will have some beneficial effect near the entrance, but not as much as a technique specifically intended for that region.

If the flow rate error is to be corrected at the channel inlet, the inlet profile may be modified as

$$U_{0,k} = \frac{1}{1 - \frac{\Delta Y}{2}} \quad (\text{C-20})$$

based on the error term (C-8). This correction is very effective near the inlet, but it has less benefit as the fully developed region is approached.

For each problem, a decision must be made as to whether a correction of the form (C-19) or (C-20) would be most beneficial. If a fully developed solution is available from another source (as it must be to get an expression of the form (C-19)), then a correction of the form (C-19) would seem to be most esthetically pleasing, since the solution would closely approach the correct fully developed velocity distribution and pressure gradient. However, since the development region would be of prime importance in such a situation, a correction of the form (C-20) would give more accurate results in that region, and any errors incurred in the fully developed region would be easily evaluated since the solution is already known in that region. On the other hand, a correction of the form (C-19) would not allow an evaluation of the error in the development region since presumably no solution is available there. If no fully developed solution is available, then a correction factor based on a uniform inlet profile such as (C-20) is the only choice. Thus, a correction of the form (C-20) would seem to the author to be most practical in all cases.

APPENDIX D—VARIABLE MESH SIZE TECHNIQUE

In the finite difference solution of viscous flows it is often advantageous to use a fine mesh size in regions of rapidly varying velocities, such as close to a wall or in a mixing region. Conversely, a relatively coarse mesh is satisfactory in regions of more slowly varying velocity, such as close to a channel centerline or near the free stream in a boundary layer flow. In references 1 and 2 Hornbeck discusses the technique of combining large and small mesh sizes. The advantage of this technique over simply applying a small mesh over the entire region is that in an implicit formulation the number of simultaneous equations to be solved can be reduced materially. This can effect a considerable saving in computer time, particularly in confined flow situations where it is usually necessary to use standard elimination methods for which the time required increases as the cube of the number of equations. In addition, the roundoff error accumulated in solving large numbers of simultaneous equations is held to a minimum.

A variable mesh technique presents no difficulties when only forward or backward first differences of error $\mathcal{O}(h)$ are required, where h is the mesh size, since such differences involve only two points and can be wholly contained in a region of any given mesh size with no difficulties encountered at the mesh size change. For this reason, the mesh size in the marching direction for any of the problems discussed in this book may be changed as desired without modification to the equations since only a first backward difference of error $\mathcal{O}(h)$ in the marching direction is involved. When it is desired to employ central differences, either first or second, as in the transverse directions for problems discussed in this book, difficulties occur in evaluating these differences at the point of mesh size change. Thus, it is not possible to vary the transverse mesh size in the field without some modification to the previously presented equations.

Suppose a mesh size change from ΔY_1 to a smaller mesh size ΔY_2 is to be made at the transverse position corresponding to $k=p$. The region of mesh size change is shown in figure D-1(a). A velocity $U_{j+1,q}$ at a point ΔY_2 below the point $k=p$ is determined by passing a parabola through the values of $U_{j+1,p+1}$, $U_{j+1,p}$, and $U_{j+1,p-1}$, and then interpolating for $U_{j+1,q}$. The interpolated value is given by

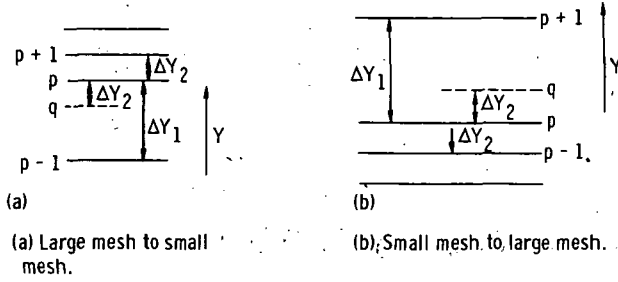


FIGURE D-1.—Region of mesh size change.

$$U_{j+1,q} = 2 \frac{\theta^2}{1+\theta} U_{j+1,p-1} + 2(1-\theta)U_{j+1,p} + \frac{\theta-1}{\theta+1} U_{j+1,p+1} \quad (D-1)$$

where

$$\theta = \frac{\Delta Y_2}{\Delta Y_1} \quad (D-2)$$

The derivatives in question at the point $k=p$ can now be expressed in difference form as

$$\frac{\partial U}{\partial Y} \Big|_{k=p} = \frac{U_{j+1,p+1} - U_{j+1,q}}{2(\Delta Y_2)} \quad (D-3)$$

$$\frac{\partial^2 U}{\partial Y^2} \Big|_{k=p} = \frac{U_{j+1,p+1} - 2U_{j+1,p} + U_{j+1,q}}{(\Delta Y_2)^2} \quad (D-4)$$

where $U_{j+1,q}$ is given by equation (D-1). These expressions apply whether the transverse direction Y is a Cartesian or radial (cylindrical) coordinate.

If the mesh size is to be changed from a smaller mesh size ΔY_2 to a larger mesh size ΔY_1 at $k=p$ as shown in figure D-1(b), then the interpolated value is given by

$$U_{j+1,q} = \frac{\theta-1}{\theta+1} U_{j+1,p-1} + 2(1-\theta)U_{j+1,p} + 2 \frac{\theta^2}{1+\theta} U_{j+1,p+1} \quad (D-5)$$

where $\theta = \Delta Y_2 / \Delta Y_1$.

The derivatives at $k=p$ are approximated as

$$\frac{\partial U}{\partial Y} \Big|_{k=p} = \frac{U_{j+1,q} - U_{j+1,p-1}}{2(\Delta Y_2)} \quad (D-6)$$

$$\frac{\partial^2 U}{\partial Y^2} \Big|_{k=p} = \frac{U_{j+1,q} - 2U_{j+1,p} + U_{j+1,p-1}}{(\Delta Y_2)^2} \quad (D-7)$$

where $U_{j+1,q}$ is given by equation (D-5).

For confined viscous flows where the integral continuity equation is applied, modification must be made if two different transverse mesh sizes are involved. As an example, consider the incompressible entrance flow between parallel plates discussed in section 6.1.1. The integral continuity equation may be written as

$$\int_0^1 U dY \Big|_{j+1} = \int_0^1 U dY \Big|_j \quad (\text{D-8})$$

If the integrals in equation (D-8) are evaluated by the trapezoidal rule for the case where the mesh size changes from a large mesh ΔY_1 to a small mesh ΔY_2 at $k=p$, somewhere in the range $0 < Y < 1$, then the finite difference form of equation (D-8) becomes

$$\begin{aligned} & \left(U_{j+1,0} + 2 \sum_{k=1}^{p-1} U_{j+1,k} + U_{j+1,p} \right) \frac{\Delta Y_1}{2} + \left(U_{j+1,p} + 2 \sum_{k=p+1}^n U_{j+1,k} \right) \frac{\Delta Y_2}{2} \\ & = \left(U_{j,0} + 2 \sum_{k=1}^{p-1} U_{j,k} + U_{j,p} \right) \frac{\Delta Y_1}{2} + \left(U_{j,p} + 2 \sum_{k=p+1}^n U_{j,k} \right) \frac{\Delta Y_2}{2} \quad (\text{D-9}) \end{aligned}$$

The extension to cylindrical geometry and other geometries is straightforward; the integration must be done in sections which cover each region of a given mesh size.

In general, the use of two (or more) different transverse mesh sizes in the same flow field does not significantly change the actual method of solution. This is true since a special form of the difference equations is needed only at the point of mesh size change, and in fact, is only needed then if central or forward or backward differences of higher error order which span the mesh size change are involved. Of course, the proper mesh size must be used in the corresponding region.

The continuity equation difference representations employed in this book almost without exception involve only simple forward or backward differences in the transverse directions, and not central differences or higher order forward or backward expressions. Thus, the only point to be observed in using continuity on a field of varying transverse mesh size is to ensure that the proper mesh size is used in the appropriate region.

REFERENCES

1. HORNBECK, ROBERT W.: The Entry Problem in Pipes with Porous Walls. Ph.D. Thesis, Carnegie Inst. Tech., 1961.
2. HORNBECK, ROBERT W.: Non-Newtonian Laminar Flow in the Inlet of a Pipe. Paper 65-WA/FE-4, ASME, Nov. 1965.

APPENDIX E—GAUSS-JORDAN ELIMINATION ROUTINE

One of the most effective methods of solving a set of simultaneous linear algebraic equations, where the matrix of coefficients is not of the band type discussed in appendix A, is a modification of Gauss elimination called Gauss-Jordan elimination. The technique will not be discussed in detail here (see Ralston, ref. 1).

The routine presented in this appendix inverts the matrix of coefficients rather than solving the set of equations. If the set of equations is written in matrix form as

$$AX = R \quad (\text{E-1})$$

where A is the square matrix of coefficients, X the column vector of unknowns, and R the column vector representing the right side, then the solution may be formally written as

$$X = A^{-1}R$$

where A^{-1} is the inverse of A . The matrix multiplication of the square matrix A^{-1} with the column vector R yields the solution column vector X .

We present first the routine to invert A and then a program segment to solve for X using A^{-1} .

The following FORTRAN IV routine employs maximization of pivotal elements (partial positioning for size) described by Ralston in reference 1. This helps to reduce roundoff error. Since the routine has no error exits, attempting to invert a singular matrix will simply give erroneous results or an overflow, depending on the computer and compiler employed. Although more sophisticated dimensioning is possible with certain systems, it is suggested that the matrix C be dimensioned as n by n ($n=70$ for the example given here) and that the integer vector J have at least a dimension of $(n+21)$.

```
C THIS IS A FORTRAN SUBROUTINE FOR INVERTING MATRICES BY
C MEANS OF GAUSS-JORDAN ELIMINATION EMPLOYING PARTIAL
C POSITIONING FOR SIZE. THERE ARE NO ERROR EXITS AND AT-
C TEMPTING TO INVERT A SINGULAR MATRIX WILL IN GENERAL
C SIMPLY GIVE NON-MEANINGFUL RESULTS.
```

C

C THE CALLING SEQUENCE IS SIMPLY

C

C CALL MIVNC(A, N)

C

C WHERE A IS THE SQUARE MATRIX TO BE INVERTED AND N IS THE
C SIZE OF THIS MATRIX. THE DUMMY ARRAY C IN THE SUBROUTINE
C IS DIMENSIONED AS 70 BY 70.

C

C THIS DIMENSION MUST BE MODIFIED BEFORE THE SUBROUTINE IS
C USED SO THAT THE ARRAY SIZE IN THE SUBROUTINE IS THE SAME
C AS THAT OF THE ARRAY IN THE CALLING PROGRAM (A IN THE
C ABOVE SAMPLE CALL). THE VALUE OF N MAY OF COURSE BE DIFFERENT
C THAN THE ROW AND COLUMN DIMENSION OF A. THE
C DIMENSION OF J IN THE SUBROUTINE MUST BE AT LEAST (N + 21).

```

SUBROUTINE MIVNC(C, J3)
  DIMENSION C(70, 70), J(120)
  DO 125 I = 1, J3
125 J(I + 20) = I
  DO 144 I = 1, J3
  C0 = 0.
  J1 = I
  DO 135 K = I, J3
  IF ((ABS(C0) - ABS(C(I, K))).GE.0.) GO TO 135
126 J1 = K
  C0 = C(I, K)
135 CONTINUE
127 IF (I.EQ.J1) GO TO 138
128 K = J(J1 + 20)
  J(J1 + 20) = J(I + 20)
  J(I + 20) = K
  DO 137 K = 1, J3
  S0 = C(K, I)
  C(K, I) = C(K, J1)
137 C(K, J1) = S0
138 C(I, I) = 1.
  DO 139 J1 = 1, J3
139 C(I, J1) = C(I, J1)/C0
  DO 142 J1 = 1, J3
  IF (I.EQ.J1) GO TO 142
129 C0 = C(J1, I)
  IF (C0.EQ.0.) GO TO 142
130 C(J1, I) = 0.
  DO 141 K = 1, J3

```

```
141 C(J1, K) = C(J1, K) - C0*C(I, K)
142 CONTINUE
144 CONTINUE
    DO 143 I = 1, J3
    IF (J(I + 20).EQ.I) GO TO 143
131 J1 = I
132 J1 = J1 + 1
    IF (J(J1 + 20).EQ.I) GO TO 133
136 IF (J3.GT.J1) GO TO 132
133 J(J1 + 20) = J(I + 20)
    DO 163 K = 1, J3
    C0 = C(I, K)
    C(I, K) = C(J1, K)
163 C(J1, K) = C0
    J(I + 20) = I
143 CONTINUE
    RETURN
    END
```

The following program segment calls the inversion routine, assuming the coefficient matrix is A and the order N , and then multiplies A^{-1} by the right side vector RH and stores the result in the vector X :

```
CALL MIVNC (A, N)
DO 10 J=1, N
SUM=0.
DO 11 K=1, N
11 SUM=SUM+A(J, K)*RH(K)
10 X(J)=SUM
```

For sets of equations of the type encountered in the confined flow chapters of this book, this routine has given accurate results on a machine with an eight-decimal digit word for N as high as 90.

REFERENCE

1. RALSTON, ANTHONY: A First Course in Numerical Analysis. McGraw-Hill Book Co., Inc., 1965.

APPENDIX F—SPECIFICATION OF TRANSVERSE VELOCITIES AT LEADING EDGES AND CHANNEL ENTRANCES

In most of the problems formulated in this book, the transverse velocity components at the leading edge in a boundary layer problem or at the entrance in a channel flow problem must be specified in order to obtain a solution to the difference equations at the first step downstream from the leading edge or entrance. However, in the great majority of these problems, these transverse velocities are not true boundary conditions in the mathematical sense. It is the purpose of this appendix to clarify this apparent paradox.

Consider first the flat plate boundary layer problem discussed in chapter 2. The differential formulation in dimensionless form is

$$U \frac{\partial U}{\partial X} + V \frac{\partial U}{\partial Y} = -\frac{dP}{dX} + \frac{\partial^2 U}{\partial Y^2} \quad (\text{F-1})$$

$$\frac{\partial U}{\partial X} + \frac{\partial V}{\partial Y} = 0 \quad (\text{F-2})$$

$$\left. \begin{aligned} U(X, 0) &= 0 \\ U(X, \infty) &= U_x(X) \\ V(X, 0) &= 0 \\ U(0, Y) &= U_x(0) \end{aligned} \right\} \quad (\text{F-3})$$

Note that $V(0, Y)$ is not specified. That this condition is not a boundary condition may be seen qualitatively by noting that there are no derivatives of V with respect to X in equations (F-1) and (F-2). That $V(0, Y)$ is not a boundary condition may be verified quantitatively by writing equations (F-1) to (F-3) in stream function form and noting that the set is complete without specifying $V(0, Y)$. The value of $V(X, Y)$ may in fact readily be shown to approach infinity as the singular point $X=0$ is approached.

Consider now the conventional implicit finite difference representation of this problem (See chapter 2 for details). Equations (F-1) and (F-2) become

$$U_{j,k} \frac{U_{j+1,k} - U_{j,k}}{\Delta X} + V_{j,k} \frac{U_{j+1,k+1} - U_{j+1,k-1}}{2(\Delta Y)} = -\frac{P_{j+1} - P_j}{\Delta X} + \frac{U_{j+1,k+1} - 2U_{j+1,k} + U_{j+1,k-1}}{(\Delta Y)^2} \quad (\text{F-4})$$

$$\frac{U_{j+1,k+1} - U_{j,k+1}}{\Delta X} + \frac{V_{j+1,k+1} - V_{j+1,k}}{\Delta Y} = 0 \quad (\text{F-5})$$

Equation (F-4) written for $k=1(1)n$ results in n simultaneous linear algebraic equations in the n unknowns $U_{j+1,k}$, each of the form

$$\left[-\frac{1}{(\Delta Y)^2} - \frac{V_{j,k}}{2(\Delta Y)} \right] U_{j+1,k-1} + \left[\frac{U_{j,k}}{\Delta X} + \frac{2}{(\Delta Y)^2} \right] U_{j+1,k} + \left[-\frac{1}{(\Delta Y)^2} + \frac{V_{j,k}}{2(\Delta Y)} \right] U_{j+1,k+1} = \frac{P_j - P_{j+1} + U_{j,k}^2}{\Delta X} \quad (\text{F-6})$$

The coefficients of the unknowns as well as the right side of equation (F-6) contain the "known" velocities $U_{j,k}$ and $V_{j,k}$. However, at the first step downstream from the leading edge, $U_{j,k}$ and $V_{j,k}$ are $U(0, Y)$ and $V(0, Y)$, respectively. Thus, $V(0, Y)$ must be specified in order to start the marching procedure. This requirement is, however, a result of the numerical scheme employed as opposed to a fundamental boundary condition. We shall emphasize this point shortly by discussing a numerical scheme which does not require the specification of $V(0, Y)$. In practice, a more important question is whether the values specified for $V(0, Y)$ in the conventional implicit scheme discussed previously have a significant effect on the solution. The fortunate answer is that they do not; the effect of even very large changes in the values chosen for $V(0, Y)$ is damped out after only a few steps downstream from the leading edge. Since a large number of small steps must be taken near the leading edge in any event to confine the effect of the leading edge singularity to small X (see chapter 2), the choice of $V(0, Y)$ is quite unimportant. The author has found that choosing $V(0, Y) = 0$ is quite acceptable. The values of $V_{j-1,k}$ calculated from equation (F-5) close to the leading edge are very large (of the order of 100) and behave in the general manner predicted by the differential equation solution in that $V(X, Y) \rightarrow \infty$ as $X \rightarrow 0$.

We now present a difference form of equation (F-1) for which it is not necessary to specify $V(0, Y)$. The form is simply an adaptation of the highly implicit formulation employed in chapter 3 for the solution of jet problems with zero or small secondary velocities and may be written as

$$\begin{aligned}
 U_{j+1,k} \frac{U_{j+1,k} - U_{j,k}}{\Delta X} + V_{j+1,k} \frac{U_{j+1,k+1} - U_{j+1,k-1}}{2(\Delta Y)} \\
 = -\frac{P_{j+1} - P_j}{\Delta X} + \frac{U_{j+1,k+1} - 2U_{j+1,k} + U_{j+1,k-1}}{(\Delta Y)^2} \quad (\text{F-7})
 \end{aligned}$$

This equation and equation (F-5) written for $k=1(1)n$ provide $2n$ simultaneous algebraic equations in the $2n$ unknowns $U_{j+1,k}$ and $V_{j+1,k}$. Since equation (F-7) is nonlinear in the unknowns, these equations must be solved by an iterative process (see chapter 3 for details). It may now be noted that $V_{j,k}$ does not appear in either equation (F-7) or equation (F-5); hence, the marching procedure may be started from the leading edge without specifying $V(0, Y)$. Solving equation (F-7) is more time consuming than solving the conventional implicit representation (F-4); therefore, it would seldom be used in practice since the results obtained are virtually identical for both equations. (For special exceptions see chapter 3.) We have, however, illustrated our point that the necessity for specifying $V(0, Y)$ is a function only of the difference scheme chosen.

Completely analogous arguments may be made for all of the other formulations presented in chapters 2 to 7, in that the transverse velocities at the plate leading edge, beginning of the boundary layer, jet mouth, channel or tube entrance, etc., are not true boundary conditions but may have to be specified in order to apply the suggested finite difference scheme. In all of these cases these transverse velocities may be specified as zero without noticeably affecting the solution.

A notable exception to the discussion given in this appendix occurs for the second approximate model for the velocity solution in a rectangular channel (sections 8.1.2 and 8.1.4). In these models, three momentum equations are employed, and the first axial derivatives of the transverse velocity components are present, indicating that values must be specified for the transverse velocity components $V(0, Y, Z)$ and $W(0, Y, Z)$ as true mathematical boundary conditions. These velocity components at the channel entrance have been rather arbitrarily specified as zero in chapter 8 since in order to specify any other values we would have to be able to describe in detail the upstream conditions prior to the channel entrance.

NATIONAL AERONAUTICS AND SPACE ADMINISTRATION
WASHINGTON, D.C. 20546

OFFICIAL BUSINESS
PENALTY FOR PRIVATE USE \$300

SPECIAL FOURTH CLASS MAIL
Book

POSTAGE AND FEES PAID
NATIONAL AERONAUTICS AND
SPACE ADMINISTRATION
451



POSTMASTER : If Undeliverable (Section 158
Postal Manual) Do Not Return

"The aeronautical and space activities of the United States shall be conducted so as to contribute . . . to the expansion of human knowledge of phenomena in the atmosphere and space. The Administration shall provide for the widest practicable and appropriate dissemination of information concerning its activities and the results thereof."

—NATIONAL AERONAUTICS AND SPACE ACT OF 1958

NASA SCIENTIFIC AND TECHNICAL PUBLICATIONS

TECHNICAL REPORTS: Scientific and technical information considered important, complete, and a lasting contribution to existing knowledge.

TECHNICAL NOTES: Information less broad in scope but nevertheless of importance as a contribution to existing knowledge.

TECHNICAL MEMORANDUMS: Information receiving limited distribution because of preliminary data, security classification, or other reasons. Also includes conference proceedings with either limited or unlimited distribution.

CONTRACTOR REPORTS: Scientific and technical information generated under a NASA contract or grant and considered an important contribution to existing knowledge.

TECHNICAL TRANSLATIONS: Information published in a foreign language considered to merit NASA distribution in English.

SPECIAL PUBLICATIONS: Information derived from or of value to NASA activities. Publications include final reports of major projects, monographs, data compilations, handbooks, sourcebooks, and special bibliographies.

TECHNOLOGY UTILIZATION PUBLICATIONS: Information on technology used by NASA that may be of particular interest in commercial and other non-aerospace applications. Publications include Tech Briefs, Technology Utilization Reports and Technology Surveys.

Details on the availability of these publications may be obtained from:

SCIENTIFIC AND TECHNICAL INFORMATION OFFICE

NATIONAL AERONAUTICS AND SPACE ADMINISTRATION
Washington, D.C. 20546